



This work is licensed under a [Creative Commons Attribution-NonCommercial-ShareAlike 4.0 International License](https://creativecommons.org/licenses/by-nc-sa/4.0/).

How to cite this thesis / dissertation (APA referencing method):

Surname, Initial(s). (Date). *Title of doctoral thesis* (Doctoral thesis). Retrieved from [http://scholar.ufs.ac.za/rest of thesis URL on KovsieScholar](http://scholar.ufs.ac.za/rest_of_thesis_URL_on_KovsieScholar)

Surname, Initial(s). (Date). *Title of master's dissertation* (Master's dissertation). Retrieved from [http://scholar.ufs.ac.za/rest of thesis URL on KovsieScholar](http://scholar.ufs.ac.za/rest_of_thesis_URL_on_KovsieScholar)

Expression of rotavirus capsid protein, VP6, in various yeasts

By

Matshepo Elizabeth Rakaki

Dissertation submitted for the degree Master of Science (M.Sc.) in Biochemistry at the Department of Microbial, Biochemical and Food Biotechnology

Faculty of Natural and Agricultural Sciences

University of the Free State

Supervisor: Ass. Prof. Hester G. O'Neill

Co-supervisor: Prof. Jacobus Albertyn

UNIVERSITY OF THE
FREE STATE
UNIVERSITEIT VAN DIE
VRYSTAAT
YUNIVESITHI YA
FREISTATA

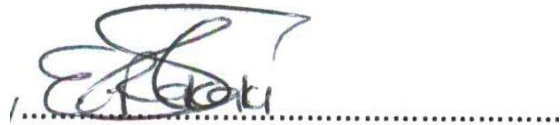


UFS·UV
NATURAL AND
AGRICULTURAL SCIENCES
NATUUR- EN
LANDBOUWETENSAPPE
MICROBIAL, BIOCHEMICAL
AND FOOD BIOTECHNOLOGY
MIKROBIESE, BIOCHEMIESE
EN VOEDSELBIOTEGNOLOGIE

Declarations:

“I, **Matshepo Elizabeth Rakaki**, declare that the Master’s Degree research dissertation that I herewith submit for the Master’s Degree qualification of **Biochemistry** at the University of the Free State is my independent work, and that I have not previously submitted it for a qualification at another institution of higher education.”

Signature:

A handwritten signature in black ink, appearing to read 'Matshepo Elizabeth Rakaki', is written over a horizontal dotted line. The signature is stylized and cursive.

Date: 05/02/2018

It always seems impossible until it's done

Nelson Mandela

You are capable of more than you know. Choose a goal that seems right for you and strive to be the best, however hard the path. Aim high. Behave honorably. Prepare to be alone at times, and to endure failure. Persist! The world needs all you can give.

E O Wilson

A dream doesn't become reality through magic; it takes sweat, determination and hard work.

Colin Powell

Desire is the key to motivation, but it's determination and commitment to an unrelenting pursuit of your goal - a commitment to excellence - that will enable you to attain the success you seek.

Mario Andretti

Acknowledgements

GOD: For the Gift of life

Ass Prof (Supervisor): Hester G O'Neill: I would like to give my devoted acknowledgement to my supervisor for giving me this opportunity to pursue this study under her supervision. Thank you for your support, encouragement and constructive criticism.

Prof Jacobus Albertyn (Co-supervisor): For your contribution to this work and giving helpful opinions

Prof A van Dijk: From the North West University for providing us with TAKARA bacteria expression pCOLD containing VP6 as positive control for VP6 expression

Prof J. Görgens: From Stellenbosch University for providing us with VP6 ORF codon optimised for *P. pastoris/P. angusta*

Mr MS Makatsa: For being the first post-graduate student to start with the project

Mr OS Folorunso: For providing the modified VP6 open reading frame optimised for *P. pastoris/P. angusta* construct (delATG_pKM177_POVP6).

Dr A Strydom: For assistance with purification protocol and transmission electron microscope

Centre of microscopy: Allowing us to use the transmission electron microscope

Department of Microbial, Biochemical and Food Biotechnology: For allowing me to pursue my MSc at the department

NRF and PRF (Funders): For financial support

Colleagues: For the constant support and laughter we shared

Mohailane and Malefu Rakaki (Parents): For your devoted support and loving me unconditionally

Puleng Dinoko (Sibling): For words of encouragement and devoted support

Family and Friends: For devoted support

Abstract

Rotavirus infection is one of the six leading causes of death among children under the age of five years. Globally it causes more than 215 000 deaths annually of which 65% occur in low- and/or middle-income countries. The two licenced live-attenuated vaccines (Rotarix™ and RotaTeq™) tend to have a lower efficacy in low- and/or middle-income countries. The lower efficacy of rotavirus live-attenuated vaccines could be due to maternal antibodies and oral polio vaccines interfering with rotavirus vaccine uptake. Rotavirus live-attenuated vaccines have been associated with reassortment with circulating genotype strains. As alternative, subunit vaccines such as viral proteins can be considered. Rotavirus VP6 protein is considered as a candidate for subunit vaccine development. Rotavirus VP6 antibodies are responsible for long lasting immunity and the antibodies against VP6 block the release of the viral mRNA. Previous studies showed rotavirus VP6 provide heterologous protection by a significant reduction of virus shedding in mice and gnotobiotic pigs.

Various recombinant yeasts were engineered by a previous MSc student, Mr M.S. Makatsa, using a unique yeast expression vector (pKM177). The recombinant yeasts contained an open reading frame (ORF) encoding rotavirus VP6 for the RVA/Human wt/ZAF/GR10924/1999/G9P[6] strain. The ORF was codon optimised to favour expression in *Arxula adenivorans* (AO), *Kluyveromyces lactis* (KO) and *Pichia pastoris/Pichia angusta* (PO). However, there was no expression of VP6 optimised for expression in *A. adenivorans* and *K. lactis* due to an additional out-of-frame ATG in the promoter region of the expression vector. In this study, the additional ATG was successfully removed by site-directed mutagenesis and the Kozak sequence was optimised to produce modified delATG_pKM177_AOVP6 and delATG_pKM177_KOVP6 constructs.

The modified delATG_pKM177_AOVP6, delATG_pKM177_KOVP6 as well as delATG_pKM177_POVP6, the modified plasmid containing the VP6 ORF codon optimised for expression in *P. pastoris/P. angusta* and obtained from a colleague, were transformed into 14 different yeast strains. Partial PCR amplification of the VP6 ORFs was conducted to screen for integration of the expression cassettes into the yeast genomes. *Debaryomyces hansenii* UFS0610 and *Yarrowia lipolytica* UFS2415 resulted in no colony formation. Integration into the *P. angusta* genome was efficient for all the VP6 optimised ORFs.

Integration of the VP6 ORFs in the *Y. lipolytica* PO 1F, UFS0097 and UFS2221 strains were relatively poor as only 16% of the clones screened showed integrated into the genome. The delATG_pKM177_AOVP6 and delATG_pKM177_POVP6 had 75-80% integration in the various yeast genomes, while delATG_pKM177_KOVP6 integration was relatively low at 46%. Expression of VP6 from all the ORFs was effective in *P. angusta* strains followed by *A.*

adenivorans strains from the UNESCO-MIRCEN yeast culture collection (*A. adenivorans* UFS1219 and *A. adenivorans* UFS1220), *S. cerevisiae* and *K. lactis*. High expression of VP6 in *P. angusta* and *P. pastoris* has been reported in previous studies. In this study, almost all *P. angusta* colonies screened, expressed VP6, while only 13% of *P. pastoris* colonies screened expressed VP6. There was relatively low expression of VP6 in *Y. lipolytica* strains as well as the prototype *A. adenivorans* strain, LS3.

Six yeasts were identified that successfully expressed rotavirus VP6. Rotavirus VP6 has a unique feature of assembling into oligomeric structures depending on the pH and ionic strength. Assembly of nanotubes or nanosphere have only been reported for VP6 produced by insect cells and *E. coli*, but not in yeast cells. A simple method was adapted to purify and allowed VP6 to assemble in oligomeric structures. Only VP6 produced in *A. adenivorans* UFS1219 was able to assemble in both nanotubes and nanospheres, while VP6 produced in *Y. lipolytica* only assembled in nanospheres. The recombinant *A. adenivorans* 1219 strain shows great potential as producer of a rotavirus subunit vaccine candidate.

Key word: Rotavirus VP6, Codon optimisation, Site-directed mutagenesis, Kozak, Subunit vaccine, Yeast expression, VP6 tubular formation.

Table of Contents

Acknowledgements	iv
Abstract	vi
Table of Figures	xii
List of Tables	xix
List of abbreviations:	xxi
Chapter 1:	1
Literature review - Overview of rotavirus capsid protein, VP6, as a candidate for vaccine development	1
1.1 Introduction	1
1.2 Genome organization and viral proteins	1
1.2.1 Structural proteins	2
1.2.2 Non-structural proteins	4
1.3 Classification	5
1.4 Epidemiology and Prevalence	7
1.5 Replication cycle	9
1.5.1 Virion attachment	10
1.5.2 Rotavirus cell penetration and uncoating	11
1.5.3 Transcription and translation of viral mRNA	11
1.5.4 Genome replication and core assembly	11
1.5.5 Outer-capsid assembly	12
1.5.6 Virion release from the infected cells	13
1.6 Pathogenesis	13
.....	14
1.7 Immunity following natural infection	14
1.7.1 Innate immunity	15
1.7.2 Acquired immunity	15
1.8 Vaccines	18
1.8.1 Live attenuated vaccines	18
1.8.1.1 RotaTeq®	18
1.8.1.2 Rotarix®	19
1.8.1.3 Other live-attenuated rotavirus vaccines	20
1.8.1.4 Impact of rotavirus vaccines	21
1.8.2 Inactivated vaccines	24
1.8.3 Sub-unit vaccines	24

1.9 Expression systems	26
1.10 Problem identification	28
1.11 Preliminary data.....	28
1.12 Aims and objectives	29
1.13 References	30
Chapter 2: Modification of the rotavirus VP6 open reading frame containing expression cassettes	47
2.1 Introduction	47
2.2 Materials and Method	48
2.2.1 General reagents, kits and enzymes.....	48
2.2.2 Virus stain, bacterial strains and culture cultivation	49
2.2.3 Recombinant constructs.....	49
2.2.4 General methods.....	50
2.2.4.1 Agarose gel electrophoresis.....	50
2.2.4.2 Bacteria Competent cells.....	50
2.2.4.3 Gel Purification of DNA fragments	51
2.2.4.4 Transformation of bacterial competent cells	51
2.2.4.5 Minilystate plasmid extraction	51
2.2.4.6 Restriction digest.....	52
2.2.4.7 Plasmid extraction of selected positive clones	52
2.2.4.8 DNA sequencing	53
2.2.5 Site directed mutagenesis.....	53
2.2.5.1 Polymerase chain reaction (PCR) amplification for site-directed mutagenesis	54
2.2.5.2 Dpn I digests, purification of PCR amplicon	54
2.2.5.3 Ligation and transformation of mutant PCR product	55
2.2.5.4 Screening for mutated transformants and confirmation with Sanger sequencing.	55
2.2.6 Cloning of VP6_KO into delATG_pKM177.....	55
2.2.6.1 Sub-cloning	56
2.3. Results	57
2.3.1 Manipulation of <i>A. adenivorans</i> optimised rotavirus VP6 ORF-containing expression cassette	57
2.3.2 Manipulation of <i>K. lactis</i> optimised rotavirus VP6 ORF containing expression cassette.....	60

2.4 Discussion.....	61
2.5 References	64
Chapter 3: Recombinant expression of Rotavirus VP6 in various yeasts	67
3.1 Introduction.....	67
3.2 Materials and methods	68
3.2.1 General chemicals, reagents and enzymes.....	68
3.2.2 Yeast strains and cultivation.....	68
3.2.3 Preparation of yeast competent cells.....	69
3.2.4 Yeast transformation.....	69
3.2.5 Evaluation of successful integration of the VP6 codon optimized ORFs into the yeast genomes	70
3.2.6 Expression of rotavirus VP6 in various yeasts.....	72
3.2.7 Bacterial expression of rotavirus VP6 as a positive control.....	72
3.2.8 Protein concentration determination.....	73
3.2.9 Sodium dodecyl sulphate polyacrylamide gel electrophoresis (SDS-PAGE)	73
3.2.10 Western Blot analysis	74
3.3 Results	75
3.3.1 Transformation of yeast strains with recombinant yeast expression plasmids.....	75
3.3.2 Integration of expression cassettes containing VP6 ORFs into the yeast genomes	76
3.3.2.1 Integration of the expression cassette containing VP6 ORF codon optimised for expression in <i>A. adenivorans</i> in various yeasts.....	76
3.3.2.2 Integration of the expression cassette containing VP6 ORF codon optimised for expression in <i>K. lactis</i> in various yeast stains.....	79
3.3.2.3 Integration of the expression cassette containing VP6 ORF codon optimised for expression in <i>P. pastoris/P. angusta</i> in various yeasts	83
3.3.3 Expression of rotavirus VP6 ORFs in various yeasts.....	88
3.3.3.1 Bacterial expression of VP6	88
3.3.3.2 Yeast expression of rotavirus VP6 encoded by the ORF codon optimised for expression in <i>A. adenivorans</i>	89
3.3.3.3 Yeast expression of rotavirus VP6 encoded by the ORF codon optimised for expression in <i>K. lactis</i>	91
3.3.3.4 Yeast expression of rotavirus VP6 encoded by the ORF codon optimised for expression in <i>P. angusta/P. pastoris</i>	94
3.4 Discussion.....	96
3.5 References	98

Chapter 4: Investigation into the oligomeric structure formation of rotavirus VP6 produced by various yeasts	101
4.1 Introduction.....	101
4.2 Materials and methods	102
4.2.1 Growth studies.....	102
4.2.2 Purification of VP6 produced in various yeasts	103
4.2.3 Preparations of oligomeric structures of rotavirus VP6 proteins produced in various yeasts.....	104
4.2.3.1 Nanotubes and nanospheres particles preparations.....	104
4.3 Results	105
4.3.1 Identification of optimum harvesting times for the various yeast strains	105
4.3.2 Purification of VP6 protein in various yeasts.....	107
4.3.3 Evaluation of VP6 nanotubes and nanospheres particles	114
4.4 Discussion.....	116
4.5 References	118
Chapter 5: Conclusions	120
5.1 References	123
Appendix A: Alignment of Sanger sequence result of delATG_pKM177_ AO VP6 with <i>in silico</i> clones using EMBOSS Needle Pairwise Sequence Alignment.	125
Appendix B: Alignment of Sanger sequence result of delATG_pKM177_ KO VP6 with <i>in silico</i> clones using EMBOSS Needle Pairwise Sequence Alignment.	127
Appendix C: Protein concentration	130
Appendix D: Integration of the expression cassette containing VP6 ORF codon optimised for <i>A. adenivorans</i>.	131
Appendix E: Integration of the expression cassette containing VP6 ORF codon optimised for <i>K. lactis</i> in various yeast stains	134
Appendix F: Integration of the expression cassette containing VP6 ORF codon optimised for <i>P. pastoris/P. angusta</i> in various yeast.	139
Appendix G: Yeast expression of rotavirus VP6 encoded by the ORF codon optimised for expression in <i>A. adenivorans</i>.	141
Appendix H: Yeast expression of rotavirus VP6 encoded by the ORF codon optimised for expression in <i>K. lactis</i>.	148
Appendix I: Yeast expression of rotavirus VP6 encoded by the ORF codon optimised for expression in <i>P. pastoris/P. angusta</i>	153
Appendix J: Western blot analysis of optimal times of harvest of VP6 protein in various yeasts	158
Appendix K: Purification of VP6 protein in <i>K. lactis</i>.	161

List of Figures

Chapter 1

	Page
Figure 1.1: The 11 viral dsRNA genome segments that encodes for 12 viral proteins, 6 structural and 6 non-structural proteins.	2
Figure 1.2: Viral capsid structure.	3
Figure 1.3: Estimated rotavirus deaths in 2013.	8
Figure 1.4: Schematic representation of rotavirus replication cycle.	10
Figure 1.5: Model of viral assembly	13
Figure 1.6: Induction of diarrhoea by NSP4	14
Figure 1.7: VP6 specific antibodies blocking the release of the viral mRNA	17
Figure 1.8: Diagram of the RotaTeq® vaccine reassortment.	19

Chapter 2

Figure 2.1: Western blot analysis of VP6 expression in <i>K. lactis</i>	48
Figure 2.2: Recombinant plasmid constructs.	50
Figure 2.3: <i>In silico</i> clone of pKM177_AOVP6.	57
Figure 2.4: Deletion-mutagenesis using PCR.	58

Figure 2.5:	Agarose gel analysis of the restriction enzyme screening of positive clones for delATG_pKM177_VP6 AO construct	59
Figure 2.6:	Sequencing chromatogram of AO VP6 ORF clones alignment with the <i>in silico</i> clone	60
Figure 2.7:	Agarose gel analysis of the restriction enzyme screening for positive clones of delATG_pKM177_VP6KO construct transformed into bacterial cells	61
Figure 2.8:	Analysis of sequence chromatogram of modified delATG_pKM177_AOVP6 and delATG_pKM177_KOVP6 aligned with <i>in silico</i> clones of the expected sequence using Geneious 6.1.2	62

Chapter 3

Figure 3.1:	Primer annealing to the AO VP6 ORF containing expression Cassette	76
Figure 3.2:	Analysis of the AO VP6 ORF containing expression cassette integration into the genome of <i>A. adenivorans</i> UFS1220 on a 1% agarose gel.	76
Figure 3.3:	Analysis of the AO VP6 ORF containing expression cassette Integration into the genome of <i>A. adenivorans</i> UFS1219 on a 1% agarose gel	77
Figure 3.4:	Analysis of the AO VP6 ORF containing expression cassette integration into the genome of <i>P. angusta</i> UFS0915 on a 1% agarose gel	77

Figure 3.5:	Analysis of the AO VP6 ORF containing expression cassette integration into the genome of <i>P. angusta</i> UFS1507 on a 1% agarose gel	78
Figure 3.6:	Analysis of the AO VP6 ORF containing expression cassette integration into the genome of <i>Y. lipolytica</i> PO 1F on a 1% agarose gel	78
Figure 3.7:	Primer annealing to the KO VP6 ORF containing expression cassette	80
Figure 3.8:	Analysis of the KO VP6 ORF containing expression cassette integration into the genome of <i>A. adenivorans</i> UFS1219 on a 1% agarose gel	80
Figure 3.9:	Analysis of the KO VP6 ORF containing expression cassette integration into the genome of <i>A. adenivorans</i> UFS1220 on a 1% agarose gel	80
Figure 3.10:	Analysis of the KO VP6 ORF containing expression cassette integration into the genome of <i>K. lactis</i> UFS1167 on a 1% agarose gel	81
Figure 3.11:	Analysis of the KO VP6 ORF containing expression cassette integration into the genome of <i>P. angusta</i> UFS0915 on a 1% agarose gel	81
Figure 3.12:	Analysis of the KO VP6 ORF containing expression cassette integration into the genome of <i>P. pastoris</i> GS115 on a 1% agarose gel	82

Figure 3.13:	Analysis of the KO VP6 ORF containing expression cassette integration into the genome of <i>Y. lipolytica</i> UFS0097 on a 1% agarose gel.	82
Figure 3.14:	Primer annealing to the PO VP6 ORF containing expression Cassette	84
Figure 3.15:	Analysis of the PO VP6 ORF containing expression cassette integration into the genome of <i>P. angusta</i> UFS0915 on a 1% agarose gel	85
Figure 3.16:	Analysis of the PO VP6 ORF containing expression cassette integration into the genome of <i>P. angusta</i> UFS1507 on a 1% agarose gel	85
Figure 3.17:	Analysis of the PO VP6 ORF containing expression cassette integration into the genome of <i>P. pastoris</i> GS115 on a 1% agarose gel	86
Figure 3.18:	Analysis of the PO VP6 ORF containing expression cassette integration into the genome of <i>P. pastoris</i> UFS1552T on a 1% agarose gel	86
Figure 3.19:	Analysis of the PO VP6 ORF containing expression cassette integration into the genome of <i>S. cerevisiae</i> CENPK on a 1% agarose gel	87
Figure 3.20:	Analysis of the PO VP6 ORF-containing expression cassette integration into the genome of <i>Y. lipolytica</i> PO 1F on a 1% agarose gel	87
Figure 3.21:	Western blot analysis of bacterial-expressed VP6 as positive	

	control	89
Figure 3.22:	Western blot analysis of rotavirus VP6 expression by <i>A. Adenivorans</i> UFS1220 colonies containing the AO VP6 ORF containing expression cassette	90
Figure 3.23:	Western blot analysis of rotavirus VP6 expression by <i>P. angusta</i> UFS0915 colonies containing the AO VP6 ORF-containing expression cassette	90
Figure 3.24:	Western blot analysis of rotavirus VP6 expression by <i>P. angusta</i> UFS1507 colonies containing the AO VP6 ORF-containing expression cassette	91
Figure 3.25:	Western blot analysis of rotavirus VP6 expression by <i>K. lactis</i> UFS1167 colonies containing the KO VP6 ORF containing Expression cassette	92
Figure 3.26:	Western blot analysis of rotavirus VP6 expression by <i>P. angusta</i> UFS0915 colonies containing the KO VP6 ORF containing expression cassette	92
Figure 3.27:	Western blot analysis of rotavirus VP6 expression by <i>P. angusta</i> UFS1507 colonies containing the KO VP6 ORF containing expression cassette	93
Figure 3.28:	Western blot analysis of rotavirus VP6 expression by <i>P. angusta</i> UFS1507 colonies containing the PO VP6 ORF containing expression cassette	94
Figure 3.29:	Western blot analysis of rotavirus VP6 expression by <i>P. angusta</i> UFS0915 colonies containing the PO VP6 ORF	

	containing expression cassette	95
Figure 3.30:	Western blot analysis of rotavirus VP6 expression by <i>S. cerevisiae</i> CENPK colonies containing the PO VP6 ORF containing expression cassette	95
Figure 3.31:	Western blot analysis of rotavirus VP6 expression by <i>Y. lipolytica</i> PO 1F colonies containing the PO VP6 ORF containing expression cassette	96
Chapter 4		
Figure 4.1:	Cryo-Electron microscopy images showing VP6 assembly in different pH environments	101
Figure 4.2:	Flow diagram illustrating VP6 purification and assembly of VP6 oligomeric structures	105
Figure 4.3:	Growth curves of the yeast expressing VP6 protein.	106
Figure 4.4:	SDS-PAGE analysis of sucrose gradient fractions obtained following ultracentrifugation of the VP6 produced <i>A. adenivorans</i> cell lysate	108
Figure 4.5:	Western blot analysis of purified VP6 protein in sucrose fractions 18-20	108
Figure 4.6:	SDS-PAGE analysis of sucrose gradient fractions obtained following ultracentrifugation of the VP6 produced <i>P. pastoris</i> cell lysate	109

Figure 4.7:	SDS-PAGE analysis of sucrose gradient fractions obtained following ultracentrifugation of the VP6 produced <i>Y. lipolytica</i> cell lysate	110
Figure 4.8:	Western blot analysis of purified VP6 protein in sucrose fractions 10-13	110
Figure 4.9:	SDS-PAGE analysis of sucrose gradient fractions obtained following ultracentrifugation of the VP6 produced <i>S. cerevisiae</i> cell lysate	111
Figure 4.10:	SDS-PAGE analysis of sucrose gradient fractions obtained following ultracentrifugation of the VP6 produced <i>P. angusta</i> cell lysate	112
Figure 4.11:	Western blot analysis of fractions obtained from sucrose gradient ultracentrifugation of VP6 produced <i>P. angusta</i> cell lysate	112
Figure 4.12:	Analysis of the integration of VP6 ORF in <i>K. lactis</i> using colony PCR on 1% agarose gel	113
Figure 4.13:	SDS-PAGE analysis of sucrose gradient fractions obtained following ultracentrifugation of the VP6 produced <i>K. lactis</i> cell lysate	114
Figure 4.14:	Transmission electron micrograph of rotavirus VP6 nanotubes structure produced in <i>A. adenivorans</i>	115
Figure 4.15:	Evaluation of rotavirus VP6 nanopsheres with TEM	115

List of Tables

Chapter 1

	Page
Table 1.1: Description of rotavirus non-structural proteins base on the human rotavirus Wa strain	4
Table 1.2: Description of rotavirus non-structural proteins base on the human rotavirus Wa strain	5
Table 1.3: Updated genotypes of all the 11 genome segments to date	7

Chapter 2

Table 2.1: Primers used to carry our site-directed mutagenesis for pKM177_AOVP6	54
Table 2.2: Primers used for Sanger sequence verification of positive clones of the pKM177_AO VP6 construct	55
Table 2.3: Primers used for Sanger sequence verification of positive clones of the pKM177_KO VP6 construct	57

Chapter 3

Table 3.1: Primers used for screening the integration of VP6 ORFs in various yeasts genome	71
Table 3.2: Colony formation by transformed yeasts	75
Table 3.3: Summary of the AO VP6 ORF containing expression cassette integration into the genomes of various yeast strains	79

Table 3.4:	Summary of the KO VP6 ORF containing expression cassette integration into the genomes of various yeast strains	83
Table 3.5:	Summary of the KO VP6 ORF containing expression cassette integration into the genomes of various yeast strains	88
Table 3.6:	Summary of rotavirus VP6 expression by yeast colonies containing AO VP6 ORF	91
Table 3.7:	Summary of rotavirus VP6 expression by yeast colonies containing KO VP6 ORF	93
Table 3.8:	Summary of rotavirus VP6 expression by yeast colonies containing PO VP6 ORF	96
Table 3.9:	Summary of the integration of the VP6 ORFs optimised for expression in different yeasts and expression of rotavirus VP6 in various yeasts	91

Chapter 4

Table 4.1:	Random selection of representative yeast colonies containing VP6 ORF for evaluation of growth studies, purification and evaluation of oligomeric structure formation	102
Table 4.2:	Optimal times of harvest of VP6 protein in various yeasts with their respective concentrations.	106

List of abbreviations:

ADRV: adult diarrhoea rotavirus

AGE: acute gastroenteritis

AGE: acute gastroenteritis

APS: ammonium persulfate

BCA: bicinchoninic acid

bp: base pair

Ca²⁺: calcium

CaCl₂: calcium chloride

DLP: double-layered particle

DMSO: dimethyl sulfoxide

DNA: deoxyribonucleic acid

dNTPs: deoxyribonucleotide triphosphate

DRC: Democratic Republic of Congo

dsRNA: double-stranded RNA

EDTA: ethylenediaminetetraacetate

EPI: Expanded Programme for Immunisation

ER: endoplasmic reticulum

FDA: Food and Drug Administration

g: gram

GAVI: Global Alliance for Vaccines and Immunisation

***hph*:** hygromycin B resistance gene

HPV: human papillomavirus

ICTV: International Committee on Taxonomy of Viruses

IFN: interferon

IgA: immunoglobulin A

IgG: immunoglobulin G

IPTG: isopropyl β -D-1-thiogalactopyranoside

IRFs: interferon-regulatory factors

kan^R: kanamycin resistance gene

Kb: kilobase

kmINUt: *K. marxianus inulinase* terminator

KOAc: potassium acetate

LB: Luria-Bertani

MA104: monkey kidney epithelial cells

MAVS: mitochondrial antiviral signalling

MgCl₂: magnesium chloride

MnCl₂: manganese(II) chloride

MOPS: N-morpholino propanesulfonic acid

NaOH: sodium hydroxide

NCDV: Nebraska Calf Diarrhea Virus

NF- κ B: nuclear factor kappa-light-chain-enhancer of activated B cells

ng: nanogram

NGS: next generation sequencing

NSP: non-structural protein

OD: optical density

OPV: oral poliovirus vaccine

ORF: open reading frame

P2: tetanus toxoid universal CD4+ T cell epitope

PABP: poly-A binding protein

PAMP: pathogen associated molecular patterns

PCR: polymerase chain reaction

PLC-IP3: phospholipase C–inositol 1,3,5-triphosphate

PNK: polynucleotide 5'-hydroxyl-kinase

PRRs: pathogen recognition receptors

RbCl₂: rubidium chloride

RCWG: Rotavirus Classification Working Group

rDNA: ribosomal DNA

RdRP: RNA-dependent RNA polymerase

RNA: ribonucleic acid

scTEFp: *S. cerevisiae* TEF promoter

SDS-PAGE: sodium dodecyl sulphate polyacrylamide gel electrophoresis

siRNA: small interfering ribonucleic acid

ssRNA: single-stranded ribonucleic acid

TAE: Tris- Acetate-EDTA

TBS: Tris-buffered saline

TE: Tris-EDTA

TEF: translation elongation factor

TEM: transmission electron microscope

TEMED: tetramethylethylenediamine

TGS: Tris-Glycine-SDS

TLP: triple-layered particle

UFS: University of the Free State

USA: United States of America

UV: ultraviolet

VAERS: Vaccine Adverse Event Reporting System

VH: heavy chain

VL: light chain

VLPs: virus-like particles

VP: viral protein

WC3: bovine rotavirus parent strain

WHO: World Health Organisation

yITEFp: *Y. lipolytica* TEF promoter

YM: yeast mold

YPD: yeast extract peptone dextrose agar

Chapter 1:

Literature review - Overview of rotavirus capsid protein, VP6, as a candidate for vaccine development

1.1 Introduction

Rotavirus infection causes severe diarrhoea among infants and young children. Rotavirus is one of the six leading causes of diarrhoea among children younger than five years of age. It causes more than 215 000 deaths annually, mostly in low- and middle-income countries (Tate *et al.*, 2016b). Rotavirus infects the small intestine and the mode of transmission is through the faecal-oral route (Estes & Greenberg, 2013). Symptoms are mainly characterised by early onset of vomiting with watery diarrhoea for four to eight days, and low-grade fever (Osonuga *et al.*, 2013). Rotavirus was first described in 1973 by Bishop and co-workers. They studied duodenal biopsies from children with acute gastroenteritis using an electron microscope and observed viral particles with a wheel-like structure in the cytoplasm of mature epithelial cells originating from the lining of the duodenal villi and in faeces (Bishop *et al.*, 1973). Rotavirus was named after its wheel-like structure (rota = Latin for wheel).

Rotavirus belongs to the *Reoviridae* family and genus of Rotavirus. Rotavirus genome has a size of approximately 18 500 bp and consists of 11 double-stranded RNA (dsRNA) genome segments which encode six structural and six non-structural proteins. These genome segments are enclosed within the viral capsid proteins which are composed of an outer layer, an intermediate layer and an inner core layer (Trask *et al.*, 2012a), forming a triple-layered particle (TLP).

1.2 Genome organisation and viral proteins

The 11 genome segments encode for 12 viral proteins: six structural viral proteins (VPs) and six non-structural proteins (NSPs) (Figure 1.1). The structural or capsid proteins VP1, VP2, VP3, VP4, VP6 and VP7 form the triple-layered particle (Table 1.1). The non-structural proteins, NSP1, NSP2, NSP3, NSP4, NSP4 and NSP5 mainly function in the replication of the virus, pathogenesis and are only produced when the virus infects cells (Ramig, 2004) (Table 1.2).

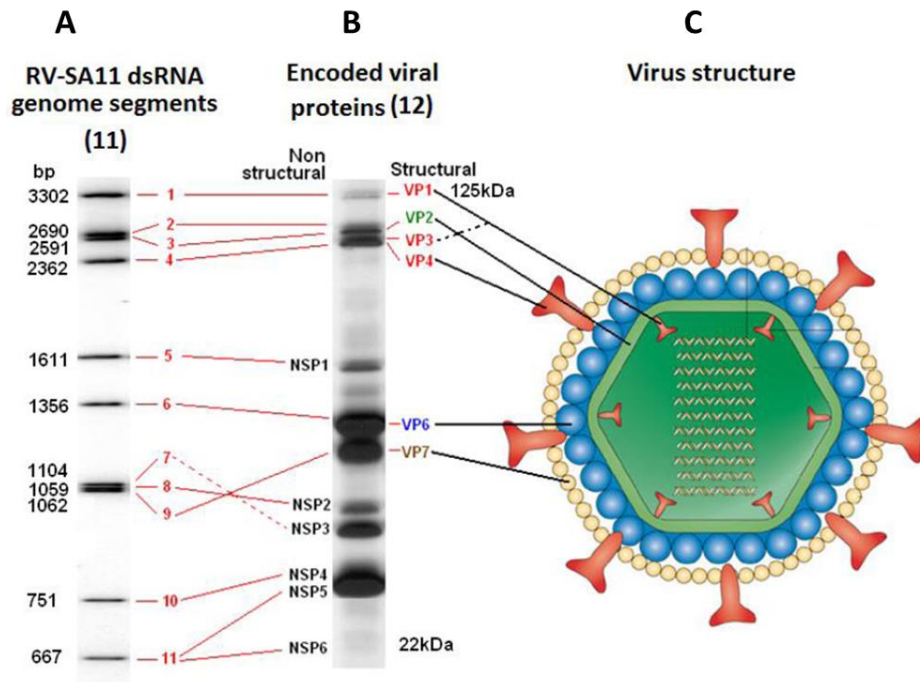


Figure 1.1: A, The 11 viral dsRNA genome segments that encodes for 12 viral proteins, 6 structural and 6 non-structural proteins. A, Separation of 11 dsRNA segments of the prototype strain SA11 by means of polyacrylamide gel (PAGE). Genome segment sizes range from 3302 to 667 bp. B & C, The VP4 spike protein (red) is attached to the intermediate protein VP6 (blue) and the outer protein VP7 (yellow) stabilize the spike proteins to VP6. The inner protein VP2 (green) forms a complex with VP1 (polymerase) and VP3 (capping enzyme), to form the viral polymerase complex. (Copied from Ramig, 2007).

1.2.1 Structural proteins

The six structural proteins have distinct functions, but interact with each other to keep the virus intact (Table 1.1). The 60 VP4 spike proteins are thought to protrude through the VP7 layers bound to the VP6 protein (Settembre *et al.*, 2010) and interact with host receptors upon entry. The inner viral protein, VP2, is surrounded by the VP6 protein forming the double-layered particle (DLP). The DLP is covered by the outer capsid protein, VP7, which is a glycoprotein (Figure 1.2a) and it appears to lock the VP4 spikes onto the virion (Settembre *et al.*, 2010). The stability of VP7 is dependent on the calcium ions bound on the trimmers (Aoki *et al.*, 2010). The inner capsid protein, VP2, forms little knobs in a 5-fold symmetry (McClain *et al.*, 2010) where 11 genome segments are enclosed in the inner capsid protein. The VP2 is thought to be a scaffold by interacting with the viral polymerase complex (McClain *et al.*, 2010). The viral polymerase complex is composed of the viral capping enzyme, VP3 and RNA-dependent RNA polymerase (RdRP), VP1 (Figure 1.2b).

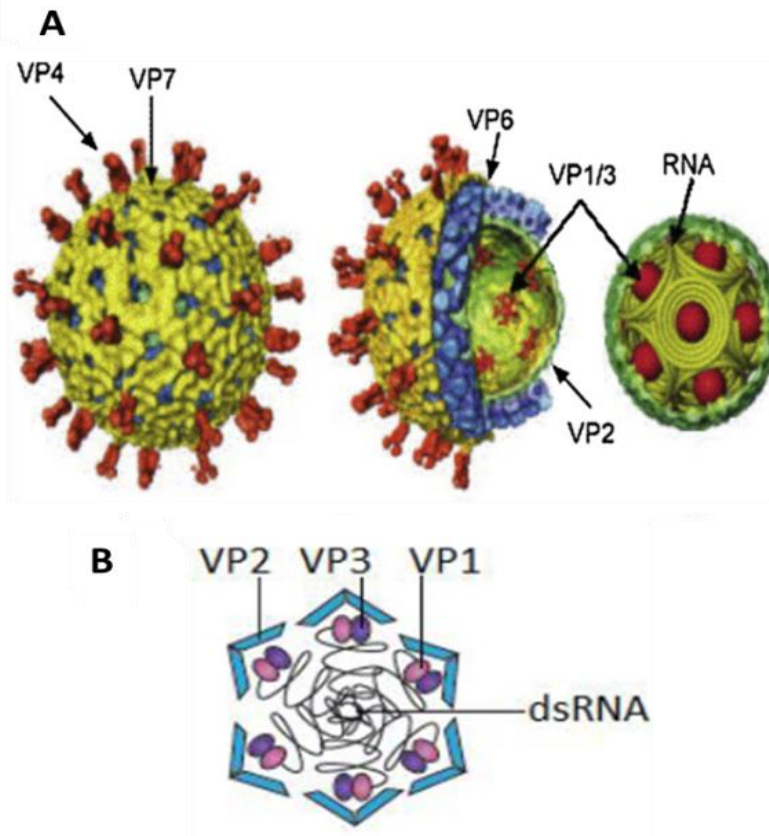


Figure 1.2: Viral capsid structure. A, Illustrates the capsid proteins with inner layer VP2 (green) (102 kDa) and middle-layer VP6 (blue) (45 kDa) which forms the double-layer particle (DLP). The DLP is covered by VP7 (yellow) (37kDa) and the viral protein spikes of VP4 (red) (87 kDa) forming a triple-layer particle (TLP) (copied from Desselberger *et al.*, 2009). B: Shows the viral polymerase complex consisting of the viral RNA-dependent RNA polymerase (VP1) (pink) and RNA capping enzyme (VP3) (purple). These proteins are attached to the inner surface of the VP2 (blue) as VP2 acts as a scaffolding protein (copied from Jayaram *et al.*, 2004 and Trask *et al.*, 2012a).

Table 1.1: Description of rotavirus structural proteins based on the human rotavirus Wa strain

Structural proteins	Viral segment	Length (bp)	Molecular weight (kDa)	Functions
VP1	1	3302	125	VP1 functions as an RNA-dependent RNA polymerase and occurs within the DLP. It also has an ssRNA binding domain and is responsible for the transcription of rotavirus positive-sense RNAs from the negative-sense RNA (Lawton <i>et al.</i> , 1997).
VP2	2	2717	102	VP2 binds to ssRNA and dsRNA and encloses the viral polymerase complex (McDonald & Patton, 2011). VP2 initiate genome replication through interaction with VP1 (Patton <i>et al.</i> , 1997).
VP3	3	2591	98	VP3 functions as the RNA capping and methylation enzyme and responsible for minus-strand synthesis (Chen <i>et al.</i> , 1999; Pizarro <i>et al.</i> , 1991).
VP4	4	2360	88	VP4 function in interacting with host receptors during infection (Trask <i>et al.</i> , 2012a). The hemagglutination domain lies on VP8* (Fuentes-Pananá <i>et al.</i> , 1995).
VP8*/VP5*	4		VP8*= 27 VP5*= 60	Production VP8* and VP5* is due to proteolytic cleavage by VP4 during infection (Settembre <i>et al.</i> , 2010). VP5* is responsible for the permeability of the virus (Denisova <i>et al.</i> , 1999) while VP8* interacts with host receptor upon entry.
VP6	6	1356	45	VP6 is the major antigen target for detection of rotavirus groups. VP6 functions as an anchor for VP4 and VP7 (Trask <i>et al.</i> , 2012a).
VP7	9	1062	37	VP7 is a glycoprotein and it locks the VP6 into the viron (Settembre <i>et al.</i> , 2010).

1.2.2 Non-structural proteins

The non-structural proteins (NSPs) are only produced once the virus enters the host cell to function in the replication of the virus (Hu *et al.*, 2012; Trask *et al.*, 2012b) (Table 1.2). The NSPs are also responsible for antagonizing the antiviral host response (Barro & Patton, 2007). The NSPs have the ability to use the host machinery during translation and are responsible for the formation of inclusion bodies known as viroplasm where rotavirus replication occurs (Fabbretti *et al.*, 1999; Keryer-Bibens *et al.*, 2009).

Table 1.2: Description of rotavirus non-structural proteins based on the human rotavirus Wa strain

Non-structural proteins	Viral segment	Length (bp)	Size (kDa)	Functions
NSP1	5	1567	58	NSP1 suppresses the host antiviral response that results in antagonising the function of interferon regulatory factors IRF3, IRF5, and IRF7 (Barro & Patton, 2005, 2007).
NSP2	7	1059	37	NSP2 interacts with NSP5 to form viroplasm (Fabbretti <i>et al.</i> , 1999) where replication occurs. NSP2 also interact VP2 and VP1 during replication (Patton <i>et al.</i> , 2006).
NSP3	8	1059	36	NSP3 is responsible for the translation of viral mRNAs and suppresses the host protein synthesis by having a high affinity with the poly A binding protein (PABP) (Keryer-Bibens <i>et al.</i> , 2009; Piron <i>et al.</i> , 1998a; Poncet <i>et al.</i> , 1993).
NSP4	10	750	20	NSP4 acts as the viral enterotoxin (Ball <i>et al.</i> , 1996) and function in the assembling of DLPs synthesized through the ER from the viroplasm.
NSP5/6	11	664	NSP5: 21 NSP6: 12	NSP5 associates with NSP2 to form viroplasm. NSP5 also regulates NSP2-RNA interactions during genome replication (Jiang <i>et al.</i> , 2006). NSP6 has sequence independent nucleic acid binding properties. NSP6 interacts with NSP5 which is also localized in the viroplasm (Rainsford & McCrae, 2007; Torres-Vega <i>et al.</i> , 2000).

1.3 Classification

Rotavirus belongs to the subfamily of *Sedoreovirinae* and is classified under the family of *Reoviridae* along with orthoreovirus, orbivirus, coltivirus, aquareovirus, oryzavirus, Cypovirus, Fijivirus, Mycoreovirus, phytoreovirus and Seadornavirus (King *et al.*, 2012) .

Based on the antigenic properties of VP6, rotavirus is classified into eight groups (A-H) recognized by International Committee on Taxonomy of Viruses (ICTV) (Matthijnssens *et al.*, 2012). In the recent Rotavirus Classification Working Group (RCWG) meeting, an additional group was proposed, group I, which was discovered in Hungarian sheltered dogs but has not yet been accepted by ICTV (Matthijnssens & Theuns, 2015). Groups A, B, C and H are commonly seen in mammals. Group A is most common in infants, young children and young animals. Furthermore, Group A have also recently been identified in bats located in Africa

and China (Esona *et al.*, 2010; He *et al.*, 2017; Xia *et al.*, 2014; Yinda *et al.*, 2016). In addition, Group A has also been detected in avian species (Ito *et al.*, 2001; Trojnar *et al.*, 2009, 2013). Groups D, F, and G rotaviruses have been detected only in avian species, while group E has been identified in porcine (Pedley *et al.*, 1983; Trojnar *et al.*, 2009, 2010). Group H, previously known as adult diarrhoea rotavirus (ADRV), is found in human adults (Hung *et al.*, 1983; Matthijssens *et al.*, 2011). In addition, Group H has also been identified in porcine (Marthaler *et al.*, 2014; Nyaga *et al.*, 2016).

Group A is the most important of the groups infecting humans and also the best studied. Group A is further classified into G genotypes (glycoprotein VP7) and P genotypes (protease sensitive protein VP4) (Matthijssens & Van Ranst, 2012). In 2008, Matthijssens and co-workers proposed a new classification system based on all 11 genome segments. The nomenclature is as follows: Gx-P[x]-Ix-Rx-Cx-Mx-Ax-Nx-Tx-Ex-Hx (where x represents numbers of the corresponding genotypes) representing VP7, VP4, VP6, VP1, VP2, VP3, NSP1, NSP2, NSP3, NSP4, and NSP5 encoding genome segments (Matthijssens *et al.*, 2008a). The capital letters in the genotype were derived from the function associated with the protein encoded by the genome segment i.e., **G**lycoprotein (VP7), **P**rotease-sensitive (VP4), **I**nter capsid (VP6), **R**NA-dependent RNA polymerase (VP1), **C**ore protein (VP2) and **M**ethyltransferase (VP3). This annotation also applies to the NSPs for instance: **I**nterferon antagonist (NSP1), **N**TPase (NSP2), **T**ranslation enhancer (NSP3), **E**nterotoxin (NSP4) and **P**hosphoprotein (NSP5) (Matthijssens *et al.*, 2008a). The RCWG proposed guidelines for the nomenclature of individual strains are based on: (A) wild-type RV strains, (B) tissue culture-adapted rotavirus strains or rotavirus strains passaged *in vivo* in their homologous host species, (C) generated in a laboratory for which a host species can be assigned unambiguously, (D) generated in a laboratory for which a host species cannot be assigned unambiguously and (E) vaccine strains (Matthijssens & Van Ranst, 2012). The P genotype is annotated by an Arabic number between square brackets (P1A[8]: serotype 1A, genotype 8 (Matthijssens *et al.*, 2008a)

To date 288 genotypes for all the 11 genome segments of rotavirus A have been described, with 35 G genotypes and 50 P genotypes (Table 1.3) (<https://rega.kuleuven.be/cev/viralmetagenomics/virus-classification/rcwg>).

Table 1.3: Updated genotypes of all the 11 genome segments to date.
<https://rega.kuleuven.be/cev/viralmetagénomics/virus-classification/rcwg>.

Protein	Genotype	Total No. of genotypes
VP7	G	35
VP4	P	50
VP6	I	26
VP1	R	21
VP2	C	19
VP3	M	19
NSP1	A	30
NSP2	N	20
NSP3	T	21
NSP4	E	26
NSP5	H	21
TOTAL:		288

The human reference strains include the Wa, DS-1 and AU-1 strains (Matthijnssens *et al.*, 2008b). The occurrence of interspecies reassortment between human and animal strains has been shown using molecular evidence like RNA–RNA hybridization (Matthijnssens *et al.*, 2008b) and next generation sequencing (NGS) (Dennis *et al.*, 2014; Jamnikar-Ciglenecki *et al.*, 2017; Komoto *et al.*, 2016). Data analysis of whole genome sequencing reported in 2008 by Matthijnssens and co-workers indicated that DS-1-like strains are descendant from bovine rotaviruses, while Wa-like strains share a common ancestor with porcine rotaviruses.

1.4 Epidemiology and Prevalence

From 2000 - 2013 annual rotavirus deaths for children under the age of 5 years were estimated at approximately 215 000 (Tate *et al.*, 2016b). Low- and middle-income countries in Asia and sub-Saharan Africa have the highest death rates (Figure 1.3a). India has the highest death rate of 22% compared to other countries shown in Figure 1.3B (Tate *et al.*, 2016b). Four countries, India, Nigeria, Pakistan and DRC account for approximately half (49%) of the global estimated deaths (Tate *et al.*, 2016b). Figure 1.3B indicates the top 10 counties (Afghanistan, Pakistan, India, Nigeria, Democratic Republic of Congo (DRC), Angola, Ethiopia, Chad, Niger, and Kenya) with the highest number of deaths. These deaths occur mostly in low- and/or middle-income countries which accounts for more than (65%) half death rates compared to other countries worldwide (Tate *et al.*, 2016b).

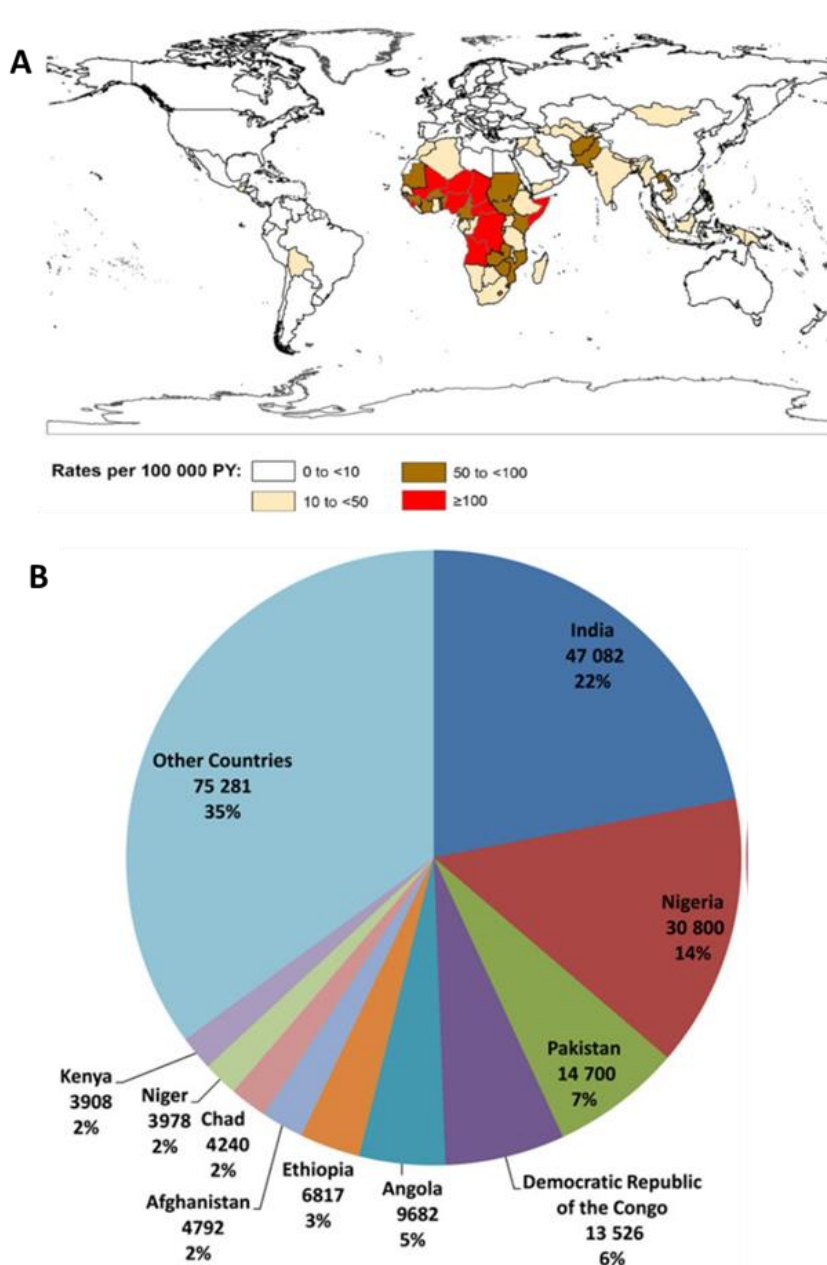


Figure 1.3: Estimated rotavirus deaths in 2013. A, Geographical map showing death rates worldwide that indicates the high mortality in Africa and Asia. The majority (56%) of rotavirus deaths were in countries of sub-Saharan Africa. B, Chart illustrating the top 10 countries with a high number of deaths. India has the highest mortality rate (22%) followed by Nigeria (14%), Pakistan (7%), DRC (6%), Angola (5%), Ethiopia (3%), Afghanistan (2%), Chad (2%), Niger (2%), and Kenya (2%) (copied from Tate *et al.*, 2016b).

Globally, at least 90% of G-genotypes namely G1-G4, G9 and G12 are circulating strains. Predominant P-genotypes consist of P[8] and P[4] (Delogu *et al.*, 2015; Esona & Gautam, 2015; Santos & Hoshino, 2005). The G and P genotype combinations G1P[8], G2P[4], G3P[8], G4P[8], G9P[8] and G12P[8] are the most predominant strains globally (Bányai *et al.*, 2012; Delogu *et al.*, 2015; Matthijnsens & Van Ranst, 2012).

Globally predominant genotypes are G1 – G4, G9 and G12 with association with P[4], P[6] or P[8] (Bányai *et al.*, 2012; Esona & Gautam, 2015; Santos & Hoshino, 2005). In Africa G1 is the most predominant (28.8%) genotype, followed by G9 (17.3%), G2 (16.8%), G8 (8.2%), G12 (6.2%) and G3 (5.9%) (Seheri *et al.*, 2014). The P[8] is the most predominant P genotype globally which is also seen as the most predominant genotype in Africa (40.6%). This is followed by P[6] (30.9%) and P[4] (13.9%) in Africa (Seheri *et al.*, 2014). The top G/P combinations in Africa are G1P[8] (18.4%), G9P[8] (11.7%), G2P[4] (8.6%), G2P[6] (6.2%), G1P[6] (4.9%), G8P[4] (4.5%), G3P[6] (4.3%), G8P[6] (3.8%) and G12P[8] (3.1%) (João *et al.*, 2018; Seheri *et al.*, 2014). The predominance of the unusual strain, G9P[4], has been reported in countries like Mexico, Guatemala, Bangladesh, Honduras and recently in India (Chitambar *et al.*, 2014; Quaye *et al.*, 2013). There are other rare strains that are emerging like G5P[8] in Brazil and G9P[6] in India. In Africa the G6 genotype has become a predominate genotype in countries like Kenya, Zimbabwe, Zambia and Cameroon which are considered as unusual as a result of zoonotic transmission (Seheri *et al.*, 2014). From Burkina Faso it has been reported that the unusual G6P[6] is the second most predominant strain (Nordgren *et al.*, 2012). Animal-human reassortment strains including G8P[14], G6P[6], G4P[6], G9P[14] and G10P[6] have been reported from African countries like Mauritius, Tanzania, Guinea Bissau, Senegal, Kenya and Nigeria (Seheri *et al.*, 2014).

1.5 Replication cycle

Most studies on the replication cycle have been done using Caco-2 cells as Caco-2 cells are a good cell culture model of human intestinal cells (Cuadras *et al.*, 2002). The viral replication cycle occurs in the mature epithelial cells of the small intestine near the tips of the villus.

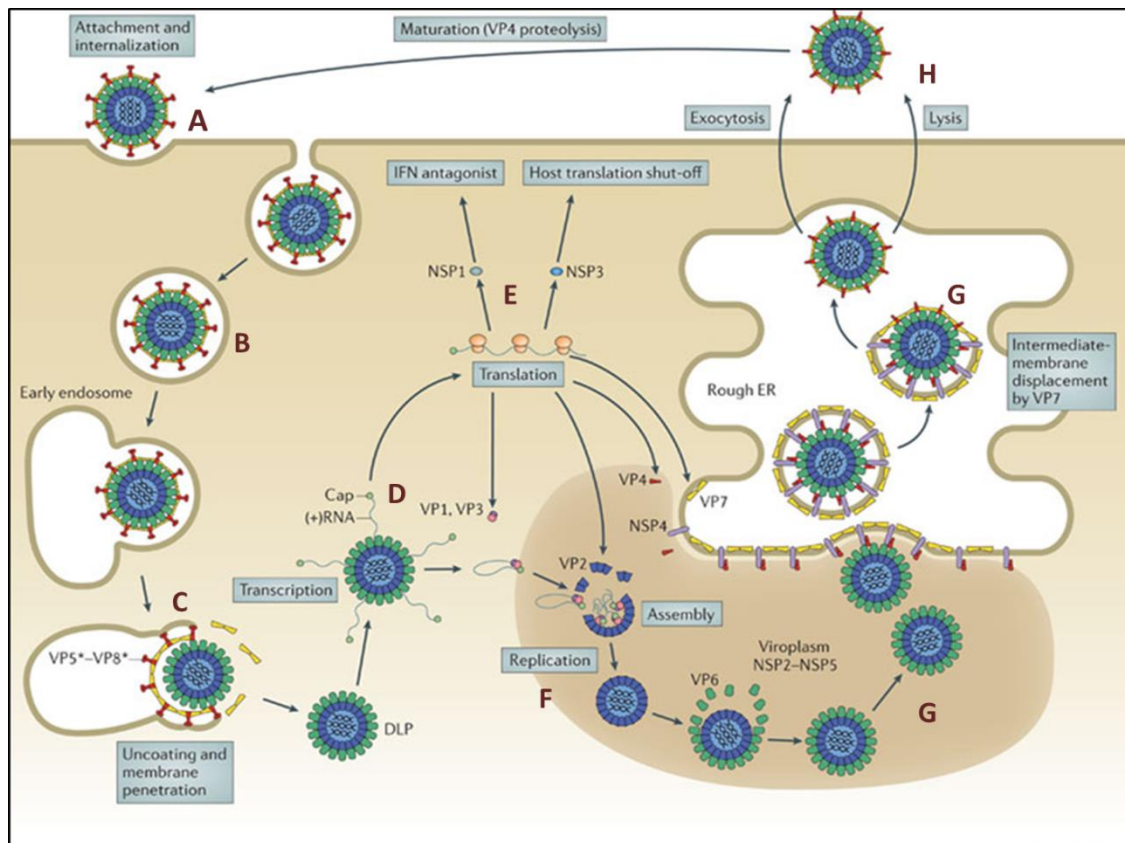


Figure 1.4: Schematic representation of rotavirus replication cycle. The spike proteins initiate (A) the attachment to host cell receptors initiated by VP4 spike proteins; (B) penetration of the virus to the host cytoplasm; (C) uncoating where the outer capsid proteins VP4 and VP7 are removed from the particle in the cytoplasm releasing the DLP; (D) transcription occurs when the DLP is transcriptionally active and the mRNA are released; (E), translation occurs and the 6 structural and 6 non-structural proteins are produced; (F) replication of the viral nucleic acid which occurs in viroplasm; (G) assembly of the virion where the DLP is assembled in the viroplasm and the outer capsid proteins in the ER membrane; (H) release of virions by cell lysis (adapted from Trask *et al.*, 2012b).

The spike proteins initiate the attachment (Figure 1.4A) to host cell receptors. This is followed by penetration (B), uncoating (C), transcription (D), translation (E), replication of the viral nucleic acid (F), assembly of viral components (G), and finally release of virions by cell lysis (H). The replication cycle is summarised in Figure 1.4.

1.5.1 Virion attachment

The attachment (Figure 1.4A) is mediated by the 60 spike proteins to the cellular receptors which contain sialic acid (SA) and cellular glycans such as histo-blood group antigens (Dormitzer *et al.*, 2002b; Hu *et al.*, 2012b; Stencel-baerenwald *et al.*, 2014). To be fully infectious, VP4 spike proteins are proteolytically cleaved into two fragments, VP8* and VP5*, by trypsin-like proteases in the intestinal lumen (Estes *et al.*, 1981; Trask *et al.*, 2012b). Experiments using MA104 cells showed that the VP8* domain is responsible for attachment

since VP8* is positioned at the tip of the cleaved spike (Fiore *et al.*, 1991). A shallow groove of the VP8* surface interacts with the SAs on the cellular glycans (Dormitzer *et al.*, 2002b).

1.5.2 Rotavirus cell penetration and uncoating

The penetration (Figure 1.4B) of rotavirus is mediated by the outer capsid protein, VP7, and VP5*. Penetration is due to the hydrophobic loops in VP5* being exposed, a phenomenon that occurs in many viral membrane fusion proteins during entry (Settembre *et al.*, 2010). Due to the low concentrations of calcium (Ca^{2+}) in the cytoplasm of the host cell, solubilisation of the outer layer proteins, VP7, is promoted and yields the DLP (Figure 1.4C).

1.5.3 Transcription and translation of viral mRNA

The DLP yielded after uncoating of the outer capsid proteins, is transcriptionally active. As mentioned before, rotavirus has its own polymerase complex which produce nascent (+) RNAs through the VP2-VP6 channel I (Lawton *et al.*, 1997) using the minus strands of dsRNAs as templates (Silvestri *et al.*, 2004). The 11 (+) sense RNAs released are capped at the 5' end by the capping enzyme, VP3, and instead of having a poly-A tail at the 3' end (Lawton *et al.*, 1997; Silvestri *et al.*, 2004) it has a consensus sequence (UGACC) which is conserved in all the 11 viral genome segments (Hu *et al.*, 2012a) (Figure 1.4D). The nascent (+) sense RNAs act as mRNA templates for protein synthesis and genome replication. The capped mRNAs accumulate in the cytosol where most of the structural and non-structural proteins are synthesised by the host ribozymes (Figure 1.4E). NSP3 plays an important role in the translation of the viral mRNAs. The N-terminal domain of NSP3 binds to the 3' consensus sequence (Deo *et al.*, 2002), while the C-terminal domain of NSP3 interacts with eIF4G (Groft & Burley, 2002). It has been seen that NSP3 has a higher affinity with eIF4G than the poly-A binding protein (PABP) (Piron *et al.*, 1998). The interaction of the NSP3 with eIF4G results in the circularisation of the viral mRNA which is important for efficient translation by host ribosomes (Groft & Burley, 2002).

1.5.4 Genome replication and core assembly

Viral replication is hosted by an inclusion body known as the viroplasm and is formed through the association of various viral proteins including NSP2 and NSP5 (Figure 1.4F). In the viroplasms, it is thought that the polymerase complex is assembled and the (+) sense RNAs are selectively packaged into assembling VP2 cores which may be modulated by NSP2 (Berois *et al.*, 2003; Vende *et al.*, 2003). The (+) sense RNAs are replicated by VP1 into the dsRNA genome as shown previously with immunofluorescence analysis of bromouridine (BrU)-labeled RNA in infected cells. This study provided evidence that plus-strand RNAs are synthesized within viroplasms and that the assembly of DLPs also occur within viroplasms (Silvestri *et al.*, 2004). Using a gel mobility shift assay, it was shown that

the polymerase enzyme (VP1) binds to the 3' end of the (+) sense viral RNA indicating an enzyme-RNA complex (Patton, 1996). For the formation of the DLP, VP2 may compete with other viral proteins. The DLP assembly occurs in the viroplasm, NSP5 interacts with VP2 which modulates the assembly of VP6 onto the core shell (Berois *et al.*, 2003) (Figure 1.4G).

1.5.5 Outer-capsid assembly

It is not fully understood how the outer-capsid assembly is carried out but it is thought to occur in the endoplasmic reticulum (ER) where NSP4 is a key regulator. The NSP4 is an integral protein embedded in the ER membrane (Trask *et al.*, 2012b). Even though it is not clear how the DLP must exit the viroplasm, the NSP4 may recruit the DLP into the outer-capsid assembly pathway (Trask *et al.*, 2012b). The VP4 spike proteins and the VP7 glycoprotein are embedded in the ER membrane (Figure 1.5). The NSP4 is composed of three domains, H1, H2 and H3 (Bergmann *et al.*, 1989). The H1 domain of the NSP4 is glycosylated and is oriented to the luminal side of the ER (Bergmann *et al.*, 1989) while H2 has a longest hydrophobic domain which is anchored in the bi-layer of the ER. The H3 domain is thought to be responsible for transport of the DLP into the ER membrane by acting as an intracellular receptor (Taylor *et al.*, 1993). NSP4 tetramers result in ER membrane deformation and budding of the DLP–VP4–NSP4 complex into the ER (Figure 1.5). The VP4 assembles first onto the DLP then the ER membrane is removed and VP7 assembles onto the particle, thereby locking VP4 into place forming the TLP (Trask *et al.*, 2012b). NSP4 is critical for viral maturation. Silvestri and co-workers showed that blockage of NSP4 expression by siRNA leads to RV particle maturation defects (Silvestri *et al.*, 2005).

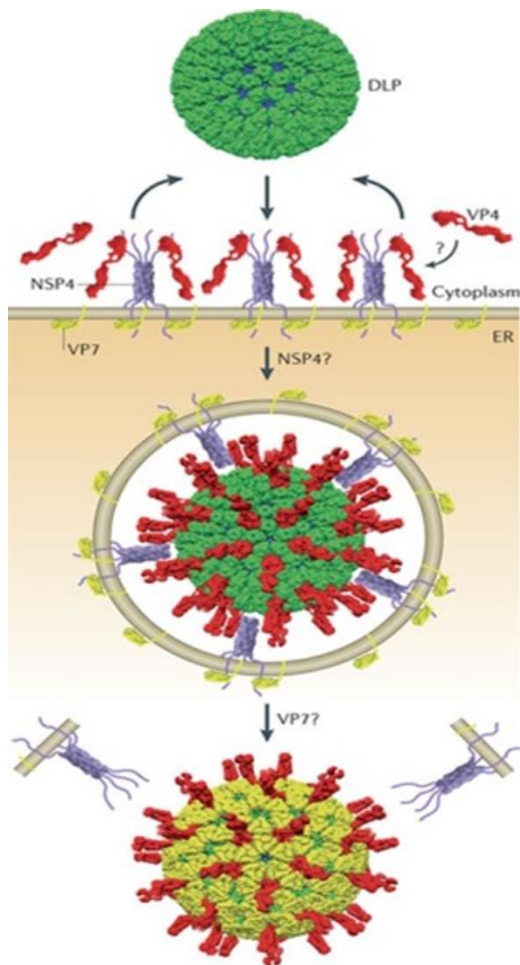


Figure 1.5: Model of viral assembly. NSP4 is thought to play a key role in the formation of triple layer particle assembly which occurs in the ER. NSP4 tetramers (blue triple helical protein) result in ER membrane deformation and budding of the DLP–VP4–NSP4 complex into the ER which recruits the DLP to the ER membrane. The VP4 spike proteins (red spikes) and the VP7 glycoprotein (yellow) are embedded in the ER. (copied from Trask *et al.*, 2012b)

1.5.6 Virion release from the infected cells

Virus release remains unclear, however work done in monkey kidney epithelial cells (MA104) showed that viral release occurs by host cell lysis, while a kind of budding process occur in Caco-2 cells that does not immediately kill the cell (Breton *et al.*, 2006).

1.6 Pathogenesis

Rotavirus infects the mature enterocytes villus of the small intestine (Figure 1.6). Villus enterocytes are arranged in finger-like projections in the walls of the small intestines and function in absorption of nutrients (Figure 1.6). Rotavirus alters the function of the small intestine which then leads to diarrhoea (Ramig, 2004). NSP4 has multiple functions and play an important role in the pathogenesis of rotavirus. It acts as an enterotoxin which induces

diarrhoea. There are certain peptides of the NSP4 that have been shown to be toxic when infected in mice (Ball *et al.*, 1996; Zhang *et al.*, 2000). These residues are responsible for the secretion of chloride through the calcium-dependent signalling pathway (Ball *et al.*, 1996). This causes an increase in the calcium $[Ca^{2+}]_i$ from the intracellular store (Zhang *et al.*, 2000) as illustrated in Figure 1.6. Infection leads to the increase in the plasma membrane permeability where there is an increase in sodium and decrease in potassium that results in a loss of fluids (Ramig, 2004). Furthermore, NSP4 binds to specific receptors which triggers the phospholipase C–inositol 1,3,5-triphosphate (PLC-IP3) cascade resulting in the release of Ca^{2+} (Dong *et al.*, 1997; Ramig, 2004). There are proteins expressed on the apical surface (disaccharidase, peptidase, etc.) that are absorbed by enterocytes and are affected by infection of rotavirus. Infection of rotavirus may lead to diarrhoea as a result of a decrease in intestinal absorption of sodium, glucose and water.

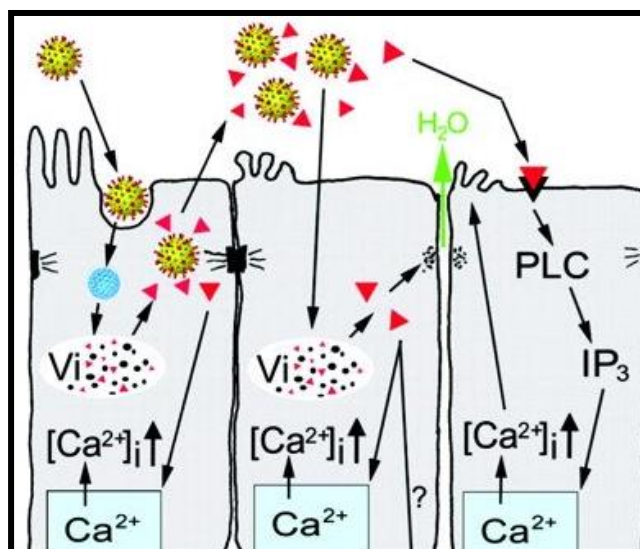


Figure 1.6: Induction of diarrhoea by NSP4: The released NSP4 protein (red triangles) mediates the release of Ca^{2+} (blue squares) from the internal stores. The tight junctions are disrupted by NSP4 which causes the flow of water (green arrow). The Ca^{2+} can also be released by binding to specific cellular receptors which triggers a signalling cascade through phospholipase C–inositol 1,3,5-triphosphate (PLC-IP3). Copied from Ramiq 2014.

1.7 Immunity following natural infection

There are many factors that play a role in rotavirus immunology causing rotavirus infection to elicit acquired and innate immune responses (Desselberger & Huppertz, 2011). The mechanism of the rotavirus immunity is, however, not fully understood.

1.7.1 Innate immunity

The innate immune response is regarded as the first protection against foreign antigens and also activates the adaptive immune response. Cytokines are involved in autocrine signalling and secretion of cytokines belonging to the interferon (IFN) family (Randall *et al.*, 2008; Takeuchi & Akira, 2010). The interferon-regulatory factors (IRFs) are essential regulators of the activation of immune cells resulting in the recognition of a virus within infected cells. There is therefore activation of the host pathogen associated molecular patterns (PAMP) (Randall *et al.*, 2008). The PAMP is recognised by the pathogen recognition receptors (PRRs) such as MDA5 caused by a viral infection which triggers the formation of the host immune regulatory proteins (Yoneyama & Fujita, 2009). When the PRRs interacts with the ssRNA/dsRNA genome of the virus, the production of IRF3/7 and nuclear factor kappa-light-chain-enhancer of activated B cells (NF- κ B) is activated through the mitochondrial antiviral signalling (MAVS) (Seth *et al.*, 2005).

NSP1 plays an important role in antagonising the innate immune system. The viral non-structural protein inhibits the expression of type I interferon by antagonising the function of interferon regulatory factors of IRF3, IRF5, and IRF7 (Barro & Patton, 2005, 2007; Graff *et al.*, 2002). NSP1 also plays a role in the degradation of the mitochondrial antiviral signalling (MAVS) protein (Nandi *et al.*, 2014).

1.7.2 Acquired immunity

Also known as humoral immune response, acquired immunity is responsible for the production of IgA and IgG antibodies (Desselberger & Huppertz, 2011; Hjelt *et al.*, 1985). IgA plays an important role in the protection against rotavirus infection, because IgA occurs predominate in the mucosal surfaces such as the gastrointestinal, respiratory, and genitourinary tracts. Rotavirus infection occurs in the gastrointestinal tract (Blutt & Conner, 2013). Serum anti-rotavirus IgA antibody seem to have better protection than serum IgG antibody (Velazquez *et al.*, 2000).

Primary infection normally elicit homotypic immune response as re-infection or multiple infections elicit both homotypic and heterotypic antibody responses (Velazquez *et al.*, 2009). Children with more than one symptomatic or asymptomatic infection have a higher degree of protection than children that are exposed to only one infection (Velazquez *et al.*, 1996; White *et al.*, 2008).

The outer capsid proteins VP7 with protruding VP4 spikes are thought to be naturally neutralized by IgG or IgA (Desselberger & Huppertz, 2011; Nair *et al.*, 2017; Velazquez *et al.*, 2000). During infection VP4 is proteolytically cleaved into two subunit proteins, VP8* and VP5*. In previous studies, VP8* appeared to have a homotypic and heterotypic activity and

showed that VP8* elicits RV neutralising antibodies against rotavirus infection (Fix *et al.*, 2015; Matsui *et al.*, 1989; Monnier *et al.*, 2006; Ruggeri & Greenberg, 1991; Wen *et al.*, 2013). However, this is in contrast to recent literature which has shown that VP8* has minimal neutralising capacity as compared with high heterotypic neutralising capacity by VP5* (Nair *et al.*, 2017). Furthermore, VP5* has the capability to mediate a broad-based protection against distinct rotavirus strains and this suggests that the VP5* heterotypic neutralising antibodies have an important role in preventing viral entry as well as initiating infection (Nair *et al.*, 2017).

Subsequent infections or immunisation seem to have a higher protection against rotavirus compared to primary infection and heterotypic infection (Bhandari *et al.*, 2014; Ruiz-Palacios *et al.*, 2006; Velazquez *et al.*, 1996). These study indicated the importance of vaccination and also to take consideration of modifying dose or number of doses of vaccine to protect children against rotavirus. Gladstone and co-workers evaluated the protective effect of natural rotavirus infection in Indian children and showed that frequent re-infection in a high viral diversity setting lowered protection as compared to previous studies done in Mexico and Guinea-Bissau (Fischer *et al.*, 1998; Gladstone *et al.*, 2011).

VP6 is responsible for the production of IgA antibodies (Yuan *et al.*, 2004). These antibodies are produced from B lymphocytes (Weitkamp *et al.*, 2003). Aiyegbo and co-workers showed that human rotavirus VP6-specific antibodies can block the transcriptional pores of the activated DLP (Figure 1.7A) which can result in the intracellular neutralisation of the virus as shown in Figure 1.7B (Aiyegbo *et al.*, 2013). The viral architecture of the virion results in 3 types of channels, namely type I, II, and III channels (Aiyegbo *et al.*, 2014) (Figure 7C). The 12 type I channels is thought to be those responsible for the release of the viral RNAs since it has a narrow opening compared to the other channels and is located at the icosahedral five-fold axes (Prasad *et al.*, 1996) (Figure 1.7C). Type II channels (60 types) are directly adjacent to the type I channel (Aiyegbo *et al.*, 2014; Prasad *et al.*, 1988). Lastly type III channels (60 types) are located at the quasi-six-fold axes and positioned around icosahedral three-fold axes (Aiyegbo *et al.*, 2013).

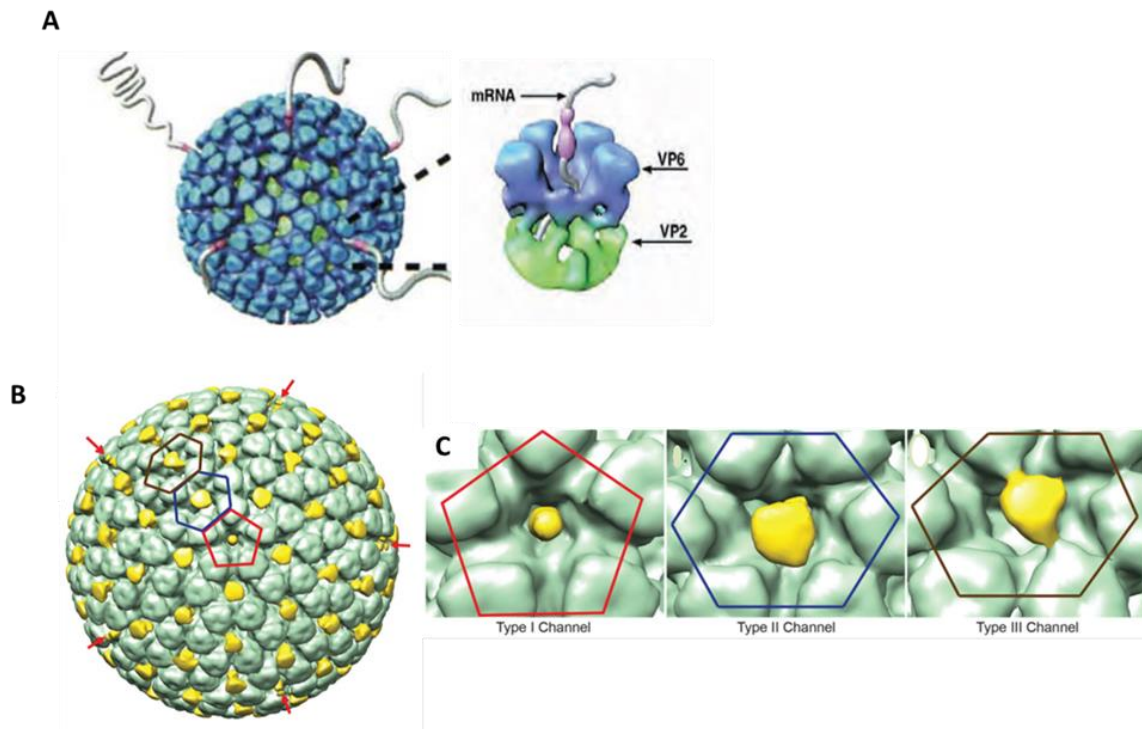


Figure 1.7: VP6 specific antibodies blocking the release of the viral mRNA. A, transcriptionally active DLP with the release of viral mRNA from the DLP pores during replication. B, illustrates the 3D structure of DLP in complex with the VP6-specific antibodies (yellow), indicated with the red arrows, blocking the transcriptional pores of the activated DLP at the five-fold axis symmetry. C, the three channels located on the VP6 structural proteins. Type I channel is responsible for the release of the viral RNA with a narrow opening, type II channel is directly adjacent to the type I channel and type III channels re located at the quasi-six-fold axes. (copied from Aiyegbo *et al.*, 2013 and 2014).

The antibody structure consists of two subunits, a heavy chain (VH) and a light chain (VL), on the antigen binding site. It was initially thought that infants have a limited antibody repertoire due to constrained VH and VL domain usage resulting in a poor antibody response (Lucas & Reason, 1998; Schroeder & Mortari, 1995). However, a study done by Weitkamp and co-workers showed that infants (2 to 11 months of age) exhibits a very strong VH dominance similar to adults (Weitkamp *et al.*, 2003). The rotavirus intestinal homing B cells in response to VP6 produce antibody repertoire is dominated by the single antibody heavy chain variable gene, VH1-46 (Weitkamp *et al.*, 2003, 2005). The VP6 capsid protein elicits immune responses to inhibit viral replication (Choi *et al.*, 2002; Lappalainen *et al.*, 2014, 2015; Vega *et al.*, 2013). VP6 has been reported to have a protective immunity in mice seen in a study by Choi and co-workers indicating protection by viral shedding (Choi *et al.*, 2002). In a recent study done by Lappalainen and co-workers also showed inhibition of viral shedding in mice by at least 65% (Lappalainen *et al.*, 2015). Furthermore, a reduction in viral reduction in shedding was also seen in gnotobiotic pigs (Vega *et al.*, 2013).

1.8 Vaccines

Since the introduction of rotavirus vaccines, the number of severe rotavirus incidence has been reduced in high- and some low income countries. Since the licencing of the two vaccines, RotaTeq® and Rotarix®, which were recommended for global use by the World Health Organisation (WHO) in 2006, the number of hospitalisations due to diarrhoea of children <5 years has reduced to 38% globally (Burnett *et al.*, 2017). In addition, there was a 46%, 30% and 41% reduction of hospitalisation in countries with high, medium and low rotavirus mortality, respectively (Burnett *et al.*, 2017). To date the vaccine effectiveness of the Rotarix® is 57% and 84% in countries with high rotavirus mortality and low mortality, respectively (Jonesteller *et al.*, 2017). While vaccine effectiveness of RotaTeq® is 45% and 90% in countries with high mortality and low mortality, respectively (Jonesteller *et al.*, 2017).

The first rotavirus vaccine to be licensed was RotaShield® in 1998. RotaShield® was a tetravalent live oral reassortant vaccine that contained a mixture of four virus strains (G1 to G4) with a rhesus rotavirus backbone. However, nine months after being licensed, Rotashield® was withdrawn from the market due to incidents of intussusception (Murphy *et al.*, 2001). Within 3 to 14 days of oral administration of the second dose of RotaShield® vaccine, the risk of intussusception was most elevated. Intussusception results in a pathological event where one part of the intestine fold into itself and usually occurs in children aged between 6 months and 2 years (Del-Pozo *et al.*, 1999). Intussusception results in a block in blood supply and therefore a lack in oxygen to the immediate tissue and this can be fatal if it is not treated quickly.

1.8.1 Live attenuated vaccines

There are two licensed live-attenuated vaccines, RotaTeq® and Rotarix®, recommended for global use by the WHO. Currently 86 countries have introduced either of the two vaccines. In Africa, 36 countries introduced either RotaTeq® or Rotarix®. Only five countries, South Africa, Botswana, Namibia, Libya, Morocco, introduced the vaccines without the support of the Global Alliance for Vaccines and Immunisation (GAVI) (<http://rotacouncil.org/vaccineintroduction/global-introduction-status>), indicating the dependence of most African countries on external financial support to implement vaccines. Immunity due to vaccination elicits strong IgA antibody responses. At least two or more doses of the vaccines are required to have sufficient protection against rotavirus infection.

1.8.1.1 RotaTeq®

RotaTeq® is a pentavalent vaccine produced by Merck Research Co and licensed by the Food and Drug Administration (FDA) and recommended by the WHO in 2006. The vaccine contains five reassortant rotaviruses (Figure 8). Four of the reassortants contain the VP7 protein derived from human rotavirus strains (G1-G4) and the spike protein (P7[5]) from the

bovine rotavirus parent strain (WC3) (Dennehy, 2008). The fifth reassortment virus expresses the spike protein (P1A[8]) derived from a human parental strain and from a bovine WC3 strain that expresses the outer capsid protein G6 (Dennehy, 2008). RotaTeq® is safe to use, but shedding of the vaccine strain is high after vaccination (after first 87.0%, second 57.4% and third 47.3% dose). Symptomatic rotavirus disease is, however, uncommon (Ye *et al.*, 2017).

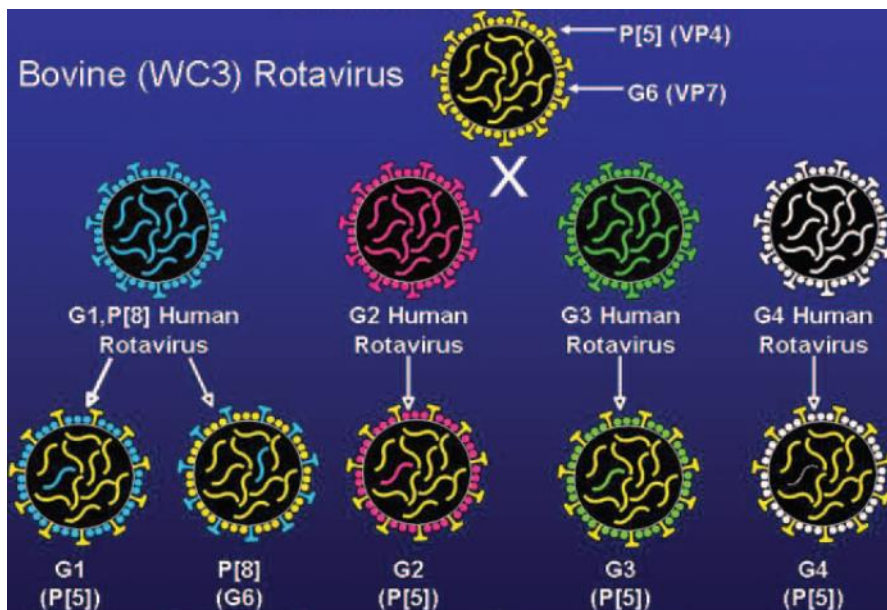


Figure 1.8: Diagram of the RotaTeq® vaccine showing the reassortment of human-bovine strains where the bovine WC3 strain is the backbone of the vaccine containing the VP7 protein (G1, G2, G3, or G4) from human rotavirus strains and VP4 protein (P1A[8]) from another human rotavirus. (copied from Offit & Clark, 2006)

RotaTeq® is administered orally in 3 doses within first 36 weeks of life. The first dose is given at 6 to 12 weeks after birth, the second dose 4 to 10 weeks after the first dose and the third dose is given at 32 weeks of age weeks. A study done in USA between February 2006, and April 2012 using the Vaccine Adverse Event Reporting System (VAERS) showed that the risk of intussusception for RotaTeq® was ~0.8 events per 100 000 vaccinated infant after the third dose (Haber *et al.*, 2013). However, in Australia the risk of intussusception was higher with 5.6 events per 100 000 per vaccinated infants (Carlin *et al.*, 2013).

1.8.1.2 Rotarix®

Rotarix® is a live-attenuated monovalent vaccine manufactured by GlaxoSmithKline and licensed in April 2008. It is also recommended by the WHO to be included in country-based immunisation programmes globally. The vaccine strain contains the most common human rotavirus VP7 and VP4 antigens, G1P[8], consisting of the Wa-like human strain, 89-12 (Matthijssens & Van Ranst, 2012). The most cross-neutralising epitopes of the Rotarix®

vaccine have been shown to be elicited to VP4 (Bernstein *et al.*, 1998). The vaccine has a higher vaccine efficacy against Wa-like strains such as G1P[8], G3P[8], G4P[8] and G9P[8] (Breuer *et al.*, 2006; Linhares *et al.*, 2008; Payne, 2009; Vesikari *et al.*, 2007).

Rotarix® is orally administered in two doses and was approved for use in infants between 6 weeks to 24 weeks of age. The first dose is given at 6 weeks of age while the second dose is administered at an interval of 4 weeks between the first and second dose. The administration of the vaccine should be completed by the end of 24 weeks of age. However, infants with a history of intussusception should not be given the Rotarix® vaccines as it could lead to death after the administration of the second dose as this has been reported in Mexico (Parashar & Patel, 2010). A large clinical trial done in 11 Latin American countries and Finland with more than 63 000 infants enrolled, showed after two years of vaccination a decrease of 83.0% of hospitalisation related cases and reached 100% against more severe rotavirus gastroenteritis (Guillermo *et al.*, 2006; Mantel *et al.*, 2009). The vaccine effectiveness of Rotarix® and RotaTeq® post-vaccination is documented in section 1.8.1.4.

1.8.1.3 Other live-attenuated rotavirus vaccines

Other developing countries such as Vietnam, India and China have developed their own vaccines due to high vaccine demand. The two companies (Merck and GlaxoSmithKline) can only produce 25% of the global demand (WHO, 2015). ROTAVAC™ (Bharat Biotech International Ltd., Hyderabad, India) developed in India is a live-attenuated monovalent vaccine derived from the human-bovine 116E rotavirus strain, G9P[11] (Gentsch *et al.*, 1993; Das *et al.*, 1993) which was a novel reassortant strain. The ROTAVAC™ has an advantage for protection against cross infection transmission from animals to humans. The vaccine was developed from a neonatal human rotavirus strain identified in India. The clinical trial, comprising of 4752 infants and 2360 infants in the placebo group, showed an efficacy of 56.3% against severe rotavirus-induced diarrhoea. Six cases of intussusception in the vaccine group and two in the placebo group were reported (Bhandari *et al.*, 2014). During the second year of life a similar vaccine efficacy of 55.1% was reported (Bhandari *et al.* 2014). The vaccine was introduced in March 2016 in the Universal Immunization Program (UIP) system in 4 states of India, Andhra Pradesh, Himachal Pradesh, Haryana and Orissa (Pradesh, 2016).

Rotavin-M™, developed in Vietnam, is a monovalent vaccine that is derived from a G1P[8] strain isolated from Vietnam infants with diarrhoea (Le *et al.*, 2009). The safety of the vaccine was compared with the Rotarix® vaccine evaluated in adults during Phase II trial. After the second dose of the two vaccines, Rotavin-M™ induced an IgA immune response to rotavirus that ranged from 51% to 73%. A 58% IgA response was observed for Rotarix®

(Anh *et al.*, 2012). These results indicated that Rotavin-M™ provided similar protection than Rotarix™ in Vietnam (Anh *et al.*, 2012). The vaccine was licenced in 2014 for use in Vietnam.

Lanzhou Lamb Rotavirus (LLR-85) vaccine was developed in China and is a monovalent vaccine containing the lamb rotavirus strain G10P[12]. The strain was passaged in primary kidney cells of newborn calf (Bai *et al.*, 1994). The vaccine was licenced in 2000 in China and is manufactured by the Lanzhou Institute of Biological Products in China (Wang *et al.*, 2009). A study conducted from 2009 to 2011 showed 44% effectiveness of the vaccine for children ranging from 9–11 months old after one dose (Fu *et al.*, 2012). For children 12–17 months old, an effectiveness of 52.8% was shown and for children 18–35 months old, 51.8% after one dose (Fu *et al.*, 2012). The low efficacy could however be due to a low vaccination rate. There are very few reports on the efficacy of the LLR-85 vaccine.

Lastly the human neonatal rotavirus vaccine (RV3-BB), the RV3-BB was developed from a human neonatal rotavirus strain, RV3 (G3P[6]). The strain was identified from stool samples of asymptomatic infants (Cameron *et al.*, 1978b). One of the advantages of the RV3 strain is that it can replicate well in the presence of maternal antibodies (Cameron *et al.*, 1978a). In a recent study conducted in Indonesia showed that the RV3-BB provided a vaccine efficacy of 94% at 12 months and 75% at 18 months (Bines *et al.*, 2018) indicating protection against severe rotavirus gastroenteritis. The vaccine was also well tolerated.

1.8.1.4 Impact of rotavirus vaccines

Rotavirus vaccination has reduced cases of hospitalisation in high income countries and this reduction of hospitalisation due to vaccination has also been observed in middle- low income countries (Bar-Zeev *et al.*, 2016; de Deus *et al.*, 2017; Groome *et al.*, 2016). Surveillance on the impact of vaccination in Africa has been conducted by WHO which has played an important role to monitor the rotavirus disease burden after introduction of vaccines. The vaccine effectiveness in high income countries in Europe is much higher accounting for 68% to 98% (Karafillakis *et al.*, 2015) and 80% in USA (Payne *et al.*, 2015). In Latin America and the Caribbean which are considered as middle income countries, the vaccine effectiveness for both Rotarix® and RotaTeq® was 73%- 83% (Velázquez *et al.*, 2017). An overall vaccine effectiveness of Rotarix® since 2006-2016 is 84%, 75%, and 57% in countries with low, medium, and high mortality, respectively, (Jonesteller *et al.*, 2017). The vaccine effectiveness of RotaTeq® is 90% for countries with low child mortality and 45% for countries with high child mortality (Jonesteller *et al.*, 2017).

South Africa was the first African country to introduce the rotavirus vaccine in 2009 in the Expanded Programme for Immunisation (EPI). In South Africa there has been a reduction of

rotavirus incidences since the introduction of vaccines. Surveillance done showed there was a reduction of 54% in 2010 and 58% in 2011 of rotavirus hospitalisations (Msimang *et al.*, 2013). To date the vaccine effectiveness in South Africa is 54% (Groome *et al.*, 2014a) which seem to be lower than the efficacy of the clinical trial (72%) (Madhi *et al.*, 2010). However, it has been seen that vaccine effectiveness is age dependent as children from age group 2-11 months tend to have a higher vaccine effectiveness compared to children ≥ 12 months. The higher vaccine effectiveness of younger children (2-11 months) compared to older children ≥ 12 months has been documented in several African countries such as Ghana (Armah *et al.*, 2016), Malawi (Bar-Zeev *et al.*, 2016), Togo (Tsolenyanu *et al.*, 2016), Tanzania (Abeid *et al.*, 2016), Rwanda (Tate *et al.*, 2016a) and recently in Burkina Faso (Bonkougou *et al.*, 2017).

There are several factors that may be responsible for the lower efficacy of vaccines in low- to middle-income countries compared to high-income countries. Firstly, maternal (transplacental) antibodies are passed to infants which can neutralise the vaccine and may interfere with immunogenicity of the vaccine (Appaiahgari *et al.*, 2014; Armah *et al.*, 2010; Becker-Dreps *et al.*, 2015; Zaman *et al.*, 2010). Maternal antibodies lasts up to 3 weeks after birth and that is why the first dose of vaccination is administered at 6 weeks of age (Moon *et al.*, 2016). It was shown that Rotarix® efficacy can be improved when the vaccine schedule is changed from 6 and 10 weeks of age to 10 and 14 weeks of age shown in a study done in South Africa (Madhi *et al.*, 2010). Another factor is breastfeeding practices. It is thought that breast milk contain IgA antibodies against rotavirus which may diminish vaccine response shown in meta-analysis studies (Moon *et al.*, 2010, 2013). Breast milk from women in low-income countries have higher IgA and neutralising activity against rotavirus compared to women in high-income countries (Moon *et al.*, 2010, 2013). Apart from antibodies present in breast milk, it was shown that higher levels of lactoferrin present in breast milk from women in low-income countries compared to women in high-income countries. Lactoferrin exhibits inhibitory activity against rotavirus vaccine strains (Moon *et al.*, 2013). Interestingly, a study conducted in Soweto, South Africa, showed that there was no significant difference when infants that did not receive breast milk an hour before and after vaccination to those that received breast milk. Previous studies showed low efficacy due to breast feeding before and after vaccination (Groome *et al.*, 2014b).

Micronutrient malnutrition is one important efficacy factor especially in low-income countries. Zinc supplementation are given to improve gastrointestinal function and also reduce the frequency and severity of diarrhoea (Bajait & Thawani, 2011; Boran *et al.*, 2006; Malik *et al.*, 2013). Oral poliovirus vaccine (OPV) can also affect rotavirus vaccine efficacy since both poliovirus and rotavirus replicate in the intestine. It was seen that OPV interferes with oral

rotavirus vaccine immunity in low-income countries (Patel *et al.*, 2012) as compared to studies done in Latin America where it seem that OPV has no effect (Ciarlet *et al.*, 2008; Patel *et al.*, 2012; Tregnaghi *et al.*, 2011). Since the first rotavirus vaccines dose (6 weeks of age) seems to have a greater negative impact on efficacy as compared to the second dose (10 and 14 weeks of age), this observation can also be due to high maternal antibodies circulating in infants at 6 weeks of age (Patel *et al.*, 2012, 2013). To overcome this problem of low efficacy for rotavirus vaccines when co-administrated with OPV, the use of the inactivated polio vaccine is recommended instead of OPV (Neuzil *et al.*, 2014; Patel *et al.*, 2012).

It was previously thought that strain diversity also plays an important role in the efficacy of vaccines. Animal-human reassortant strains result in unusual strains and the vaccine strains do not recognise these unusual strains resulting in low efficacy of the vaccine (Gentsch *et al.*, 2005). However, a recent study showed that strain diversity plays no role in the efficacy of rotavirus vaccines as both Rotarix® and RotaTeq® elicits a broad effectiveness against homotypic and heterotypic strains (Velasquez *et al.*, 2014). G1P[8] strain accounts for over 70% in high income countries like North America, Europe and Australia, but only about 30–40% of the infections has been shown in Latin America and Africa (Santos and Hoshino, 2005). Despite the fact that the G1P[8] which is regarded as the common strain globally was not frequent in Latin America there was a good effectiveness (on average 77%) against rotavirus induced hospitalisation (Bucardo & Nordgren, 2015).

On the other hand rotavirus vaccines have been associated with temporal changes in circulating genotypes mainly in low- and middle-income countries (Donato *et al.*, 2014; Gurgel *et al.*, 2007; Jere *et al.*, 2018; Martínez *et al.*, 2014; Page *et al.*, 2017; Zeller *et al.*, 2010). In South Africa there has been an increase in G2P[4] genotype in 2013 (Page *et al.*, 2017) however this could be due high incidence of G2P4 strains in neighbouring Mozambique in 2013 as at that time rotavirus vaccines were not yet introduced in Mozambique (João *et al.*, 2018). Similar results have also been observed in Botswana in 2013 after the introduction of Rotarix® vaccines in 2012 (Gastañaduy *et al.*, 2016). The G12P[8] also seem to be emerging after vaccination in South Africa (Groome *et al.*, 2014a; Page *et al.*, 2017). Jere and co-workers conducted a study in Malawi which illustrated the distribution of DS-1-like G1P[8] rotavirus strains instead of Wa-like G1P[8] strain after vaccination (Jere *et al.*, 2018). RotaTeq® tends to reassort with itself or the co-infection with a field strain after vaccination can lead to reassortment as this may revert to virulence (Bucardo *et al.*, 2012; Donato *et al.*, 2012; Hemming & Vesikari, 2014; Payne *et al.*, 2010).

As stated above there are several disadvantages associated with rotavirus live-attenuated vaccines. As alternatives, inactivated or subunit vaccines can be considered which are regarded safer to use compared to live-attenuated vaccines.

1.8.2 Inactivated vaccines

Inactivated vaccines are produced by weakening the virus using heat or chemicals. Rotavirus inactivated vaccines are produced by heat, formalin, binary ethylenimine and β -propiolactone treatment (Jiang *et al.*, 2008, 2013; Wang *et al.*, 2010; Yuan *et al.*, 1998; Zissis *et al.*, 1983). The immunity of rotavirus inactivated vaccines have been evaluated in mice and gnotobiotic piglets. Wang and co-workers have evaluated the protective immunity of a heat inactivated and aluminum phosphate formulated vaccine in gnotobiotic piglets. After the third dose the vaccine had induced high titers of rotavirus-specific IgG and neutralising activity in the sera of gnotobiotic piglets was seen (Wang *et al.*, 2010). In the case of mice, the rotavirus inactivated vaccine induced rotavirus-specific IgA and IgG in the presence of adjuvants to increase immunogenicity (McNeal *et al.*, 1999). The monovalent inactivated rotavirus vaccines showed cross-neutralising activity against homotypic and heterotypic human strains in guinea pigs as an animal model (Jiang *et al.*, 2013; Velasquez *et al.*, 2015). However, neutralising activity tend to be low against reassortant strains. Administration of the monovalent inactivated rotavirus vaccine is dose dependent, two doses induced elevated neutralising activity against homotypic and heterotypic human strains while the three dose regimen induced low levels of neutralising activity (Jiang *et al.*, 2013).

1.8.3 Sub-unit vaccines

Attractive candidates for vaccine development are virus-like particles (VLPs). The VLPs are composed of viral proteins and resembles the virion but are not infectious as they lack the viral genome. Hepatitis B virus vaccines, Engerix® (GlaxoSmithKline) and Recombivax HB® (Merck), were the first vaccines to be developed based on VLPs. Furthermore, human papillomavirus vaccines (HPV), Cervarix® (GlaxoSmithKline) and Gardasil® (Merck), have also been developed based on VLPs.

Rotavirus VLPs are either composed of the double layer particles, VP2 and VP6, (2/6DLP) or triple layered particles, VP2, VP6 and VP7, (2/6/7 TLP). In insect cells, it has been seen that there are similarities between the native rotavirus particles and VLPs produced in insects cells (Crawford *et al.*, 1994). Production of VLPs in insect cells have been evaluated in different animal models. In gnotobiotic pigs, three dose oral inoculation of 2/6DLP produced in insect cells without an adjuvant did not elicit protection against rotavirus (Iosef *et al.*, 2002). In mice the evaluation of rotavirus 2/6DLPs produced in Sf9 cells indicated a more heterotypic immune response (Bertolotti-Ciarlet *et al.*, 2003). Furthermore, rectal immunisation with rotavirus 2/6/7TLPs with toxin adjuvants such as cholera toxin and

attenuated *E. coli* derived heat-labile toxins had significantly higher titers of anti-rotavirus IgA antibodies in both serum and faeces as compared to rotavirus VLPs without an adjuvant (Parez *et al.*, 2006). Combination of live-attenuated human rotavirus and 2/6DLP vaccines had the most effective immunogenicity and induced IFN- γ -producing T cells in the ileum of gnotobiotic pigs (Azevedo *et al.*, 2013). Administration of VLPs in parental rabbits elicited high level of rotavirus-specific serum antibodies (Ciarlet *et al.*, 1998).

Rotavirus VLPs have also been produced in transgenic plants. Even though there was successful production of the VLPs, the VLP induced high serum IgG antibodies with low production of IgA antibodies (Yang *et al.*, 2011). Furthermore, emerging novel rotavirus genotypes in Africa and Asia such as G9P[6] had prompted fears that the current vaccines might not be fully effective. Therefore, a 2/6/4TLP using G9P[6] genotype produced in *Nicotiana benthamiana* was seen as a rapid production of antigens at lower costs (Pêra *et al.*, 2015). However, serum IgG antibodies are less associated with protection than serum IgA antibodies (Velazquez *et al.*, 2000).

Apart from VLPs, viral proteins are also considered good candidates for vaccine development. These proteins should induce a high immune response and should be able to have a good stability without the aid of other viral proteins. In the case of rotavirus, viral proteins such as VP6, VP8* and NSP4 have been considered good candidates for rotavirus vaccine development. It was shown that NSP4 induces a more heterotypic antibody response during a natural rotavirus infection in children (Ray *et al.*, 2003). Rotavirus NSP4 can also act as an adjuvant for 2/6DLPs as the addition of NSP4 to 2/6DLPs increased immunogenicity of rotavirus vaccines when administered in mice (Kavanagh *et al.*, 2010). Furthermore, a recent study by Afchangi and co-workers showed fusion of the capsid protein VP6 and NSP4 elicited stronger humoral immune responses compared with administration of VP6 protein alone (Afchangi *et al.*, 2017).

Rotavirus VP8* is produced by trypsin cleavage of VP4 upon entry and is responsible for the initial binding of rotavirus host glycans (Hu *et al.*, 2012b; Settembre *et al.*, 2010). This protein is considered a vaccine candidate as antibodies raised against VP8* can block the binding of rotavirus to the host receptors preventing entry of the virus to the host cells (Kovacs-Nolan *et al.*, 2003; Larralde *et al.*, 1991; Zhou *et al.*, 1994). In mice VP8* protein is capable of eliciting antibodies which have neutralisation activity (Andre *et al.*, 2005; Kovacs-Nolan & Mine, 2006; Lentz *et al.*, 2011; Marelli *et al.*, 2011). The construction of VP8* subunit vaccine candidate expressed in *E. coli* contains amino acid residues 64 (or 65)-223 Δ VP8* of P[8], P[4] or P[6] fused with tetanus toxoid universal CD4+ T cell epitope (P2) to improve its vaccine potential (Wen *et al.*, 2013). The immunogenicity of the P2-P[8] Δ VP8*-P[8] Δ VP8*

or P2-P[8] Δ VP8*-P[6] Δ VP8* subunit vaccines were previously evaluated in guinea pigs which showed high titers and homotypic and heterotypic neutralizing antibodies against rotavirus human genotype, G1-G4, G8, G9 and G12 with P[8], P[4] or P[6] combination (Wen *et al.*, 2014, 2015).

The parental P2-VP8-P[8] subunit rotavirus vaccine produced in *E. coli* has recently been evaluated for safety and immunogenicity in toddlers and infants in South Africa (Wen *et al.*, 2013). There was a strong elicited neutralising antibody response against P[4] and P[8] strains. However, there was no neutralising activity against the P[6] strain (Groome *et al.*, 2017). However, this work done on rotavirus VP8* vaccine contradicts the work done by Nair and co-workers as they showed that VP5* protein is a good candidate for a subunit vaccine compared to VP8*, since VP5* induces heterotypic responses compared to VP8* (Nair *et al.*, 2017).

Rotavirus VP6 is also an attractive vaccine development target with an advantage that anti-VP6 IgA antibodies neutralise rotavirus intracellular by blocking transcription of RNA of the DLP seen in Figure 1.7B (Aiyegbo *et al.*, 2013). Using mice and gnotobiotic pigs as animal models, a reduction in rotavirus shedding was observed as a result of rotavirus VP6-specific IgA that inhibited rotavirus replication (Lappalainen *et al.*, 2014, 2015; Vega *et al.*, 2013). Recently a seed-based bivalent rotavirus vaccine containing VP6 and NSP4 was orally administered in mice which showed induction of immune responses (Afchangi *et al.*, 2017; Feng *et al.*, 2017). The combination vaccine containing norovirus VLPs and rotavirus VP6 showed VP6 acts as an adjuvant for norovirus in mice (Blazevic *et al.*, 2016). The use of VP6 protein based vaccine as a booster to oral rotavirus live-attenuated vaccines can have an impact on the cost of vaccination as only one dose instead of 2 or 3 of the live-attenuated vaccine can be administered with VP6 as booster (Azevedo *et al.*, 2010). Furthermore, a VP6 vaccine can also be safer to be administered to older children as previously stated that infants' ≥ 12 months seem to have lower vaccine effectiveness (Abeid *et al.*, 2016; Armah *et al.*, 2016; Bar-Zeev *et al.*, 2016; Tate *et al.*, 2016a; Tsolenyanu *et al.*, 2016).

1.9 Expression systems

There are many expression systems used to produce rotavirus VLPs such as baculovirus infected insect cells, transgenic plants and yeasts. Baculoviruses are DNA viruses that replicate in the nucleus of insect cells (Guarino, 2011). This expression system employs the introduction of a foreign gene into the baculovirus genome using appropriate vectors. The recombinant protein is then transfected into insect cells resulting in the production of a recombinant virus (Contreras-Gomez *et al.*, 2013; Gomez-Sebastian *et al.*, 2014). Even though there has been successful VLP expression in insects cell using baculovirus, up-

scaling of rotavirus-VLP production in insect cells/baculovirus is expensive as cell death occurs in a few days after infection (Hu, 2005). The production of VLPs in plants can be cost effective and suitable for oral administration as it is not pathogenic to humans and animals. Despite the glycosylation of the N-glycans being structurally similar between plants and humans, plants can add sugars that are foreign to humans (Sil & Jha, 2014). For instance, N-glycans for humans consists of α -1, 6-fucose and β -1, 4-N-acetylglucosamine while plants are composed of 1, 3-fucose and a bisecting β -1, 2-xylose (Broglie & Cedex, 2004).

Yeast expression is an attractive alternative expression system because it is easy to manipulate and cost effective. Yeast expression system has been used extensively in the pharmaceutical industry to produce large scale products such as hepatitis vaccines, insulin, HPV, polio vaccine and tetanus vaccine to name the few and can express proteins at very high yields (Kim *et al.*, 2015). Protein production is determined by its correct folding capacity in the endoplasmic reticulum (ER) since incorrect folding can lead to a decrease in protein yield due to physiological instability (Werten *et al.*, 1999). There is a wide range of yeasts that have been used as expression system such as *Saccharomyces cerevisiae*, *Pichia pastoris*, *Pichia angusta* previously known as *Hansenula polymorpha* and *Yarrowia lipolytica*. There are several factors to be considered for recombinant expression in yeast such as proteolytic cleavage and glycosylation. Yeast cells express numerous proteases whereby recombinant proteins can be proteolytically cleaved, resulting in a truncated protein. To overcome proteolytic cleavage of yeast cells, protease-deficient strains can be used. Such strains have been engineered for *S. cerevisiae* and *P. pastoris* (Cho *et al.*, 2010; Sohn *et al.*, 2010; Wu *et al.*, 2013). Alternatively, protease inhibitor cocktails which are commercially available can be used to overcome proteolytic cleavage.

Another factor to be considered is glycosylation which plays an important role for heterogeneous expression. *S. cerevisiae* is a successful expression system for vaccine development of human papillomavirus (HPV) (Kim *et al.*, 2011). However the N-linked glycosylation of the recombinant protein differs from the native protein resulting in long α 1,6-linked mannose backbone with mannose side chains of α 1,2- and α 1,3-linked mannose side chains which may be allergenic (Jigami & Odani, 1999; Kim *et al.*, 2015; Sudbery, 1996). Alternatively, methylotrophic yeast such as *P. pastoris* and *P. angusta* have become an attractive heterologous protein production vectors. The advantage of *P. pastoris* and *P. angusta* compared to *S. cerevisiae* is its glycosylation pattern which tends to glycosylate at correct positions compare to *S. cerevisiae* (Bretthauer, 2003; Kim *et al.*, 2004). Furthermore, a *Y. lipolytica* strain was previously engineered for the production of a recombinant protein that have similar glycosylation patterns seen in *P. pastoris* and *P. angusta* (Song *et al.*, 2007). These two methylotrophic yeasts as well as *Y. lipolytica* have been used as

alternative hosts for product of pharmaceuticals products. There are other yeasts that can be used for heterologous protein production such as *Kluyveromyces lactis*, *Kluyveromyces marxinaus*, *Arxula adenivorans* and *Deberomyces hansenii*.

1.10 Problem identification

GlaxoSmithKline and Merck can only produce about 25% of the projected global demand of the Rotarix™ and RotaTeq® worldwide (WHO, 2015). It is a declared goal of the WHO and other organisations that rotavirus vaccines should be produced locally. Countries like India (ROTAVAC™), Vietnam (Rotavin-M™) and China (Lanzhou Lamb Rotavirus (LLR-85)) have started producing their own local vaccines (Fu *et al.*, 2012; Le *et al.*, 2009; Pradesh, 2016).

In Africa, around 36 countries have introduced rotavirus vaccines. Only five countries in Africa, South Africa, Botswana, Namibia, Libya and Morocco did so without the support of the Vaccine Alliance (GAVI), indicating the high cost associated with these vaccines. The two vaccines are live-attenuated vaccines that may revert to virulence and possibility cause intussusception. An alternative to overcome these challenges is the use of subunit vaccines like virus-like particles or the use of a viral protein as a vaccine candidate. Antibodies directed against VP6 neutralise rotavirus intracellularly by blocking transcription of RNA by the DLP particle (Aiyegbo *et al.*, 2013) and most importantly rotavirus VP6 antibodies provide a humoral memory (Nair *et al.*, 2016) making VP6 an attractive vaccine development target. Rotavirus VP6 has been produced for many years in insect cells, however up-scaling of rotavirus-VLP production in insect cells is expensive and not commercially viable. Rotavirus VP6 has also been produced in transgenic plants but the yield tends to be low. Yeast expression is considered as an attractive alternative expression system, because it is easy to manipulate and cost effective. First production of rotavirus-VLP was successfully performed in *S. cerevisiae* (Rodriguez-Limas *et al.*, 2011). Bredell and co-workers recently conducted a study that showed that the methylotrophic yeasts (*P. angusta* and *P. pastoris*) showed a high capacity of VP6 production (Bredell *et al.*, 2016). A unique wide-range yeast expression system that allows for the transformation and the subsequent protein expression in any yeast was developed at the University of the Free State (UFS).

1.11 Preliminary data

Previously a wide-range yeast expression system was developed by researchers at the UFS (Albertyn *et al.*, 2011). The availability of this wide-range yeast expression system as well as the UNESCO-MIRCEN yeast culture collection in the Department of Microbial, Biochemical and Food Biotechnology at UFS offer a novel approach for recombinant protein expression.

The consensus sequence encoding rotavirus VP6 structural protein from the neonatal South African rotavirus strain G9P[6] (Jere *et al.*, 2011; Potgieter *et al.*, 2009) was used in a

previous M.Sc study to construct recombinant wide-range yeast expression vectors (Makatsa, 2015). The VP6 open reading frame (ORF) codon optimised for expression in *Kluyveromyces lactis* and *Arxula adenivorans* were purchased from GenScript and an ORF optimised for expression in *Pichia pastoris/Pichia angusta*, previously purchased from GeneArt, was provided by Prof. J. Görgens from Stellenbosch University under agreement.

A control to monitor rotavirus VP6 protein expression in yeast was successfully prepared in bacterial cells. The positive control indicated specific reaction with the polyclonal rotavirus antibody raised against Nebraska Calf Diarrhea Virus (NCDV) rotavirus strain by western blot. Rotavirus VP6 expression in yeast strains showed no reactions for *K. lactis* and *A. adenivorans* codon optimised VP6 ORF in all nine yeast strains (*K. lactis*, *K. marxianus*, *A. adenivorans*, *C. deformans*, *Debaromyces hansenii*, *P. angusta*, *S. cerevisiae*, *Y. lipolytica* and *P. pastoris*) that tested positive for integration of the VP6 ORF into the yeast genomes. However, all yeast strains except *K. marxianus* showed reaction for VP6 expression for *P. pastoris/P. angusta* codon optimised VP6 ORF (Makatsa, 2015).

1.12 Aims and objectives

The aim of the study was to produce rotavirus VP6 capsid protein encoded by yeast codon optimised open reading frames in various yeast strains.

The objectives for this specific project were:

1. To alter the *K. lactis* and *A. adenivorans* optimised VP6 open reading frames containing expression cassettes to enable expression of VP6;
2. Evaluation of rotavirus VP6 expression encoded by *K. lactis*, *A. adenivorans* and *P. angusta/P. pastoris* optimised open reading frames in various yeasts;
3. To evaluate the ability of the yeasts, that expressed VP6, to produce VP6 tubular structures.

1.13 References

- Abeid, K. A., Jani, B., Cortese, M. M., Kamugisha, C., Mwenda, J. M., Pandu, A. S., Msaada, K. A., Mohamed, A. S., Khamis, A. U. & other authors. (2016). Monovalent Rotavirus Vaccine Effectiveness and Impact on Rotavirus Hospitalizations in Zanzibar, Tanzania_ Data From the First 3 Years After Introduction. *J Infect Dis* **215**, 183–191.
- Afchangi, A., Arashkia, A., Shahosseini, Z., Jalilvand, S., Marashi, S. M., Roohvand, F., Mohajel, N. & Shoja, Z. (2017). Immunization of Mice by Rotavirus NSP4-VP6 Fusion Protein Elicited Stronger Responses Compared to VP6 Alone. *Viral Immunol* , **2918**, 1–9.
- Aiyegbo, M. S., Eli, I. M., Spiller, B. W., Williams, D. R., Kim, R., Lee, D. E., Liu, T., Li, S., Stewart, P. L. & Crowe, J. E. (2014). Differential Accessibility of a Rotavirus VP6 Epitope in Trimers Comprising Type I, II, or III Channels as Revealed by Binding of a Human Rotavirus VP6-Specific Antibody Mohammed. *J Virol* **88**, 469–76.
- Aiyegbo, M. S., Sapparapu, G., Spiller, B. W., Eli, I. M., Williams, D. R., Kim, R., Lee, D. E., Liu, T., Li, S. & other authors. (2013). Human Rotavirus VP6-Specific Antibodies Mediate Intracellular Neutralization by Binding to a Quaternary Structure in the Transcriptional Pore. *PLoS One* **8**, 12–14.
- Albertyn, J., Labuschagne, M., Theron, C. & Smit, M. (2011). Novel expression constructs.
- Andre, I., Rodriguez-Diaz, J., Buesa, J. & Zueco, J. (2005). Yeast Expression of the VP8 * Fragment of the Rotavirus Spike Protein and Its Use as Immunogen in Mice. *Biotechnol Bioeng* **93**, 89–98.
- Anh, D. D., Van Trang, N., Thiem, V. D., Anh, N. T. H., Mao, N. D., Wang, Y., Jiang, B., Hien, N. D. & Luan, L. T. (2012). A dose-escalation safety and immunogenicity study of a new live attenuated human rotavirus vaccine (Rotavin-M1) in Vietnamese children. *Vaccine* **30**, 114–121.
- Aoki, S. T., Settembre, E., Trask, S. D., Greenberg, H. B., Stephen, C. & Dormitzer, P. R. (2010). Structure of rotavirus outer-layer protein VP7 bound with a neutralizing Fab. *Science (80-)* **324**, 1444–1447.
- Appaiahgari, M. B., Glass, R., Singh, S., Taneja, S., Rongsen-Chandola, T., Bhandari, N., Mishra, S. & Vрати, S. (2014). Transplacental rotavirus IgG interferes with immune response to live oral rotavirus vaccine ORV-116E in Indian infants. *Vaccine* **32**, 651–656.
- Armah, G., Pringle, K., Enweronu-laryea, C. C., Ansong, D., Mwenda, J. M., Diamenu, S. K., Narh, C., Lartey, B., Binka, F. & other authors. (2016). Impact and Effectiveness of Monovalent Rotavirus Vaccine Against Severe Rotavirus Diarrhea in Ghana. *Clin Infect Dis* **62**, S200–S207.
- Armah, G. E., Sow, S. O., Breiman, R. F., Dallas, M. J., Tapia, M. D., Feikin, D. R., Binka, F. N., Steele, A. D., Laserson, K. F. & other authors. (2010). Efficacy of pentavalent rotavirus vaccine against severe rotavirus gastroenteritis in infants in developing countries in sub-Saharan Africa: A randomised, double-blind, placebo-controlled trial. *Lancet* **376**, 606–614.
- Azevedo, M. S. P., Gonzalez, A. M., Yuan, L., Jeong, K., Iosef, C., Nguyen, T. Van, Lovgren-bengtsson, K., Morein, B. & Saif, L. J. (2010). An Oral versus Intranasal Prime / Boost Regimen Using Attenuated Human Rotavirus or VP2 and VP6 Virus-Like Particles with Immunostimulating Complexes Influences Protection and Antibody-Secreting Cell Responses to Rotavirus in a Neonatal Gnotobiotic Pig Mo. *Clin Vaccine Immunol* **17**, 420–428.

- Azevedo, M., Vlasova, A. & Saif, L. (2013).** Human rotavirus virus-like particle vaccines evaluated in a neonatal gnotobiotic pig model of human rotavirus disease. *Expert Rev vaccines* **12**, 169–81.
- Bai, Z., Chen, D. & Shen, S. (1994).** Selection and Characterization of Strain LLR-85 for Oral Rotavirus Live Vaccine. *Chinese J Biol* **7**, 49–52.
- Bajait, C. & Thawani, V. (2011).** Role of zinc in pediatric diarrhea. *India J Pharmacol* **43**, 232–235.
- Ball, J. M., Tian, P., Zeng, C. Q., Morris, A. P. & Estest, M. K. (1996).** Age-Dependent Diarrhea Induced by a Rotaviral Nonstructural Glycoprotein. *Science* **272**, 101–4.
- Bányai, K., László, B., Duque, J., Steele, A. D., Nelson, E. A. S., Gentsch, J. R. & Parashar, U. D. (2012).** Systematic Review of Regional and Temporal Trends in Global Rotavirus Strain Diversity in the Pre Rotavirus Vaccine era_ Insights for Understanding the Impact of Rotavirus. *Vaccine* **30**, A122–A130.
- Bar-Zeev, N., Jere, K. C., Bennett, A., Pollock, L., Tate, J. E., Nakagomi, O. & Iturriza-gomara, M. (2016).** Population Impact and Effectiveness of Monovalent Rotavirus Vaccination in Urban Malawian Children 3 Years After Vaccine Introduction : Ecological and Case-Control Analyses. *Clin Infect Dis* **62**, 213–219.
- Barro, M. & Patton, J. T. (2005).** Rotavirus nonstructural protein 1 subverts innate immune response by inducing degradation of IFN regulatory factor 3. *Proc Natl Acad Sci USA* **102**, 4114–9.
- Barro, M. & Patton, J. T. (2007).** Rotavirus NSP1 Inhibits Expression of Type I Interferon by Antagonizing the Function of Interferon Regulatory Factors IRF3 , IRF5 , and IRF7. *J Virol* **81**, 4473–4481.
- Becker-dreps, S., Vilchez, S., Velasquez, D., Moon, S.-S., Hudgens, M. G., Zambrana, L. E. & Jiang, B. (2015).** Rotavirus-Specific IgG Antibodies from Mothers' Serum may Inhibit Infant Immune Responses to the Pentavalent Rotavirus Vaccine. *Pediatr Infect Dis J* **34**, 115–116.
- Bergmann, C. C., Maass, D., Poruchynsky, S., Atkinson, P. H. & Bellamy, A. R. (1989).** Topology of the non-structural rotavirus. *EMBO J* **8**, 1695–1703.
- Bernstein, D. I., Smith, V. E., Sherwood, J. R., Schiff, G. M., Sander, D. S., DeFeudis, D., Spriggs, D. R. & Ward, R. L. (1998).** Safety and immunogenicity of live, attenuated human rotavirus vaccine 89-12. *Vaccine* **16**, 381–387.
- Berois, M., Sapin, C., Erk, I., Poncet, D. & Cohen, J. (2003).** Rotavirus Nonstructural Protein NSP5 Interacts with Major Core Protein VP2. *J Virology* **77**, 1757–1763.
- Bertolotti-Ciarlet, A., Ciarlet, M., Crawford, S. E., Conner, M. E. & Estes, M. K. (2003).** Immunogenicity and protective efficacy of rotavirus 2 / 6-virus-like particles produced by a dual baculovirus expression vector and administered intramuscularly , intranasally , or orally to mice. *Vaccine* **21**, 3885–3900.
- Bhandari, N., Rongsen-Chandola, T., Bavdekar, A., John, J., Antony, K., Taneja, S., Goyal, N., Kawade, A., Kang, G. & other authors. (2014).** Efficacy of a monovalent human-bovine (116E) rotavirus vaccine in Indian infants: A randomised, double-blind, placebo-controlled trial. *Vaccine* **32**, A110–A116.
- Bines, J. E., Thobari, J. A., Satria, C. D., Handley, A., Watts, E., Cowley, D., Nirwati, H., Ackland, J., Standish, J. & other authors. (2018).** Human neonatal rotavirus vaccine (RV3-BB) targets rotavirus from birth. *N Engl J Med* **278**, 719–730

- Bishop, R. F., Davidson, G. P., Holmes, I. H. & Ruck, B. J. (1973).** Virus particles in epithelial cell of duodenal mucosa from children with acute non bacterial gastroenteritis. *Lancet* **302**, 1281–1283.
- Blazevic, V., Malm, M., Arinobu, D., Lappalainen, S. & Vesikari, T. (2016).** Rotavirus capsid VP6 protein acts as an adjuvant in vivo for norovirus virus-like particles in a combination vaccine. *Hum Vaccines Immunother* **12**, 740–748. Taylor & Francis.
- Blutt, S. E. & Conner, M. E. (2013).** The gastrointestinal frontier : IgA and viruses. *Front Immunol* **4**, 1–12.
- Bonkougou, I. J. O., Aliabadi, N., Leshem, E., Kam, M., Nezien, D., Drabo, M. K., Nikiema, M., Ouedraogo, B., Medah, I. & other authors. (2017).** *Impact and effectiveness of pentavalent rotavirus vaccine in children <5 years of age in Burkina Faso.* *Vaccine*. doi.org/10.1016
- Boran, P., Tokuc, G., Vagas, E., Oktem, S. & Gokduman, M. K. (2006).** Impact of zinc supplementation in children with acute diarrhoea in Turkey. *Arch Dis Child* **91**, 296–299.
- Bredell, H., Smith, J. J., Prins, W. A., Görgens, J. F. & Zyl, W. H. Van. (2016).** Expression of rotavirus VP6 protein : A comparison amongst *Escherichia coli* , *Pichia pastoris* and *Hansenula polymorpha*. *FEMS Yeast Res* **16**, 1–12.
- Breton, M., Fontanges, P., Trugnan, G. & Chwetzoff, S. (2006).** Rotavirus Spike Protein VP4 Binds to and Remodels Actin Bundles of the Epithelial Brush Border into Actin Bodies **80**, 3947–3956.
- Bretthauer, R. K. (2003).** Genetic engineering of *Pichia pastoris* to humanize N-glycosylation of proteins. *Trends Biotechnol* **21**, 459–462.
- Breuer, T., Clemens, S. C., Cheuvart, B., Espinoza, F., Gillard, P., Innis, B. L., Cervantes, Y., Linhares, A. C., López, P. & other authors. (2006).** Safety and Efficacy of an Attenuated Vaccine against Severe Rotavirus Gastroenteritis Guillermo. *N Engl J Med* **354**, 11–22.
- Brogie, B. De & Cedex, A. (2004).** Posttranslational modification of therapeutic proteins in plants. *Curr Opin Plant Biol* **7**, 171–181.
- Bucardo, F. & Nordgren, J. (2015).** Impact of vaccination on the molecular epidemiology and evolution of group A rotaviruses in Latin America and factors affecting vaccine efficacy. *Infect Genet Evol* **34**, 106–113.
- Bucardo, F., Rippinger, C. M., Svensson, L. & Patton, J. T. (2012).** Vaccine-Derived NSP2 Segment in Rotaviruses from Vaccinated Children with Gastroenteritis in Nicaragua. *Infect Genet Evol* **12**, 1282–1294.
- Burnett, E., Jonesteller, C. L., Tate, J. E., Yen, C. & Parashar, U. D. (2017).** Global Impact of Rotavirus Vaccination on Childhood Hospitalizations and Mortality From Diarrhea. *J Infect Dis* **215**, 1666–1672.
- Cameron, D. J. S., Bishop, R. F., Veenstra, A. A. & Barnes, G. L. (1978a).** Noncultivable viruses and neonatal diarrhea: Fifteen-month survey in a newborn special care nursery. *J Clin Microbiol* **8**, 93–98.
- Cameron, D. J. S., Bishop, R. F., Veenstra, A. A., Barnes, G. L., Holmes, I. H. & Ruck. (1978b).** Pattern of shedding of two noncultivable viruses in stools of newborn babies. *J Med Virol* **2**, 7–13.

- Carlin, J. B., Macartney, K. K., Lee, K. J., Quinn, H. E., Buttery, J., Lopert, R., Bines, J. & McIntyre, P. B. (2013).** Intussusception Risk and Disease Prevention Associated With Rotavirus Vaccines in Australia ' s National Immunization Program. *Clin Infect Dis* **57**, 1427–34.
- Chen, D., Luongo, C. L., Nibert, M. L. & Patton, J. T. (1999).** Rotavirus open cores catalyze 5'-capping and methylation of exogenous RNA: evidence that VP3 is a methyltransferase. *Virology* **265**, 120–30.
- Chitambar, S. D., Ranshing, S. S., Pradhan, G. N., Kalrao, V. R., Dhongde, R. K. & Bavdekar, A. R. (2014).** Changing trends in circulating rotavirus strains in Pune, western India in 2009-2012: Emergence of a rare G9P[4] rotavirus strain. *Vaccine* **32**, A29–A32.
- Cho, E. Y., Cheon, S. A., Kim, H., Choo, J., Lee, D. J., Ryu, H. M., Rhee, S. K., Chung, B. H., Kim, J. Y. & Kang, H. A. (2010).** Multiple-yapsin-deficient mutant strains for high-level production of intact recombinant proteins in *Saccharomyces cerevisiae*. *J Biotechnol* **149**, 1–7.
- Choi, A. H., Mcneal, M. M., Basu, M., Flint, J. A., Stone, S. C., Clements, J. D., Bean, J. A., Poe, S. A., Vancott, J. L. & Ward, R. L. (2002).** Intranasal or oral immunization of inbred and outbred mice with murine or human rotavirus VP6 proteins protects against viral shedding after challenge with murine rotaviruses. *Vaccine* **20**, 3310–3321.
- Ciarlet, M. A. X., Crawford, S. U. E. E., Barone, C., Bertolotti-ciarlet, A., Ramig, R. F., Estes, M. K. & Conner, M. E. (1998).** Subunit Rotavirus Vaccine Administered Parenterally to Rabbits Induces Active Protective Immunity. *J Virolgy* **72**, 9233–9246.
- Ciarlet, M., Sani-Grosso, R., Yuan, G., Liu, G. F., Heaton, P. M., Gottesdiener, K. M., Arredondo, J. L. & Schödel, F. (2008).** Concomitant Use of the Oral Pentavalent Human-Bovine Reassortant Rotavirus Vaccine and Oral Poliovirus Vaccine. *Pediatr Infect Dis J* **27**, 874–880.
- Contreras-Gomez, A., Sanchez-Miron, A., Garcia-Camacho, F. & Molina-Grima, E. (2013).** Protein Production Using the Baculovirus-Insect Cell Expression System. *Biotechnol Progr* **30**, 1–18.
- Crawford, S. U. E. E., Labbe, M., Cohen, J., Burroughs, M. H., Zhou, Y. & Estes, M. K. (1994).** Characterization of Virus-Like Particles Produced by the Expression of Rotavirus Capsid Proteins in Insect Cells. *J Virol* **68**, 5945–5952.
- Cuadras, M. A., Feigelstock, D. A., An, S. & Greenberg, H. B. (2002).** Gene Expression Pattern in Caco-2 Cells following Rotavirus Infection. *J Virolgy* **76**, 4467–4482.
- Del-Pozo, G., Albillos, J. C., Tejedor, D., Calero, R., Rasero, M., De-la-Calle, U. & López-Pacheco, U. (1999).** Intussusception in children: current concepts in diagnosis and enema reduction. *Radiographics* **19**, 299–319.
- Delogu, R., Ianiro, G., Camilloni, B., Fiore, L. & Ruggeri, F. M. (2015).** Unexpected Spreading of G12P[8] Rotavirus Strains Among Young Children in a Small Area of Central Italy. *J Med Virol* **87**, 1292–1302.
- Denisova, E., Dowling, W., Monica, R. L. A., Shaw, R., Scarlata, S., Ruggeri, F. & Mackow, E. R. (1999).** Rotavirus Capsid Protein VP5 * Permeabilizes Membranes. *J Virolgy* **73**, 3147–3153.
- Dennehy, P. H. (2008).** Rotavirus vaccines: An overview. *Clin Microbiol Rev* **21**, 198–208.
- Dennis, F. E., Fujii, Y., Haga, K., Damanka, S., Lartey, B., Agbemabiese, C. A., Ohta, N., Armah, G. E. & Katayama, K. (2014).** Identification of Novel Ghanaian G8P [6] Human-Bovine Reassortant Rotavirus Strain by Next Generation Sequencing. *PLoS One* **9**, 1–11.

- Deo, R. C., Groft, C. M., Rajashankar, K. R. & Burley, S. K. (2002).** Recognition of the Rotavirus mRNA 3' Consensus by an Asymmetric NSP3 Homodimer. *Cell* **108**, 71–81.
- Desselberger, U. & Huppertz, H. (2011).** Immune Responses to Rotavirus Infection and Vaccination and Associated Correlates of Protection **203**.
- Desselberger, U., Manktelow, E., Li, W., Cheung, W., Iturriza-Gómara, M. & Gray, J. (2009).** Rotaviruses and rotavirus vaccines. *Br Med Bull* **90**, 37–51.
- de Deus, N., Chilaúle, J. J., Cassocera, M., Bambo, M., Langa, J. S., Siteo, E., Chissaque, A., Anapakala, E., Sambo, J. & other authors. (2017).** Early impact of rotavirus vaccination in children less than five years of age in Mozambique. *Vaccine*, 1-5.
- Donato, C. M., Ch'ng, L. S., Boniface, K. F., Crawford, N. W., Buttery, J. P., Lyon, M., Bishop, R. F. & Kirkwood, C. D. (2012).** Identification of Strains of RotaTeq Rotavirus Vaccine in Infants With Gastroenteritis Following Routine Vaccination. *J Infect Dis* **206**, 377–83.
- Donato, C. M., Zhang, Z. A., Donker, N. C. & Kirkwood, C. D. (2014).** Characterization of G2P[4] rotavirus strains associated with increased detection in Australian states using the RotaTeq® vaccine during the 2010–2011 surveillance period. *Infect Genet Evol* **28**, 398–412.
- Dong, Y., Zeng, C. Q.-Y., Ball, J. M., Estes, M. K. & Morris, A. P. (1997).** The rotavirus enterotoxin NSP4 mobilizes intracellular calcium in human intestinal cells by stimulating phospholipase C-mediated inositol 1, 4, 5-trisphosphate production. *Proc Natl Acad Sci USA* **94**, 3960–3965.
- Dormitzer, P. R., Sun, Z. J., Wagner, G. & Harrison, S. C. (2002a).** The rhesus rotavirus VP4 sialic acid binding domain has a galectin fold with a novel carbohydrate binding site. *EMBO J* **21**, 885–897.
- Dormitzer, P., Sun, Z., Blixt, O., James, C., Wagner, G. & Harrison, S. (2002b).** Specificity and Affinity of Sialic Acid Binding by the Rhesus Rotavirus VP8 * Core Specificity and Affinity of Sialic Acid Binding by the Rhesus. *Am Soc Microbiol* **76**, 10512–10517.
- Esona, M. D. & Gautam, R. (2015).** Rotavirus. *Clin Lab Med* **35**, 363–391.
- Esona, M., Mijatovic-Rustempasic, S., Conrardy, C., Tong, S., Kuzmin, I., Agwanda, B., Breiman, R., Banyai, K., Niezgodá, M. & other authors. (2010).** Reassortant Group A Rotavirus from Straw-colored Fruit Bat (*Eidolon helvum*). *Emerg Infect Dis* **16**, 1-9.
- Estes, M. K. & Greenberg, H. B. (2013).** Rotaviruses. In *Fields Virol*, 2nd edn., pp. 1347–1401.
- Estes, M. K., Graham, D. Y. & Mason, B. B. (1981).** Proteolytic Enhancement of Rotavirus Infectivity : Molecular Mechanisms. *J Virology* **39**, 879–888.
- Fabbretti, E., Afrikanova, I., Vascotto, F. & Burrone, O. R. (1999).** Two non-structural rotavirus proteins, NSP2 and NSP5, form viroplasm-like structures in vivo. *J Gen Virol* **80**, 333–339.
- Feng, H., Li, X., Song, W., Duan, M., Chen, H., Wang, T. & Dong, J. (2017).** Oral Administration of a Seed-based Bivalent Rotavirus Vaccine Containing VP6 and NSP4 Induces Specific Immune Responses in Mice. *Front Plant Sci* **8**, 1–13.
- Fiore, L., Greenberg, H. B. & Mackow, E. R. (1991).** The VP8 Fragment of VP4 Is the Rhesus Rotavirus Hemagglutinin. *Virology* **181**, 553–563.
- Fischer, T. K., Valentiner-branth, P., Steinsland, H., Perch, M., Santos, G. & Aaby, P. (1998).** Protective Immunity after Natural Rotavirus Infection : A Community Cohort Study of Newborn Children in Guinea-Bissau , West Africa. *J Infect Dis* **186**, 593–597.

- Fix, A. D., Harro, C., Mcneal, M., Dally, L., Flores, J., Robertson, G., Boslego, J. W. & Cryz, S. (2015).** Safety and immunogenicity of a parenterally administered rotavirus VP8 subunit vaccine in healthy adults. *Vaccine* **33**, 3766–3772.
- Fredj, M. B. H., BenHamida-Rebaï, M. Ben, Zeller, M., Heylen, E., Ranst, M. Van, Matthijssens, J. & Trabelsi, A. (2014).** Sequence and structural analyses of NSP4 proteins from human group A rotavirus strains detected in Tunisia. *Pathol Biol* **62**, 146–151.
- Fu, C., He, Q., Xu, J., Xie, H., Ding, P., Hu, W., Dong, Z., Liu, X. & Wang, M. (2012).** Effectiveness of the Lanzhou lamb rotavirus vaccine against gastroenteritis among children. *Vaccine* **31**, 154–158.
- Fuentes-Pananá, E. M., López, S., Gorziglia, M. & Arias, C. F. (1995).** Mapping the Hemagglutination Domain of Rotaviruses. *J Virolgy* **69**, 2629–2632.
- Gastañaduy, P. A., Steenhoff, A. P., Mokomane, M., Esona, M. D., Bowen, M. D., Jibril, H., Pernica, J. M., Mazhani, L., Smieja, M. & other authors. (2016).** Effectiveness of Monovalent Rotavirus Vaccine After Programmatic Implementation in Botswana : A Multisite Prospective Case-Control Study. *Clin Infect Dis* **62**, 161–167.
- Gentsch, J. R., Laird, A. R., Bielfelt, B., Griffin, D. D., Jain, V., Cunliffe, N. A., Nakagomi, O., Kirkwood, C. D., Fischer, T. K. & other authors. (2005).** Serotype Diversity and Reassortment between Human and Animal Rotavirus Strains : Implications for Rotavirus Vaccine Programs. *J Infect Dis* **192**, S146-59.
- Gladstone, B. P., Ramani, S., Mukhopadhyaya, I., Muliyl, J., Sarkar, R., Rehman, A. M., Jaffar, S., Gomara, M. I., Gray, J. J. & other authors. (2011).** Protective Effect of Natural Rotavirus Infection in an Indian Birth Cohort. *N Engl J Med* **365**, 337–346.
- Gomez-Sebastian, S., Lopez-Vidal, J. & Escibano, J. M. (2014).** Significant Productivity Improvement of the Baculovirus Expression Vector System by Engineering a Novel Expression Cassette. *PLoS One* **9**, 1–10.
- Graff, J. W., Mitzel, D. N., Weisend, C. M., Flenniken, M. L. & Hardy, M. E. (2002).** Interferon Regulatory Factor 3 Is a Cellular Partner of. *J Virol* **76**, 9545–9550.
- Groft, C. M. & Burley, S. K. (2002).** Recognition of eIF4G by Rotavirus NSP3 Reveals a Basis for mRNA Circularization. *Mol Cell* **9**, 1273–1283.
- Groome, M. J., Page, N., Cortese, M. M., Moyes, J., Zar, H. J., Kapongo, C. N., Mulligan, C., Diedericks, R., Cohen, C. & other authors. (2014a).** Effectiveness of monovalent human rotavirus vaccine against admission to hospital for acute rotavirus diarrhoea in South African children : a case-control study. *Lancet Infect Dis* **14**, 1096–104.
- Groome, M. J., Moon, S.-S., Velasquez, D., Jones, S., Koen, A., van Niekerk, N., Jiang, B., Parashar, U. D. & Madhi, S. A. (2014b).** Effect of breastfeeding on immunogenicity of oral live-attenuated human rotavirus vaccine: a randomized trial in HIV-uninfected infants in Soweto, South Africa. *Bull World Health Organ* **92**, 238–45.
- Groome, M. J., Zell, E. R., Solomon, F., Nzenze, S., Parashar, U. D., Izu, A. & Madhi, S. A. (2016).** Temporal Association of Rotavirus Vaccine Introduction and Reduction in All-Cause Childhood Diarrheal Hospitalizations in South Africa. *Clin Infect Dis* **62**, S188–S195.
- Groome, M. J., Koen, A., Fix, A., Page, N., Jose, L., Madhi, S. A., Mcneal, M., Dally, L., Cho, I. & other authors. (2017).** Safety and immunogenicity of a parenteral P2-VP8-P [8] subunit

rotavirus vaccine in toddlers and infants in South Africa : a randomised , double-blind , placebo-controlled trial. *Lancet Infect Dis* **17**, 843–853.

- Rohrmann, G. F. (2011).** Baculoviruses as insecticides_ Three examples - Baculovirus Molecular Biology - 3rd edition.
- Gurgel, R. Q., Cuevas, L. E., Vieira, S. C. F., Barros, V. C. F., Fontes, P. B., Salustino, E. F., Dove, W., Cunliffe, N. & Hart, C. A. (2007).** Predominance of Rotavirus P[4]G2 in a Vaccinated Population, Brazil. *Emerg Infect Dis* **13**, 1571–1573.
- Haber, P., Patel, M., Pan, Y., Baggs, J., Haber, M., Yue, X., Lewis, P. & Parashar, U. D. (2013).** Intussusception After Rotavirus Vaccines Reported to US VAERS , 2006 – 2012. *Pediatrics* **131**, 1042–9.
- He, B., Huang, X., Zhang, F., Tan, W., Matthijnsens, J., Qin, S., Xu, L., Zhao, Z., Yang, L. & other authors. (2017).** Group A rotaviruses in Chinese bats: genetic composition, serology and evidence for bat-to-human transmission and reassortment. *J Virol* **91**, 1844–1852.
- Hemming, M. & Vesikari, T. (2014).** Detection of rotateq vaccine-derived, double-reassortant rotavirus in a 7-year-old child with acute gastroenteritis. *Pediatr Infect Dis J* **33**, 655–656.
- Hjelt, K., Grauballe, P. C., Schiotz, P. O., Andersen, L. & Krasilnikoff, P. A. (1985).** Intestinal and Serum Immune Response to a Naturally Acquired Rotavirus Gastroenteritis in Children. *J Pediatr Gastroenterol Nutr* **4**, 60–66.
- Hu, L., Crawford, S. E., Hyser, J. M., Estes, M. K. & Prasad, B. V. V. (2012a).** Rotavirus non-structural proteins: structure and function. *Curr Opin Virol* **2**, 380–8.
- Hu, L., Crawford, S. E., Czako, R., Cortes-penfield, N. W., Smith, D. F., Pendu, J. Le, Estes, M. K. & Prasad, B. V. V. (2012b).** interacts with A-type histo-blood group antigen. *Nature* **485**, 256–259.
- Hu, Y. (2005).** Baculovirus as a highly efficient expression vector in insect and mammalian cells. *Acta Pharmacol Sin* **26**, 405–416.
- Hung, T., Chen, G. M., Wang, C. G., Chou, Z. Y., Chao, T. X., Ye, W. W., Yao, H. L. & Meng, K. H. (1983).** Rotavirus-like agent in adult non-bacterial diarrhoea in China. *Lancet* **322**, 1078–1079.
- Iosef, C., Nguyen, T. Van, Jeong, K., Bengtsson, K., Morein, B., Kim, Y., Chang, K., Azevedo, M. S. P., Yuan, L. & other authors. (2002).** Systemic and intestinal antibody secreting cell responses and protection in gnotobiotic pigs immunized orally with attenuated Wa human rotavirus and Wa 2/6-rotavirus-like-particles associated with immunostimulating complexes. *Vaccine* **20**, 1741–1753.
- Ito, H., Sugiyama, M., Masubuchi, K., Mori, Y. & Minamoto, N. (2001).** Complete nucleotide sequence of a group A avian rotavirus genome and a comparison with its counterparts of mammalian rotaviruses. *Virus Reseach* **75**, 123–138.
- Jamnikar-Ciglenecki, U., Kuhar, U., Steyer, A. & Kirbis, A. (2017).** Whole genome sequence and a phylogenetic analysis of the G8P [14] group A rotavirus strain from roe deer. *BioMed Cent Vet Res* **13**, 1–15.
- Jayaram, H., Estes, M. K. & Prasad, B. V. V. (2004).** Emerging themes in rotavirus cell entry, genome organization, transcription and replication. *Vaccine Res* **101**, 67–81.
- Jere, K. C., Mlera, L., O'Neill, H. G., Potgieter, C. A., Page, N. A., Seheri, M. L. & Van Dijk, A. A.**

- (2011). Whole Genome Analyses of African G2, G8, G9, and G12 Rotavirus Strains Using Sequence-Independent Amplification and 454 Pyrosequencing. *J Med Virol* **83**, 2018–2042.
- Jere, K. C., Chaguza, C., Bar-Zeev, N., Lowe, J., Peno, C., Kumwenda, B., Nakagomi, O., Tate, J. E., Parashar, U. D. & other authors. (2017).** Emergence of double- and triple-gene reassortant G1P[8] rotaviruses possessing a DS-1-like backbone post rotavirus vaccine introduction in Malawi. *J Virology* doi:10.112, 1–48.
- Jere, K. C., Chaguza, C., Bar-zeev, N., Lowe, J., Peno, C., Kumwenda, B., Nakagomi, O., Tate, J. E., Parashar, U. D. & other authors. (2018).** Emergence of Double- and Triple-Gene Reassortant G1P[8] Rotaviruses Possessing a DS-1-Like Backbone after Rotavirus Vaccine Introduction in Malawi Khuzwayo. *J Virology* **92**, 1–15.
- Jiang, B., Gentsch, J. R. & Glass, R. I. (2008).** Inactivated rotavirus vaccines: A priority for accelerated vaccine development. *Vaccine* **26**, 6754–6758.
- Jiang, B., Wang, Y. & Glass, R. I. (2013).** Does a monovalent inactivated human rotavirus vaccine induce heterotypic immunity? *Hum Vaccin Immunother* **9**, 1634–1637.
- Jiang, X., Jayaram, H., Kumar, M., Ludtke, S. J., Estes, M. K. & Prasad, B. V. V. (2006).** Cryoelectron microscopy structures of rotavirus NSP2-NSP5 and NSP2-RNA complexes: implications for genome replication. *J Virol* **80**, 10829–35.
- Jigami, Y. & Odani, T. (1999).** Mannosylphosphate transfer to yeast mannan. *Elsevier Sci* **1426**, 335–345.
- João, E. D., Strydom, A., O’Neill, H. G., Cuamba, A., Cassocera, M., Acácio, S., Mandomando, I., Motanyane, L., Page, N. & de Deus, N. (2018).** Rotavirus A strains obtained from children with acute gastroenteritis in Mozambique, 2012 - 2013 : G and P genotypes and phylogenetic analysis of VP7 and partial VP4 genes. *Arch Virol* **163**, 153–165.
- Jonesteller, C. L., Burnett, E., Yen, C., Tate, J. E. & Parashar, U. D. (2017).** Effectiveness of Rotavirus Vaccination : A Systematic Review of the First Decade of Global Postlicensure Data , 2006 – 2016. *Clin Infect Dis* **65**, 840–50.
- Karafillakis, E., Hassounah, S. & Atchison, C. (2015).** Effectiveness and impact of rotavirus vaccines in Europe , 2006 – 2014. *Vaccine* **33**, 2097–2107.
- Kavanagh, O., Ajami, N., Cheng, E., Ciarlet, M., Guerrero, R., Zeng, C., Crawford, S. & Estes, M. (2010).** Rotavirus Enterotoxin NSP4 Has Mucosal Adjuvant Properties. *Vaccine* **18**, 54–56.
- Keryer-Bibens, C., Legagneux, V., Namanda-Vanderbeken, A., Cosson, B., Paillard, L., Poncet, D. & Osborne, H. B. (2009).** The rotaviral NSP3 protein stimulates translation of polyadenylated target mRNAs independently of its RNA-binding domain. *Biochem Biophys Res Commun* **390**, 302–6.
- Kim, H. J., Kwag, H., Jin, Y. & Kim, H. (2011).** The composition of the carbon source and the time of cell harvest are critical determinants of the final yield of human papillomavirus type 16 L1 protein produced in *Saccharomyces cerevisiae*. *Protein Expr Purif* **80**, 52–60.
- Kim, H., Yoo, S. J. & Kang, H. A. (2015).** Yeast synthetic biology for the production of recombinant therapeutic proteins. *FEMS Yeast Res* **15**, 1–16.
- Kim, M. W., Rhee, S. K., Kim, J. Y., Shimma, Y. I., Chiba, Y., Jigami, Y. & Kang, H. A. (2004).** Characterization of N-linked oligosaccharides assembled on secretory recombinant glucose

oxidase and cell wall mannoproteins from the methylotrophic yeast *Hansenula polymorpha*. *Glycobiology* **14**, 243–251.

King, A. M. Q., Adams, M. J., Carsten, E. B. & Lefkowitz, E. J. (2012). *Virus Taxonomy: Classification and Nomenclature of Viruses. Ninth Report of the International Committee on Taxonomy of Viruses.* Elsevier Inc.

Komoto, S., Tacharoenmuang, R., Guntapong, R. & Ide, T. (2016). Reassortment of Human and Animal Rotavirus Gene Segments in Emerging DS-1- Like G1P [8] Rotavirus Strains. *PLoS One* **11**, 1–26.

Kovacs-Nolan, J. & Mine, Y. (2006). Tandem copies of a human rotavirus VP8 epitope can induce specific neutralizing antibodies in BALB/c mice. *Biochim Biophys Acta - Gen Subj* **1760**, 1884–1893.

Kovacs-Nolan, J., Yoo, D. & Mine, Y. (2003). Fine mapping of sequential neutralization epitopes on the subunit protein VP8 of human rotavirus. *Biochem J* **376**, 269–275.

Lappalainen, S., Pastor, A. R., Tamminen, K., López-guerrero, V. & Esquivel-guadarrama, F. (2014). Immune responses elicited against rotavirus middle layer protein VP6 inhibit viral replication in vitro and in vivo. *Hum Vaccin Immunother* **10**, 2039–2047.

Lappalainen, S., Pastor, A. R., Malm, M., Lopez-Guerrero, V., Esquivel-Guadarrama, F., Palomares, L. A., Vesikari, T. & Blazevic, V. (2015). Protection against live rotavirus challenge in mice induced by parenteral and mucosal delivery of VP6 subunit rotavirus vaccine. *Arch Virol* **160**, 2075–2078.

Larralde, G., Li, B. G., Kapikian, a Z. & Gorziglia, M. (1991). Serotype-specific epitope(s) present on the VP8 subunit of rotavirus VP4 protein. *J Virol* **65**, 3213–3218.

Lawton, J. a, Estes, M. K. & Prasad, B. V. (1997). Three-dimensional visualization of mRNA release from actively transcribing rotavirus particles. *Nat Struct Mol Biol* **4**, 118–121.

Le, L. T., Nguyen, T. V., Nguyen, P. M., Huong, N. T., Huong, N. T., Huong, N. T. M., Hanh, T. B., Ha, D. N., Anh, D. D. & other authors. (2009). Development and characterization of candidate rotavirus vaccine strains derived from children with diarrhoea in Vietnam. *Vaccine* **27**, 5–8.

Lentz, E. M., Mozgovej, M. V, Bellido, D., Santos, M. J. D., Wigdorovitz, A. & Bravo-almonacid, F. F. (2011). VP8 * antigen produced in tobacco transplastomic plants confers protection against bovine rotavirus infection in a suckling mouse model. *J Biotechnol* **156**, 100–107.

Linhares, A. C., Velázquez, F. R., Pérez-Schael, I., Sáez-Llorens, X., Abate, H., Espinoza, F., López, P., Macías-Parra, M., Ortega-Barría, E. & other authors. (2008). Efficacy and safety of an oral live attenuated human rotavirus vaccine against rotavirus gastroenteritis during the first 2 years of life in Latin American infants: a randomised, double-blind, placebo-controlled phase III study. *Lancet (London, England)* **371**, 1181–9.

Lucas, A. H. & Reason, D. C. (1998). Aging and the Immune Response to the *Haemophilus influenzae* Type b Capsular Polysaccharide : Retention of the Dominant Idiotypic and Antibody Function in the Elderly **66**, 1752–1754.

Madhi, S. A., Cunliffe, N. A., Steele, D., Witte, D., Kirsten, M., Louw, C., Ngwira, B., Victor, J. C., Gillard, P. H. & other authors. (2010). Effect of Human Rotavirus Vaccine on Severe Diarrhea in African Infants. *N Engl J Med* **362**, 2251–2259.

- Makatsa, M. S. (2015).** *Engineering yeast strains for the expression of South African G9P [6] rotavirus VP2 and VP6 structural proteins* By. University of the Free State.
- Malik, A., Taneja, D. k, Taneja, D. K., Devasenapathy, N. & Rajeshwari, K. (2013).** Short-Course Prophylactic Zinc Supplementation for Diarrhea Morbidity in Infants of 6 to 11 Months. *Pediatrics* **132**, e46–e52.
- Mantel, W. H. O. S. C., Wang, S., Mayers, G. & Derobert, E. (2009).** Detailed Review Paper on Rotavirus Vaccines 1–57.
- Marelli, B., Perez, A. R., Banchio, C., de Mendoza, D. & Magni, C. (2011).** Oral immunization with live *Lactococcus lactis* expressing rotavirus VP8* subunit induces specific immune response in mice. *J Virol Methods* **175**, 28–37.
- Marthaler, D., Rossow, K., Culhane, M., Goyal, S., Collins, J., Matthijnsens, J., Nelson, M. & Ciarlet, M. (2014).** Widespread Rotavirus H in Domesticated Pigs, United States. *Emerg Infect Dis* **20**, 1195–1198.
- Martínez, M., Carvalho-costa, F. A., Mello, E. De, Lundgren, T., Figueira, M., Madi, A., Maria, R., Assis, S., Ribeiro, S. & other authors. (2014).** Prevalence and genomic characterization of G2P [4] group A rotavirus strains during monovalent vaccine introduction in Brazil. *Infect Genet Evol* **28**, 486–494.
- Matsui, S. M., Offit, P. A., Vo, P. T., Mackow, E. R., David, A., Shaw, R. D., Padilla-noriega, L. & Greenberg, H. B. (1989).** Passive Protection against Rotavirus-Induced Diarrhea by Monoclonal Antibodies to the Heterotypic Neutralization Domain of VP7 and the VP8 Fragment of VP4. *J Clin Microbiol* **27**, 780–782.
- Matthijnsens, J. & Van Ranst, M. (2012).** Genotype constellation and evolution of group A rotaviruses infecting humans. *Curr Opin Virol* **2**, 426–433.
- Matthijnsens, J. & Theuns, S. (2015).** Minutes of the 7th Rotavirus Classification Working Group (RCWG) Meeting (9 Oct 2015). *12th Int Double Stranded RNA Virus Symp* 1–7.
- Matthijnsens, J., Ciarlet, M., Rahman, M., Attoui, H., Bányai, K., Estes, M. K., Gentsch, J. R., Iturriza-Gómara, M., Kirkwood, C. D. & other authors. (2008a).** Recommendations for the classification of group a rotaviruses using all 11 genomic RNA segments. *Arch Virol* **153**, 1621–1629.
- Matthijnsens, J., Ciarlet, M., Heiman, E., Arijs, I., Delbeke, T., McDonald, S. M., Palombo, E. a, Iturriza-Gómara, M., Maes, P. & other authors. (2008b).** Full genome-based classification of rotaviruses reveals a common origin between human Wa-Like and porcine rotavirus strains and human DS-1-like and bovine rotavirus strains. *J Virol* **82**, 3204–3219.
- Matthijnsens, J., Ciarlet, M., McDonald, S. M., Attoui, H., Bányai, K., Brister, J. R., Buesa, J., Esona, M. D., Estes, M. K. & other authors. (2011).** Uniformity of rotavirus strain nomenclature proposed by the Rotavirus Classification Working Group (RCWG). *Arch Virol* **156**, 1397–1413.
- Matthijnsens, J., Otto, P. H., Ciarlet, M., Desselberger, U., van Ranst, M. & Johne, R. (2012).** VP6-sequence-based cutoff values as a criterion for rotavirus species demarcation. *Arch Virol* **157**, 1177–1182.
- McClain, B., Settembre, E., Temple, B. R. S., Bellamy, A. R. & Harrison, S. C. (2010).** X-ray crystal structure of the rotavirus inner capsid particle at 3.8 Å resolution. *J Mol Biol* **397**, 587–599.

- McDonald, S. M. & Patton, J. T. (2011).** Rotavirus VP2 core shell regions critical for viral polymerase activation. *J Virol* **85**, 3095–105.
- McNeal, M. M., Rae, M. N. & Ward, R. L. (1999).** Effects of different adjuvants on rotavirus antibody responses and protection in mice following intramuscular immunization with inactivated rotavirus. *Vaccine* **17**, 1573–1580.
- Monnier, N., Higo-moriguchi, K., Sun, Z. J., Prasad, B. V. V., Taniguchi, K. & Dormitzer, P. R. (2006).** High-Resolution Molecular and Antigen Structure of the VP8 * Core of a Sialic Acid-Independent Human Rotavirus Strain †. *J Virolgy* **80**, 1513–1523.
- Moon, S., Groome, M. J., Velasquez, D. E., Parashar, U. D., Jones, S., Koen, A. & Niekerk, N. Van. (2016).** Pre vaccination Rotavirus Serum IgG and IgA Are Associated With Lower Immunogenicity of Live , Oral Human Rotavirus Vaccine in South African Infants. *Clin Infect Dis* **62**, 157–65.
- Moon, S.-S., Wang, Y., Shane, A. L., Nguyen, T., Ray, P., Dennehy, P. H., Baek, L. J., Parashar, U., Glass, R. I. & Jiang, B. (2010).** Inhibitory Effect of Breast Milk on Infectivity of Live Oral Rotavirus Vaccines. *Pediatr Infect Dis J* **29**, 919–923.
- Moon, S.-S., Tate, J. E., Ray, P., Dennehy, P. H., Archary, D., Coutsoudis, A., Bland, R., Newell, M.-L., Glass, R. I. & other authors. (2013).** Differential Profiles and Inhibitory Effect on Rotavirus Vaccines of Nonantibody Components in Breast Milk From Mothers in Developing and Developed Countries. *Pediatr Infect Dis J* **32**, 863–870.
- Morelli, M., Ogden, K. M. & Patton, J. T. (2015).** Silencing the alarms: Innate immune antagonism by rotavirus NSP1 and VP3. *Virology* **479–480**, 75–84.
- Msimang, V. M. Y., Page, N., Groome, M. J., Moyes, J., Cortese, M. M., Seheri, M., Kahn, K., Chagan, M., Madhi, S. a & Cohen, C. (2013).** Impact of rotavirus vaccine on childhood diarrheal hospitalization after introduction into the South African public immunization program. *Pediatr Infect Dis J* **32**, 1359–64.
- Murphy, T. V, Gargiullo, P. M., Massoudi, M. S., Nelson, D. B., Jumaan, A. O., Okoro, C. A., Zanardi, L. R., Setia, S., Fair, E. & other authors. (2001).** Intussusception among infants given an oral rotavirus vaccine. *N Engl J Med* **344**, 564–572.
- Nair, N., Newell, E. W., Vollmers, C., Quake, S. R., Morton, J. M., Davis, M. M., He, X. S. & Greenberg, H. B. (2016).** High-dimensional immune profiling of total and rotavirus VP6-specific intestinal and circulating B cells by mass cytometry. *Mucosal Immunol* **9**, 68–82.
- Nair, N., Feng, N., Blum, L. K., Sanyal, M., Ding, S., Jiang, B., Sen, A., Morton, J. M., He, X.-S. & other authors. (2017).** VP4- and VP7-specific antibodies mediate heterotypic immunity to rotavirus in humans. *Sci Transl Med* **9**, 1–12.
- Nandi, S., Chanda, S., Bagchi, P., Nayak, M. K., Bhowmick, R. & Chawla-sarkar, M. (2014).** MAVS Protein Is Attenuated by Rotavirus Nonstructural Protein 1. *PLoS One* **9**, e92126.
- Neuzil, K. M., Zaman, K. & Victor, J. C. (2014).** A proposed framework for evaluating and comparing efficacy estimates in clinical trials of new rotavirus vaccines. *Vaccine* **32S**, A179–A184.
- Nordgren, J., Bonkoungou, I. J. O., Nitiema, L. W., Sharma, S., Ouermi, D., Simpoire, J., Barro, N. & Svensson, L. (2012).** Rotavirus in diarrheal children in rural Burkina Faso: High prevalence of genotype G6P[6]. *Infect Genet Evol* **12**, 1892–1898. Elsevier B.V.

- Nyaga, M. M., Peenze, I., Potgieter, C. A., Seheri, L. M., Page, N. A., Yinda, C. K., Steele, A. D., Matthijnsens, J. & Mphahlele, M. J. (2016).** Infection , Genetics and Evolution Complete genome analyses of the first porcine rotavirus group H identified from a South African pig does not provide evidence for recent interspecies transmission events. *Infect Genet Evol* **38**, 1–7.
- Offit, A. & Clark, H. (2006).** RotaTeq a pentavalent bovine human reassortant rotavirus vaccine. *Pediatr Ann* **35**, 29–34.
- Osonuga, A., Osonuga, O. A. & Emegoakor, C. (2013).** A Review of Current Practices for Management of Rotavirus Infection in Children Under - 5 Years in Ghana. *Int J Sci Study* **1**, 40–44.
- Page, N. A., Seheri, L. M., Groome, M. J., Moyes, J., Walaza, S., Mphahlele, J., Kahn, K., Kapongo, C. N., Zar, H. J. & other authors. (2017).** Temporal association of rotavirus vaccination and genotype circulation in South Africa : Observations from 2002 to 2014. *Vaccine* **S0264–410X**, doi: 10.1016/j.vaccine.2017.10.062. Elsevier Ltd.
- Parashar, U. & Patel, M. (2010).** Effect of Rotavirus Vaccination on Death from Childhood Diarrhea in Mexico. *NEW Engl J Med Engl J of Med* **362**, 299–305.
- Parez, N., Fourceux, C., Mohamed, A., Dubuquoy, C., Pillot, M., Dehee, A., Charpilienne, A., Poncet, D., Schwartz-cornil, I. & Garbarg-chenon, A. (2006).** Rectal Immunization with Rotavirus Virus-Like Particles Induces Systemic and Mucosal Humoral Immune Responses and Protects Mice against Rotavirus Infection †. *J Virology* **80**, 1752–1761.
- Patel, M., Steele, A. D. & Parashar, U. D. (2012).** Influence of oral polio vaccines on performance of the monovalent and pentavalent rotavirus vaccines. *Vaccine* **30S**, A30–A35.
- Patel, M., Shane, A. L., Parashar, U. D., Jiang, B., Gentsch, J. R. & Glass, R. I. (2013).** Oral Rotavirus Vaccines: How Well Will They Work Where They Are Needed Most? *J Infect Dis* **2009**, S39–S48.
- Patton, J. T., Jones, M. T., Kalbach, A. N., He, Y. W. & Xiaobo, J. (1997).** Rotavirus RNA polymerase requires the core shell protein to synthesize the double-stranded RNA genome. *J Virol* **71**, 9618–9626.
- Patton, J. T., Silvestri, L. S., Tortorici, M. a, Vasquez-Del Carpio, R. & Taraporewala, Z. F. (2006).** Rotavirus genome replication and morphogenesis: role of the viroplasm. *Curr Top Microbiol Immunol* **309**, 169–87.
- Patton, J. T. (1996).** Rotavirus VP1 Alone Specifically Binds to the 3' End of Viral mRNA , but the Interaction Is Not Sufficient To Initiate Minus-Strand Synthesis. *J Virology* **70**, 7940–7947.
- Payne, D. (2009).** *Detailed Review Paper on Rotavirus Vaccines.*
- Payne, D. C., Edwards, K. M., Bowen, M. D., Keckley, E., Peters, J., Esona, M. D., Teel, E. N., Kent, D., Parashar, U. D. & Gentsch, J. R. (2010).** Sibling Transmission of Vaccine-Derived Rotavirus (RotaTeq) Associated With Rotavirus Gastroenteritis. *Pediatrics* **125**, e438-41.
- Payne, D. C., Selvarangan, R., Azimi, P. H., Boom, J. A., Englund, J. A., Staat, M. A., Halasa, N. B., Weinberg, G. A., Szilagyi, P. G. & other authors. (2015).** Long-term Consistency in Rotavirus Vaccine Protection : RV5 and RV1 Vaccine Effectiveness in US Children , 2012 – 2013. *Clin Infect Dis* **61**, 1792–1799.
- Pedley, S., Bridger, J. C., Brown, J. F. & McCrae, M. A. (1983).** Molecular characterization of

- rotaviruses with distinct group antigens. *J Gen Virol* **64**, 2093–2101.
- Pêra, F. F. P. G., Mutepfa, D. L. R., Khan, A. M., Els, J. H., Mbewana, S., Dijk, A. A. A. Van, Rybicki, E. P. & Hitzeroth, I. I. (2015).** Engineering and expression of a human rotavirus candidate vaccine in *Nicotiana benthamiana*. *Virology* **12**, 1–11.
- Piron, M., Vende, P., Cohen, J. & Poncet, D. (1998a).** Rotavirus RNA-binding protein NSP3 interacts with eIF4G1 and evicts the poly(A) binding protein from eIF4F. *EMBO J* **17**, 5811–21.
- Piron, M., Vende, P., Piron, M., Vende, P., Cohen, J. & Poncet, D. (1998b).** Rotavirus RNA-binding protein NSP3 interacts with eIF4G1 and evicts the poly (A) binding protein from eIF4F Rotavirus RNA-binding protein NSP3 interacts with eIF4F. *EMBO J* **17**, 5811–5821.
- Pizarro, J. L., Sandino, a M., Pizarro, J. M., Fernández, J. & Spencer, E. (1991).** Characterization of rotavirus guanylyltransferase activity associated with polypeptide VP3. *J Gen Virol* **72 (Pt 2)**, 325–32.
- Poncet, D., Aponte, C. & Cohen, J. (1993).** Rotavirus protein NSP3 (NS34) is bound to the 3' end consensus sequence of viral mRNAs in infected cells. *J Virol* **67**, 3159–65.
- Potgieter, A. C., Page, N. A., Liebenberg, J., Wright, I. M., Landt, O. & van Dijk, A. A. (2009).** Improved strategies for sequence-independent amplification and sequencing of viral double-stranded RNA genomes. *J Gen Virol* **90**, 1423–1432.
- Pradesh, H. (2016, March 26).** Achieving a new milestone towards expanding full immunization coverage in the country to reduce child mortality. *Press Inf Bur Gov India Minist Heal Fam Welf* 2–3.
- Quaye, O., McDonald, S., Esona, M. D., Lyde, F. C., Mijatovic-Rustempasic, S., Roy, S., Banegas, D. J. C., Quiñonez, Y. M., Chinchilla, B. L. & other authors. (2013).** Rotavirus G9P[4] in 3 countries in Latin America, 2009-2010. *Emerg Infect Dis* **19**, 1332.
- Rainsford, E. W. & McCrae, M. a. (2007).** Characterization of the NSP6 protein product of rotavirus gene 11. *Virus Res* **130**, 193–201.
- Ramig, R. F. (2004).** MINIREVIEW Pathogenesis of Intestinal and Systemic Rotavirus Infection. *J Virol* **78**, 10213–10220.
- Ramig, R. F. (2007).** Systemic Rotavirus Infection. *Expert Rev Anti Infect Ther* **5**, 591–612.
- Randall, R. E., Goodbourn, S. & Randall, R. E. (2008).** Interferons and viruses : an interplay between induction , signalling , antiviral responses and virus countermeasures. *J Gen Virol* **89**, 1–47.
- Ray, P., Malik, J., Singh, R. K., Bhatnagar, S., Bahl, R., Kumar, R. & Bhan, M. K. (2003).** Rotavirus nonstructural protein NSP4 induces heterotypic antibody responses during natural infection in children. *J Infect Dis* **187**, 1786–1793.
- Rodriguez-Limas, W. A., Tyo, K. E. J., Nielsen, J., Ramirez, O. T. & Palomares, L. A. (2011).** Molecular and process design for rotavirus-like particle production in *Saccharomyces cerevisiae*. *Microb Cell Fact* **10**, 33.
- Ruggeri, F. & Greenberg, H. (1991).** Antibodies to the Trypsin Cleavage Peptide VP8 * Neutralize Rotavirus by Inhibiting Binding of Virions to Target Cells in Culture. *J Virology* **65**, 2211–2219.
- Ruiz-Palacios, G. M., Pérez-Schael, I., Velázquez, F. R., Abate, H., Breuer, T., Clemens, S. C., Chevart, B., Espinoza, F., Gillard, P. & other authors. (2006).** Safety and Efficacy of an

- Attenuated Vaccine against Severe Rotavirus Gastroenteritis. *N Engl J Med* **354**, 11–22.
- Santos, N. & Hoshino, Y. (2005).** Global distribution of rotavirus serotypes/genotypes and its implication for the development and implementation of an effective rotavirus vaccine. *Rev Med Virol* **15**, 29–56.
- Schroeder, H. W. & Mortari, F. (1995).** Developmental Regulation of the Human Antibody Repertoire. *Ann N Y Acad Sci* **764**, 242–260.
- Seheri, M., Nemarude, L., Peenze, I., Netshifhefhe, L., Nyaga, M. M., Ngobeni, H. G., Maphalala, G., Maake, L. L., Steele, A. D. & other authors. (2014).** Update of Rotavirus Strains Circulating in Africa From 2007 Through 2011. *Pediatr Infect Dis J* **33**, S76–S84.
- Seth, R. B., Sun, L., Ea, C. & Chen, Z. J. (2005).** Identification and Characterization of MAVS, a Mitochondrial Antiviral Signaling Protein that Activates NF κ B and IRF3. *Cell* **122**, 669–682.
- Settembre, E. C., Chen, J. Z., Dormitzer, P. R., Grigorieff, N. & Harrison, S. C. (2010).** Atomic model of an infectious rotavirus particle. *EMBO J* **30**, 408–416.
- Sil, B. & Jha, S. (2014).** Plants : The Future Pharmaceutical Factory. *Am J Plant Sci* **5**, 319–327.
- Silvestri, L., Tortorici, M., Carpio, V. & Patton, J. (2005).** Rotavirus Glycoprotein NSP4 Is a Modulator of Viral Transcription in the Infected Cell Rotavirus Glycoprotein NSP4 Is a Modulator of Viral Transcription in the Infected Cell. *J Virol* **79**, 15165–15174.
- Silvestri, L. S., Taraporewala, Z. F. & Patton, J. T. (2004).** Rotavirus Replication : Plus-Sense Templates for Double-Stranded RNA Synthesis Are Made in Viroplasm **78**, 7763–7774.
- Sohn, S. B., Graf, A. B., Kim, T. Y., Gasser, B., Maurer, M., Ferrer, P., Mattanovich, D. & Lee, S. Y. (2010).** Genome-scale metabolic model of methylotrophic yeast *Pichia pastoris* and its use for in silico analysis of heterologous protein production. *Biotechnol J* **5**, 705–715.
- Song, Y., Min, H. C., Park, J. N., Moo, W. K., Eun, J. K., Hyun, A. K. & Kim, J. Y. (2007).** Engineering of the yeast *Yarrowia lipolytica* for the production of glycoproteins lacking the outer-chain mannose residues of N-glycans. *Appl Environ Microbiol* **73**, 4446–4454.
- Stencel-baerenwald, J. E., Reiss, K., Reiter, D. M., Stehle, T. & Dermody, T. S. (2014).** The sweet spot: defining virus–sialic acid interactions. *Nat Rev Microbiol* **12**, 739–749.
- Sudbery, P. E. (1996).** The expression of recombinant proteins in yeasts. *Curr Opin Biotechnol* **7**, 517–524.
- Takeuchi, O. & Akira, S. (2010).** Review Pattern Recognition Receptors and Inflammation. *Cell* **140**, 805–820.
- Tate, J. E., Ngabo, F., Donnen, P., Gatera, M., Uwimana, J., Rugambwa, C., Mwenda, J. M. & Parashar, U. D. (2016a).** Effectiveness of Pentavalent Rotavirus Vaccine Under Conditions of Routine Use in Rwanda. *Clin Infect Dis* **62**, S208–12.
- Tate, J. E., Burton, A. H., Boschi-Pinto, C. & Parashar, U. D. (2016b).** Global, Regional, and National Estimates of Rotavirus Mortality in Children <5 Years of Age, 2000–2013. *Clin Infect Dis* **62**, S96–S105.
- Torres-Vega, M. A., González, R. A., Duarte, M., Poncet, D., López, S. & Arias, C. F. (2000).** The C-terminal domain of rotavirus NSP5 is essential for its multimerization, hyperphosphorylation and interaction with NSP6. *J Gen Virol* **81**, 821–830.

- Trask, S. D., Ogden, K. M. & Patton, J. T. (2012a).** Interactions among capsid proteins orchestrate rotavirus particle functions. *Curr Opin Virol* **2**, 373–9.
- Trask, S. D., McDonald, S. M. & Patton, J. T. (2012b).** Structural insights into the coupling of virion assembly and rotavirus replication. *Nat Rev Microbiol* **10**, 165–77.
- Tregnaghi, M. W., Abate, H. J., Valencia, A., Lopez, P., Reverbel Da Silveira, T., Rivera, L., Medina, D. M. R., Saez-Llorens, X., Ayala, S. E. G. & other authors. (2011).** Human Rotavirus Vaccine Is Highly Efficacious When Coadministered With Routine Expanded Program of Immunization Vaccines Including Oral Poliovirus Vaccine in Latin America. *Pediatr Infect Dis J* **30**, e103–e108.
- Trojnar, E., Otto, P. & Johne, R. (2009).** The first complete genome sequence of a chicken group A rotavirus indicates independent evolution of mammalian and avian strains. *Virology* **386**, 325–333.
- Trojnar, E., Otto, P., Roth, B., Reetz, J. & Johne, R. (2010).** The genome segments of a group D rotavirus possess group A-like conserved termini but encode group-specific proteins. *J Virol* **84**, 10254–10265.
- Trojnar, E., Sachsenro, J., Twardziok, S., Reetz, J., Otto, P. H. & Johne, R. (2013).** Identification of an avian group A rotavirus containing a novel VP4 gene with a close relationship to those of mammalian rotaviruses. *J Gen Virol* **94**, 136–142.
- Tsolenyau, E., Mwenda, J. M., Dagnra, A., Leshem, E., Godonou, M., Nassoury, I., Landoh, D., Tate, J. E., Atakouma, Y. & Parashar, U. D. (2016).** Early Evidence of Impact of Monovalent Rotavirus Vaccine in Togo. *Clin Infect Dis* **62**, S196–S199.
- Vega, C. G., Bok, M., Vlasova, A. N., Chattha, K. S., Gómez-Sebastián, S., Nuñez, C., Alvarado, C., Lasa, R., Escribano, J. M. & other authors. (2013).** Recombinant Monovalent Llama-Derived Antibody Fragments (VHH) to Rotavirus VP6 Protect Neonatal Gnotobiotic Piglets against Human Rotavirus-Induced Diarrhea. *PLOS Pathog* **9**, 1–17.
- Velasquez, D. E., Parashar, U. D. & Jiang, B. (2014).** Strain diversity plays no major role in the varying efficacy of rotavirus vaccines : An overview. *Infect Genet Evol* **28**, 561–571.
- Velasquez, D. E., Wang, Y. & Jiang, B. (2015).** Inactivated human rotavirus vaccine induces heterotypic antibody response : Correction and development of IgG avidity assay. *Hum Vaccin Immunother* **11**, 531–533.
- Velazquez, R. F., Matson, D. O., Guerrero, M. L., Shults, J., Calva, J. J., Morrow, A. L., Glass, R. I., Pickering, L. K. & Ruiz-palacios, G. M. (2000).** Serum Antibody as a Marker of Protection against Natural Rotavirus Infection and Disease. *J Infect Dis* **182**, 1602–9.
- Velazquez, R. F., Matson, D. O., Calva, J. J., Guerrero, L., Morrow, A. L., Carter-Campbell, S., Glass, R. I., Estes, M. K., Pickering, L. K. & Ruaiz-Palacios, G. M. (1996).** Rotavirus Infection in Infants as Protection against Subsequent Infections. *N Engl J Med* **335**, 1022–8.
- Velázquez, R. F., Linhares, A. C., Muñoz, S., Seron, P., Lorca, P., Deantonio, R. & Ortega-barria, E. (2017).** Efficacy , safety and effectiveness of licensed rotavirus vaccines : a systematic review and meta-analysis for Latin America and the Caribbean. *BMC Pediatr* **17**, 1–12.
- Vende, P., Tortorici, M. A., Taraporewala, Z. F. & Patton, J. T. (2003).** Rotavirus NSP2 interferes with the core lattice protein VP2 in initiation of minus-strand synthesis. *Virology* **313**, 261–273.
- Vesikari, T., Karvonen, A., Prymula, R., Schuster, V., Tejedor, J., Cohen, R., Meurice, F., Han, H.,**

- Damaso, S. & Bouckenoghe, A. (2007).** Efficacy of human rotavirus vaccine against rotavirus gastroenteritis during the first 2 years of life in European infants: randomised, double-blind controlled study. *Lancet* **370**, 1757–1763.
- Wang, X., Riewpaiboon, A., Seidlein, L. Von, Chen, X., Kilgore, P. E., Ma, J., Qi, S., Zhang, Z., Hao, Z. & other authors. (2009).** Potential Cost-Effectiveness of a Rotavirus Immunization Program in Rural China. *Clin Infect Dis* **49**, 1202– 1210.
- Wang, Y., Azevedo, M., Saif, L. J., Gentsch, J. R., Glass, R. I. & Jiang, B. (2010).** Inactivated rotavirus vaccine induces protective immunity in gnotobiotic piglets. *Vaccine* **28**, 5432–5436.
- Weitkamp, J., Kallewaard, N., Bures, E., Williams, J. V, Greenberg, H. B. & Crowe, J. E. (2003).** Infant and Adult Human B Cell Responses to Rotavirus Share Common Immunodominant Variable Gene Repertoires. *J Immunol* **171**, 4680–4688.
- Weitkamp, J., Kallewaard, N. L., Amber, L., Lafleur, B. J., Greenberg, H. B., James, E., Kallewaard, N. L., Bowen, A. L. & Lafleur, B. J. (2005).** VH1– 46 Is the Dominant Immunoglobulin Heavy Chain Gene Segment in Rotavirus-Specific Memory B Cells Expressing the Intestinal Homing Receptor α 4 β 7. *J Immunol* **174**, 3454–3460.
- Wen, X., Cao, D., Jones, R., Li, J., Szu, S. & Hoshino, Y. (2013).** Construction and Characterization of Human Rotavirus Recombinant VP8* Subunit Parenteral Vaccine Candidates. *Vaccine* **30**, 6121–6126.
- Wen, X., Wen, K., Cao, D., Li, G., Jones, R., Li, J., Szu, S., Hoshino, Y. & Yuan, L. (2014).** Inclusion of a universal tetanus toxoid CD4(+) T cell epitope P2 significantly enhanced the immunogenicity of recombinant rotavirus Δ VP8* subunit parenteral vaccines. *Vaccine* **32**, 4420–4427.
- Wen, X., Cao, D., Jones, R. W., Hoshino, Y. & Yuan, L. (2015).** Tandem truncated rotavirus VP8 * subunit protein with T cell epitope as non-replicating parenteral vaccine is highly immunogenic. *Hum Vaccin Immunother* **11**, 2483–2489.
- Wentzel, J. F. (2014).** *Investigating the importance of co- expressed rotavirus proteins in the development of a selection-free rotavirus reverse genetics system.* North-West University.
- Werten, M. W. T., van den Bosch, T. J., Wind, R. D., Mooibroek, H. & De Wolf, F. A. (1999).** High-yield Secretion of Recombinant Gelatins by *Pichia pastoris*. *Yeast* **15**, 1087–1096.
- White, L. J., Buttery, J., Cooper, B., Nokes, D. J. & Medley, G. F. (2008).** Rotavirus within day care centres in Oxfordshire , UK : characterization of partial immunity. *J R Soc* **5**, 1481–1490.
- WHO. (2015).** *Immunization coverage.*
- Wu, M., Shen, Q., Yang, Y., Zhang, S., Qu, W., Chen, J., Sun, H. & Chen, S. (2013).** Disruption of YPS1 and PEP4 genes reduces proteolytic degradation of secreted HSA/PTH in *Pichia pastoris* GS115. *J Ind Microbiol Biotechnol* **40**, 589–599.
- Xia, L., Fan, Q., He, B., Xu, L., Zhang, F., Hu, T., Wang, Y., Li, N., Qiu, W. & other authors. (2014).** The complete genome sequence of a G3P[10] Chinese bat rotavirus suggests multiple bat rotavirus inter-host species transmission events. *Infect Genet Evol* **28**, 1–4.
- Yang, Y., Li, X., Yang, H., Qian, Y., Zhang, Y., Fang, R. & Chen, X. (2011).** Immunogenicity and virus-like particle formation of rotavirus capsid proteins produced in transgenic plants. *Sci China Life Sci* **54**, 82–9.

- Ye, S., Division, M., Queensland, P., Whiley, D. M., Division, M., Queensland, P., Ware, R. S., Coast, G., Kirkwood, C. D. & other authors. (2017).** Multivalent rotavirus vaccine and wild-type rotavirus strain shedding in Australian infants: a birth cohort study. *Clin Infect Dis* doi.org/10.1093/cid.
- Yinda, C. K., Zeller, M., Conceição-neto, N., Maes, P., Deboutte, W., Beller, L., Heylen, E., Ghogomu, S. M. & Ranst, M. Van. (2016).** Novel highly divergent reassortant bat rotaviruses in Cameroon , without evidence of zoonosis. *Sci Rep* **6**, 1–10.
- Yoneyama, M. & Fujita, T. (2009).** Recognition of viral nucleic acids in innate immunity. *Med Virol* **20**, 4–22.
- Yuan, L., Kang, S., Ward, L. A., To, T. L. & Saif, L. J. (1998).** Antibody-Secreting Cell Responses and Protective Immunity Assessed in Gnotobiotic Pigs Inoculated Orally or Intramuscularly with Inactivated Human Rotavirus †. *J Virol* **72**, 330–338.
- Yuan, L., Ishida, S., Honma, S., Patton, J. T., Hodgins, D. C., Kapikian, A. Z. & Hoshino, Y. (2004).** Homotypic and Heterotypic Serum Isotype – Specific Antibody Responses to Rotavirus Nonstructural Protein 4 and Viral Protein (VP) 4 , VP6 , and VP7 in Infants Who Received Selected Live Oral Rotavirus Vaccines. *J Infect Dis* **189**, 1833–1845.
- Zaman, K., Dang, D. A., Victor, J. D., Shin, S., Yunus, M., Dallas, M. J., Podder, G., Vu, D. T., Le, T. P. & other authors. (2010).** Efficacy of pentavalent rotavirus vaccine against severe rotavirus gastroenteritis in infants in developing countries in Asia: a randomised, double-blind, placebo-controlled trial. *Lancet* **376**, 615–23.
- Zeller, M., Rahman, M., Heylen, E., De Coster, S., De Vos, S., Arijs, I., Novo, L., Verstappen, N., Van Ranst, M. & Matthijssens, J. (2010).** Rotavirus incidence and genotype distribution before and after national rotavirus vaccine introduction in Belgium. *Vaccine* **28**, 7507–7513.
- Zhang, M., Zeng, C. Q., Morris, A. P., Estes, M. K. & Irol, J. V. (2000).** A Functional NSP4 Enterotoxin Peptide Secreted from Rotavirus-Infected Cells **74**, 11663–11670.
- Zhou, Y. J., Burns, J. W., Morita, Y., Tanaka, T. & Estes, M. K. (1994).** Localization of rotavirus VP4 neutralization epitopes involved in antibody-induced conformational changes of virus structure. *J Virol* **68**, 3955–64.
- Zisis, G., Lambert, J. P., Marbebant, P., Marissens, D., Lobmann, M., Charlier, P., Delem, A. & Zygraich, N. (1983).** Protection studies in colostrum-deprived piglets of a bovine rotavirus vaccine candidate using human rotavirus strains for challenge. *J Infect Dis* **148**, 1061–1068.

Chapter 2: Modification of the rotavirus VP6 open reading frame containing expression cassettes

2.1 Introduction

Rotavirus capsid protein, VP6, has been reported as the most abundant protein and also a highly conserved protein (Estes & Kapikian, 2007). Rotavirus VP6 is considered a good candidate for vaccine development as VP6 has been shown to elicit humoral immune response (Nair *et al.*, 2016). In addition, the antibodies against VP6 bind to channel I thereby blocking the release of the viral mRNA (Aiyegbo *et al.*, 2013, 2014). This phenomenon has been proven in animal models through administration of VP6 as a subunit rotavirus vaccine which showed heterologous protection by a significant reduction of virus shedding (Lappalainen *et al.*, 2014, 2015; Vega *et al.*, 2013). In addition, rotavirus VP6 can also act as an adjuvant to other antigens (Blazevic *et al.*, 2016; Malm *et al.*, 2017). Rotavirus VP6 has been produced in different expression systems such as transgenic plants, insect cells using baculovirus, bacteria and yeasts (Bredell *et al.*, 2016; Dong *et al.*, 2005; Feng *et al.*, 2017; Lappalainen *et al.*, 2016a). One way to achieve high yields of VP6 protein in these different expression systems is due to codon optimisation.

Codon optimisation is a technique mostly used for expression of recombinant protein in heterologous hosts (Elena *et al.*, 2014; Gupta, 2003; Sharp & Li, 1986, 1987). Organisms each have their own codon usage. Genes from a specific organism may present with rare codons when expressed in a heterologous host, resulting in inefficient translation. Codon optimisation is therefore used to overcome this problem. It involves the introduction of synonymous mutations that favours expression of heterologous proteins in a desired host. There are different companies using different algorithms to design codon-optimised sequences. One example is GenScript that uses a patented algorithm that involves an *in silico* evaluation of around 10 000 candidate sequences in each round of analyses and the sorting matrix selects the 10 best sequence optimisations. Codon optimisation has been used in the recombinant production of pharmaceuticals, biofuels and industrial enzymes. An interesting example is the use of codon optimised genes for an anticancer drug (Huber *et al.*, 2014). Furthermore, it has been recently shown that codon optimisation in DNA vaccines targeting avian influenza virus H5N1 antigen coding sequences improved the immune potential in mice and chickens (Stachyra *et al.*, 2016).

In a previous M.Sc. study by Mr. M.S. Makatsa, various recombinant yeasts were engineered (Makatsa, 2015). These yeasts contained the open reading frame (ORF) encoding rotavirus VP6 for the RVA/Human wt/ZAF/GR10924/1999/G9P[6] strain. The ORF was codon optimised to favour expression in *Arxula adenivorans*, *Kluyveromyces lactis*

and *Pichia pastoris/Pichia angusta*. However, VP6 expression could only be obtained for the *Pichia pastoris/Pichia angusta* ORF shown in Figure 2.1 by the absence of bands in lanes VP6 KO and VP6 AO.

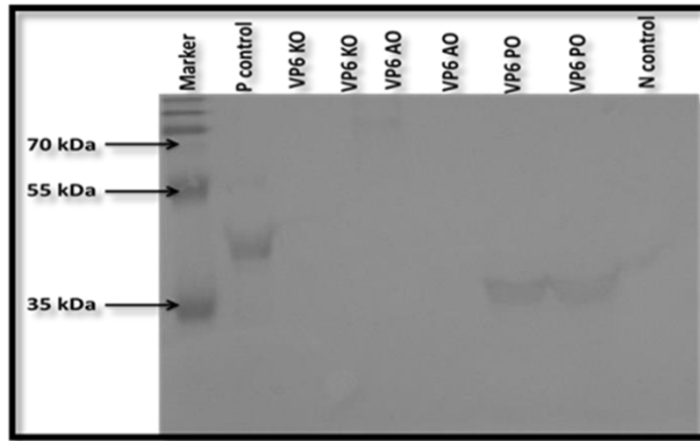


Figure 2.1: Western blot analysis of VP6 expression in *K. lactis*. Lane Marker is the PageRuler™ plus Prestained Protein Ladder (Thermo Scientific), lane P control is the bacterial expressed VP6, lanes VP6 KO is VP6 ORF codon optimised for expression in *K. lactis*, lanes VP6 AO is VP6 ORF codon optimised for expression in *A. adenivorans*, lanes, VP6 PO is VP6 ORF codon optimised for expression in *P. pastoris/P. angusta* and lane N control is untransformed yeast cells (copied from Makatsa, 2015).

In this chapter, the expression cassettes containing the *A. adenivorans* and *K. lactis* codon optimised ORFs were evaluated, and modified. Furthermore, to enhance the expression of VP6, the Kozak sequence, required for efficient translation in eukaryotes, was assessed for the different expression cassettes.

2.2 Materials and Method

2.2.1 General reagents, kits and enzymes

The following restriction enzymes *DpnI*, *EcoRI*, *BglIII*, *BamHI*, *BstXI*, *Eco47III*, *XhoI* together with their recommended buffers as well as other molecular biology enzymes and reagents such as T4 ligase, polynucleotide 5'-hydroxyl-kinase (PNK), Phusion High-fidelity DNA polymerase, 1KB DNA ladder, 6X loading dye, ATP, dNTPs were purchased from Thermo Fischer Scientific (USA). The BigDye® Terminator v3.1 Cycle Sequencing Kit was purchased from Applied Biosystems (USA).

For extraction and purification of DNA, the NucleoSpin® gel and PCR clean-up kits as well as the NucleoSpin® plasmid extraction kits were purchased from Macherey-Nagel (Germany). ethylenediaminetetraacetate (EDTA), 2-propanol, Tris (hydroxymethyl)

aminomethane, glacial acetic acid and absolute ethanol were purchased from Merck (Germany).

2.2.2 Virus stain, bacterial strains and culture cultivation

The consensus sequence of the South African rotavirus neonatal strain, RVA/Human wt/ZAF/GR10924/1999/G9P[6], was previously determined using 454 pyrosequencing directly from a stool sample obtained from the Dr George Mukhari Hospital at the Sefako Makgatho Health Sciences University (Potgieter *et al.*, 2009; Jere *et al.*, 2011). During a previous study, the rotavirus VP6 open reading frames (ORFs) were codon optimised for expression in *A. adenivorans* and *K. lactis*. The synthetic genes with desired restriction sites were purchased from GenScript™, cloned in pUC57 plasmid, while the VP6 *P. pastoris/P. angusta* codon optimised ORF (GeneArt™) was provided by Prof. J. Görgens from the Stellenbosch University (Makatsa, 2015).

Escherichia coli cells were purchased from New England BioLabs® (NEB®) [F' *proA+B+lac^f Δ(lacZ)M15 zzz::Tn10 (Tet^R) Δ(ara-leu) 7697 araD139 fhuA ΔlacX74 galK16 galE15 e14- Φ80dlacZΔM15 recA1 relA1 endA1 nupG rpsL (Str^R) rph spoT1 Δ(mrr-hsdRMS-mcrBC)*] and were used for plasmid manipulations. Cultivation of the *E. coli* cells was achieved using Luria-Bertani (LB) media which consisted of, per litre, 10 g tryptone (Merck), 5 g yeast extract (Merck), 10 g sodium chloride (Merck). To obtain solid media, 15 g agar (Merck) was added per litre of liquid LB media. For selection of transformed recombinant clones 100 µg/ml kanamycin (Calbiochem®) antibiotics was used.

2.2.3 Recombinant constructs

The VP6 *A. adenivorans* (AO) and *K. lactis* (KO) codon optimised ORFs were previously cloned into the wide-range yeast expression vector, pKM177 (Makatsa, 2015) to produce three recombinant expression vectors. The yeast expression vector contains the 18S rDNA and ITS rDNA (enhance integration) target sequence from *K. marxianus* that allows for genomic integration into the host yeast strain (Figure 2.2). The vector is under the control of a *Yarrowia lipolytica* TEF promoter and a *K. marxianus* inulinase terminator. The selection markers present in the expression vector are the *hph* gene which provides resistance to hygromycin B (Merck) to facilitate selection of successful integration of the ORFs into the yeasts genomes and a *Kan* gene which provide resistance to kanamycin to facilitate sub-cloning in *E. coli* cells (Figure 2.2). The ORFs were cloned into the *XhoI* and *Eco47III* restriction sites illustrated in Figure 2.2.

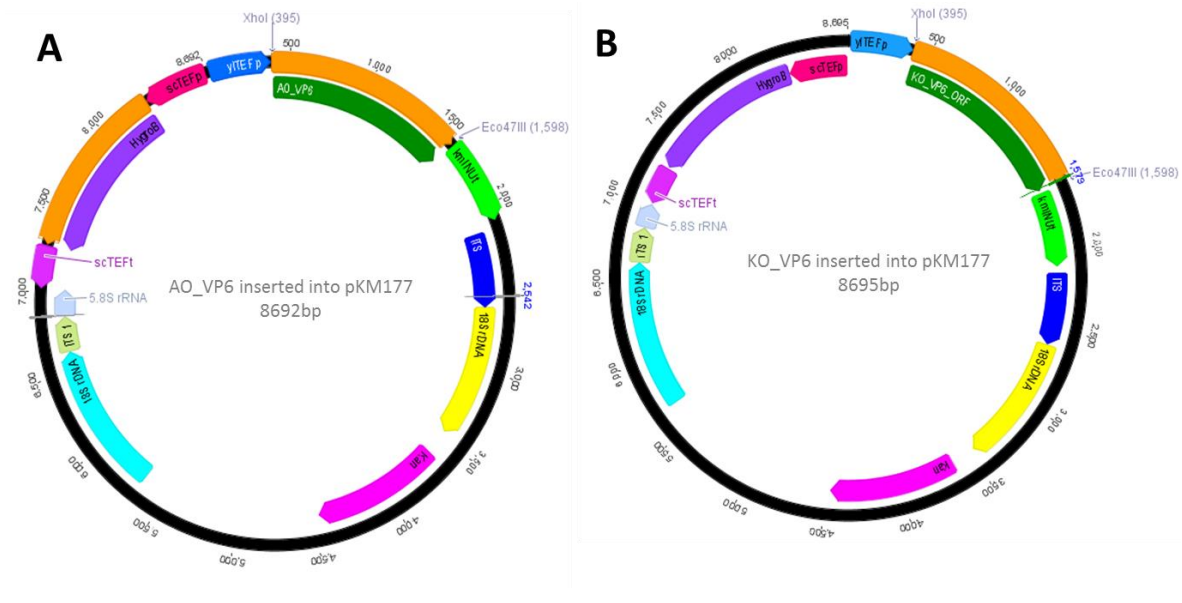


Figure 2.2: Recombinant plasmid constructs containing, A, *Axruia adeninivirans* optimised VP6 ORF (AO_VP6) and B, *Kluyveromyces lactis* optimised VP6 ORF (KO_VP6). The vector contains the hygromycin B resistance gene (hph) ■, *Y. lipolytica* TEF promoter (yITEFp) ■, *K. marxianus* inulinase terminator (kminUt) ■, kanamycin resistance gene (kan^R) ■, 18S rDNA target sequence that allows for genomic integration of the *Kluyveromyces marxianus* yeast ■ and *S. cerevisiae* TEF promoter (scTEFp) ■. The VP6 ORF was cloned at the *XhoI* and *Eco47III* restriction site.

2.2.4 General methods

2.2.4.1 Agarose gel electrophoresis

The 1% agarose gel contained 1 g agarose powder in 100 ml of 1 x Tris Acetic EDTA (TAE) electrophoresis buffer (40 mM Tris pH 8.3, 2 mM EDTA, 20 mM glacial acetic acid). To visualise the DNA under the UV light, the agarose gel was mixed with 0.5 µg/mL ethidium bromide (Sigma). The 1 kb GeneRuler DNA Ladder mix (Thermo Fisher Scientific) was used to track the amplicon size. To track the migration of the DNA samples during electrophoresis and to ensure the DNA samples sink into the wells a 1 X loading dye was mixed with the samples upon loading on the agarose gel. The electrophoresis was done using a BioRad™ system at 90 V for 45 minutes. The gel pictures were obtained with ChemiDoc™ MP Imaging System (Bio-Rad, USA).

2.2.4.2 Bacteria Competent cells

The *E. coli* competent cells were prepared using the rubidium chloride (RbCl₂) method (Hanahan, 1983) resulting in an expulsion of membrane proteins by allowing negatively charged DNA to bind to the membrane (Hanahan, 1983; Roychoudhury *et al.*, 2009). Briefly, a colony from a streaked LB culture plate was inoculated in 5 ml LB broth and incubated at 37°C overnight. A volume of 1.5 ml of the pre-inoculum was transferred to 50 ml LB media in a 500 ml flask and the culture was incubated at 37°C and shaking at 220 rpm using an Incubator Shaker ZWY – 240 (LABWIT) until the cells reached an OD₅₃₀ of 0.35. The cells

were transferred to a 50 ml centrifuge tube and left on ice for 15 minutes. The cells were harvested at 804 x g for 5 minutes at 4 °C. The cells were gently resuspended with 21ml ice-cold TF buffer 1 (100 mM RbCl₂, 50 mM MnCl₂, 30 mM KOAc, 10 mM CaCl₂, 15% glycerol) and incubated on ice for 90 minutes. The cells were harvested at 804 x g for 5 minutes at 4°C. The cells were further resuspended with 3.5 ml ice-cold TF buffer 2 (10 mM MOPS pH 7, 10 mM RbCl₂, 75 mM CaCl₂ and 15% glycerol) and 200 µl aliquots were prepared in 1.5 ml microfuge tubes. The cells were snap-frozen in liquid nitrogen and stored at -80°C.

2.2.4.3 Gel Purification of DNA fragments

The gel purification of digests and PCR products were carried out using NucleoSpin® Gel and PCR Clean-up kit (Macherey-Nagel, Germany) according to the manufacturer's protocol. Briefly, to dissolve the agarose slice containing the DNA the NTI buffer (200µl NTI per 100 mg gel) was added to the gel slice incubated at 50°C for 5-10 minutes with intermittent vortexing until the gel slice was completely dissolved. The samples were transferred to the NucleoSpin® Gel and PCR Clean-up Columns and centrifugation at 11 000 x g for 30 seconds to trap the DNA to the silica membrane. The flow-through was discarded. The columns were washed with 700 µl NT3 buffer containing ethanol to remove any remaining contaminants at 11 000 x g for 30 seconds. This step was repeated to minimise the presence of chaotropic salts from the NTI buffer. The flow-through was discarded. To remove any remaining NT3 in the column, the column was centrifuged again at 11 000 x g for 1 minute. The DNA was eluted with 15-30 µl elution buffer (pre-heated to 50°C) in a clean 1.5 ml microfuge tube incubated at room temperature for 1 minute and centrifuged at 11 000 x g for 1 minute.

2.2.4.4 Transformation of bacterial competent cells

The 200 µl competent cell aliquots were thawed on ice. A volume of 10 µl of the ligation mixture was added to the competent cells and incubated on ice for an hour. The cells were heat shocked at 42°C for 40 seconds. To allow the exogenous plasmid DNA to enter the bacteria, immediately after heat shock the cells were incubated on ice for 2 minutes. To revive the cells, 800 µl of LB media was added to the cells and incubated at 37°C Incubator Shaker ZW 240 (LABWIT) for an hour. Cells were plated on LB plates containing 30 µg/ml kanamycin and incubated at 37°C overnight.

2.2.4.5 Minilyate plasmid extraction

The plasmid extraction was carried out by STET boiling lysate miniprep protocol (Holmes & Quigley, 1981) for screening of positive clones. Prior to the plasmid extraction, several transformed bacterial colonies obtained following transformation (section 2.2.4.4) were inoculated with a sterile toothpick in 5 ml LB media containing 30 µg/ml kanamycin. A reference agar plate was also prepared. The cultures were incubated in 37°C shaking

overnight. The cells were harvested by centrifugation at 16 000 x g for 2 minutes at room temperature. The cells were resuspended in 250 µl STET buffer (8 g sucrose, 5 g Triton X-100, 50 mM EDTA (pH 8.0), 50 mM Tris (pH 8.0) per 100ml) containing 1 mg/ul lysozyme. The mixture was boiled for 1 minute which degrades chromosomal DNA as well as bacterial plasma membrane proteins forming a yellow to white pellet. Immediately after boiling the mixture was centrifuged at 16 000 x g for 8 minutes at room temperature. The pellet was removed with a sterile toothpick and discarded. The plasmid DNA was precipitated with 250 µl isopropanol and the plasmid DNA was pelleted by centrifugation at 16 000 x g for 8 minutes at room temperature. The supernatant was carefully removed and the precipitated DNA was vacuum-dried with a Speedy-vac at 60°C (Eppendorf). The plasmid DNA was resuspended with 0.1 x TE buffer from a stock solution of 1 xTE (1 M Tris and 0.5 M EDTA) containing (0.25 µg/ml) RNase.

2.2.4.6 Restriction digest

Digestions were performed according to manufacturer's instructions specific for each restriction enzyme. Generally the reactions contained 500-1000 ng DNA template, 1 x buffer, 1 U restriction enzyme and nuclease free water up to 20 µl. The digest reaction was incubated overnight at 37°C. If a double digest was carried out a web program (<http://www.thermoscientificbio.com/webtools/doubledigest/>) was used for recommendation of buffer. Digested DNA samples were analysed using agarose gel electrophoresis.

2.2.4.7 Plasmid purification for selected positive clones

The recombinant clones were purified according to the high-copy plasmid DNA extraction protocol from the NucleoSpin® Plasmid kit (Macherey-Nagel). Briefly, the corresponding positive colonies from the reference agar plates were inoculated in 5 ml LB media containing 30 µg/ml kanamycin. The cultures were grown at 37°C Incubator Shaker ZWY – 240 (LABWIT) overnight and the cells were harvested at 11 000 x g for 30 seconds. The supernatant was discarded and the pelleted cells were resuspended with 250 µl A1 buffer containing 0.4 mg/ml RNase. A volume of 250 µl lysis buffer (A2) was added and mixed by carefully inverting the tube 6-8 times and incubated at room temperature for 5 minutes. This was followed by the addition of 300 µl neutralisation buffer (A3), again mixed gently by inverting until the solution turns completely colourless. The neutralisation buffer precipitates the chromosomal DNA, proteins and cell debris. To separate these contaminants from the plasmid DNA, the solution was centrifuged for 5 minutes at 11 000 x g. A volume of 750 µl of the supernatant containing the plasmid DNA was transferred to the NucleoSpin® Plasmid/Plasmid (NoLid) column followed by centrifugation at 11 000 x g for 1 minute allowing the DNA to bind to the silica membrane and the flow-through was discarded. Contaminates such as salts, metabolites and soluble macromolecule cellular components

were removed by washing the membrane with 600 µl A4 buffer containing ethanol followed by centrifugation at 11 000 x g for 1 minute and the flow-through was discarded. The silica membrane was dried to remove the residual ethanol by centrifugation for 2 minutes at 11 000 x g. To elute the pure plasmid DNA, the NucleoSpin® Plasmid/Plasmid (NoLid) column was placed in a clean 1.5 ml microcentrifuge tube followed by the addition of 50 µl of alkaline buffer AE (5 mM Tris/HCl, pH 8.5) incubated at room temperature for 5 minutes and centrifuged at 11 000 x g for 1 minute.

2.2.4.8 DNA sequencing

The BigDye™ Terminator Cycle Sequencing Kit v3.1 (Applied Biosystems™) was used to verify the positive clones. The primers used are given in Table 2.1 and Table 2.2. Each sequence reaction contained 1 X sequencing buffer, 3.2 pmol of primer, 450 ng of template, 0.5 ul of premix (containing dNTPs, polymerase) and nuclease free water to a final volume of 10 µl. Thermal cycling was performed using the G-Storm Thermal Cycler System with the following conditions: initial denaturation 96°C for 1 minute, each reaction was subjected to 25 cycles of denaturation at 96°C for 10 sec, primer annealing at 50°C for 5 sec and extension at 60°C for 4 minutes.

The sequencing clean-up step was carried out according to the EDTA/Ethanol precipitation protocol recommended by the BigDye manual. The sequencing reaction was adjusted to 20µl with nuclease free water and transferred to a 1.5 ml microcentrifuge tube containing 125 mM EDTA and 60 µl 100% ethanol. The reaction was mixed by vortexing for 5 seconds. The reaction was subsequently incubated at room temperature for 15 minutes to precipitate, followed by centrifugation at 20 000 x g for 15 minutes at 4°C. The supernatant was carefully aspirated without disturbing the pellet. A volume of 200 µl of 70% ethanol was added to the precipitated DNA and centrifuged at 20 000 x g for 5 minutes at 4°C. The supernatant was carefully aspirated without disturbing the pellet. The reaction was vacuum dried with a Speedy-Vac (Eppendorf) for 5 minutes at 60°C. The samples were analysed on a 313xl Genetic Analyzer (Applied Biosystems™) at the Department of Microbial, Biochemical and Food Biotechnology, University of Free State. The nucleotide sequences obtained were compared to the *in silico* clones constructed with Geneious 6.1.2 (Biomatters). Only raw sequencing reads with quality scores of 60% and higher were used to conduct a *de novo* assemble.

2.2.5 Site directed mutagenesis

Site-directed mutagenesis was carried out using deletion-PCR by designing primers that exclude the first ATG codon at the promoter (γ TEF) site of the vector for pKM177_AOVP6

construct. The primers (Integrated DNA Technologies; IDT) used for the ORFs are shown in the Table 2.1.

Table 2.1: Primers used to carry out site-directed mutagenesis for pKM177 AOV6.

Codon optimized		Primer Name	Sequence	Melting temperature (T_m)
AO	Forward	pKMdelATG_AO_F	5'- CTCGAGCATGGATGTTTTGTATTC -3'	54.3°C
AO	Reverse	pKM177delATG_R	5'- TTCGGGTGTGAGTTGACAAGG -3'	57.3°C

2.2.5.1 Polymerase chain reaction (PCR) amplification for site-directed mutagenesis

To delete the ATG codon upstream of the cloned ORF, Phusion High-fidelity DNA polymerase (ThermoFisher Scientific) was used. The reaction had a final volume of 50µl which contained 1 x Phusion HF buffer, 200 µM dNTPs mix (Thermo Fisher Scientific), 0.5 µM of the forward and reverse primer (Table 2.1), 10 ng of the template DNA, 0.02 U Phusion DNA Polymerase and nuclease free water up to 50 µl. The reaction was subjected to 30 cycles using the G-Storm2 Thermal Cycler System. The initial denaturation was carried out at 98°C for 30 seconds. Each subsequent cycle consisted of 10 seconds denaturation at 95°C, 30 seconds for 64.3°C annealing and 15 seconds for 72°C annealing. A final extension step was included at 72°C for 5 minutes. A volume of 2 µl of the amplicon was analysed on a 1% agarose gel electrophoresis (section 2.2.4.1).

2.2.5.2 DpnI digests, purification of PCR amplicon

To ensure that only the PCR product would be used in subsequent experiments, a *DpnI* digest was carried out. In *E. coli*, DNA is usually methylated. Therefore, the *DpnI* restriction enzyme recognises the methylated sites of the plasmid DNA which will cleave the template plasmid DNA but does not cleave the PCR product as the PCR product is not methylated. The final volume of the digest reaction was 50 µl and contained 4 x Tango buffer, 2 U *DpnI* and 45 µl of the PCR reaction. The digest reaction was incubated at 37°C for 16 hours. The reaction was analysed on a 1% agarose electrophoresis 90 V for 45 minutes (section 2.2.4.1). The agarose gel containing the PCR products were weighed and transferred to a sterile 2 ml microcentrifuge tube. The purification of the amplicons were carried out using NucleoSpin® Gel and PCR Clean-up kit (Macherey-Nagel, Germany) as described in Section 2.2.4.3. The DNA was eluted with 100 µl of distilled water in a clean 1.5 microfuge tube incubated at room temperature for 1 minute and centrifuged at 11 000 x g for 1 minute. The DNA was concentrated by vacuum drying with a Concentrator (Eppendorf) for 3 hours. The dried DNA pellet was resuspended in 13 µl nuclease free water.

2.2.5.3 Ligation and transformation of mutant PCR product

The purified PCR product was self-ligated by performing a T4 ligation reaction. Since the PCR product resulted in a blunt end lacking a phosphate group at the 5' end, 0.75 U T4 polynucleotide kinase (Thermo Fisher Scientific) was used to catalyse the transfer of the γ -phosphate group to the 5'-OH group and 1 mM ATP (Thermo Fisher Scientific) acted as a cofactor. In addition, 1 X T4 ligase buffer (Thermo Scientific), 13 μ l purified DNA and 5 U T4 ligase (Thermo Fisher Scientific) were added making a final reaction volume of 20 μ l. The reaction was incubated for 3 hours at room temperature. The ligated recombinants were transformed in *E. coli* competent cells as described in Section 2.2.4.4.

2.2.5.4 Screening for mutated transformants and confirmation with Sanger sequencing.

The clones of the mutated transformants were extracted using the STET boiling lysate miniprep protocol (2.2.4.5). The digest reaction contained 2 μ l pKM177_ AOVP6 DNA, 1 X buffer O, 0.5 U *Bst*XI and nuclease free water to a final reaction volume of 20 μ l. The reactions were incubated at 37°C for 2 hours. The digest reaction were analysed with 1% agarose gel electrophoresis as described in section 2.2.4.1. The digest reactions were compared to the *in silico* cloning performed using Geneious 6.1.2.

Sanger sequencing was carried out to confirm successful site-directed ATG deletion of the construct at the promoter site (Section 2.2.4.8). The VP6 ORF was also sequenced to verify that no base change has occurred Table 2.2.

Table 2.2: Primers used for Sanger sequence verification of positive clones of the pKM177 AO VP6 construct.

Primer Name	Sequence	Melting temperature (T_m)	Manufacturer
VP6Seq AF1	5' -GGATGAGATGGTCCGAGA -3'	53.2°C	IDT
VP6Seq AF2	5' - ACTTATCAGGCCCGATTG -3'	54.5°C	IDT
VP6Seq AF3	5' -TCTATGCTGGTCAAGTAGAGC -3'	53.8°C	IDT
VP6Seq AR1	5'-CTTATCTCGGGCATCCTTCAG -3'	54.9°C	IDT
VP6Seq AR2	5' -CGGTTAAGAGTAAACGAGGC -3'	53.1°C	IDT
pKM_SeqF1	5' -GTCAAGACTGTCAAGGAGGG -3'	60.50°C	Inqaba

2.2.6 Cloning of VP6_KO into delATG_pKM177

The Kozak motif for the KO_VP6 ORF-containing expression cassette was corrected through sub-cloning of the original VP6_KO purchased from GenScript into the

delATG_pKM177 modified vector. This vector was prepared by a colleague, Mr. O.S. Folorunso.

2.2.6.1 Sub-cloning

The VP6_KO purchased from GenScript was supplied cloned into pUC57 vector at the *XhoI* and *Eco47III* sites. To obtain the KO VP6-encoding ORF from the pUC57, plasmid DNA was digested with *XhoI* and *Eco47III* restriction enzymes. Previously, a PhD student, Mr. O. S. Folorunso, performed site-directed mutagenesis to remove the ATG codon in the γ TEF promoter of the pKM177 cloning vector (delATG_pKM177). This plasmid, delATG_pKM177, was therefore also digested with *XhoI* and *Eco47III* restriction enzymes. The reaction contained 500 ng of template (delATG_pKM177/ pUC57_ KO VP6), 4 X Tango buffer, 1 U *XhoI* restriction enzyme, 1 U of *Eco47III* restriction enzyme and the nuclease free water up to 20 μ l.

The digest reactions were incubated overnight at 37°C. The digest was analysed using agarose gel electrophoresis as described in Section 2.2.4.1. The bands were excised with a sterile blade and the DNA purified from the gel with NucleoSpin Kit (Macherey-Nagel) as described in section 2.2.4.3, except that the DNA was eluted in 20 μ l elution buffer (NE buffer).

Prior to ligation, a ligation calculator (http://www.insilico.uni-duesseldorf.de/Lig_Input.html) was used to calculate the concentration of the insert that should be ligated to the vector using a vector:insert ratio of 3:1. Therefore, 47.9 ng of KO_VP6 ORF was ligated with 100 ng of delATGdel_pKM177 using 1 U T4 ligase enzyme in 1X ligation buffer and nuclease free water up to 20 μ l.

The ligation mixture was incubated for 18 hours at 16°C. A volume of 10 μ l of the ligation reaction was transformed in competent *E. coli* Top10 cells using the RbCl₂ method described in section 2.2.4.4. The screening of positive clones was firstly carried out by doing mini plasmid preparations as described in section 2.2.4.5. The *BglIII* restriction enzyme was used to screen for positive clones as described in Section 2.2.4.6. The enzyme has three restriction sites in the recombinant construct at 8 689 nucleotide (vector), 900 nucleotide (insert) and 4 471 nucleotide (vector) resulting in 3 fragment sizes of 903 bp, 4 218 bp and 3 571 bp. A control delATG_pKM177, was also included that resulted in two fragment sizes of 4 222bp and 3 352 bp. The positive clones were purified using the NucleoSpin® Plasmid kit (Macherey-Nagel) described in section 2.2.4.7. Verification of the clones were carried by Sanger sequencing using the BigDye™ Terminator Cycle Sequencing Kit v3.1, as described in section 2.2.4.8. The primers used are shown in Table 2.3 which were supplied from the Integrated DNA Technologies (IDT).

Table 2.3: Primers used for Sanger sequence verification of positive clones of the pKM177 KO VP6 construct.

Primer Name	Sequence	Melting temperature (T_m)	Manufacturer
VP6Seq KF1	5' -GGATGAAATGGTTAGAGAATCAC -3'	51.3°C	IDT
VP6Seq KF2	5' - CCAAGCAAGATTCGGTAC -3'	50.7°C	IDT
VP6Seq KF3	5' -GAGTGTTCACTGTCGCTTC -3'	53.4°C	IDT
VP6Seq KR1	5' - CTCAATGAATACAATACATCCATGCTCG -3'	56.0°C	IDT
VP6Seq KR2	5' -GTGAAAGATGCAGAGTAAGGGAAG -3'	55.4°C	IDT

2.3. Results

As indicated in the introduction of this chapter, no expression was seen for the AO and KO VP6 ORF-containing constructs during a previous study (Makatsa, 2015). This chapter focused therefore on the manipulation of these expression cassettes to enable expression.

Close inspection of the expression cassettes (pKM177_AOVP6 and pKM177_KOVP6) indicated an additional ATG codon at the promoter site upstream of the VP6 codon optimised ORFs (Figure 2.3).

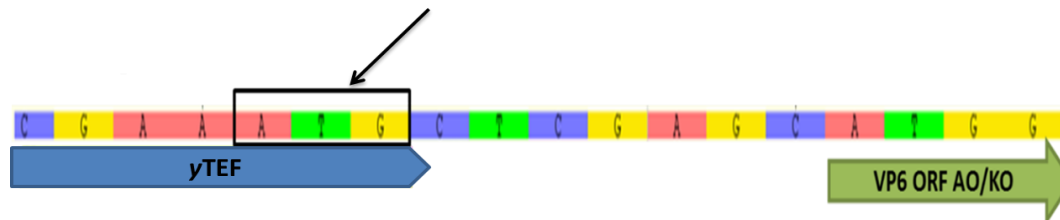


Figure 2.3: *In silico* clone of pKM177_AOVP6. The additional ATG (arrow) at the yTEF promoter site upstream the AO/KO ORF.

It was hypothesised that expression initiated at the first ATG which was not in-frame with the AO and KO VP6 ORFs and therefore no rotavirus VP6 expression was detected during the previous study. Another factor that was also considered is the Kozak sequence which enhances expression in eukaryotes (Kozak, 1981, 1986, 2002). The pKM177_AOVP6 and pKM177_KOVP6 clones were compared to the Kozak sequence.

2.3.1 Manipulation of *A. adenivorans* optimised rotavirus VP6 ORF-containing expression cassette

In order to remove the ATG sequence upstream of the AO rotavirus ORF, site-directed mutagenesis was performed by designing primers that excluded the ATG nucleotides as illustrated in Figure 2.4a. As can be seen in Figure 2.4b, the expected amplicon size for pKM177_AOVP6 without the ATG at the promoter site, 8 689 bp, was obtained. Non-

specific amplification during the delATG_pKM177_ AOVP6 amplification (Figure 2.4b, Lane1), but in Lane 2 in Figure 2.4b no non-specific amplification was observed.

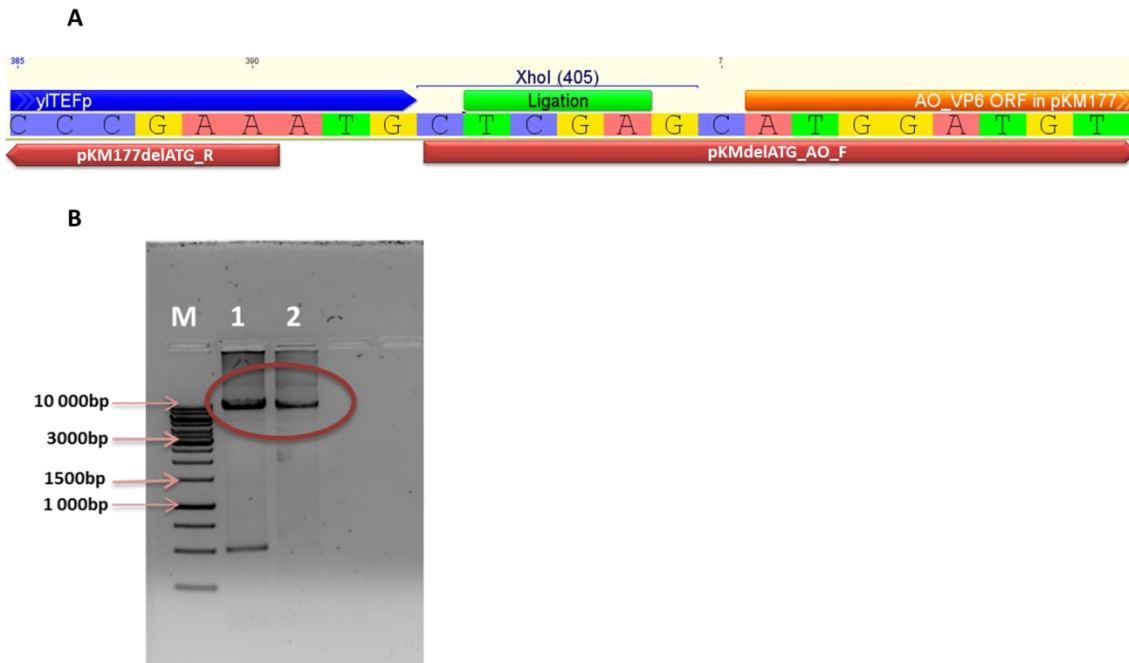


Figure 2.4: Deletion-mutagenesis using PCR. A, primer design, red, excluding the ATG at the pKM177 promoter site, blue. The AO VP6 ORF, orange, ligated, into the expression vector pKM177 at the *XhoI* restriction enzyme site, green. B, The reaction was analysed on a 1% agarose gel. Lane M is the 1 kb marker (ThermoFisher Scientific), lane1, 2 are the PCR products of pKM177_VP6 AO with an amplicon size of 8 689 bp (red circle).

The ligation reactions performed from the purified *DpnI* digest reaction were transformed into the competent cells. Thirty colonies were chosen for screening of positively transformed delATG_pKM177_AO VP6. *BstXI* restriction enzyme was used to screen for positive clones which has two restriction sites, namely at the vector site (at nucleotide 8 647) as well as at the VP6 insert (at nucleotide 1 172) resulting in two fragment sizes of 7 475 bp and 1 214 bp seen in Figure 2.5. Of the 30 clones screened, 12 clones (clone 1, 7, 8, 10, 11, 13, 15, 19, 21, 23, 25 and 30) showed the expected restriction enzyme profile, suggesting therefore that the AO VP6 ORF is present in these clones (Figure 2.5a).

The *BstXI* enzyme only indicated the presence of the AO VP6-encoding ORF and not if the deletion of the ATG was successful. Nucleotide sequencing was, therefore, performed to evaluate the success of the mutagenesis (Figure 2.6). Only 1 clone (clone 8 indicated with an arrow) out of the 9 clones screened had the correct ATG deletion at the promoter site (Figure 2.6).

The entire AO VP6 ORF was also sequenced to ensure that no additions or deletion of nucleotides occurred. The AO VP6 ORF from the delATG_pKM177_AOVP6 recombinant was aligned with the original AO VP6 ORF from GenScript shown in APPENDIX A and no base changes were detected in the ORF.

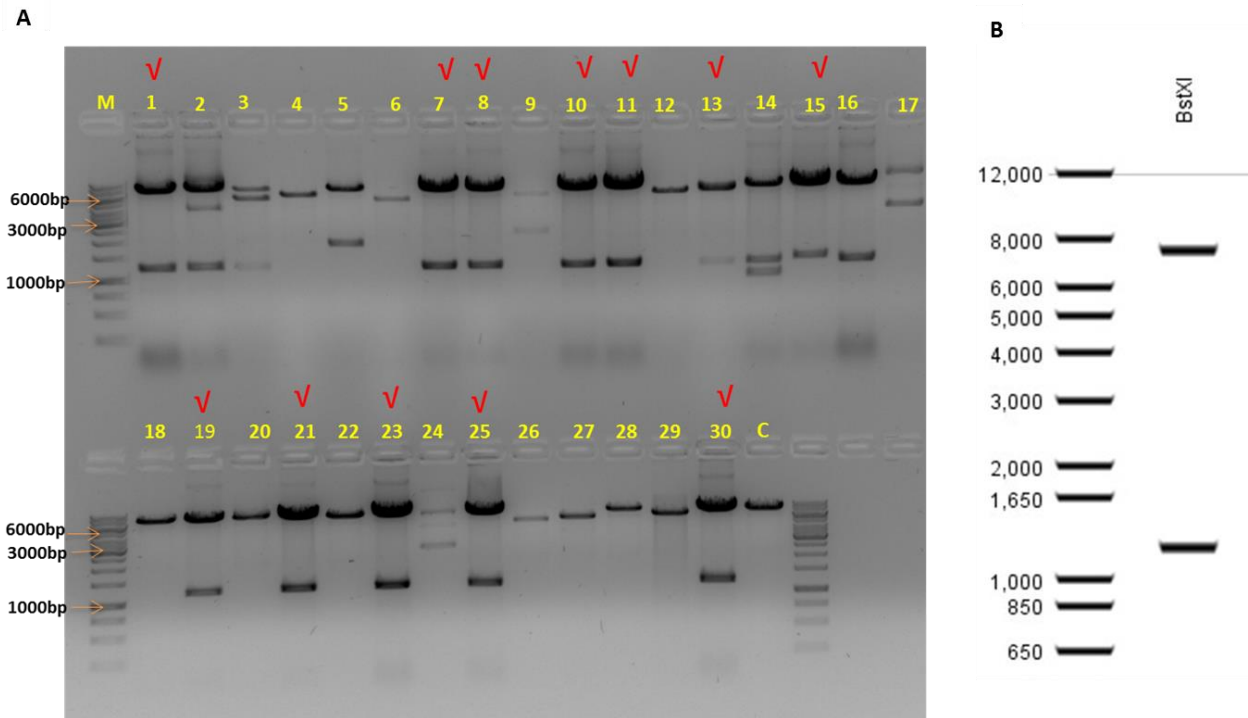


Figure 2.5: Agarose gel analysis of the restriction enzyme screening of positive clones for delATG_pKM177_VP6 AO construct. The *BstXI* restriction enzyme was used resulting in two fragment sizes of 7 475 bp and 1 214 bp. A, the digest reactions were analysed on a 1% agarose gel, M= 1 kb marker (ThermoFisher Scientific), lane 1-30 are the clones screened, lane C= the control which is the pKM177 cloning vector. Out of 30 clones 12 positive clones were identified, indicated with a red tick. B, an *in silico* clone was constructed using Geneious 6.1.2. to give the predicted sizes of the fragments.

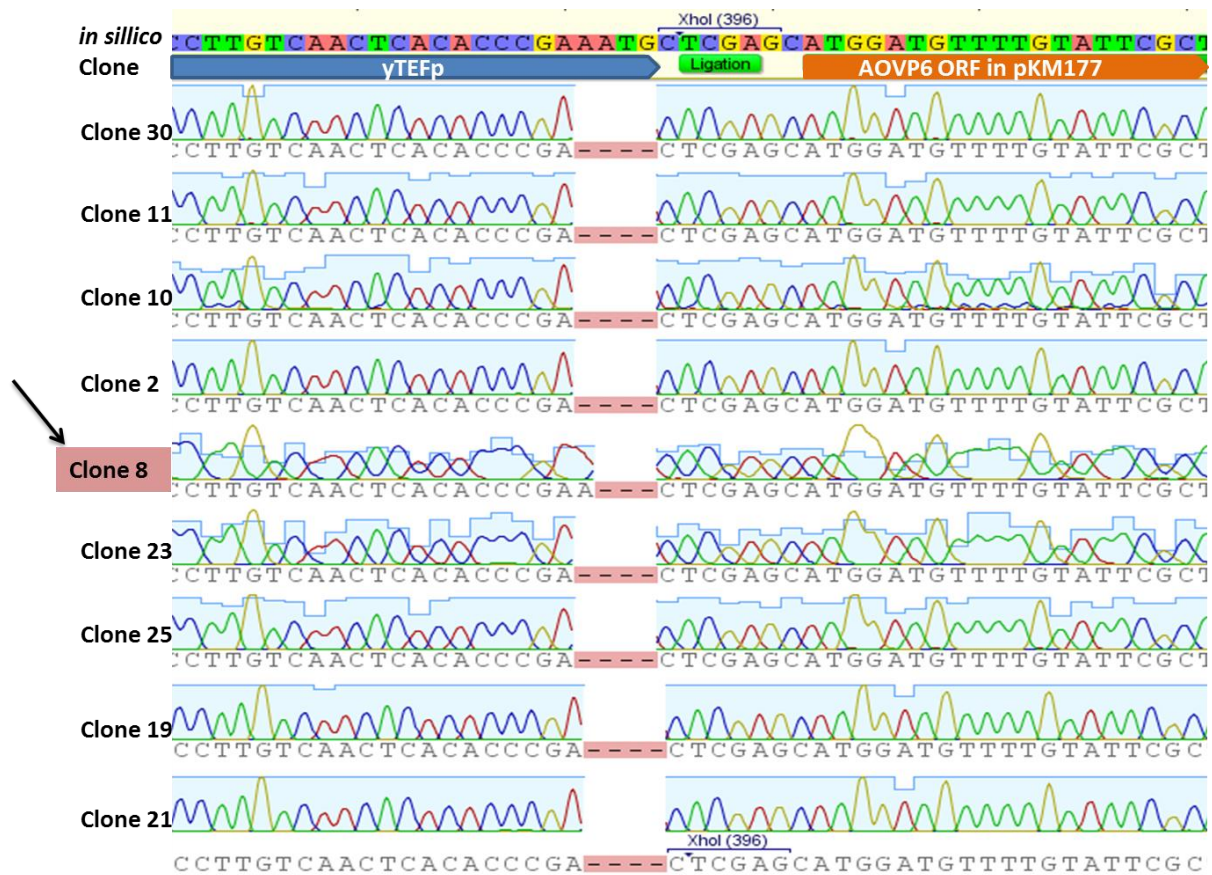


Figure 2.6: Sequencing chromatogram of AO VP6 ORF clones alignment with the *in silico* clone. Blue, *Y. lipolytica* TEF promoter. The AO VP6 ORF, orange, ligated, into the expression vector pKM177 at the *XhoI* restriction enzyme site, green. Correct ATG deletion indicated with an arrow, red.

2.3.2 Manipulation of *K. lactis* optimised rotavirus VP6 ORF containing expression cassette

Attempts to remove the upstream ATG in the KO VP6 ORF containing expression cassette were unsuccessful (results not shown). Since the ATG sequence in the original cloning vector was successfully removed by Mr. O.S. Folorunso, delATG_pKM177, the KO VP6 ORF was sub-cloned into this modified vector.

Both the vector and VP6 KO ORF cloned in pUC57 were successfully digested with the *XhoI* and *Eco47III* restriction enzymes (not shown). The *BglIII* restriction enzyme was used to screen for the correct ligated clones. The enzyme has three restriction sites at 8689 nucleotide (vector), 900 nucleotide (insert) and 4471 nucleotide (vector) resulting in 3 fragment sizes of 903 bp, 4 218 bp and 3 571 bp. A control was also included which was the cloning vector that resulted in two fragment sizes of 4 222 bp and 3 352 bp. Of the 20 clones screened 16 (1, 2, 3, 4, 5, 7, 9, 12, 13, 14, 15, 16, 17, 18, 19, and 20) showed the correct insertion (Figure 2.7a) and had the same profile as the *in silico* clones (Figure 2.7b).

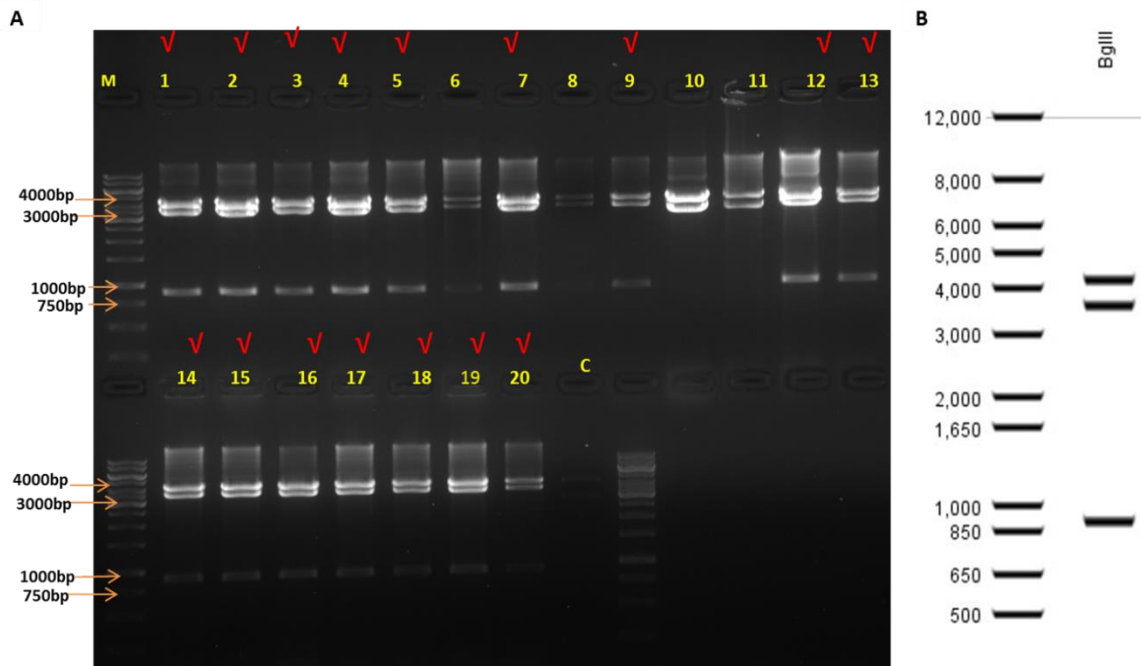


Figure 2.7: Agarose gel analysis of the restriction enzyme screening for positive clones of delATG_pKM177_VP6KO construct transformed into bacterial cells. The *BglIII* restriction enzyme was used and resulted in three fragment sizes of 903 bp, 3 571 bp and 4 218 bp. A, the digest reactions were analysed on a 1% agarose gel, M=1 kb marker (ThermoFisher Scientific), lane 1-20 are the clones screened, lane C= the control which is the delATG_pKM177 cloning vector. Of 20 clones, 16 showed have positive insertion indicated with a red tick. B, an *in silico* clone was constructed using Geneious 6.1.2. to give the predicted sizes of the fragments.

Of the 16 clones that showed to have the same profile as the *in silico* clone, 3 clones (1, 2, and 3) were verified by Sanger sequencing. Of the three clones, one clone showed the correct insertion of the ORF into the vector shown in Appendix B. As seen in Figure 2.8, ATG in the promoter region was present and the modified delATG_pKM177_KOVP6 expression cassette contained an optimal Kozak seq with a purine at -3 and C at -1. The entire KO VP6 ORF was also sequenced and no additions or deletions of nucleotides were observed (APPENDIX B).

2.4 Discussion

No rotavirus VP6 expression was previously observed for the AO and KO VP6 ORF-containing constructs (Makatsa, 2015) possibly due to the additional ATG that was out of frame with the ORF. Site-directed mutagenesis was used in this chapter to correct delATG_pKM177_AOVP6 (Figure 2.4 and Figure 2.8a). In Figure 2.4, non-specific amplification in lane 1, but not in lane 2, was observed. Since these were duplicate samples, the reason for the non-specific amplification in only lane 1 and not in lane 2 is unclear. Contamination in lane 1 could be a possible explanation for the non-specific amplification. A

low efficiency for site-directed mutagenesis was observed as the correct deletion of the ATG was observed in only 1 clone. The deleted ATG is preceded by 2 adenine bases and, indeed, in various of the clones screened it was observed that 2 adenine bases, instead of only 1, were deleted. This could be due to slippage by the DNA polymerase.

The delATG_pKM177_KOVP6 was corrected through sub cloning into the previously mutated pKM177 expression vector (delATG_pKM177) (Figure 2.8b). Site-directed mutagenesis using deletion PCR has been used as early as the 1980's (Hemsley *et al.*, 1989; Ho *et al.*, 1989). This method has been used for modification of products in various industries such as biocatalysis (Liu *et al.*, 2017; Madhavan *et al.*, 2017; Wang *et al.*, 2017).

Another factor to consider is the Kozak motif which plays a vital function in expression of proteins in eukaryotes (Kozak, 1981, 1984, 1986, 2002; Nakagawa *et al.*, 2008). Marilyn Kozak proposed a scanning mechanism for the initiation of translation in eukaryotes (Kozak, 1978, 1984). Efficient translation initiation is enhanced by a Kozak consensus sequence of GCCGCC(A/G)CCATGG (A/G represents A or G and ATG represents the translation initiation codon (Kozak, 1978, 1984; Nakagawa *et al.*, 2008). It was proposed that a purine (A/G) nucleotide at the -3 position and (C) nucleotide at the -1 position plays a crucial role in translation initiation in eukaryotes (Kochetov, 2014; Kozak, 1986; Pesole *et al.*, 2000). These nucleotides is thought to interact with eIF2 α which is required for initiation of translation in eukaryotes.

The ATG was successfully deleted for the delATG_pKM177_AOVP6 and delATG_pKM177_KOVP6 (Figure 2.8). In addition, these constructs contain a similar sequence as the Kozak sequence with adenine nucleotide at -3 position as well as cytosine nucleotide at the -1 position as seen in Figure 2.8 (indicated with arrows).

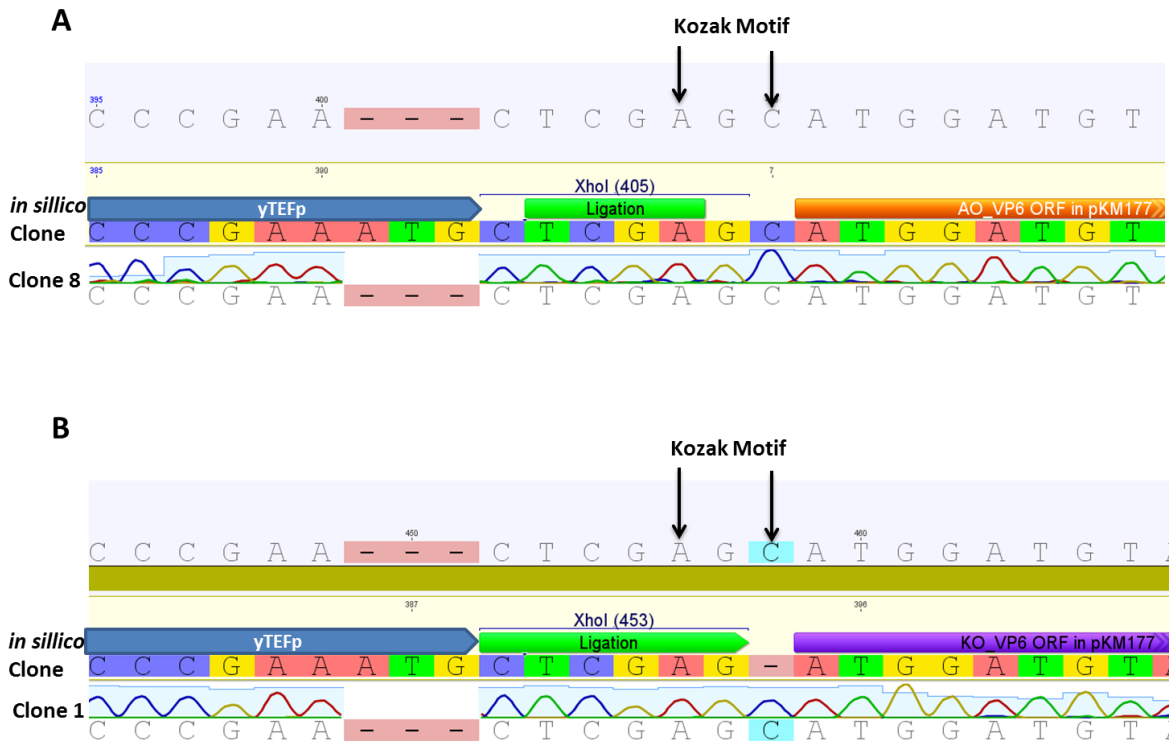


Figure 2.8: Analysis of sequence chromatogram of modified delATG_pKM177_AOVP6 and delATG_pKM177_KOVP6 aligned with *in silico* clones of the expected sequence using Geneious 6.1.2. A, *in silico* clone of AO VP6 ORF (orange) cloned into pKM177 expression vector aligned with modified delATG_pKM177_AOVP6 sequence at the promoter site (blue). B, *in silico* clone of KO VP6 ORF (purple) cloned into pKM177 expression vector aligned with modified delATG_pKM177_KOVP6 sequence at the promoter site (blue). The arrows indicates the -3 and -1 positions nucleotide playing a crucial role for Kozak sequence.

2.5 References

- Aiyegbo, M. S., Eli, I. M., Spiller, B. W., Williams, D. R., Kim, R., Lee, D. E., Liu, T., Li, S., Stewart, P. L. & Crowe, J. E. (2014). Differential accessibility of a rotavirus VP6 epitope in trimers comprising type I, II, or III channels as revealed by binding of a human rotavirus VP6-specific antibody. *J Virol* **88**, 469–76.
- Aiyegbo, M. S., Sapparapu, G., Spiller, B. W., Eli, I. M., Williams, D. R., Kim, R., Lee, D. E., Liu, T., Li, S. & other authors. (2013). Human Rotavirus VP6-Specific Antibodies Mediate Intracellular Neutralization by Binding to a Quaternary Structure in the Transcriptional Pore. *PLoS One* **8**, 12–14.
- Blazevic, V., Malm, M., Arinobu, D., Lappalainen, S. & Vesikari, T. (2016). Rotavirus capsid VP6 protein acts as an adjuvant in vivo for norovirus virus-like particles in a combination vaccine. *Hum Vaccines Immunother* **12**, 740–748.
- Bredell, H., Smith, J. J., Prins, W. A., Görgens, J. F. & Zyl, W. H. Van. (2016). Expression of rotavirus VP6 protein : A comparison amongst Escherichia coli , Pichia pastoris and Hansenula polymorpha. *FEMS Yeast Res* **16**, 1–12.
- Dong, J., Liang, B., Jin, Y., Zhang, W. & Wang, T. (2005). Oral immunization with pBsVP6-transgenic alfalfa protects mice against rotavirus infection. *Virology* **339**, 153–163.
- Elena, C., Ravasi, P., Castelli, M. E., Peir, S. & Menzella, H. G. (2014). Expression of codon optimized genes in microbial systems: Current industrial applications and perspectives. *Front Microbiol* **5**, 1–8.
- Estes, K. M. & Kapikian, A. (2007). Rotaviruses. In *Fields Virol*, 5 th., pp. 1917–74. Edited by D. Knipe, P. Howley, D. Griffin, R. Lamb, M. Martin, B. Roizman & S. Straus.
- Feng, H., Li, X., Song, W., Duan, M., Chen, H., Wang, T. & Dong, J. (2017). Oral Administration of a Seed-based Bivalent Rotavirus Vaccine Containing VP6 and NSP4 Induces Specific Immune Responses in Mice. *Front Plant Sci* **8**, 1–13.
- Gupta, S. (2003). Codon Optimization Shubhra Gupta. *Proj Report, Arizona State Univ* 1–12. www.guptalab.org/shubhg/pdf/shubhra_codon.pdf
- Hanahan, D. (1983). Studies on transformation of Escherichia coli with plasmids. *J Mol Biol* **166**, 557–580.
- Hemsley, A., Arnheim, N., Toney, M. D., Cortopassi, G. & Galas, D. J. (1989). A simple method for site-directed mutagenesis using the polymerase chain reaction. *Nucleic Acids Research* **17**, 6545–6551.
- Ho, S. N., Hunt, H. D., Horton, R. M., Pullen, J. K. & Pease, L. R. (1989). Site-directed mutagenesis by overlap extension using the polymerase chain reaction. *Gene* **77**, 51–59.
- Holmes, D. S. & Quigley, M. (1981). A rapid boiling method for the preparation of bacterial plasmids. *Anal Biochem* **114**, 193–197.
- Huber, K. V. M., Salah, E., Radic, B., Gridling, M., Elkins, J. M., Stukalov, A., Jemth, A. S., Göktürk, C., Sanjiv, K. & other authors. (2014). Stereospecific targeting of MTH1 by (S)-crizotinib as an anticancer strategy. *Nature* **508**, 222–227.
- Jere, K. C., Mlera, L., O'Neill, H. G., Potgieter, C. A., Page, N. A., Seheri, M. L. & Van Dijk, A. A.

- (2011). Whole Genome Analyses of African G2, G8, G9, and G12 Rotavirus Strains Using Sequence-Independent Amplification and 454 Pyrosequencing. *J Med Virol* **83**, 2018–2042.
- Kochetov, A. V. (2014).** Genome analysis AUG codons at the beginning of protein coding sequences are frequent in eukaryotic mRNAs with a suboptimal start codon context. *Bioinformatics* **21**, 837–840.
- Kozak, M. (1978).** How do eukaryotic ribosomes select initiation regions in messenger RNA *Cell* **15**, 1109–1123.
- Kozak, M. (1981).** Interaction of Eukaryotic Ribosomes with Messenger RNA: Evidence for a Scanning Mechanism. In *Int Cell Biol 1980–1981*, pp. 85–92. Edited by G. H. Schweiger. Springer, Berlin, Heidelberg.
- Kozak, M. (1984).** Compilation and analysis of sequences upstream from the translational start site in eukaryotic. *Nucleic Acids Research* **12**, 857–872.
- Kozak, M. (1986).** Point Mutations Define a Sequence Flanking the AUG Initiator Codon That Modulates Translation by Eukaryotic Ribosomes. *Cell* **44**, 283–292.
- Kozak, M. (2002).** Pushing the limits of the scanning mechanism for initiation of translation. *Gene* **299**, 1–34.
- Lappalainen, S., Pastor, A. R., Tamminen, K., López-guerrero, V. & Esquivel-guadarrama, F. (2014).** Immune responses elicited against rotavirus middle layer protein VP6 inhibit viral replication in vitro and in vivo. *Hum Vaccin Immunother* **10**, 2039–2047.
- Lappalainen, S., Pastor, A. R., Malm, M., Lopez-Guerrero, V., Esquivel-Guadarrama, F., Palomares, L. A., Vesikari, T. & Blazevic, V. (2015).** Protection against live rotavirus challenge in mice induced by parenteral and mucosal delivery of VP6 subunit rotavirus vaccine. *Arch Virol* **160**, 2075–2078.
- Lappalainen, S., Vesikari, T. & Blazevic, V. (2016).** Simple and efficient ultrafiltration method for purification of rotavirus VP6 oligomeric proteins. *Arch Virol* **161**, 3219–3223.
- Liu, Y., Huang, L., Jia, L., Gui, S., Fu, Y., Zheng, D. & Guo, W. (2017).** Improvement of the acid stability of *Bacillus licheniformis* alpha amylase by site-directed mutagenesis. *Process Biochem* **58**, 174–180.
- Madhavan, A., Sindhu, R., Binod, P., Sukumaran, R. K. & Pandey, A. (2017).** Bioresource Technology Strategies for design of improved biocatalysts for industrial applications. *Bioresour Technol* **245**, 1304–1313.
- Makatsa, M. S. (2015).** *Engineering yeast strains for the expression of South African G9P [6] rotavirus VP2 and VP6 structural proteins.* University of the Free State.
- Malm, M., Heinim, S., Vesikari, T. & Blazevic, V. (2017).** Rotavirus capsid VP6 tubular and spherical nanostructures act as local adjuvants when co-delivered with norovirus VLPs. *Clin Exp Immunology* **189**, 331–341.
- Nair, N., Newell, E. W., Vollmers, C., Quake, S. R., Morton, J. M., Davis, M. M., He, X. S. & Greenberg, H. B. (2016).** High-dimensional immune profiling of total and rotavirus VP6-specific intestinal and circulating B cells by mass cytometry. *Mucosal Immunol* **9**, 68–82.
- Nakagawa, S., Niimura, Y., Gojobori, T. & Tanaka, H. (2008).** Diversity of preferred nucleotide

sequences around the translation initiation codon in eukaryote genomes. *Nucleic Acids Research* **36**, 861–871.

Pesole, G., Gissi, C., Grillo, G., Licciulli, F., Liuni, S. & Saccone, C. (2000). Analysis of oligonucleotide AUG start codon context in eukariotic mRNAs. *Gene* **261**, 85–91.

Roychoudhury, A., Basu, S. & Sengupta, D. N. (2009). Analysis of comparative efficiencies of different transformation methods of *E. coli* using two common plasmid vectors. *Indian J Biochem Biophys* **46**, 395–400.

Sharp, P. M. & Li, W. (1986). Codon usage In regulatory genes in *Escherichia coli* does not reflect selection for 'rare' codons. *Nucleic Acids Research* **14**, 7737–7749.

Sharp, P. M. & Li, W. (1987). The codon adaptation index - a measure of directional synonymous codon usage bias, and its potential applications. *Nucleic Acids Research* **15**, 1281–1295.

Stachyra, A., Redkiewicz, P., Kosson, P., Protasiuk, A., Góra-sochacka, A., Kudla, G. & Sirko, A. (2016). Codon optimization of antigen coding sequences improves the immune potential of DNA vaccines against avian influenza virus H5N1 in mice and chickens. *Virology* **13**, 1–11.

Vega, C. G., Bok, M., Vlasova, A. N., Chattha, K. S., Gómez-Sebastián, S., Nuñez, C., Alvarado, C., Lasa, R., Escibano, J. M. & other authors. (2013). Recombinant Monovalent Llama-Derived Antibody Fragments (VHH) to Rotavirus VP6 Protect Neonatal Gnotobiotic Piglets against Human Rotavirus-Induced Diarrhea. *PLoS Pathog* **9**, 1–17.

Wang, C., Zhang, H., Li, M., Hu, X. & Li, Y. (2017). Functional analysis of truncated and site-directed mutagenesis dextranucrases to produce different type dextrans. *Enzyme Microb Technol* **102**, 26–34.

Chapter 3: Recombinant expression of Rotavirus VP6 in various yeasts

3.1 Introduction

Heterologous expression has been widely used in industry as well as in molecular research. The fundamental goal of heterologous expression especially in biotechnology is to produce high yield of a product to minimise cost. Rotavirus VP6 has been expressed in insect cells using baculovirus expression resulting in high yield production of proteins (Bertolotti-Ciarlet *et al.*, 2003; Crawford *et al.*, 1994), but scale-up of the VP6 protein is not commercially viable as this expression system is expensive. It does, however, remain the gold standard in recombinant rotavirus protein expression. Although *E. coli* can rapidly produce high yields of rotavirus VP6, a recent study by Bredell and co-workers showed that the VP6 protein produced tends to be insoluble (Bredell *et al.*, 2016) which correlates to what has been seen in previous studies (Mathieu *et al.*, 2001). The production of the insoluble VP6 protein in *E. coli* could be due to misfolding during over-expression. This may be due to overloading of the folding machinery as a result of high level protein expression, most likely during induced expression (Baneyx & Mujacic, 2004).

When using transgenic plants as an expression system for vaccine development, the plants should be edible. However, plants like tobacco leaves, which were used for rotavirus VP6 expression (Birch-Machin *et al.*, 2004; Inka *et al.*, 2012), are not edible. On the other hand, expression of rotavirus VP6 in plants like potatoes (Yu & Langridge, 2003) cannot be eaten raw as they have to be cooked first. Heat can denature the transgenic protein which could subsequently decrease the immunogenic property of the transgenic protein. Expression of rotavirus VP6 of an edible plant such as alfalfa resulted, however, in low antigen production (Dong *et al.*, 2005). Alternative approaches have been considered for using maize seed as an expression system and resulted in high yields of VP6 protein (Feng *et al.*, 2017).

Using yeast as an expression system is advantageous because it is easy to manipulate and scale-up is commercially viable. Rotavirus VP6 has been expressed in *S. cerevisiae* (Rodríguez-Limas *et al.*, 2011). However, *S. cerevisiae* tend to add high mannose glycans which results in hyperglycosylation (Cueva *et al.*, 2004). Methylotrophic yeasts such as *P. angusta* and *P. pastoris* are less prone to hyperglycosylation compared to *S. cerevisiae* (Ahmad *et al.*, 2014; Kang *et al.*, 1998; Teh *et al.*, 2011). Production of rotavirus VP6 in these methylotrophic yeasts had a sufficient production yield (Bredell *et al.*, 2016). Currently there are no reports on expression of VP6 protein in yeasts such as *Arxula adeninivorans*, *Kluyveromyces lactis*, *Debaryomyces hansenii* and *Yarrowia lipolytica*. *A. adeninivorans* is a

dimorphic yeast which has been used in biotechnological applications and is considered as safe for production of foreign proteins (Bischoff *et al.*, 2017; Böer *et al.*, 2009). *K. lactis* is mainly known to have the ability to convert lactone to lactic acid and had been extensively used in industrial applications (Breunig & Steensma, 2003). *Y. lipolytica* has a unique feature of biofuel production (Tai & Stephanopoulos, 2013) as well as lipase production (Najjar *et al.*, 2011). *D. hansenii* is an osmotolerant and an oleaginous yeast (Breuer & Harms, 2006; Kumar *et al.*, 2012; Onishi, 1986; Ratledge & H, 1986). This yeast is mostly in biotechnological applications (Breuer & Harms, 2006; Kumar *et al.*, 2012; Kurtzman *et al.*, 2011; Ratledge & H, 1986).

In this chapter, these yeasts as well as *P. angusta*, *P. pastoris* and *S. cerevisiae* from the UNESCO-MIRCEN yeast culture collection at UFS were screened for expression of rotavirus VP6 protein.

A unique wide-range yeast expression system has been developed at UFS containing a *Y. lipolytica* TEF promoter and a *K. marxianus* inulinase terminator. Genomic integration to the yeast cells is allowed by the *K. marxianus* 18S rDNA sequence with the addition of the ITS gene which enhances multiple homologous integration into the host genome (Albertyn *et al.*, 2011). The wide-range yeast expression system was used to achieve heterologous expression of rotavirus VP6 in the various yeasts described above.

3.2 Materials and methods

3.2.1 General chemicals, reagents and enzymes

The *NotI* restriction enzyme was purchased at Thermo Fisher Scientific. Hygromycin B antibiotic was supplied by Merck. Kanamycin antibiotic and Sodium Dodecyl Sulfate were supplied by Calbiochem®. The primary Goat polyclonal antibody raised against the Nebraska calf diarrhoea virus (NCDV) and secondary donkey polyclonal anti-goat IgG antibody were both supplied by Abcam. Tris (hydroxymethyl) aminomethane, yeast extract, peptone and methanol were purchased at Merck. D-(+)-glucose monohydrate, ammonium persulfate (APS) and sorbitol were purchased from Sigma.

3.2.2 Yeast strains and cultivation

To generate a control, rotavirus VP6 was expressed in bacteria. The VP6 ORF was previously cloned in the pCold II vector (pCold_VP6) was kindly provided by Prof. A. Van Dijk, North West University. The pCold_VP6 was transformed in *E. coli* BL21 (DE3) cells [F⁻, ompT, hsdSB (rB⁻, mB⁻), dcm, gal, λ(DE3); Stratagene] and the transformation was carried out using the rubidium chloride (RbCl₂) transformation method (Hanahan, 1983) as described in Chapter 2, Section 2.2.4.

The following yeast strains, *Arxula adenivorans* UFS1219, *Arxula adenivorans* UFS1220, *Debaryomyces hansenii* UFS0610, *Kluyveromyces lactis* UFS1167, *Pichia angusta* UFS0915, *Pichia angusta* UFS1507, *Pichia pastoris* UFS1552T, *Yarrowia lipolytica* UFS0097, *Yarrowia lipolytica* UFS 2221 and *Yarrowia lipolytica* UFS2415, were obtained from the UNESCO-MIRCEN yeast culture collection, Department of Microbial, Biochemical and Food Biotechnology, UFS. The following yeast strains, *Arxula adenivorans* LS3 and *Saccharomyces cerevisiae* CENPK, were kindly provided by Prof. J. Albertyn from the Department of Microbial, Biochemical and Food Biotechnology, UFS. The *Pichia pastoris* GS115 is a commercial strain (Invitrogen) and was kindly provided by to Prof. Smit and Prof. Opperman from the Department of Microbial, Biochemical and Food Biotechnology, UFS. *Yarrowia lipolytica* PO 1F was provided by Prof. Smit, the Department of Microbial, Biochemical and Food Biotechnology stored in liquid nitrogen. The yeast strains were revived on yeast mold (YM) agar plates incubated at 25°C for 3-4 days. The yeast colonies were inoculated in 5ml yeast extract peptone dextrose agar (YPD) broth and incubated at 30°C for 24 hours. The cultures were frozen at -80°C for short term storage containing 50% glycerol. The YPD broth or agar composition contained 20 g peptone (Merck), 20 g glucose (Sigma) and 10 g yeast extract (Merck) and for agar 15 g agar (Merck) to make 1 L.

3.2.3 Preparation of yeast competent cells

Yeast competent cells were prepared according to Klebe and co-workers, using bicine to make the cells competent by creating pores in the membrane (Klebe *et al.*, 1983). A pre-inoculum was prepared by inoculating a colony from the revived yeast cells on the YPD agar plate in 5 ml YPD broth. The culture was incubated for 24 hours at 30°C shaking, except for *P. angusta* which was incubated at 37°C. A volume of 1 ml of the pre-inoculum was transferred to 100 ml YPD media in a 1 L flask. The yeast cultures were incubated at 30°C shaking, except for *P. angusta* which was incubated at 37°C, until all the cultures reached OD₆₀₀ 0.6-0.8. The cells were harvested at 1 000 x g for 5 minutes. The cells were resuspended in 0.5 volume of solution 1 (1 M sorbitol, 10 mM bicine-NaOH (pH 8.35), 3 % ethylene glycol, 5% (v/v) DMSO (added before used) filter sterilised). The cells were centrifuged at 1000 x g for 5 minutes and resuspended with 2 ml of solution 1. A volume of 200 µl of the competent cells were aliquoted in 1.5 ml microfuge tubes. To increase the viability of the competent cells, the cells were slow-frozen by storing them at -20°C for 4-8 hours before transferring the competent cells to -80°C.

3.2.4 Yeast transformation

The modified constructs containing either AO or KO VP6 ORF cloned into the expression cassette (pKM177) without the ATG in the promoter region as described in Chapter 2 (delATG_pKM177_AOVP6 and delATG_pKM177_KOVP6) were transformed in 14 yeast

strains. The *P. pastoris/P. angusta* codon optimised VP6 ORF (delATG_pKM177_POVP6) construct, obtained from a colleague, Mr OS Folorunso, was also transformed into the 14 different yeast strains as described in Section 3.2.2. Mr. Folorunso modified the construct to include an optimal Kozak sequence and remove the promoter-region ATG.

Yeast transformation was carried out using the bicine protocol (Chen *et al.*, 1997). Briefly, 1 µg of the plasmid DNA, either delATG_pKM177_AOVP6 or delATG_pKM177_KOVP6 or delATG_pKM177_POVP6 were linearized with *NotI* endonuclease (Thermo Scientific) for 90 minutes at 37°C. The *NotI* endonuclease was inactivated at 80°C for 20 minutes. The linearized plasmid DNA was transformed into the competent cells along with 50 µg of salmon sperm carrier DNA (Life Technologies) and 1.4 ml of solution 2 (40% v/v PEG 1000; 200 mM bicine-NaOH, pH8.4). The mixture was vortexed for 1 minute and incubated at 30°C for an hour, except for *P. angusta* which was incubated at 37°C. The cells were heat shocked at 37°C for 10 minutes, except for *P. angusta* which was heat shocked at 42°C for 10 minutes. Cells were harvested at 2 328 x g for 5 minutes and resuspended in 500 µl of solution 3 (150 mM NaCl; 10 mM bicine-NaOH, pH8.4) and 500 µl YPD media. The cells were allowed to recover by incubating at 30°C (37°C for *P. angusta*) shaking for 2 hours and harvested again at 2 328 x g for 5 minutes. Approximately 800 µl of the supernatant was decanted and the remaining supernatant was used to resuspend the cells. The cells were plated on selective YPD plates containing 600 µg/ml hygromycin B (Merck) and incubated at 30°C (37°C for *P. angusta*) for 2-5 days until colonies were formed.

3.2.5 Evaluation of successful integration of the VP6 codon optimised ORFs into the yeast genomes

Screening for genomic integration of the expression cassette containing VP6 codon optimised ORFs to the yeast genomes was carried out by colony PCR. The colonies of the yeast clones that formed after transformation described in section 3.2.4 were transferred to a higher concentration of hygromycin B (800 µg/ml) YPD plates and incubated in MEMMERT oven (Lasec) at 30 °C, or *P. angusta* at 37°C, overnight. Positive integration of the respective expression cassettes were evaluated by KAPA Taq DNA polymerase (KAPA Biosystems) or Dream Taq polymerase (Thermo Scientific) or DreamTaq Green PCR Master Mix (2 X) (Thermo Scientific) according to the manufacturer's instructions. The primers (IDT) that were used are given in Table 3.1.

Table 3.1: Primers used for screening the integration of VP6 ORFs in various yeasts genome.

	Primer Name	Sequence	Amplicon size
VP6_AO	VP6Seq_AF2	5'- ACTTATCAGGCCCGATTTCG -3'	665 bp
	pKM173/177_R	5'- GAACAGCTAGAGTGCGTT -3'	
VP6_KO	VP6Seq_KF2	5'- CCAAGCAAGATTTCGGTAC -3'	667 bp
	pKM173/177_R	5'- GAACAGCTAGAGTGCGTT -3'	
VP6_PO	VP6Seq_PF2	5'- CAACACCTACCAAGCTAGA -3'	670 bp
	pKM173/177_R	5'- GAACAGCTAGAGTGCGTT -3'	
VP6_PO	VP6Seq_PF3	5'- GAGTTTTTCACCGTTGCTTC -3'	330 bp
	pKM173/177_R	5'- GAACAGCTAGAGTGCGTT -3'	

Prior to the amplification reaction, cells from 800 µg/ml hygromycin B YPD plates were selected and transferred with a sterile toothpick to 25 µl nuclease free water. The cells were denatured at 98°C for 10 minutes using the G-Storm PCR System to liberate the yeasts genomes. The KAPA Taq DNA polymerase (Roche) reaction contained 1 x KAPA Taq Buffer, 0.4 µM forward and reverse primer, respectively, 0.2 mM dNTP mix, 1 U KAPA Taq DNA Polymerase and nuclease free water to a final reaction volume of 50 µl. The Dream Taq Green Polymerase (Thermo Fisher Scientific) reaction contained 1 X DreamTaq Green Buffer, 0.4 µM forward and reverse primer, respectively, 0.2 mM dNTP mix, 1.25 U DreamTaq DNA Polymerase and nuclease free water to a final reaction volume of 50 µl. The DreamTaq Green PCR Master Mix (2 X) reaction contained 1 X DreamTaq Buffer, 0.4 µM forward and reverse primer, respectively, 12.5 µl of DreamTaq Green PCR Master Mix (containing 2 X DreamTaq Green buffer, 0.4 mM dNTP mix, 4 mM MgCl₂, 1.25 U Dream Taq Polymerase) and nuclease free water to a final reaction volume of 50 µl.

The conditions for the partial amplification of the AO VP6 ORF containing expression AO VP6 ORF containing expression cassette were as follows: initial denaturation was at 95°C for 3 minutes, followed by 35 cycles of denaturation at 95°C for 30 seconds, annealing at 46.5°C for 30 seconds and extension at 72°C for 1 minute. Final extension was at 72°C for 5 minutes. The conditions for the partial amplification of the KO VP6 ORF containing expression cassette were as follows: initial denaturation was at 95°C for 3 minutes, followed by 35 cycles of denaturation at 95°C for 30 seconds, annealing at 48.4°C for 30 seconds and extension at 72°C for 1 minute. Final extension was at 72°C for 5 minutes. Lastly, conditions

for the partial amplification of the PO VP6 ORF containing expression cassette were as follows: initial denaturation was at 95°C for 3 minutes, followed by 35 cycles of denaturation at 95°C for 30 seconds, annealing at 47.1°C for 30 seconds and extension at 72°C for 40 1 minute. Final extension was at 72°C for 5 minutes.

The template plasmids were also partially amplified as positive controls. A no template-containing reaction, as PCR negative control, was included as well as untransformed yeast cells as a negative cell control. The reactions were analysed on a 1% agarose gel as described in section 2.2.4.1. The bands were stained with 0.5 µg/mL ethidium bromide and visualised using ChemiDoc™ MP imaging system (Bio-Rad).

3.2.6 Expression of rotavirus VP6 in various yeasts

The yeast colonies that showed integration of the respective rotavirus VP6 ORF-containing expression cassettes into the yeast genomes were evaluated for expression in the 14 yeast stains (Section 3.2.2). A pre-inoculum was prepared for each of the yeast colonies in 5 ml YPD media and incubated in a 30°C, shaking for 24 hours except for *P. angusta* which was incubated at 37°C. A volume of 500 µl of the pre-inoculum was transferred to 50ml YPD media in a 500 ml Erlenmeyer flask. The culture was incubated at 30°C (37°C for *P. angusta*), shaking for 14-16 hours. The cells were harvested at 10 000 x g for 10 minutes at 4°C and resuspended in 50 mM Tris buffer pH 7.4 (3 ml per gram wet cells) containing Protease Inhibitor Cocktail (Sigma). The cells were lysed using a One Shot Constant Cell Disruption System (Constant Systems, United Kingdom) at 35 kPsi. The insoluble debris was separated from the soluble fraction by centrifugation at 20 000 x g for 30-45 minutes at 4°C. The supernatant which contained the soluble fraction was transferred to a clean sterile 1.5 ml microfuge tube. Evaluation of VP6 expression by the yeasts strains was carried out by western blot analysis as described in Section 3.2.10.

3.2.7 Bacterial expression of rotavirus VP6 as a positive control

E. coli previously transformed with pCOLD_VP6 (Makatsa, 2015) were revived by streaking on 100ug/ml ampicillin containing LB plates and incubated overnight at 37°C. A colony was transferred to 5 ml LB broth containing 100 µg/ml ampicillin and incubated overnight in a 37°C shaker as a pre-inoculum. The expression was carried out according to the pCold™ Cold Shock Expression System (TAKARA) protocol. Briefly, 500 µl of the pre-inoculum was transferred to 50 ml LB media containing 100 µg/ml ampicillin in a 500 ml Erlenmeyer flask. The culture was incubated at 37°C shaking until the cells reached an OD₆₀₀ ~0.4-0.5. The cells were cooled to 20°C and 1 mM isopropyl β-D-1-thiogalactopyranoside (IPTG) (Sigma) was added as inducer. The culture was incubated at 20°C shaking for 3 hours. Cells were harvested at 10 000 x g for 10 minutes at 4°C. Cells were lysed using a lysis buffer

containing 1% SDS and 1 X TE (3 ml per 1 g) containing cOmplete™ Protease Inhibitor Cocktail (Roche) and incubated for 30 minutes. The insoluble debris was separated from the soluble fraction by centrifugation at 16 000 x g for 20 minutes at 4°C. The supernatant which contained the soluble fraction was transferred to a clean 1.5 ml microfuge tube and was analysed by western blot as described in Section 3.2.10.

3.2.8 Protein concentration determination

Total protein concentration was determined with the Pierce™ BCA protein assay kit (Thermo Scientific™ Pierce™) using the microtiter plate protocol and performed in duplicate. The Pierce™ BCA protein assay kit quantifies total protein by means of a detergent-compatible formulation based on bicinchoninic acid (BCA). Reaction of BCA with amino acids, cysteine, tryptophan and tyrosine, as well as peptide bonds is responsible for colour formation (Wiechelman *et al.*, 1988).

Firstly, a standard was constructed using bovine serum albumin (BSA). Dilutions were prepared in 50 mM Tris buffer pH 7.4 (Appendix C). A BCA Working Reagent (WR) was prepared using a 50:1 ratio (Reagent A:Reagent B). A volume of 200 µl WR was mixed with 25 µl of the sample using a vortex for 30 seconds, followed by incubation at 37°C for 30 minutes. The absorbance was measured at 562 nm on a plate reader (SpectraMax® M2; Molecular Devices). A standard curve was constructed by calculating the average of sample (as this was done in duplicates) which was subtracted using the blank (containing 50 mM Tris buffer containing Protease Inhibitor Cocktail). For determination of unknown protein concentration, 200 µl WR was added in each well and mixed with the 25 µl of the unknown protein, mixed with a vortex and incubated at 37°C for 30 minutes. The absorbance was measured at 562 nm on a plate reader (SpectraMax® M2; Molecular Devices). The protein concentration was calculated by using the standard curve equation $y=mx+c$.

3.2.9 Sodium dodecyl sulphate polyacrylamide gel electrophoresis (SDS-PAGE)

A 10% SDS-PAGE gel was prepared according to Green and Sambrook, 2012. The separation gel contained 10% acrylamide/bis-acrylamide (Sigma), 375 mM Tris (pH 8.8), 0.1% SDS, 0.1% ammonium persulfate (APS; Sigma), 0.008% tetramethylethylenediamine (TEMED; Sigma). The stacking gel contained: 5% acrylamide/bis-acrylamide (Sigma), 0.06 mM Tris (pH 6.8), 0.1% SDS, 0.1% APS, 0.008% tetramethylethylenediamine (TEMED; Sigma).

The protein concentration determined in section 3.2.8 was used to calculate the amount of total protein to be loaded. Per gel, each well contained an equal amount of total protein. The protein samples were mixed with sample buffer (50 µl beta-mercaptoethanol (Merck) and 950 µl Laemmli sample buffer (Bio-Rad) in a 1:1 ratio and heated at 98°C for 10 minutes to

denature proteins. The samples were loaded along with the 3 µl PageRuler™ Prestained Protein Ladder (Thermo Fisher Scientific) or Spectra™ Multicolor Broad Range Protein Ladder (Thermo Fisher Scientific) as a size reference. The SDS PAGE gels were electrophoresed in 1% TGS buffer (25 mM Tris; 129 mM Glycine; 0.1% (w/v) SDS, pH 8.3) with PowerPac™ Basic Power Supply (BioRad™) at 200 V for an hour.

3.2.10 Western Blot analysis

Verification of recombinant expression of the VP6 protein was carried out by Western blot analysis. The proteins were transferred to a BioTrace™ NT Nitrocellulose Transfer Membrane (Pall Corporation) from the SDS-PAGE gel for an hour at 100 V in a transfer buffer containing 0.025 M Tris, 0.2 M glycine and 20% methanol (pH 8.4). Verification of the transfer of the proteins to the Nitrocellulose Transfer Membrane was carried out by staining the membrane with 0.25% of Ponceau S (Sigma) solution in 1% acetic acid for 10 minutes at room temperature. After verification of the transfer, the Ponceau S solution was removed from the membrane by washing the membrane with distilled water.

The membrane was blocked with 5% fat free instant milk powder (Spar) in Tris-buffered saline (TBS) containing 0.2% Tween-20 (Sigma) (0.2% TBS-T). The blocking solution was discarded and the membrane was washed with 0.2% TBS-T buffer three times, each wash for a period of 10 min. The membrane was incubated with primary goat polyclonal antibody raised against the Nebraska calf diarrhoea virus (NCDV) strain (Abcam) with a dilution of 1:500 in 0.2% TBS-T buffer for 3 hours at room temperature. The primary antibody dilution was discarded from the membrane and the unbound primary antibodies were removed by washing the membrane 3 times with 0.2% TBS-T buffer for 10 minutes each. The membrane was subsequently incubated with the secondary donkey polyclonal anti-goat IgG antibody (Abcam) with a 1:1000 dilution in 0.2% TBS-T buffer for one hour at room temperature. The unbound antibodies were removed by washing the membrane with 0.2% TBS-T buffer three times, each wash for a period of 10 min

Detection of the proteins on the membrane were carried out by 4-chloro-1-naphthol peroxidase substrate detection method (Green & Sambrook, 2012). Briefly, one tablet of the 4-chloro-1-naphthol (Sigma) was dissolved in 10 ml methanol. Two millilitres of the dissolved 4-chloro-1-naphthol was added to 5 ml 1x TBS buffer containing 0.15% hydrogen peroxide to make a final volume of 6 ml. The 4-chloro-1-naphthol solution is a substrate for the horseradish peroxidase which is conjugated to the secondary antibody. A volume of 6 ml of 4-chloro-1-naphthol solution was added to the membrane at room temperature and incubated for 15 – 30 minutes in the dark as the reaction is sensitive to light. This reaction results in a purple colour precipitate.

3.3 Results

3.3.1 Transformation of yeast strains with recombinant yeast expression plasmids

The modified constructs with optimal Kozak sequences, to enable expression in yeast, were transformed into various yeast strains. There was a variation in the number of colonies formed among the strains transformed with the different modified constructs on YPD plates containing 600 µg/ml hygromycin B antibiotic (Merck) as seen in Table 3.2. The colonies were formed either after 48 hours or 72 hours (Table 3.2).

Table 3.2: Colony formation by transformed yeasts

Yeast	Strain	Time for colony formation	Average number of colonies formed
<i>Arxula adenivorans</i>	UFS1219	72 hours	≤5
<i>Arxula adenivorans</i>	UFS1220	72 hours	>50
<i>Arxula adenivorans</i>	LS3	72 hours	<20
<i>Debaryomyces hansenii</i>	UFS0610	No colonies formed	
<i>Kluyveromyces lactis</i>	UFS1167	48 hours	<50
<i>Pichia angusta</i>	UFS0915	48 hours	>50
<i>Pichia angusta</i>	UFS1507	48 hours	<50
<i>Pichia pastoris</i>	GS115	72 hours	<20
<i>Pichia pastoris</i>	UFS1552T	72 hours	<50
<i>Saccharomyces cerevisiae</i>	CENPK	48 hours	>50
<i>Yarrowia lipolytica</i>	PO 1F	72 hours	>50
<i>Yarrowia lipolytica</i>	UFS0097	72 hours	<50
<i>Yarrowia lipolytica</i>	UFS2221	72 hours	<50
<i>Yarrowia lipolytica</i>	UFS2415	No colonies formed	

The colony formation of *K. lactis*, *S. cerevisiae* and the *P. angusta* strains was faster than for the other yeast strains (Table 3.2). There were no colonies formed on the *D. hansenii* and *Y. lipolytica* UFS2415 strains. The number of colony formation among the yeasts varied as *S. cerevisiae*, *A. adenivorans* UFS1220 and *P. angusta* strains contained more than 50 colonies on the 600 µg/ml YPD plate. A low number of colonies was formed by *A. adenivorans* UFS1219 (5 or less). The colony formation by *A. adenivorans* LS3 strain varied among the three VP6 cassettes (not shown).

3.3.2 Integration of expression cassettes containing VP6 ORFs into the yeast genomes

3.3.2.1 Integration of the expression cassette containing VP6 ORF codon optimised for expression in *A. adenivorans* in various yeasts

Screening for the integration of the AO VP6 ORF containing expression cassette into the various yeast genomes was carried by colony PCR using VP6Seq_AF2 as a forward primer and pKM173/177_R resulting in an amplicon of 665 bp (Figure 3.1). The results obtained for integration into the genomes of *A. adenivorans* strains UFS1219, 1220, *P. angusta* strains UFS0915, UFS01507 and *Y. lipolytica* PO-1F are provided in Figures 3.2-3.6. The remainder of the results are shown in Appendix D.

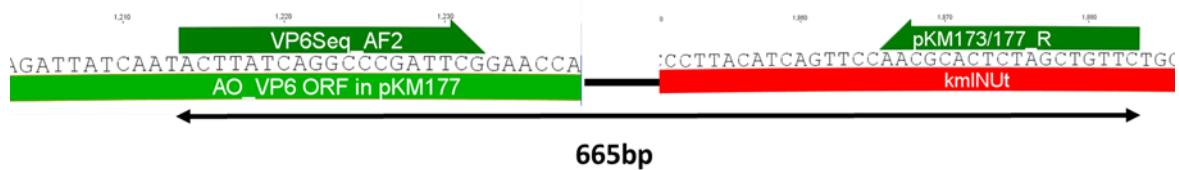


Figure 3.1: Primer annealing to the AO VP6 ORF containing expression cassette. AO VP6 ORF (light green). *K. marxianus* inulinase terminator (red). Forward and reverse primer (dark green).

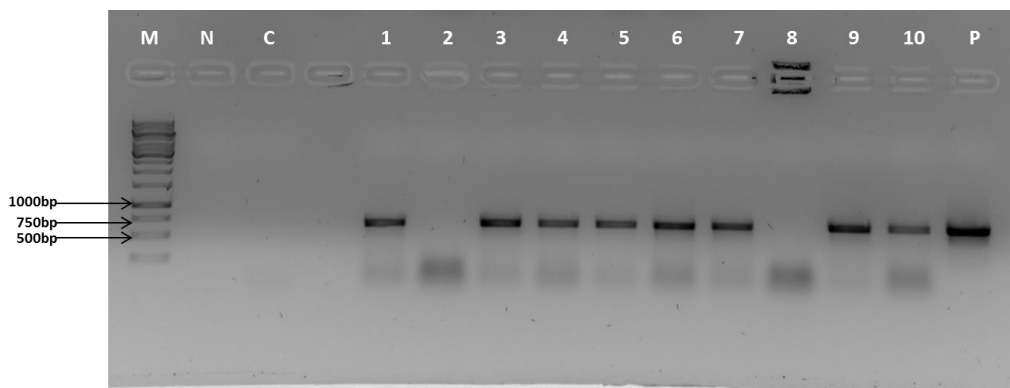


Figure 3.2. Analysis of the AO VP6 ORF containing expression cassette integration into the genome of *A. adenivorans* UFS1220 on a 1% agarose gel. Lane M: GeneRuler DNA Ladder mix. Lane N: negative PCR control, Lane C: untransformed *A. adenivorans* UFS1220 cells. Lane 1-10: Yeast colonies screened for integration of AO VP6 ORF into *A. adenivorans* UFS1220. Lane P: positive control.

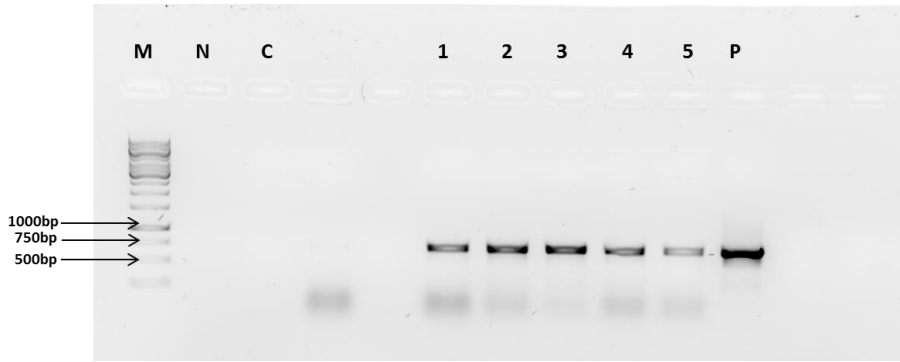


Figure 3.3: Analysis of the AO VP6 ORF containing expression cassette integration into the genome of *A. adenivorans* UFS1219 on a 1% agarose gel. Lane M: GeneRuler DNA Ladder mix. Lane N: negative PCR control, Lane C: untransformed *A. adenivorans* UFS1219 cells. Lane 1-10: Yeast colonies screened for integration of AO VP6 ORF into *A. adenivorans* UFS1219. Lane P: positive control.

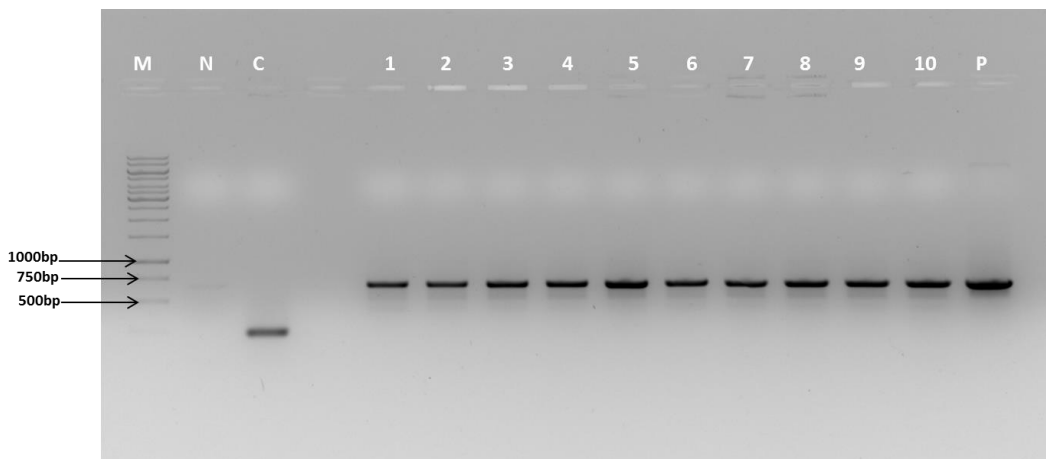


Figure 3.4: Analysis of the AO VP6 ORF containing expression cassette integration into the genome of *P. angusta* UFS0915 on a 1% agarose gel. Lane M: GeneRuler DNA Ladder mix. Lane N: negative PCR control, Lane C: untransformed *P. angusta* UFS0915 cells. Lane 1-10: Yeast colonies screened for integration of AO VP6 ORF into *P. angusta* UFS0915. Lane P: positive control.

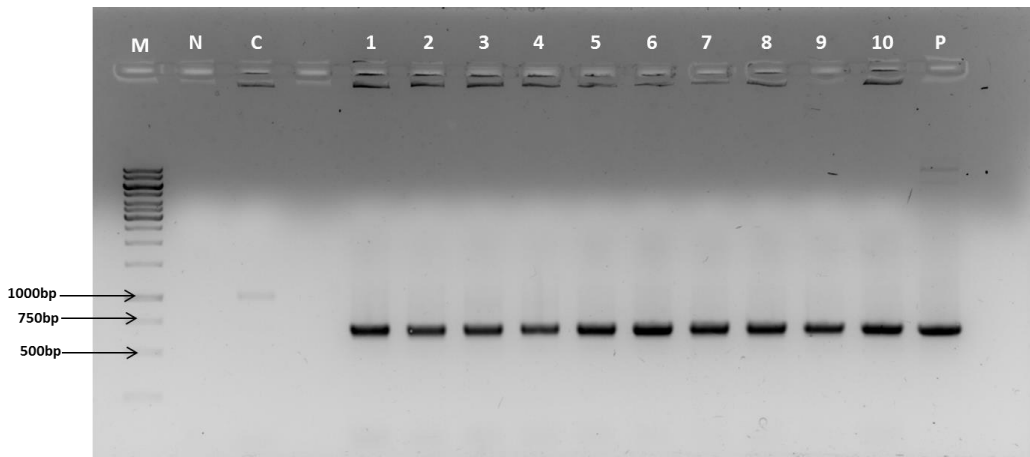


Figure 3.5: Analysis of the AO VP6 ORF containing expression cassette integration into the genome of *P. angusta* UFS1507 on a 1% agarose gel. Lane M: GeneRuler DNA Ladder mix. Lane N: negative PCR control, Lane C: untransformed *P. angusta* UFS1507 cells. Lane 1-10: Yeast colonies screened for integration of AO VP6 ORF into *P. angusta* UFS1507. Lane P: positive control.

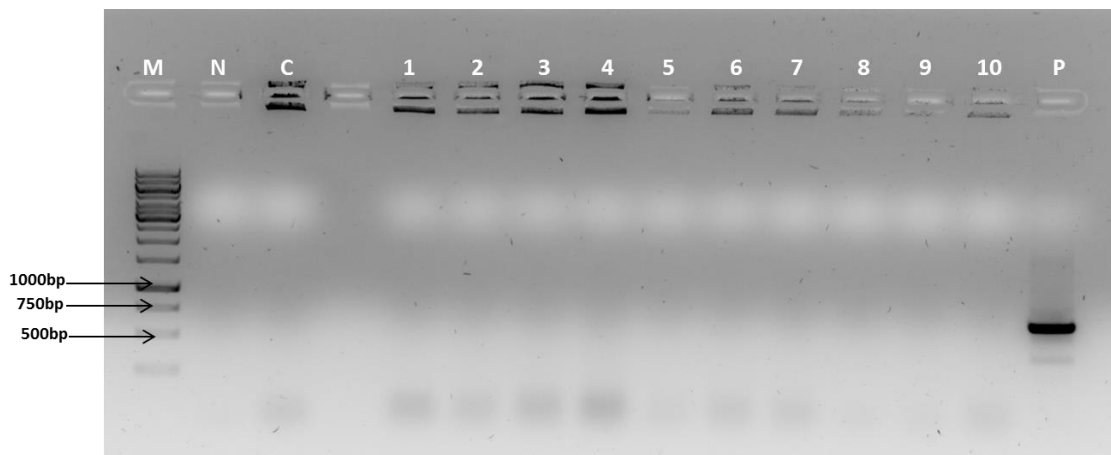


Figure 3.6: Analysis of the AO VP6 ORF containing expression cassette integration into the genome of *Y. lipolytica* PO 1F on a 1% agarose gel. Lane M: GeneRuler DNA Ladder mix. Lane N: negative PCR control, Lane C: untransformed *Y. lipolytica* PO 1F cells. Lane 1-10: Yeast colonies screened for integration of AO VP6 ORF into *Y. lipolytica* PO 1F. Lane P: positive control.

Majority (80-100%) of the colonies screened for the two *A. adenivorans* strains from the culture collection (UFS1219 and UFS1220) showed integration (Figure 3.2-3.3, Table 3.3), while the *A. adenivorans* LS3 strain, the most commonly used *A. adenivorans* strain, exhibited 60% integration. (Appendix D). The AO VP6 ORF containing expression cassette also showed efficient integration in the two *P. angusta* strains as all the colonies screened

showed integration (Figure 3.4-3.5). There was also good integration of AO VP6 ORF containing expression cassette in the *P. pastoris* (UFS1552T and GS115), *S. cerevisiae* CENPK and *K. lactis* UFS1167 strains (Appendix D). Even though there were colonies formed on the hygromycin B plate for VP6 ORF transformed in *Y. lipolytica* PO 1F, no integration was detected for any of the colonies (Figure 3.6). Almost 75% of the colonies screened for genome integration of the AO VP6 ORF-containing expression cassette exhibited integration into the various yeast strains (Table 3.3).

Table 3.3: Summary of the AO VP6 ORF containing expression cassette integration into the genomes of various yeast strains

Yeast	Strain	Integration
<i>Arxula adenivorans</i>	LS3	6/10
<i>Arxula adenivorans</i>	UFS1219	5/5
<i>Arxula adenivorans</i>	UFS1220	8/10
<i>Debaryomyces hansenii</i>	UFS0610	-
<i>Kluyveromyces lactis</i>	UFS1167	9/10
<i>Pichia angusta</i>	UFS0195	10/10
<i>Pichia angusta</i>	UFS1507	10/10
<i>Pichia pastoris</i>	GS115	9/10
<i>Pichia pastoris</i>	UFS1552T	7/10
<i>Saccharomyces cerevisiae</i>	CENPK	9/10
<i>Yarrowia lipolytica</i>	PO 1F	0/10
<i>Yarrowia lipolytica</i>	UFS0097	-
<i>Yarrowia lipolytica</i>	UFS2221	-
<i>Yarrowia lipolytica</i>	UFS2415	-

--: denotes no colony formation.

3.3.2.2 Integration of the expression cassette containing VP6 ORF codon optimised for expression in *K. lactis* in various yeast strains

Screening for integration of the expression cassette containing KO VP6 ORF into the various yeast genomes was carried by colony PCR using VP6Seq_KF2 and pKM173/177_R resulting in an amplicon of 667 bp (Figure 3.7). The results obtained for integration into the genomes of *A. adenivorans* strains UFS1219, 1220, *K. lactis* UFS1167, *P. angusta* UFS0915, *P. pastoris* GS115 and *Y. lipolytica* UFS0097 are provided in Figures 3.8-.3.13. The remainder of the results are shown in Appendix E.

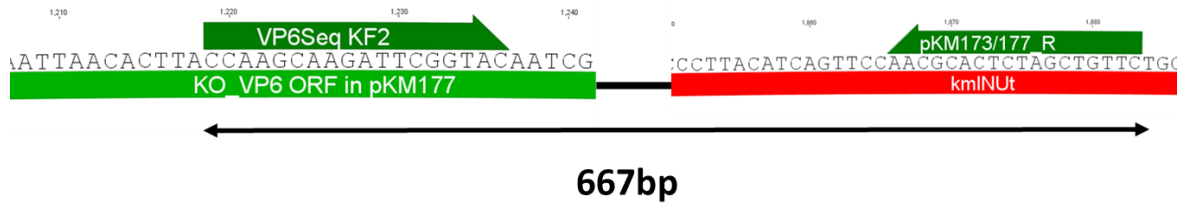


Figure 3.7: Primer annealing to the KO VP6 ORF containing expression cassette. KO VP6 ORF (light green). *K. marxianus* inulinase terminator (red). Forward and reverse primer (dark green).

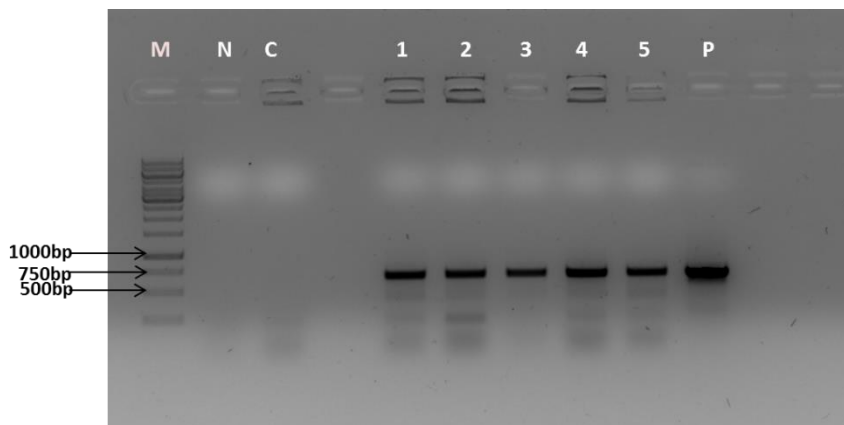


Figure 3.8: Analysis of the KO VP6 ORF containing expression cassette integration into the genome of *A. adenivorans* UFS1219 on a 1% agarose gel. Lane M: GeneRuler DNA Ladder mix. Lane N: negative PCR control, Lane C: untransformed *A. adenivorans* UFS1219 cells. Lane 1-5: Yeast colonies screened for integration of the expression cassette containing KO VP6 ORF into *A. adenivorans* UFS1219. Lane P: positive control.

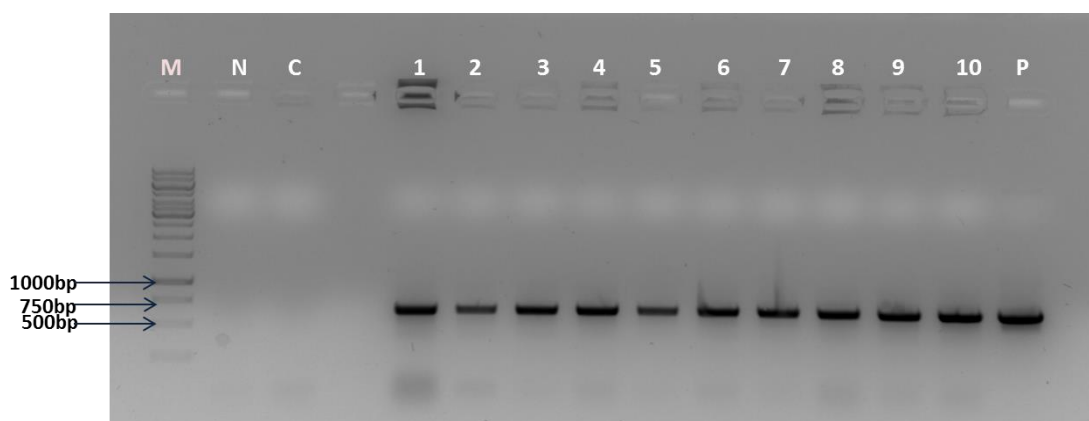


Figure 3.9: Analysis of the KO VP6 ORF containing expression cassette integration into the genome of *A. adenivorans* UFS1220 on a 1% agarose gel. Lane M: GeneRuler DNA Ladder mix. Lane N: negative PCR control, Lane C: untransformed *A. adenivorans* UFS1220 cells. Lane 1-10: Yeast colonies screened for

integration of the expression cassette containing KO VP6 ORF into *A. adenivorans* UFS1219. Lane P: positive control.

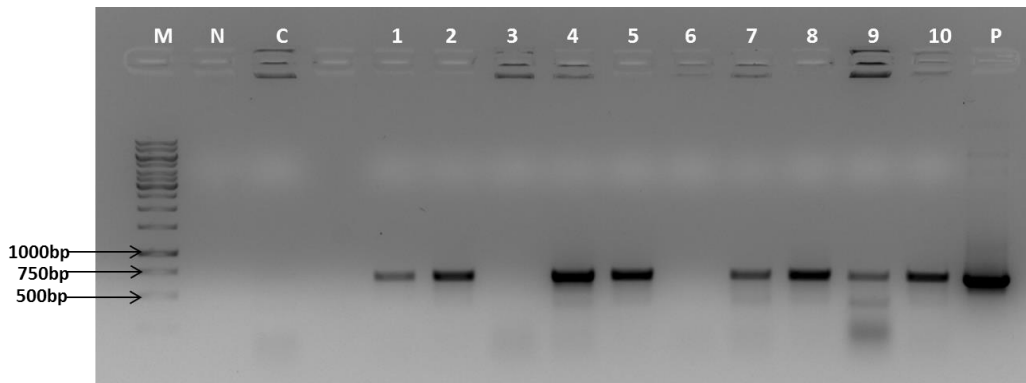


Figure 3.10: Analysis of the KO VP6 ORF containing expression cassette integration into the genome of *K. lactis* UFS1167 on a 1% agarose gel. Lane M: GeneRuler DNA Ladder mix. Lane N: negative PCR control, Lane C: untransformed *K. lactis* UFS1167 cells. Lane 1-10: Yeast colonies screened for integration of the expression cassette containing KO VP6 ORF into *K. lactis* UFS1167. Lane P: positive control.

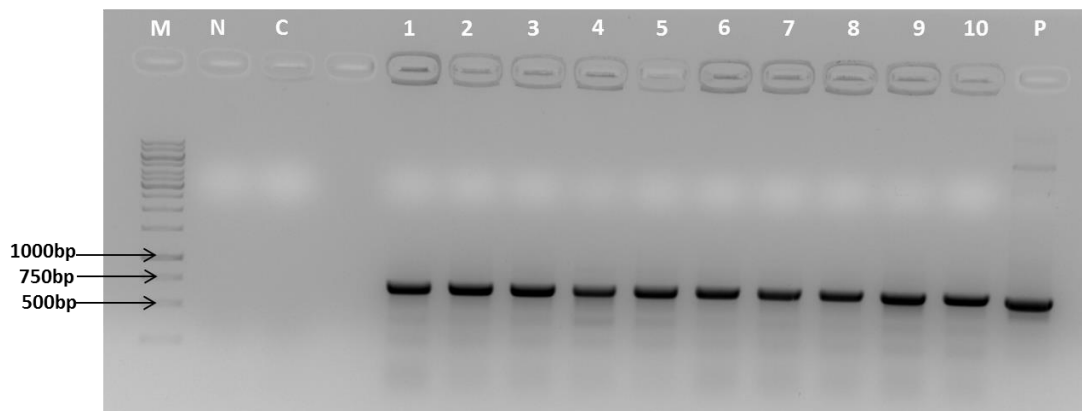


Figure 3.11: Analysis of the KO VP6 ORF containing expression cassette integration into the genome of *P. angusta* UFS0915 on a 1% agarose gel. Lane M: GeneRuler DNA Ladder mix. Lane N: negative PCR control, Lane C: untransformed *P. angusta* UFS0915 cells. Lane 1-10: Yeast colonies screened for integration of the expression cassette containing KO VP6 ORF into *P. angusta* UFS0915. Lane P: positive control.

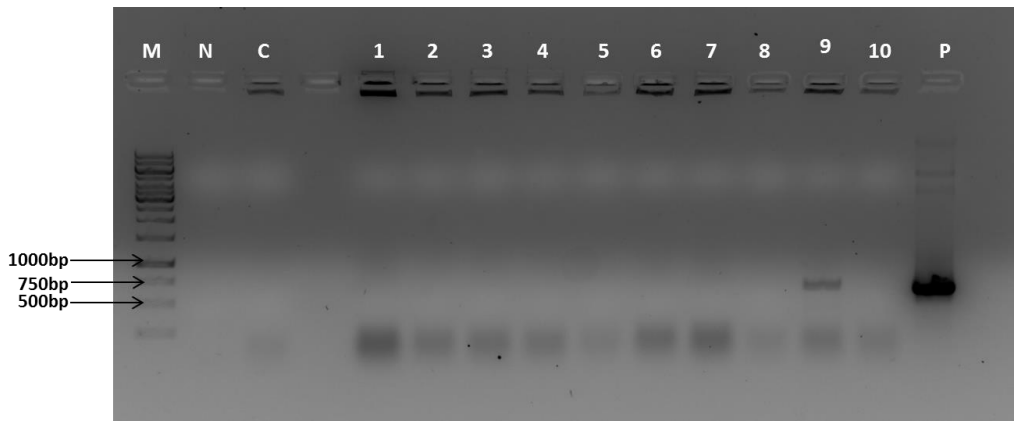


Figure 3.12: Analysis of the KO VP6 ORF containing expression cassette integration into the genome of *P. pastoris* GS115 on a 1% agarose gel. Lane M: GeneRuler DNA Ladder mix. Lane N: negative PCR control, Lane C: untransformed *P. pastoris* GS115 cells. Lane 1-10: Yeast colonies screened for integration of the expression cassette containing KO VP6 ORF into *P. pastoris* GS115. Lane P: positive control.

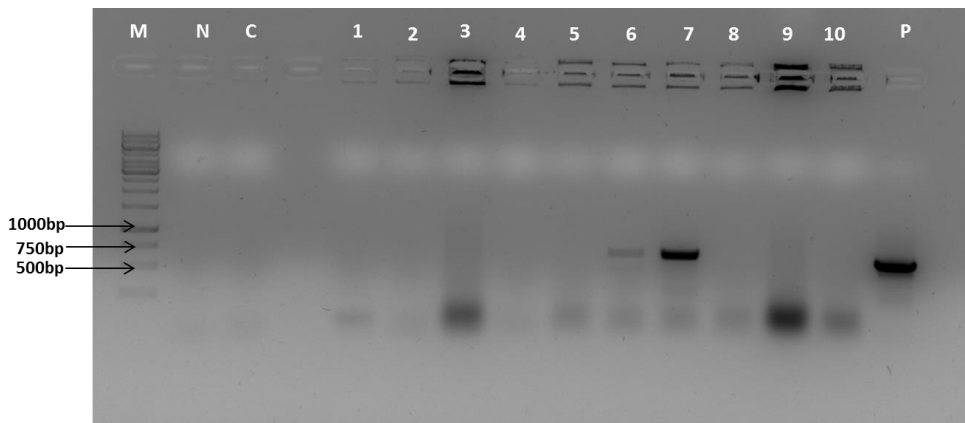


Figure 3.13: Analysis of the KO VP6 ORF containing expression cassette integration into the genome of *Y. lipolytica* UFS0097 on a 1% agarose gel. Lane M: GeneRuler DNA Ladder mix. Lane N: negative PCR control, Lane C: untransformed *Y. lipolytica* UFS0097 cells. Lane 1-10: Yeast colonies screened for integration of the expression cassette containing KO VP6 ORF into *Y. lipolytica* UFS0097. Lane P: positive control.

The KO VP6 ORF containing expression cassette exhibited efficient integration into *K. lactis* UFS1167 genome as 80% of the colonies screened showed integration (Figure 3.10). Figure 3.8-3.9 & 3.11 showed a 100% integration of the expression cassette containing KO VP6 ORF in *A. adenivorans* UFS1219, *A. adenivorans* UFS1220 and *P. angusta* UFS0097. Integration of the expression cassette containing KO VP6 ORF in *A. adenivorans* LS3 and *P. pastoris* GS115 yeast strains were low, 10% and 12%, respectively (Appendix E; Figure 3.12; Table 3.4). However, integration into the other *P. pastoris* strain, UFS1552T, was relatively good compared to the *P. pastoris* GS115. Although at a low level (20%), integration into the genome of *Y. lipolytica* UFS0097 was observed (Figure 3.13, Table 3.4).

No integration was observed in any of the *Y. lipolytica* PO 1F and *Y. lipolytica* UFS2221 colonies screened (Appendix E) even though colonies formed on the hygromycin B plates. Similar results were previously observed and when tested it was seen that the *hph* gene did insert, but not the VP6 ORF (Makatsa, 2015). No colonies formed on the hygromycin B plates when *D. hansenii* UFS0610 yeast strain was transformed with the expression cassette containing KO VP6 ORF. In summary, 46% of the yeast colonies screened showed integration in various yeast strains (Table 3.4). This was lower compared to the integration of VP6 AO containing expression cassette (Section 3.3.2.1). Integration was however seen in *Y. lipolytica* UFS0097 that were not seen in Section 3.3.2.1 (Figure 3.13), but no integration of the KO VP6-containing expression cassette in *Y. lipolytica* UFS2221 (Appendix E).

Table 3.4: Summary of the KO VP6 ORF containing expression cassette integration into the genomes of various yeast strains

Yeast	Strain	Integration
<i>Arxula adeninivorans</i>	LS3	1/10
<i>Arxula adeninivorans</i>	UFS1219	5/5
<i>Arxula adeninivorans</i>	UFS1220	10/10
<i>Debaryomyces hansenii</i>	UFS0610	-
<i>Kluyveromyces lactis</i>	UFS1167	8/10
<i>Pichia angusta</i>	UFS0915	10/10
<i>Pichia angusta</i>	UFS1507	5/7
<i>Pichia pastoris</i>	GS115	2/17
<i>Pichia pastoris</i>	UFS1552T	7/10
<i>Saccharomyces cerevisiae</i>	CENPK	4/10
<i>Yarrowia lipolytica</i>	PO 1F	0/10
<i>Yarrowia lipolytica</i>	UFS0097	2/10
<i>Yarrowia lipolytica</i>	UFS2221	0/10
<i>Yarrowia lipolytica</i>	UFS2415	-

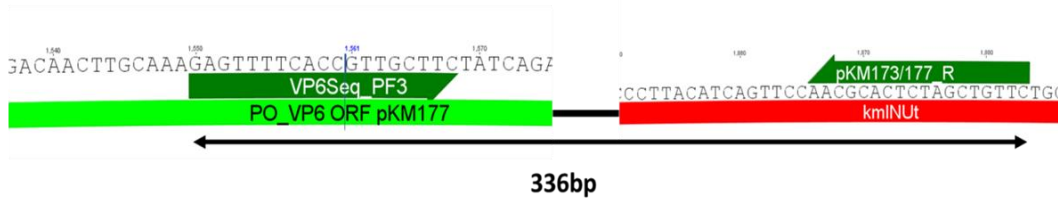
--: denotes no colony formation

3.3.2.3 Integration of the expression cassette containing VP6 ORF codon optimised for expression in *P.pastoris*/*P.angusta* in various yeasts

Screening for the integration of the expression cassette containing PO VP6 ORF into the various yeast genomes was carried by colony PCR using VP6Seq_PF3 or VP6Seq_PF2 as a forward primer and pKM173/177_R as a reverse primer resulting in an amplicon of 336 bp

(Figure 3.14a) or 6670bp (Figure 3.14b), respectively. The results obtained for integration into the genomes of *P. angusta* UFS0915, *P. angusta* UFS1507, *P. pastoris* GS115, *P. pastoris* UFS1552T, *S. cerevisiae* CENPK and *Y. lipolytica* PO 1F are provided in Figures 3.15-.3.20. The remainder of the results are shown in Appendix F.

A



B

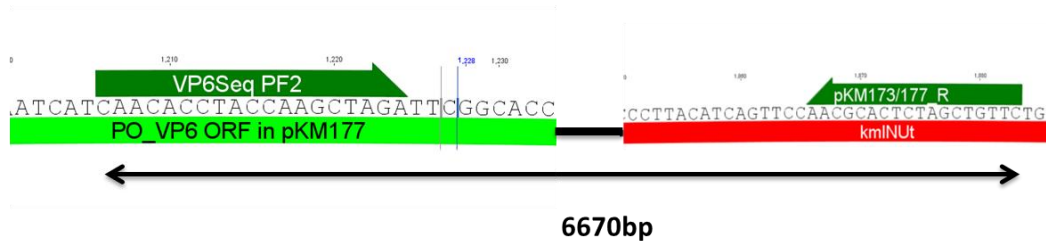


Figure 3.14: Primer annealing to the PO VP6 ORF containing expression cassette. PO VP6 ORF (light green). *K. marxianus* inulinase terminator (red). Forward and reverse primer (dark green). A, Primer annealing of VP6Seq_PF3 and pKM173/177_R resulting in an amplicon of 336 bp. B, A, Primer annealing of VP6Seq_PF2 and pKM173/177_R resulting in an amplicon of 670 bp.

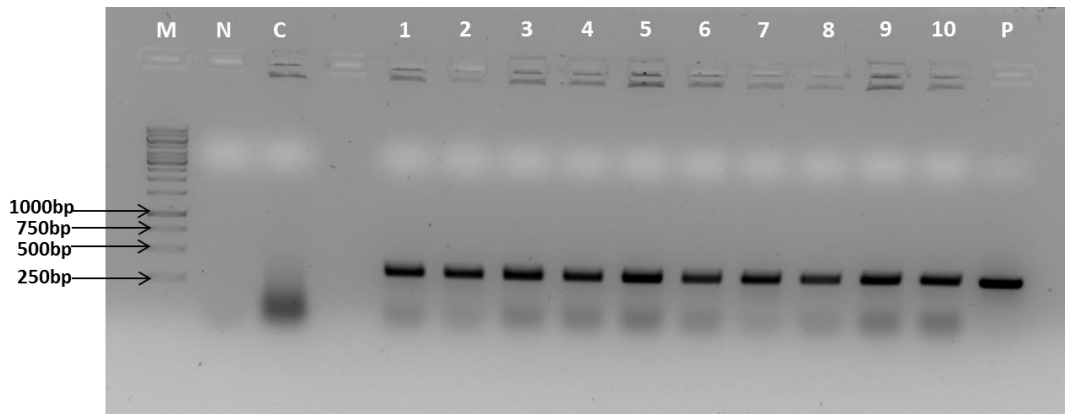


Figure 3.15: Analysis of the PO VP6 ORF containing expression cassette integration into the genome of *P. angusta* UFS0915 on a 1% agarose gel. Lane M: GeneRuler DNA Ladder mix. Lane N: negative PCR control, Lane C: untransformed *P. angusta* UFS0915 cells. Lane 1-10: Yeast colonies screened for integration of the expression cassette containing PO VP6 ORF into *P. angusta* UFS0915. Lane P: positive control.

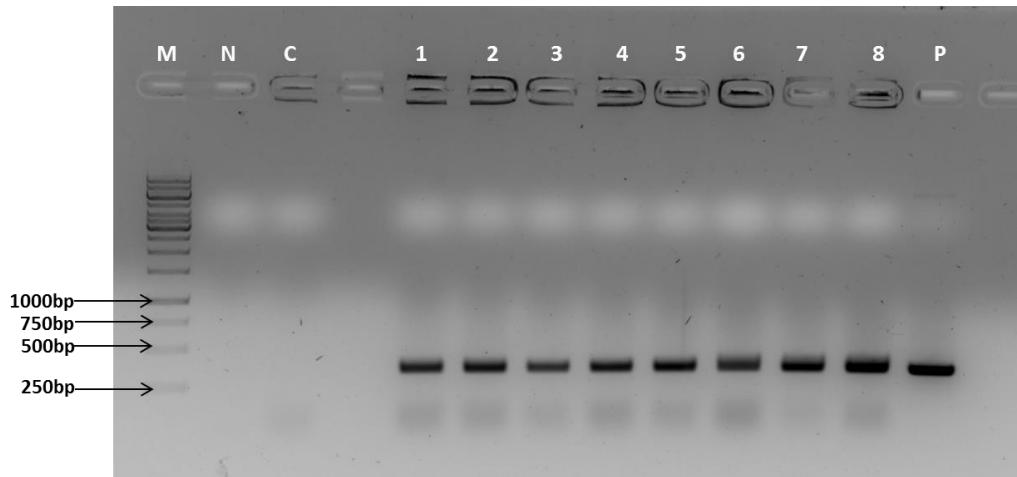


Figure 3.16: Analysis of the PO VP6 ORF containing expression cassette integration into the genome of *P. angusta* UFS1507 on a 1% agarose gel. Lane M: GeneRuler DNA Ladder mix. Lane N: negative PCR control, Lane C: untransformed *P. angusta* UFS1507 cells. Lane 1-8: Yeast colonies screened for integration of the expression cassette containing PO VP6 ORF into *P. angusta* UFS1507. Lane P: positive control.

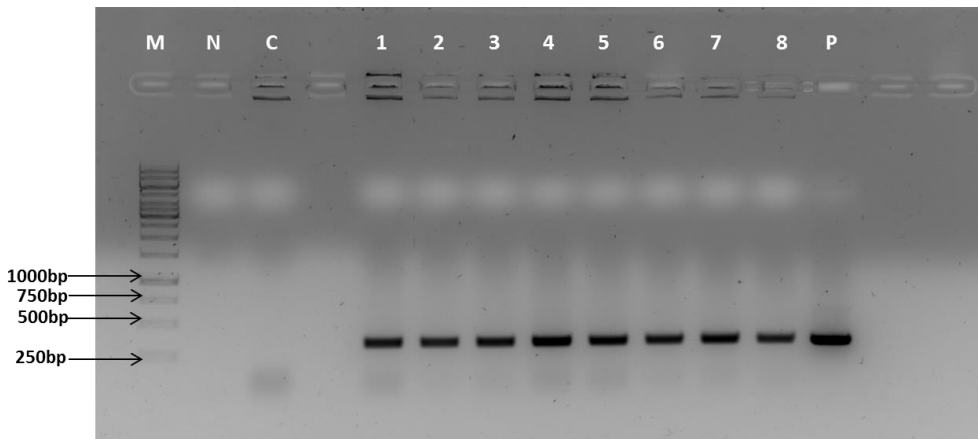


Figure 3.17: Analysis of the PO VP6 ORF containing expression cassette integration into the genome of *P. pastoris* GS115 on a 1% agarose gel. Lane M: GeneRuler DNA Ladder mix. Lane N: negative PCR control, Lane C: untransformed *P. pastoris* GS115 cells. Lane 1-8: Yeast colonies screened for integration of the expression cassette containing PO VP6 ORF into *P. pastoris* GS115. Lane P: positive control.

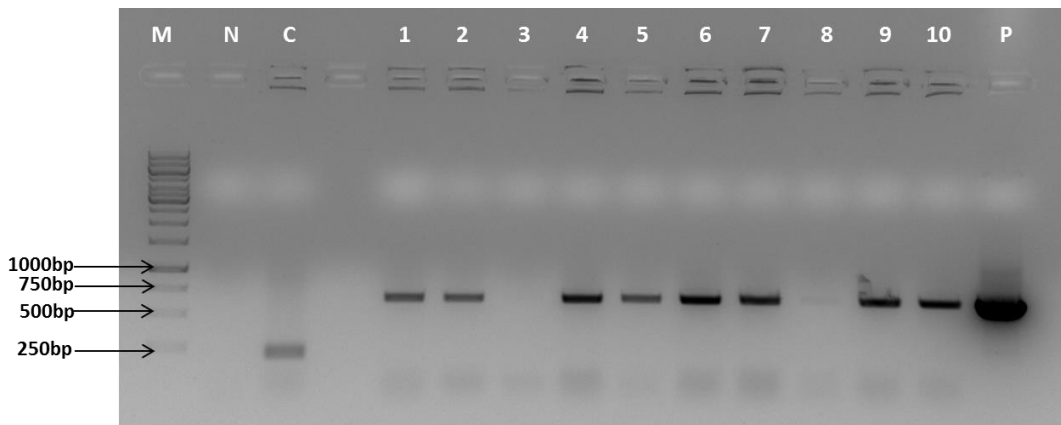


Figure 3.18: Analysis of the PO VP6 ORF containing expression cassette integration into the genome of *P. pastoris* UFS1552T on a 1% agarose gel. Lane M: GeneRuler DNA Ladder mix. Lane N: negative PCR control, Lane C: untransformed *P. pastoris* UFS1552T cells. Lane 1-10: Yeast colonies screened for integration of the expression cassette containing PO VP6 ORF into *P. pastoris* UFS1552T. Lane P: positive control.

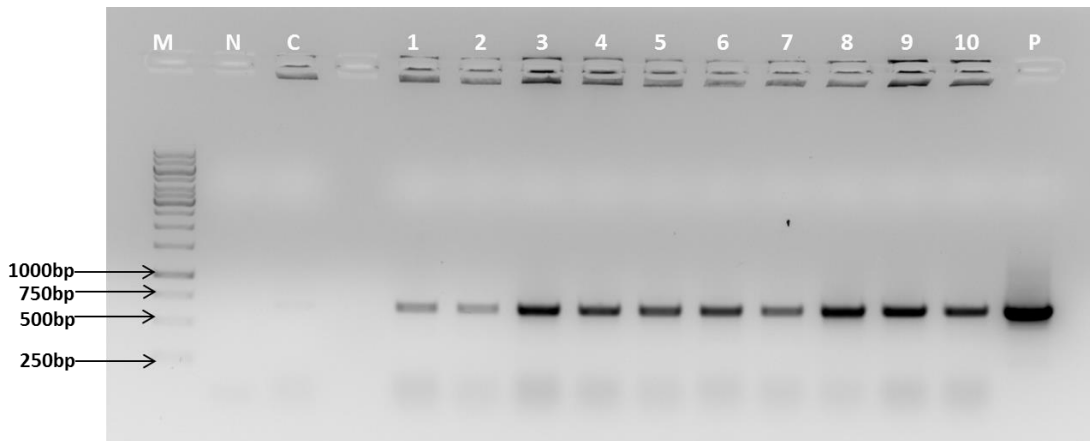


Figure 3.19: Analysis of the PO VP6 ORF containing expression cassette integration into the genome of *S. cerevisiae* CENPK on a 1% agarose gel. Lane M: GeneRuler DNA Ladder mix. Lane N: negative PCR control, Lane C: untransformed *S. cerevisiae* CENPK cells. Lane 1-10: Yeast colonies screened for integration of the expression cassette containing PO VP6 ORF into *S. cerevisiae* CENPK. Lane P: positive control.

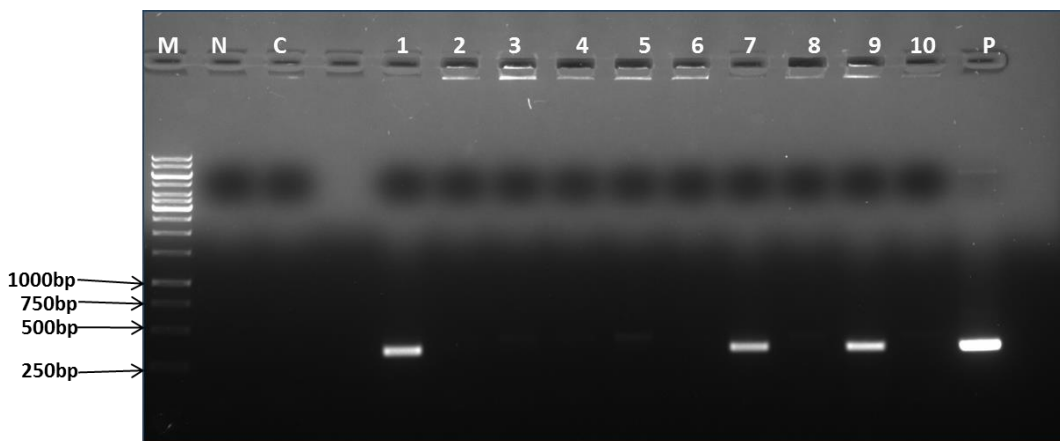


Figure 3.20: Analysis of the PO VP6 ORF-containing expression cassette integration into the genome of *Y. lipolytica* PO 1F on a 1% agarose gel. Lane M: GeneRuler DNA Ladder mix. Lane N: negative PCR control, Lane C: untransformed *Y. lipolytica* PO 1F cells. Lane 1-10: Yeast colonies screened for integration of the expression cassette containing PO VP6 ORF into *Y. lipolytica* PO 1F. Lane P: positive control.

Integration of the PO VP6 containing expression cassette was highly efficient in the *P. angusta* and *P. pastoris* yeast strains. A 100% of the colonies screened for the two *P. angusta* strains (Figure 3.15-3.16), *P. pastoris* GS115 (Figure 3.17) as well as *S. cerevisiae* CENPK (Figure 3.19) exhibited integration of PO VP6 containing expression cassette. The PO VP6 containing expression showed 70% integration into the *K. lactis* strain (Appendix F). There was an integration of 80% of the colonies screened for *P. pastoris* UFS1552T (Figure 3.18). Integration into *Y. lipolytica* PO 1F (Figure 3.20) was also observed. This was a

surprising result, as there was no integration observed for the expression cassettes investigated in sections 3.3.2.1-3.3.2.2 for this strain. Again, there were no colonies when *D. hansanii* UFS0610 was transformed with VP6 ORF optimised for *P. angusta/P. pastoris*. There were also no colonies when the PO VP6-containing expression was transformed in *A. adenivorans* UFS1220. In summary, 80% of the yeast colonies screened contained PO VP6 containing expression cassette (Table 3.5).

Table 3.5 Summary of the PO VP6 ORF containing expression cassette integration into the genomes of various yeast strains

Yeast	Strain	Integration
<i>Arxula adenivorans</i>	LS3	4/4
<i>Arxula adenivorans</i>	UFS1219	2/2
<i>Arxula adenivorans</i>	UFS1220	-
<i>Debaryomyces hansenii</i>	UFS0610	-
<i>Kluyveromyces lactis</i>	UFS1167	7/10
<i>Pichia angusta</i>	UFS0195	10/10
<i>Pichia angusta</i>	UFS1507	10/10
<i>Pichia pastoris</i>	GS115	8/8
<i>Pichia pastoris</i>	UFS1552T	8/10
<i>Saccharomyces cerevisiae</i>	CENPK	10/10
<i>Yarrowia lipolytica</i>	PO 1F	3/10
<i>Yarrowia lipolytica</i>	UFS0097	-
<i>Yarrowia lipolytica</i>	UFS2221	0/10
<i>Yarrowia lipolytica</i>	UFS2514	0/10

--: denotes no colony formation

3.3.3 Expression of rotavirus VP6 ORFs in various yeasts

Clones that showed integration described in sections 3.3.2.1-3.3.2.3 were screened for expression in various yeast strains described in sections 3.3.2.3-3.3.2.3. The expected size of VP6 expressed in the yeasts cells is 45 kDa (Estes *et al.*, 1987).

3.3.3.1 Bacterial expression of VP6

The recombinant pCOLD_VP6 plasmid was transformed into *E. coli* BL21 cells. *E. coli* BL21 cells allows for high-efficiency protein expression under control of a T7 promoter which is inducible by the addition of IPTG (Rosano & Ceccarelli, 2014).

The observed protein size was approximately 48 kDa (Figure 3.21) which is larger than the expected VP6 size of 45 kDa (Estes *et al.*, 1987). This is because the bacterial-expressed

VP6 is fused to a His-tag and a translation enhancer element (TEE). A series of dilutions were carried out for the bacterial-expressed VP6 control to evaluate which dilution and concentration to be used during analysis of VP6 expression by the yeast colonies. The use of 1 mg/ml total protein was considered suitable as a positive control (Figure 3.21).

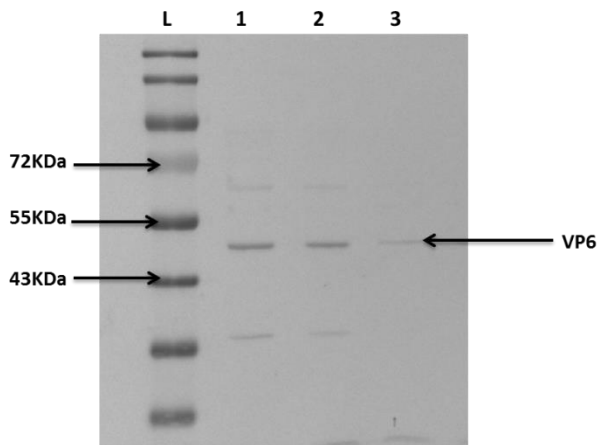


Figure 3.21: Western blot analysis of bacterial-expressed VP6 as positive control. Lane L is the PageRuler™ Prestained Protein Ladder (Thermo Fisher Scientific). Lane 1 - Total protein concentration 2.5 mg/ml; Lane 2 - 1.0 mg/ml; Lane 3 - 0.5 mg/ml.

3.3.3.2 Yeast expression of rotavirus VP6 encoded by the ORF codon optimised for expression in *A. adenivorans*

Results obtained for the expression of VP6 encoded by the ORF optimised for expression in *A. adenivorans* as detected by Western blot analyses are shown in Figures 3.22-3.24 and the remainder of the results are shown in Appendix G. Eighty percent of the *A. adenivorans* UFS1219 and UFS1220 (UNESCO-MIRCEN yeast culture collection) colonies screened (Figure 3.22; Appendix G) expressed VP6, while less than 20% of the colonies screened for the prototype strain *A. adenivorans* LS3 expressed VP6 (Appendix G). Again a high percentage (80%) of the *P. angusta* colonies screened, expressed VP6 (Figure 3.23-3.24 & Appendix G). Even though there was a high level of integration for the AO VP6 ORF containing expression cassette into *P. pastoris* strains, the expression was poor (Appendix G; Table 3.6). A total of 56% of the *K. lactis* UFS1167 colonies screened expressed VP6 (Appendix G). Overall, 60% of colonies tested positive for the AO VP6 ORF-containing expression cassette, expressed rotavirus VP6 (Table 3.6).

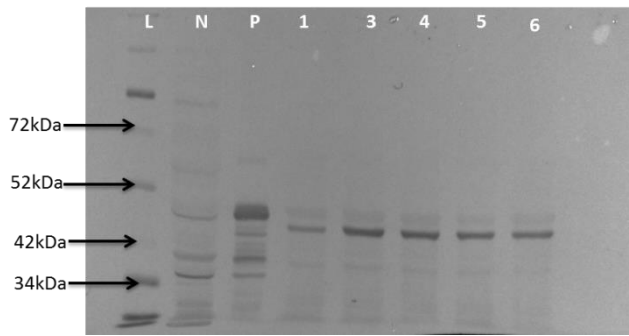


Figure 3.22: Western blot analysis of rotavirus VP6 expression by *A. adenivorans* UFS1220 colonies containing the AO VP6 ORF containing expression cassette. Lane L: Spectra™ Multicolor Broad Range Protein Ladder (Thermo Fisher Scientific). Lane N: untransformed *A. adenivorans* UFS1220 cells, negative control. Lane P: Bacterial expressed VP6, protein size 48 kDa. Lanes 1, 3, 4, 5, 6: *A. adenivorans* UFS1220 yeast colonies screened for expression of VP6 with expected size of 45 kDa. A total protein concentration of 1.9 mg/ml was used for all colonies screened.

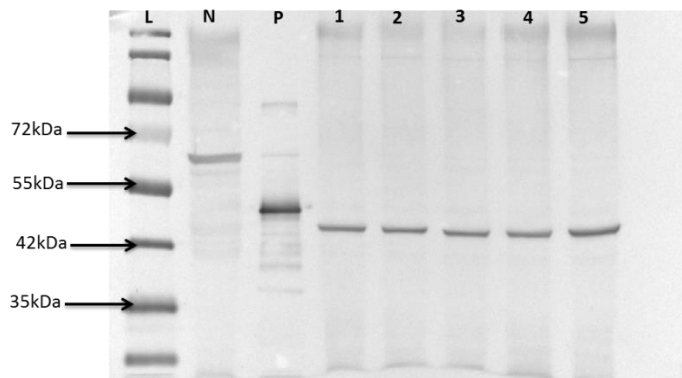


Figure 3.23: Western blot analysis of rotavirus VP6 expression by *P. angusta* UFS0915 colonies containing the AO VP6 ORF-containing expression cassette. Lane L: PageRuler™ Prestained Protein Ladder (Thermo Fisher Scientific). Lane N: untransformed *P. angusta* UFS0915 cells, negative control. Lane P: Bacterial expressed VP6, protein size 48 kDa. Lanes 1, 2, 3, 4, 5: *P. angusta* UFS0915 yeast colonies screened for expression of VP6 with expected size of 45 kDa. A total protein concentration of 2.1 mg/ml was used for all colonies screened.

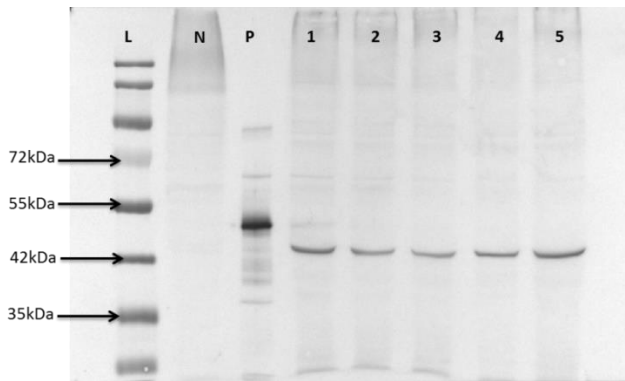


Figure 3.24: Western blot analysis of rotavirus VP6 expression by *P. angusta* UFS1507 colonies containing the AO VP6 ORF-containing expression cassette. Lane L: PageRuler™ Prestained Protein Ladder (Thermo Fisher Scientific). Lane N: untransformed *P. angusta* UFS1507 cells, negative control. Lane P: Bacterial expressed VP6, protein size 48 kDa. Lanes 1, 2, 3, 4, 5: *P. angusta* UFS1507 yeast colonies screened for expression of VP6 with expected size of 45 kDa. A total protein concentration of 2.3 mg/ml was used for all colonies screened.

Table 3.6: Summary of rotavirus VP6 expression by yeast colonies containing AO VP6 ORF.

Yeast	Strain	Expression
<i>Arxula adeninivorans</i>	LS3	1/6
<i>Arxula adeninivorans</i>	UFS1219	5/5
<i>Arxula adeninivorans</i>	UFS1220	8/10
<i>Kluyveromyces lactis</i>	UFS1167	5/9
<i>Pichia angusta</i>	UFS0195	10/10
<i>Pichia angusta</i>	UFS1507	8/10
<i>Pichia pastoris</i>	GS115	1/9
<i>Pichia pastoris</i>	UFS1552T	2/7
<i>Saccharomyces cerevisiae</i>	CENPK	4/9

3.3.3.3 Yeast expression of rotavirus VP6 encoded by the ORF codon optimised for expression in *K. lactis*

Results obtained for the expression of VP6 encoded by the ORF optimised for expression in *K. lactis* as detected by western blot analyses are shown in Figures 3.25-3.27 and the remainder of the results are shown in Appendix H. Only 60% of *K. lactis* UFS1167 colonies screened showed expression of VP6 (Figure 3.25 & Table 3.7), while 90% of the *P. angusta* colonies screened expressed VP6 (Figure 3.26 -27 & Appendix H). Even though 100% integration was observed for KO VP6 ORF containing expression cassette in *A. adeninivorans* UFS1219 and *A. adeninivorans* Y1220 (Appendix H & Table 3.7), expression

of VP6 was poor (30%) by these yeasts (Appendix H). There was no VP6 expression in any of the *P. pastoris* UFS1552T colonies screened, although all colonies of the commercial *P. pastoris* GS115 strain expressed VP6 (Appendix H & Table 3.7) despite low integration (Table 3.5) of the KO VP6 containing expression cassette into *P. pastoris* GS115 genome. Although the KO VP6 ORF containing expression cassette integrated in the *Y lipolytica* UFS0097 genome (Figure 3.20 & Table 3.7), no expression of VP6 in any of the *Y lipolytica* UFS0097 colonies screened was detected (Appendix H). Overall, 50% of colonies that tested positive for integration of the KO VP6 ORF containing expression cassette, expressed rotavirus VP6 (Table 3.7).

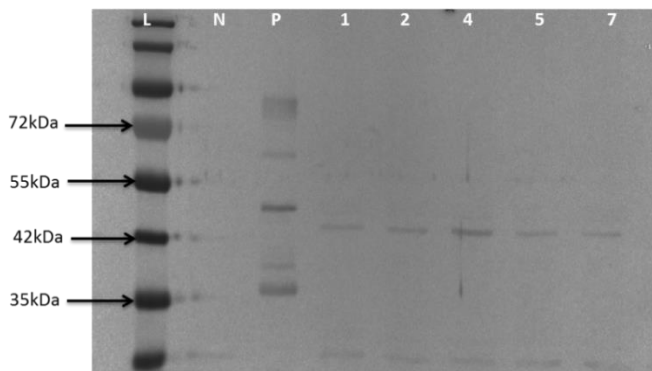


Figure 3.25: Western blot analysis of rotavirus VP6 expression by *K. lactis* UFS1167 colonies containing the KO VP6 ORF containing expression cassette. Lane L: PageRuler™ Prestained Protein Ladder (Thermo Fisher Scientific). Lane N: untransformed *K. lactis* UFS1167 cells, negative control. Lane P: Bacterial expressed VP6, protein size 48 kDa. Lanes 1, 2, 4, 5, 7: *K. lactis* UFS1167 yeast clones screened for expression of VP6 with expected size of 45 kDa. A total protein concentration of 2.1 mg/ml was used for all colonies screened.

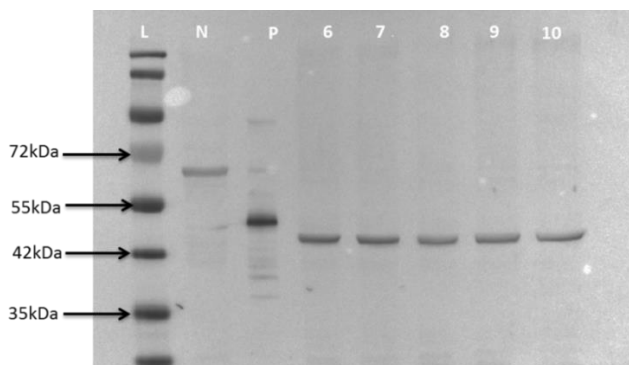


Figure 3.26: Western blot analysis of rotavirus VP6 expression by *P. angusta* UFS0915 colonies containing the KO VP6 ORF containing expression cassette. Lane L: PageRuler™ Prestained Protein Ladder (Thermo Fisher Scientific). Lane N: untransformed *P. angusta* UFS0915 cells, negative control. Lane P: Bacterial expressed VP6, protein size 48 kDa. Lanes 6, 7, 8, 9, 10: *P. angusta* UFS0915 yeast

clones screened for expression of VP6 with expected size of 45 kDa. A total protein concentration of 2.1 mg/ml was used for all colonies screened.

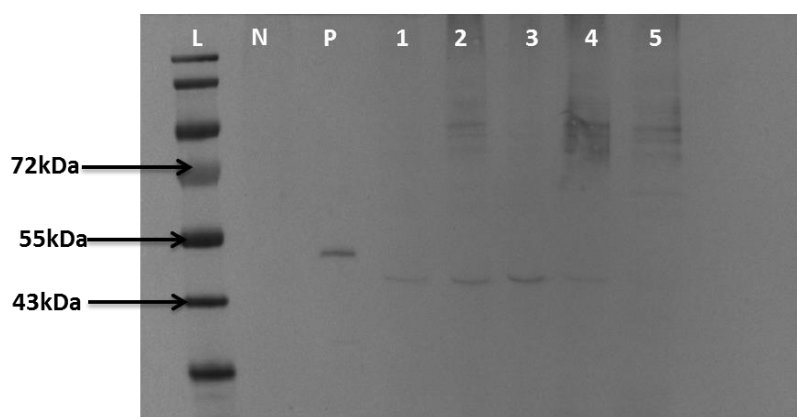


Figure 3.27: Western blot analysis of rotavirus VP6 expression by *P. angusta* UFS1507 colonies containing the KO VP6 ORF containing expression cassette. Lane L: PageRuler™ Prestained Protein Ladder (Thermo Fisher Scientific). Lane N: untransformed *P. angusta* UFS1507 cells, negative control. Lane P: Bacterial expressed VP6, protein size 48 kDa. Lanes 1, 2, 3, 4, 5: *P. angusta* UFS1507 yeast clones screened for expression of VP6 with expected size of 45 kDa. A total protein concentration of 2.4 mg/ml was used for all colonies screened.

Table 3.7: Summary of rotavirus VP6 expression by yeast colonies containing KO VP6 ORF.

Yeast	Strain	Expression
<i>Arxula adeninivorans</i>	LS3	0/1
<i>Arxula adeninivorans</i>	UFS1219	3/5
<i>Arxula adeninivorans</i>	UFS1220	2/10
<i>Kluyveromyces lactis</i>	UFS1167	5/8
<i>Pichia angusta</i>	UFS0915	10/10
<i>Pichia angusta</i>	UFS1507	4/5
<i>Pichia pastoris</i>	GS115	2/2
<i>Pichia pastoris</i>	UFS1552T	0/5
<i>Saccharomyces cerevisiae</i>	CENPK	2/4
<i>Yarrowia lipolytica</i>	UFS0097	0/2

3.3.3.4 Yeast expression of rotavirus VP6 encoded by the ORF codon optimised for expression in *P. angusta*/*P. pastoris*

Results obtained for the expression of VP6 encoded by the ORF optimised for expression in *P. angusta*/*P. pastoris* as detected by Western blot analyses are shown in Figures 3.28-3.31 and the remainder of the results are shown in Appendix I.

Of the colonies screened for the two *P. angusta* strains, 90% expressed VP6 (Figure 3.28-29). However, only 11% of the colonies for the *P. pastoris* strains expressed VP6 (Appendix I, Table 3.8). Furthermore, 100% of *S. cerevisiae* CENPK, *A. adenivorans* UFS1219 and *K. lactis* UFS1167 colonies screened expressed the VP6 protein (Figure 3.30, Table 3.8 & Appendix I). There was a 38% expression of VP6 by *Y. lipolytica* PO 1F colonies screened. Despite the low expression of VP6 by *Y. lipolytica*, expression was not seen by this strain in Sections 3.3.3.2-3.3.3.3. Low expression of VP6 was also seen for the *A. adenivorans* LS3 strain (Table 3.8 & Appendix I). Overall, 64% of colonies that previously tested positive for integration of the PO VP6 ORF containing expression cassette, expressed rotavirus VP6 (Table 3.8).

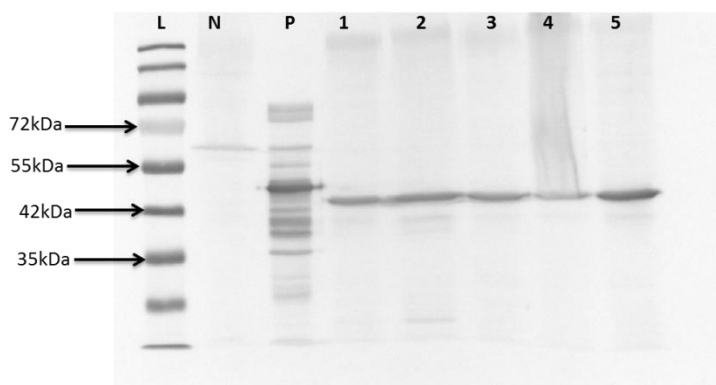


Figure 3.28: Western blot analysis of rotavirus VP6 expression by *P. angusta* UFS1507 colonies containing the PO VP6 ORF containing expression cassette. Lane L: PageRuler™ Prestained Protein Ladder (Thermo Fisher Scientific). Lane N: untransformed *P. angusta* UFS1507 cells, negative control. Lane P: Bacterial expressed VP6, protein size 48 kDa. Lanes 1, 2, 3, 4, 5: *P. angusta* UFS1507 yeast clones screened for expression of VP6 with expected size of 45 kDa. A total protein concentration of 2.1 mg/ml was used for all colonies screened.

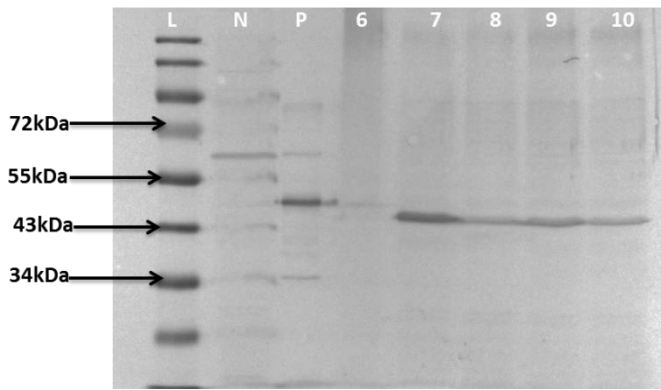


Figure 3.29: Western blot analysis of rotavirus VP6 expression by *P. angusta* UFS0915 colonies containing the PO VP6 ORF containing expression cassette. Lane L: PageRuler™ Prestained Protein Ladder (Thermo Fisher Scientific). Lane N: untransformed *P. angusta* UFS0915 cells, negative control. Lane P: Bacterial expressed VP6, protein size 48 kDa. Lanes 6, 7, 8, 9, 10: *P. angusta* UFS0915 yeast clones screened for expression of VP6 with expected size of 45 kDa. A total protein concentration of 2.6 mg/ml was used for all colonies screened.

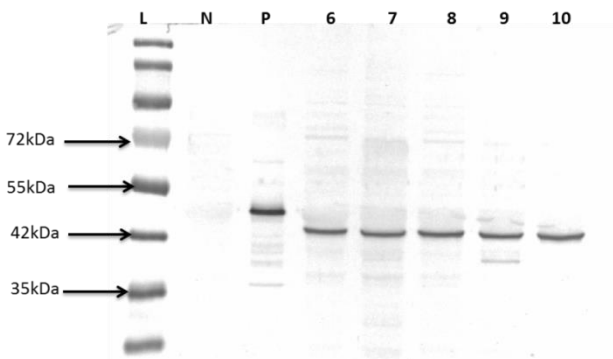


Figure 3.30: Western blot analysis of rotavirus VP6 expression by *S. cerevisiae* CENPK colonies containing the PO VP6 ORF containing expression cassette. Lane L: PageRuler™ Prestained Protein Ladder (Thermo Fisher Scientific). Lane N: untransformed *S. cerevisiae* CENPK cells, negative control. Lane P: Bacterial expressed VP6, protein size 48 kDa. Lanes 6, 7, 8, 9, 10: *S. cerevisiae* CENPK yeast clones screened for expression of VP6 with expected size of 45 kDa. A total protein concentration of 2.0 mg/ml was used for all colonies screened.

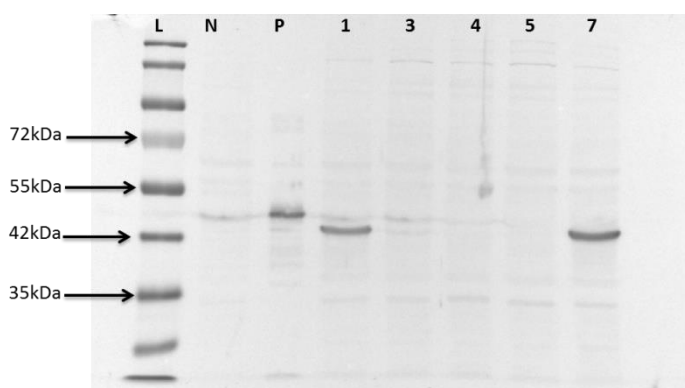


Figure 3.31: Western blot analysis of rotavirus VP6 expression by *Y. lipolytica* PO 1F colonies containing the PO VP6 ORF containing expression cassette. Lane L: PageRuler™ Prestained Protein Ladder (Thermo Fisher Scientific). Lane N: untransformed *Y. lipolytica* PO 1F cells, negative control. Lane P: Bacterial expressed VP6, protein size 48 kDa. Lanes 1, 3, 4, 5, 7: *Y. lipolytica* PO 1F yeast clones screened for expression of VP6 with expected size of 45 kDa. A total protein concentration of 2.4 mg/ml was used for all colonies screened.

Table 3.8: Summary of rotavirus VP6 expression by yeast colonies containing PO VP6 ORF.

Yeast	Strain	Integration
<i>Arxula adeninivorans</i>	LS3	1/4
<i>Arxula adeninivorans</i>	UFS1219	2/2
<i>Kluyveromyces lactis</i>	UFS1167	7/7
<i>Pichia angusta</i>	UFS0915	9/10
<i>Pichia angusta</i>	UFS1507	10/10
<i>Pichia pastoris</i>	GS115	0/8
<i>Pichia pastoris</i>	UFS1552T	2/10
<i>Saccharomyces cerevisiae</i>	CENPK	10/10
<i>Yarrowia lipolytica</i>	PO 1F	3/8

3.4 Discussion

A summary of the integration of the VP6 ORFs optimised for expression in different yeasts and expression of rotavirus VP6 by these yeasts are shown in Table 3.9. Integration in various yeast genomes by the AO and PO VP6 ORF containing expression cassettes was more efficient than the KO VP6 ORF containing expression cassette as seen in Table 3.9. There was 96% integration of all the optimised VP6 ORFs into the *P. angusta*. Methylotrophic yeasts like *P. pastoris* and *P. angusta* have gained interest for alternative

recombinant protein production due to their glycosylation patterns and high expression yield (Bretthauer, 2003; Kim *et al.*, 2015; Sohn *et al.*, 2010). From the expression results obtained in this study, 80% of the *P. angusta* colonies screened expressed VP6. Good expression of VP6 by *P. pastoris* containing the VP6 ORF codon optimised for expression in *P. angusta/P. pastoris* was expected since the VP6 ORF was codon optimised to favour expression in *P. pastoris*. However, expression by the *P. pastoris* strains was relatively poor despite efficient integration of the VP6 ORFs (Table 3.9). Although the cloning vector is under the control of the *Y. lipolytica* TEF promoter, there was poor integration of the VP6 ORFs in the *Y. lipolytica* strains. This could be due to the fact that the genome of *Y. lipolytica* does not easily recombine with foreign DNA, hence poor integration (Romanos *et al.*, 1992; Satyanarayana & Kunze, 2017). The yeasts from the UNESCO-MIRCEN Yeast Culture collection showed more efficient genome integration, especially when comparing the *A. adenivorans* strains (UFS1219 and UFS1220) and the prototype *A. adenivorans* LS3 strain (Table 3.9). Reports have shown, though, high recombinant protein production in the prototype strain (Malak *et al.*, 2016; Wartmann *et al.*, 2002).

Overall, six different yeasts (10 different yeast strains) tested positive for rotavirus VP6 expression (Table 3.9).

Table 3.9: Summary of the integration of the VP6 ORFs optimised for expression in different yeasts and expression of rotavirus VP6 in various yeasts

Yeast strains	VP6 ORF optimised for <i>A. adenivorans</i>		VP6 ORF optimised for <i>K. lactis</i>		VP6 ORF optimised for <i>P. angusta/P. pastoris</i>	
	Integration	Expression	Integration	Expression	Integration	Expression
<i>A. adenivorans</i> LS3	6/10	1/6	1/10	0/1	4/4	1/4
<i>A. adenivorans</i> UFS1219	5/5	5/5	5/5	2/5	2/2	2/2
<i>A. adenivorans</i> UFS1220	8/10	8/8	10/10	3/10	-	-
<i>D. hansenii</i> UFS0610	-	-	-	-	-	-
<i>K. lactis</i> UFS1167	9/10	5/9	8/10	5/8	7/10	7/7
<i>P. angusta</i> UFS0197	10/10	8/10	10/10	10/10	10/10	9/10
<i>P. angusta</i> UFS1507	10/10	10/10	5/7	4/5	10/10	10/10
<i>P. pastoris</i> GS115	9/10	0/9	2/17	0/2	8/8	0/8
<i>P. pastoris</i> UFS1552T	7/10	2/7	7/10	0/5	8/10	2/8
<i>S. cerevisiae</i> CENPK	9/10	4/10	4/10	2/4	10/10	10/10
<i>Y. lipolytica</i> PO 1F	0/10	-	0/10	-	8/10	3/8
<i>Y. lipolytica</i> UFS0097	-	-	2/10	0/2	-	-
<i>Y. lipolytica</i> UFS 2221	-	-	0/10	-	0/10	-
<i>Y. lipolytica</i> UFS 2415	-	-	-	-	-	-

- : Denotes either no colonies formed or no expression.

3.5 References

- Ahmad, M., Hirz, M. & Pichler, H. (2014).** Protein expression in *Pichia pastoris* : recent achievements and perspectives for heterologous protein production. *Appl Microbiol Biotechnol* **98**, 5301–5317.
- Albertyn, J., Labuschagne, M., Theron, C. & Smit, M. (2011).** Novel expression constructs.
- Baneyx, F. & Mujacic, M. (2004).** Recombinant protein folding and misfolding in *Escherichia coli*. *Nat Biotechnol* **22**, 1399–1408.
- Bertolotti-Ciarlet, A., Ciarlet, M., Crawford, S. E., Conner, M. E. & Estes, M. K. (2003).** Immunogenicity and protective efficacy of rotavirus 2 / 6-virus-like particles produced by a dual baculovirus expression vector and administered intramuscularly , intranasally , or orally to mice. *Vaccine* **21**, 3885–3900.
- Birch-Machin, I., Newell, C., Hibberd, J. & Gray, J. (2004).** Accumulation of rotavirus VP6 protein in chloroplasts of transplastomic tobacco is limited by protein stability. *Plant Biotechnol J* **2**, 261–70.
- Bischoff, F., Chamas, A., Katarzyna, L., Matthes, F., Böer, E. & Kunze, G. (2017).** Applications of *Blastobotrys (Arxula) adenivorans* in Biotechnology. In: Satyanarayana T., Kunze G. (eds) *Yeast Divers Hum Welf* 455–479.
- Böer, E., Steinborn, G., Florsch, K., Martina, K., Gellissen, G. & Kunze, G. (2009).** *Arxula adenivorans* (*Blastobotrys adenivorans*) – A Dimorphic Yeast of Great Biotechnological Potential. *Yeast Biotechnol Divers Appl* **27**, 615–616.
- Bredell, H., Smith, J. J., Prins, W. A., Görgens, J. F. & Zyl, W. H. Van. (2016).** Expression of rotavirus VP6 protein : A comparison amongst *Escherichia coli* , *Pichia pastoris* and *Hansenula polymorpha*. *FEMS Yeast Res* **16**, 1–12.
- Bretthauer, R. K. (2003).** Genetic engineering of *Pichia pastoris* to humanize N-glycosylation of proteins. *Trends Biotechnol* **21**, 459–462.
- Breuer, U. & Harms, H. (2006).** *Debaryomyces hansenii* — an extremophilic yeast with biotechnological potential. *Yeast* **23**, 415–437.
- Breunig, K. D. & Steensma, H. Y. (2003).** Functional Genetics of Industrial Yeasts. In *Kluyveromyces Lact Genet Physiol Appl*, pp. 171–205.
- Chen, D. C., Beckerich, J. M. & Gaillardin, C. (1997).** One-step transformation of the dimorphic yeast *Yarrowia lipolytica*. *Appl Microbiol Biotechnol* **48**, 232–235.
- Crawford, S. U. E. E., Labbe, M., Cohen, J., Burroughs, M. H., Zhou, Y. & Estes, M. K. (1994).** Characterization of Virus-Like Particles Produced by the Expression of Rotavirus Capsid Proteins in Insect Cells. *J Virol* **68**, 5945–5952.
- Cueva, R., Pablo, G. & Polaina, J. (2004).** A Search for Hyperglycosylation Signals in Yeast Glycoproteins. *J Biol Chem* **279**, 43789–43798.
- Dong, J., Liang, B., Jin, Y., Zhang, W. & Wang, T. (2005).** Oral immunization with pBsVP6-transgenic alfalfa protects mice against rotavirus infection. *Virology* **339**, 153–163.
- Estes, M. K., Crawford, S. U. E. E., Penaranda, M. E., Petrie, B. L., Burns, J. W., Chan, W., Ericson, B., Smith, G. E. & Summers, M. A. X. D. (1987).** Synthesis and Immunogenicity of the Rotavirus

- Major Capsid Antigen Using a Baculovirus Expression System. *J Virol* **61**, 1488–1494.
- Feng, H., Li, X., Song, W., Duan, M., Chen, H., Wang, T. & Dong, J. (2017).** Oral Administration of a Seed-based Bivalent Rotavirus Vaccine Containing VP6 and NSP4 Induces Specific Immune Responses in Mice. *Front Plant Sci* **8**, 1–13.
- Hanahan, D. (1983).** Studies on transformation of *Escherichia coli* with plasmids. *J Mol Biol* **166**, 557–580.
- Inka, B. A., Gonzalez-Rabade, N. & Gray, J. (2012).** Increased accumulation and stability of rotavirus VP6 protein in tobacco chloroplasts following changes to the 5' untranslated region and the 5' end of the coding region. *Plant Biotechnol J* **10**, 422–34.
- Kang, H., Sohn, J., Choi, E., Chung, B., Yu, M. & Rhee, S. (1998).** Glycosylation of Human 1 - Antitrypsin in *Saccharomyces cerevisiae* and Methylophilic Yeasts. *Yeast* **14**, 371–381.
- Kim, H., Yoo, S. J. & Kang, H. A. (2015).** Yeast synthetic biology for the production of recombinant therapeutic proteins. *FEMS Yeast Res* **15**, 1–16.
- Klebe, R. J., Harriss, J. V., Sharp, Z. D. & Douglas, M. G. (1983).** A general method for polyethylene-glycol-induced genetic transformation of bacteria and yeast. *Gene* **25**, 333–341.
- Kumar, S., Randhawa, A., Ganesan, K., Raghava, G. P. S. & Mondal, A. K. (2012).** Draft Genome Sequence of Salt-Tolerant Yeast *Debaryomyces hansenii*. *Eukaryot Cell* **11**, 961–962.
- Kurtzman, C. P., Fell, J. W. & Boekhout, T. (2011).** *The Yeasts*, Fourth. (C. Kurtzman, J. W. Fell & T. Boekhout, Eds.).
- Makatsa, M. S. (2015).** *Engineering yeast strains for the expression of South African G9P [6] rotavirus VP2 and VP6 structural proteins*. University of the Free State.
- Malak, A., Baronian, K. & Kunze, G. (2016).** *Blastobotrys (Arxula) adenivorans* : a promising alternative yeast for biotechnology and basic research. *Yeast* **33**, 535–547.
- Mathieu, M., Petitpas, I., Navaza, J., Lepault, J., Kohli, E., Pothier, P., Prasad, B. V. V., Cohen, J. & Rey, A. A. (2001).** Atomic structure of the major capsid protein of rotavirus : implications for the architecture of the virion. *EMBO J* **20**, 1485–1497.
- Najjar, A., Robert, S., Guérin, C., Violet-Asther, M. & Carrière, F. (2011).** Quantitative study of lipase secretion, extracellular lipolysis, and lipid storage in the yeast *Yarrowia lipolytica* grown in the presence of olive oil_ analogies with lipolysis in humans. *Appl Microbiol Biotechnol* **89**, 1947–1962.
- Onishi, H. (1986).** Osmophilic yeasts. *Adv Food Res* **12**, 53–94.
- Ratledge, C. & H, T. K. (1986).** In *Yeast Biotechnology and Biocatalysis*. In *Marcel Dekker New York*, pp. 223–253. Edited by H. J. Verachtert & R. De Mot.
- Rodríguez-Limas, W. A., Tyo, K. E. J., Nielsen, J., Ramírez, O. T. & Palomares, L. A. (2011).** Molecular and process design for rotavirus-like particle production in *Saccharomyces cerevisiae*. *Microb Cell Fact* **10**, 33.
- Romanos, M. A., Scorer, C. A. & Clare, J. J. (1992).** Foreign Gene Expression in Yeast : a Review. *Yeast* **8**, 423–488.
- Rosano, G. L. & Ceccarelli, E. A. (2014).** Recombinant protein expression in *Escherichia coli* :

advances and challenges **5**, 1–17.

- Satyanarayana, T. & Kunze, G. (Eds.). (2017).** *Yarrowia lipolytica* expression system. In *Yeast Divers Hum Welf*, pp. 223–225.
- Sohn, S. B., Graf, A. B., Kim, T. Y., Gasser, B., Maurer, M., Ferrer, P., Mattanovich, D. & Lee, S. Y. (2010).** Genome-scale metabolic model of methylotrophic yeast *Pichia pastoris* and its use for in silico analysis of heterologous protein production. *Biotechnol J* **5**, 705–715.
- Tai, M. & Stephanopoulos, G. (2013).** Engineering the push and pull of lipid biosynthesis in oleaginous yeast *Yarrowia lipolytica* for biofuel production. *Metab Eng* **15**, 1–9. Elsevier.
- Teh, S. H., Fong, M. Y. & Mohamed, Z. (2011).** Expression and analysis of the glycosylation properties of recombinant human erythropoietin expressed in *Pichia pastoris*. *Genet Mol Biol* **34**, 464–470.
- Wartmann, T., Böer, E., Pico, A. H., Sieber, H., Bartelsen, O., Gellissen, G. & Kunze, G. (2002).** High-level production and secretion of recombinant proteins by the dimorphic yeast *Arxula adenivorans*. *FEMS Yeast Res* **2**, 363–369.
- Wiechelman, K., Braun, R. D. & Fitzpatrick, J. D. (1988).** Investigation of the bicinchoninic acid protein assay_ Identification of the groups responsible for color formation. *Anal Biochem* **175**, 231–237.
- Yu, J. & Langridge, W. (2003).** Expression of rotavirus capsid protein VP6 in transgenic potato and its oral immunogenicity in mice. *Transgenic Res* **12**, 163–9.

Chapter 4: Investigation into the oligomeric structure formation of rotavirus VP6 produced by various yeasts

4.1 Introduction

One of the unique features of rotavirus VP6 is the ability to form oligomeric structures without the help of other viral capsid proteins. This ability of rotavirus VP6 to form nanotubes and nanospheres depends on the pH and ionic strength (Lepault *et al.*, 2001; Ready & Sabara, 1987). Above pH 7 it has been shown that VP6 arranges into nanotubes with a diameter of 45 nm (Figure 4.1a) while at a pH that ranges between 5.5-7, the nanotube appears to be larger with a diameter of 75 nm (Figure 4.1b). At a pH that ranges from 3.0-5.5, VP6 assembles into rough nanospheres that differ in size as shown in Figure 4.1c (Lepault *et al.*, 2001).

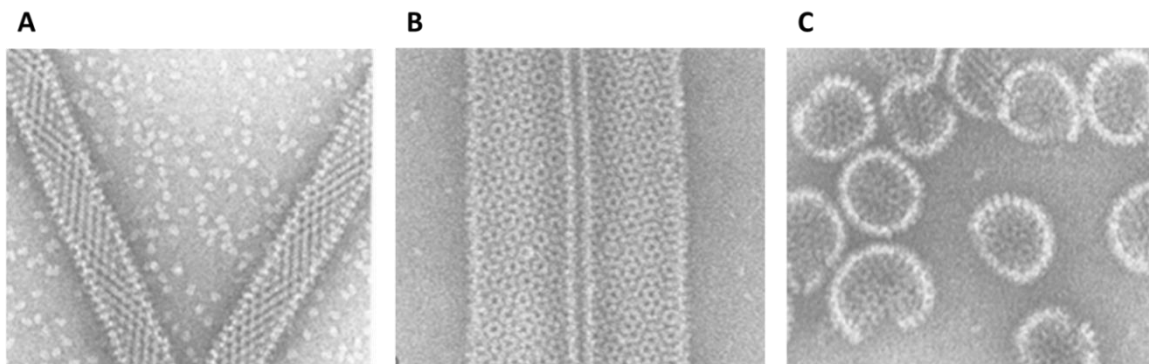


Figure 4.1: Cryo-Electron microscopy images showing VP6 assembly in different pH environments. A, the VP6 nanotube structure with a diameter of 45 nm above pH 7. B, the VP6 nanotube structure with a diameter of 75 nm at pH 5.5-7.0. C, nanosphere particles with a diameter of 75 nm at pH 3.0-5.5. (copied from Lepault *et al.*, 2001).

Rotavirus VP6 nanotubes and nanospheres have been produced in *E. coli* and also insect cells using baculovirus expression (Bugli *et al.*, 2014; Jere *et al.*, 2014; Lappalainen *et al.*, 2013, 2016a; Li *et al.*, 2014; Ready & Sabara, 1987). The rotavirus VP6 tubular particles have been associated with the induction of protective immunity in mice (Lappalainen *et al.*, 2013; Pastor *et al.*, 2014). Therefore, the ability of VP6 proteins to form tubular structures indicates that the protein is folding correctly in its native form and is expected to elicit an immune response. A study by Pastor and co-workers performed an immunological evaluation of the three different forms of the VP6 protein, nanotubes, double-layered rotavirus-like particles (VP6 & VP2) and VP6 trimers. The results showed that nanotubes induced the highest IgG titers following immunisation with a reduction of viral shedding by 70% (Pastor *et al.*, 2014).

Lappalainen and co-workers have developed a simple protocol to purify the VP6 protein and reconstruct VP6 nanotubes and nanospheres (Lappalainen *et al.*, 2016a) . To date there has not been any work conducted on the reconstruction of VP6 nanotubes and nanosphere particles produced in yeasts. In this chapter, this protocol was adapted to purify VP6 from the yeast strains identified in chapter 3 and investigate the potential of the yeast expressed VP6 to fold into tubules.

4.2 Materials and methods

4.2.1 Growth studies

The six yeasts that expressed rotavirus VP6 were identified in the previous chapter. The VP6-expressing yeast colonies were randomly selected (Table 4.1) for evaluation of growth studies. The yeast colonies were revived by streaking on a YPD plate (Section 3.2.1) and incubated overnight at 30°C, except for *P. angusta* which was incubated at 37°C. The colonies were inoculated in 5 ml YPD broth media as a pre-inoculum. A volume of 500 µl of the pre-inoculum culture was transferred sterile to 50 ml YPD broth media in a 500ml Erlenmeyer flask. Immediately after the transfer of the pre-inoculum culture to the 50 ml YPD broth, the optical density was measured at time 0 using the spectrophotometer Helios Gamma (UNICAM) at a wavelength of 600 nm. The cultures were incubated in a 30°C incubator Shaker ZWY 240 (LABWIT) except for *P. angusta* which was incubated in a 37°C. The OD₆₀₀ was measured every 2 hours for 26 hours. The experiment was carried out in duplicate. For the reconstruction of growth curves, the OD₆₀₀ measured were plotted against time.

Table 4.1: Random selection of representative yeast colonies containing VP6 ORF for evaluation of growth studies, purification and evaluation of oligomeric structure formation.

Yeast Strain	Yeast colony with VP6 ORFs	Reference of VP6 expression
<i>A. adenivorans</i> UFS1220	AO VP6 ORF colony 1 (Figure 3.3; Lane 1)	Figure 3.22; Lane 1
<i>K. lactis</i> UFS1167	KO VP6 ORF colony 1 (Figure 3.10; Lane 1)	Figure 3.25; Lane 1
<i>P. angusta</i> UFS1507	PO VP6 ORF colony 1 (Figure 3.16; Lane 1)	Figure 3.28; Lane 1
<i>P. pastoris</i> UFS1552T	AO VP6 ORF colony 1 (Figure D4; Lane 1)	Figure G8*; Lane 1
<i>S. cerevisiae</i> CENKP	PO VP6 ORF colony 6 (Figure 3.19; Lane 6)	Figure 3.30; Lane 6

<i>Y. lipolytica</i> PO 1F	PO VP6 ORF colony 7 (Figure 3.20; Lane 7)	Figure 3.31; Lane 7
----------------------------	--	---------------------

*: From Appendix G; Figure G8

To evaluate the times at which to harvest the cells in order to purify the VP6 protein, described in section 4.2.2, the ability of the clones to express VP6 were confirmed using Western blot analysis (Chapter 3, Section 3.2.10) at mid- to late-exponential phase.

4.2.2 Purification of VP6 produced in various yeasts

The yeast colonies described in section 4.2.1 were purified using sucrose gradient density centrifugation. Briefly, the colonies were expressed in a final volume of 500 ml-800 ml YPD, depending on the biomass, as described in section 3.2.5. The cells were harvested either at mid-or late-exponential phase as determined during the growth studies (Section 4.2.1). The harvested cells were resuspended with 1 ml of 50 mM Tris (pH 7.4) containing either Protease Inhibitor Mix (Sigma) or cOmplete™ ULTRA tablets (Roche) or Pierce™ Protease inhibitor Tables (Thermo Fisher Scientific) per gram of wet biomass.

The cells were lysed with a One Shot Constant Cell Disruption System (Constant Systems, United Kingdom) at 35 kPi and the soluble fraction was separated from the insoluble debris by centrifugation at 20 000 x g for 45 minutes at 4°C. The soluble fractions were transferred to 25 x 69 mm Ultra-Clear™ Tubes (Beckman Coulter). Ultracentrifugation of the soluble fraction was performed with an Optima™ L-100 XP Ultracentrifuge (Beckman Coulter) using the SW 32Ti rotor at 100 000 x g for 90 minutes at 4°C. The pellet was resuspended in either 2 ml or 3 ml (depending on the mass of the pellet) of 0.2 M Tris pH-HCl 7.3 and 0.2 M CaCl₂ buffer containing Protease Inhibitor Cocktail (Sigma) or Pierce™ Protease inhibitor (Thermo Fisher Scientific). The sucrose gradients (10%-60%) were prepared in 0.2 M Tris pH-HCl 7.3 and 0.2 M CaCl₂ buffer. The gradients were layered on top of each other in 25 x 69 mm Ultra-Clear™ Tubes (Beckman Coulter). The sample was layered on top of the 10% layer. The samples were allowed to migrate through the sucrose gradients by ultracentrifugation using the Optima™ L-100 XP Ultracentrifuge (Beckman Coulter) with SW 32Ti rotor at 100 000 x g for 3 hours at 4°C. A volume of 1 ml of each fraction was pipetted into a clean 1.5 ml microcentrifuge tube. Identification of the fractions containing VP6 was carried out with SDS-PAGE analysis (Section 3.2.9). The gels were stained by boiling the gels with 0.2% (w/v) Coomassie brilliant blue R 250 (Merck) for 40 seconds. The gels were de-stained with 10% (v/v) acetic acid, 20% (v/v) methanol 2- 3 hours on a Stuart ® rocker.

4.2.3 Preparations of oligomeric structures of rotavirus VP6 proteins produced in various yeasts

The fractions containing only VP6 were pooled. Removal of sucrose from the samples was carried out by dialysis against 1x phosphate-buffered saline (PBS) (10 mM PO_4^{3-} , 137 mM NaCl, and 2.7 mM KCl) using Slide-A-Lyzer™ G2 Dialysis Cassettes (Thermo Fisher Scientific). The samples were concentrated with Amicon Ultra-15 Centrifugal Filter Units (Merck) with a molecular cut-off of 30 kD at 4 000 x g for 10 minutes at 4°C. The concentrated VP6 protein was transferred to a clean 15ml centrifuge tube and was considered as the crude sample.

4.2.3.1 Nanotubes and nanospheres particles preparations

A flow diagram of VP6 purification and assembly of VP6 nanotubes and nanospheres is shown in Figure 4.2 based on the of the method developed by Lappalainen and co-workers (Lappalainen *et al.*, 2016). Before preparation of tubular and spherical structures, the VP6 protein in the crude sample was dissociated into monomers by addition of 100 mM sodium acetate (pH 3.0) at a final concentration of 80 mM to the crude sample (Tosser *et al.*, 1992). This was incubated overnight at 4°C. To remove any yeast proteins, the monomers were purified using an Amicon Ultra-15 Filter Unit with a molecular cut-off of 100 kDa and centrifuged at 4 000 x g for 10 minutes at 4°C. Any impurities from yeast proteins was trapped in the 100 kDa column. The filtrate containing VP6 was further concentrated with the Amicon Ultra-15 Centrifugal Filter Unit with a molecular cut-off of 30 kD.

For preparation of nanotubes and nanospheres, buffer exchange was carried out. Briefly, to reconstitute VP6 nanotubes, buffer exchange was carried out using 1x PBS (10 mM PO_4^{3-} , 137 mM NaCl, and 2.7 mM KCl) at pH 7.3-7.5 in the 30 kDa filtering unit three times at 4 000 x g for 10 minutes at 4°C. To reconstruct VP6 nanospheres, buffer exchange was carried by adding 50 mM sodium acetate containing 130 mM sodium chloride at pH4.82 to the monomers and centrifuging at 4000 x g for 10 minutes at 4°C using the 30 kDa filtering unit.

The VP6 nanotubes as well as the VP6 nanospheres were evaluated using the Philips CM100 Analytical Transmission Electron Microscope (TEM) at Centre for Microscopy, UFS. The samples were prepared by negative staining with a 1:1 dilution of 2% uranyl acetate. The samples were fixed on 3.05 mm Copper Grids (Agar Scientific) and allow to set for 1 minute. The excess uranyl acetate was washed with distilled water and the Copper Grids containing the samples were dried using Filter Paper (Whatman) by tapping the Copper Grids. The copper grids were visualised under TEM at 20 000 X magnification.

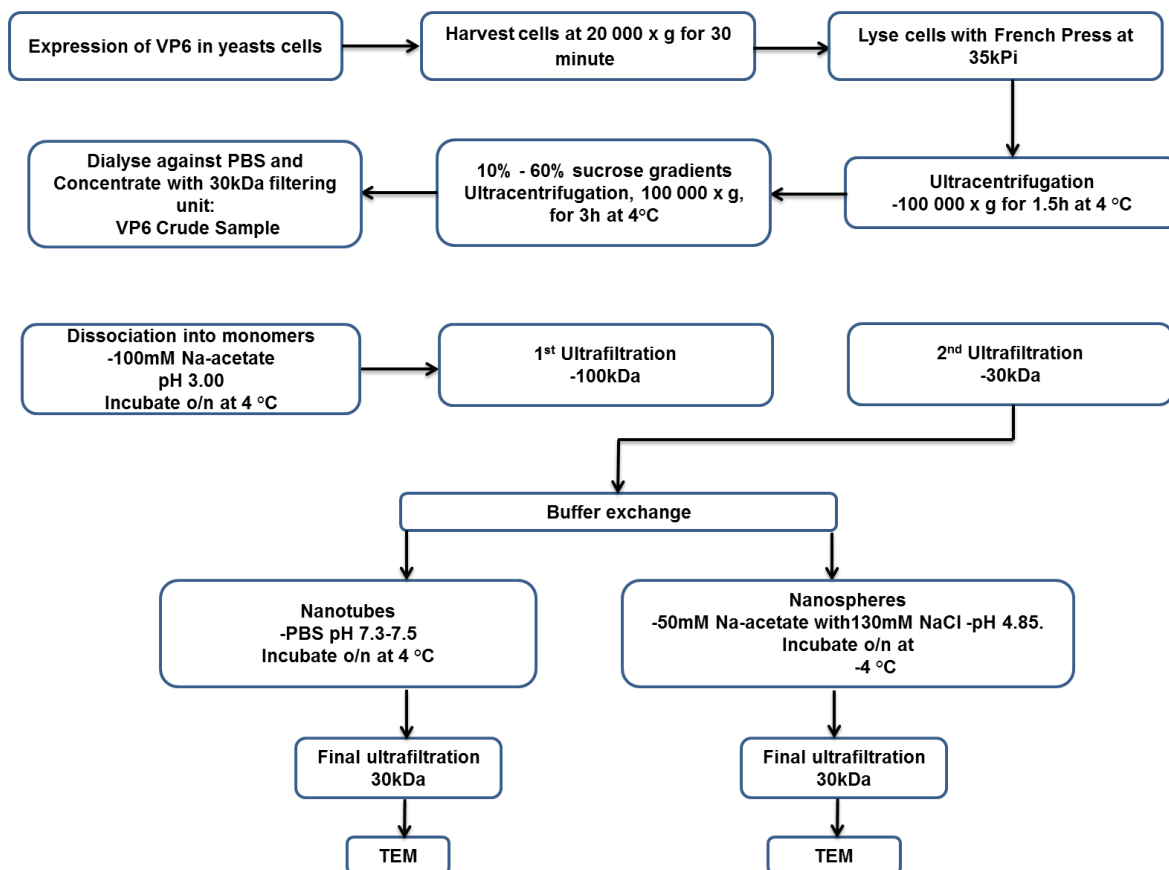


Figure 4.2: Flow diagram illustrating VP6 purification and assembly of VP6 oligomeric structures (Lappalainen *et al.*, 2016).

4.3 Results

4.3.1 Identification of optimum harvesting times for the various yeast strains

The growth curves constructed for the various yeast strains expressing VP6 protein indicated that *A. adenivorans* had a slower growth compared to other yeasts. *A. adenivorans* reached a mid-exponential phase after 12 – 16 hours and late-exponential after 18 hours as seen in Figure 4.3 or Table 4.2, while *P. pastoris*, *P. angusta*, *K. lactis* and *Y. lipolytica* reached mid-exponential phase after 8-12 hours and late-exponential phase after 14-16 hours (Figure 4.3). On the other hand, *S. cerevisiae* reached mid-exponential phase after 12 hours and late-exponential phase after 16 hours (Figure 4.3).

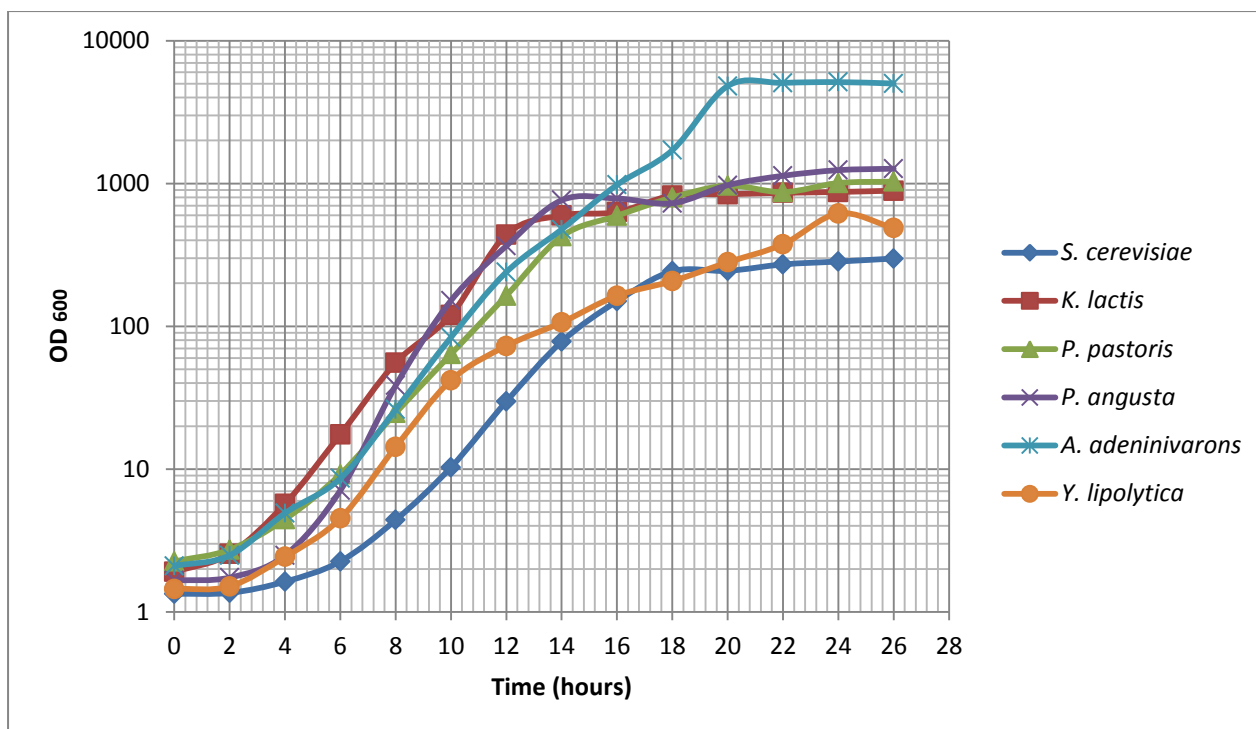


Figure 4.3: Growth curves of the yeast expressing VP6 protein.

Protein concentrations and Western blot analysis were carried out to verify the time to harvest cells. For the expression of VP6 in *Y. lipolytica*, *K. lactis* and *A. adenivorans* there was no significant difference in the protein concentration when cells were harvested at mid-exponential and late-exponential phases (Table 4.2). Expression of VP6 in *P. angusta*, *P. pastoris* and *S. cerevisiae* showed a higher total protein concentration in the late-exponential phase as seen in Table 4.2. The Western blot analyses carried out to confirm VP6 expression are shown in APPENDIX J.

Table 4.2: Optimal times of harvest of VP6 protein in various yeasts with their respective concentrations.

Yeast	Mid-Exponential Phase	Total protein concentration	Late-Exponential Phase	Total protein concentration
<i>A. adenivorans</i>	12 h	1.076 mg/ml	18 h	0.952 mg/ml
<i>K. lactis</i>	12 h	1.810 mg/ml	16 h	1.921 mg/ml
<i>P. angusta</i>	8 h	0.728 mg/ml	14 h	1.31 mg/ml
<i>P. pastoris</i>	8 h	0.985 mg/ml	14 h	1.710 mg/ml
<i>S. cerevisiae</i>	12 h	2.498 mg/ml	16 h	3.075 mg/ml
<i>Y. lipolytica</i>	10 h	2.062 mg/ml	16 h	1.945 mg/ml

h: Hour

4.3.2 Purification of VP6 protein in various yeasts

Purification of VP6 protein from the various yeasts was carried out by sucrose gradient centrifugation. Figure 4.4 shows the protein content in *A. adenivorans* of the fractions obtained following sucrose gradient centrifugation. Multiple bands were observed in fractions 1-6 (Figure 4.4a), while a clear single band of the expected size indicating a possible purified VP6 from fraction 18-22 and 32-33 without any multiple protein bands as seen in Figure 4.4b, c, d. The presence of VP6 in the fractions 18-20 was verified with Western blot analysis (Figure 4.5) with a total protein concentration of 2.5 mg/ml. Fractions 18-20 were pooled together for the evaluation of VP6 oligomeric structures which will be described in section 4.3.3.

No single bands were observed in the sucrose gradient fractions analysed for *P. pastoris* as seen in Figure 4.6. There were multiple bands observed in fractions 1-6 (Figure 4.6a) and no bands seen in fractions 10-18 (Figure 4.6b) as well as the rest of the fractions analysed (not shown).

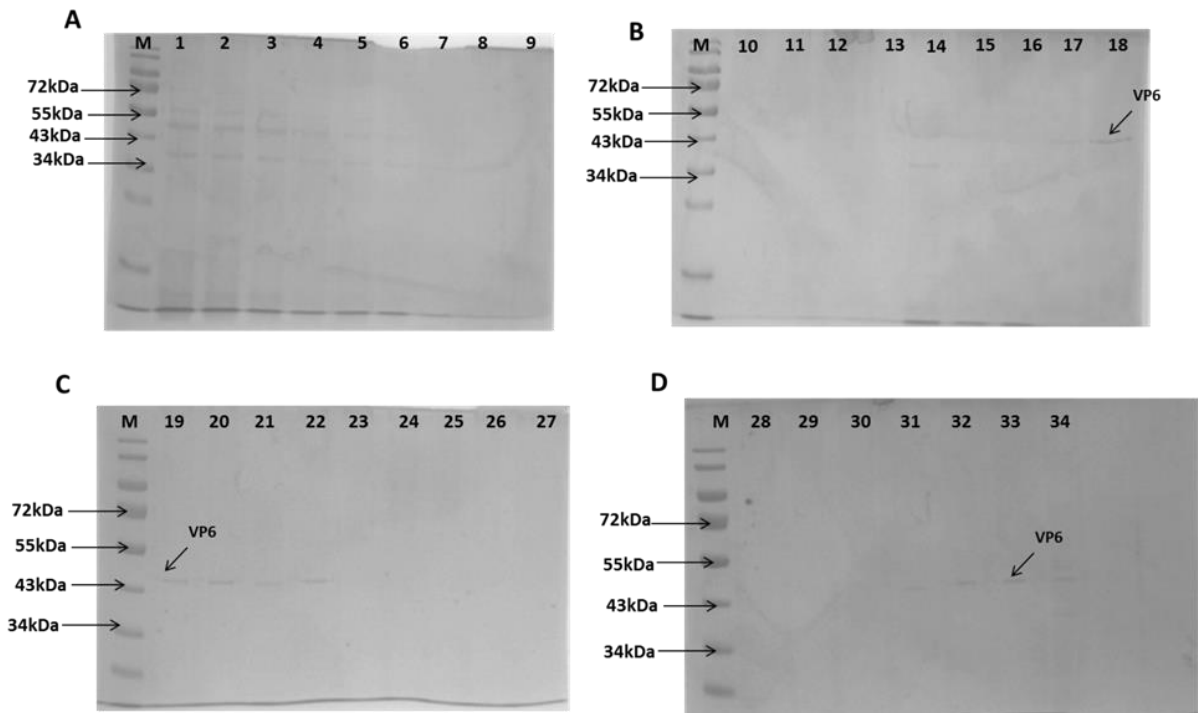


Figure 4.4: SDS-PAGE analysis of sucrose gradient fractions obtained following ultracentrifugation of the VP6 produced *A. adenivorans* cell lysate. A, Lane M is Page Ladder, Lanes 1-9 sucrose gradient fractions 1-9. B, Lane M is Page Ladder, Lanes 10-18 sucrose gradient fractions 10-18. C, Lane M is Page Ladder, Lanes 19-27 sucrose gradient fractions 19-27. D, Lane M is Page Ladder, Lanes 28-34 sucrose gradient fractions 28-34.

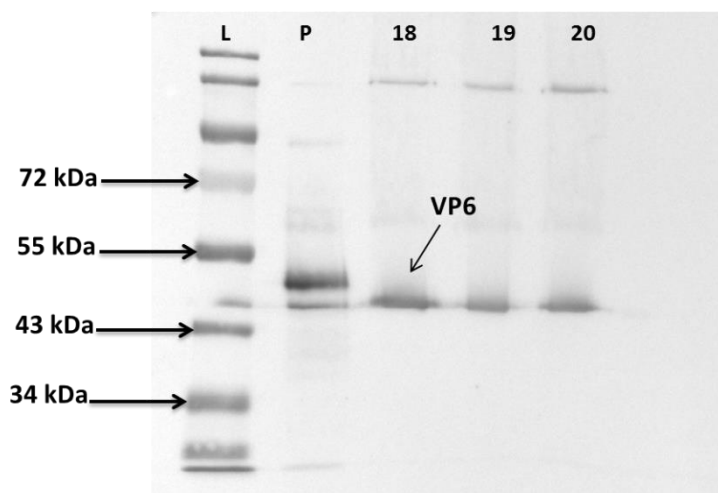


Figure 4.5: Western blot analysis of purified VP6 protein in sucrose fractions 18-20. Lane L, PageRuler™ Prestained Protein Ladder (Thermo Fisher Scientific). Lane P, positive control bacterial VP6, size of 48 kDa. Lanes 18, 19, 20 sucrose gradient fractions containing purified VP6 protein produced in *A. adenivorans*.

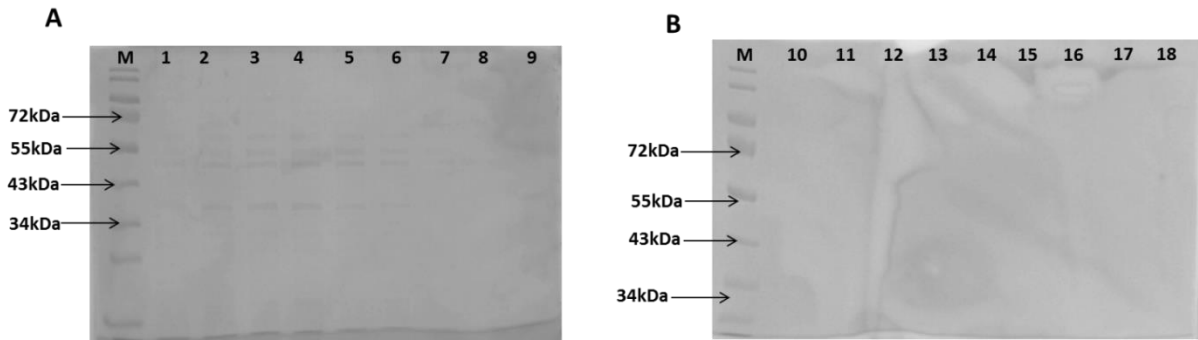


Figure 4.6: SDS-PAGE analysis of sucrose gradient fractions obtained following ultracentrifugation of the VP6 produced *P. pastoris* cell lysate. A, Lane M is Page Ladder, Lanes 1-9 sucrose gradient fractions 1-9. B, Lane M is Page Ladder, Lanes 10-18 sucrose gradient fractions 10-18.

For purification of the VP6 protein produced by *Y. lipolytica*, multiple bands were also observed in fractions 1-9 as seen in Figure 4.7a. However, less bands were observed in fractions 10-13. A band of the expected VP6 size is indicated with an arrow in Figure 4.7b. There were no bands seen from fractions 14-36 as seen in Figure 4.7b, c, d. However, the concentration was lower (1.9 mg/ml) compared to the purification of VP6 in *A. adenivorans* (Figure 4.4). Western blot analysis was carried out to confirm the presence of purified VP6 produced in *Y. lipolytica* in fractions 10-13 (Figure 4.8). Fractions 10-13 were pooled together to evaluate oligomeric structures of VP6 protein described in sections 4.3.3.

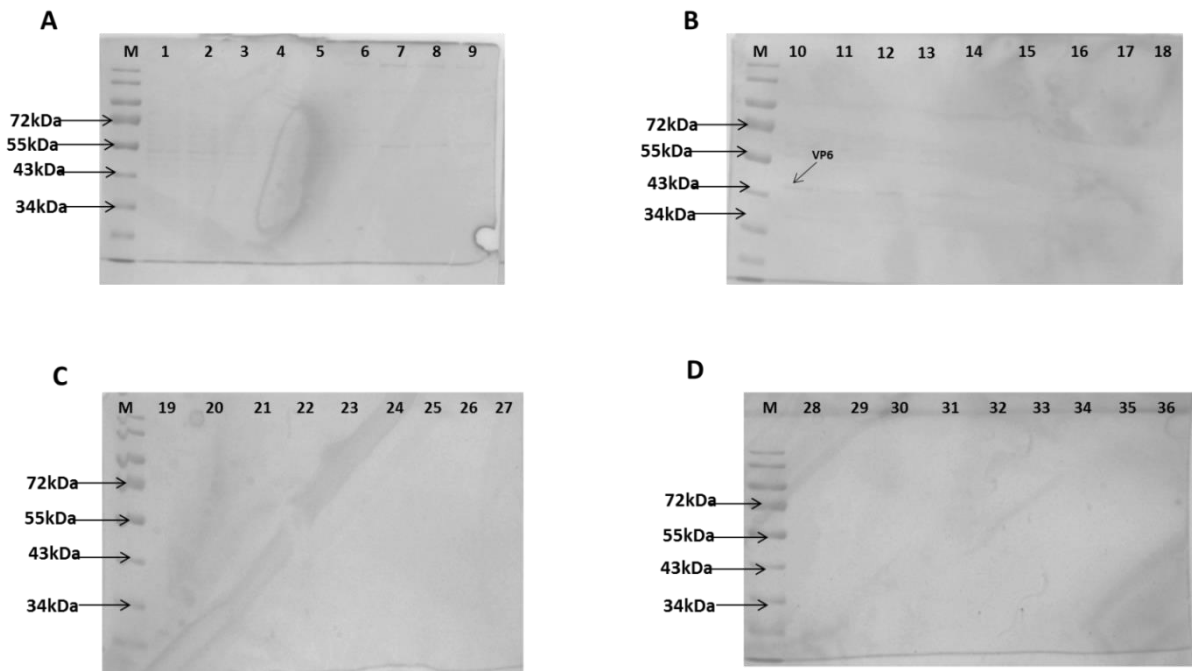


Figure 4.7: SDS-PAGE analysis of sucrose gradient fractions obtained following ultracentrifugation of the VP6 produced *Y. lipolytica* cell lysate. A, Lane M is Page Ladder, Lanes 1-9 sucrose gradient fractions 1-9. B, Lane M is Page Ladder, Lanes 10-18 sucrose gradient fractions 10-18. C, Lane M is Page Ladder, Lanes 19-27 sucrose gradient fractions 19-27. D, Lane M is Page Ladder, Lanes 28-34 sucrose gradient fractions 28-34.

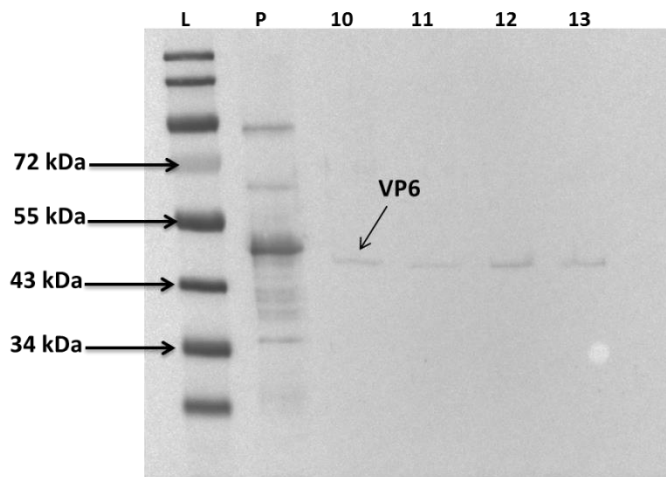


Figure 4.8: Western blot analysis of purified VP6 protein in sucrose fractions 10-13. Lane L, PageRuler™ Prestained Protein Ladder (Thermo Fisher Scientific). Lane P, VP6 bacterial positive control protein size of 48 kDa. Lanes 10, 11, 12, 13 sucrose gradient containing purified VP6 protein produced in *Y. lipolytica*.

There was no successful purification of VP6 produced by *S. cerevisiae* (Figure 4.8), similar to what was also seen for the purification of VP6 from the *P. pastoris* cell lysate. Multiple

bands were observed in fractions 1-6 (Figure 4.9a). No bands were seen in fractions 7-18 (Figure 4.9a, b). Fractions 19-36 were also analysed on the SDS-PAGE and no bands were seen (not shown).

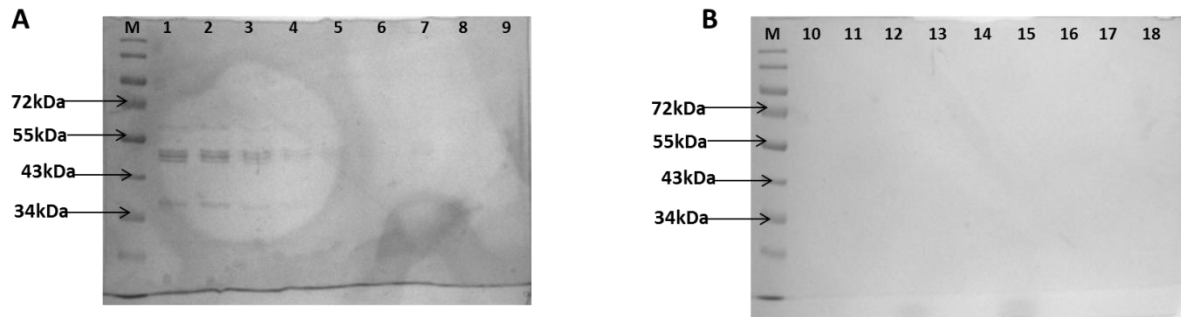


Figure 4.9: SDS-PAGE analysis of sucrose gradient fractions obtained following ultracentrifugation of the VP6 produced *S. cerevisiae* cell lysate. A, Lane M is Page Ladder, Lanes 1-9 sucrose gradient fractions 1-9. B, Lane M is Page Ladder, Lanes 10-18 sucrose gradient fractions 10-18.

Despite an efficient expression of VP6 in *P. angusta* as described in chapter 3, purification of VP6 protein in *P. angusta* resulted in a low concentration (1.2 mg/ml) of purified protein as seen in Figure 4.10. Multiple bands were seen in fractions 1-18 of Figure 4.9a, b similar to the sucrose gradient fractions obtained for the different yeast cell lysates analysed before (Figure 4.4, 4.6, 4.7 and 4.8). Despite the low concentration, a band of the expected size was detected in fraction 19 (Figure 4.10c). Western blot was carried out to verify the presence of purified VP6 protein in fractions 19-21. Fraction 18 was also in the western blot analyses. However, VP6 was only detected in fraction 18 not fraction 19. There were also low concentrations seen in the western blot carried out seen in Figure 4.11.

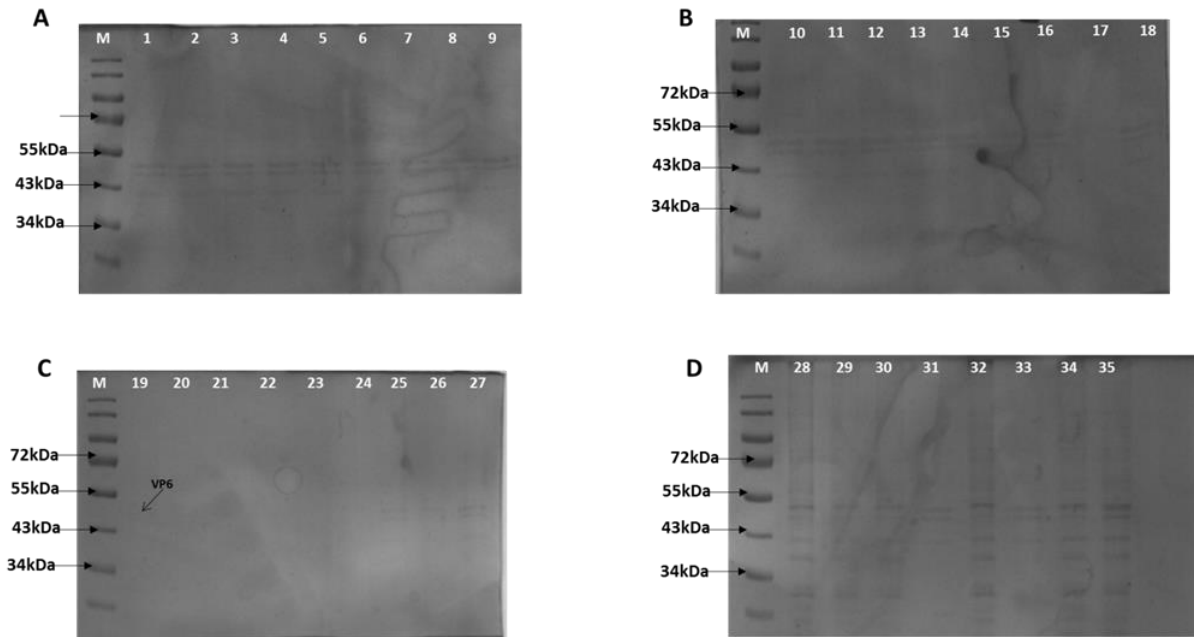


Figure 4.10: SDS-PAGE analysis of sucrose gradient fractions obtained following ultracentrifugation of the VP6 produced *P. angusta* cell lysate. A, Lane M is Page Ladder, Lanes 1-9 sucrose gradient fractions 1-9. B, Lane M is Page Ladder, Lanes 10-18 sucrose gradient fractions 10-18. C, Lane M is Page Ladder, Lanes 19-27 sucrose gradient fractions 19-27. D, Lane M is Page Ladder, Lanes 28-34 sucrose gradient fractions 28-34.

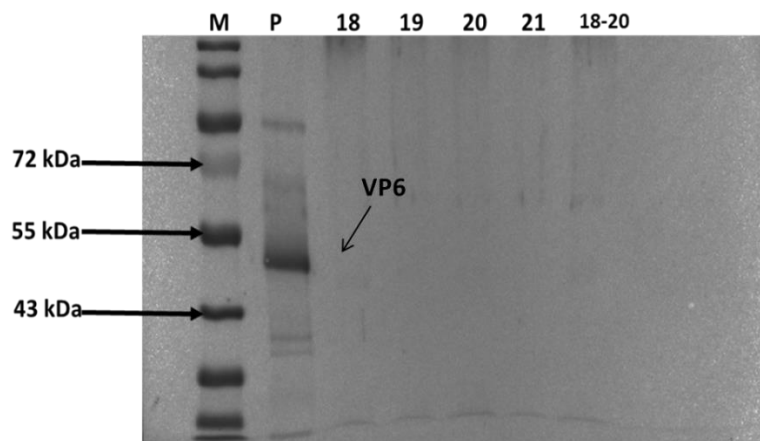


Figure 4.11: Western blot analysis of fractions obtained from sucrose gradient ultracentrifugation of VP6 produced *P. angusta* cell lysate. Lane M, Page ladder. Lane P, bacterial expressed VP6 as positive control. Lanes 18-21 purified VP6 from sucrose gradients of fractions 18-21. Lane 18-20, is fraction 18-20 pooled together.

Lastly, purification of VP6 produced by *K. lactis* resulted in no bands in any of the fractions as seen in Appendix K. Troubleshooting indicated that the KO VP6 ORF was lost as verified by colony PCR (Figure 4.12a), the same colonies containing KO VP6 containing expression

cassette that earlier showed expression of VP6 in *K. lactis* (Section 3.3.3.3, Figure 3.25). The clone used for purification is indicated with an arrow in Figure 4.12a. The *K. lactis* clones containing the PO VP6 ORF containing expression cassette that showed expression of VP6 (Appendix I, Figure I2 and I3) were also screened to confirm if the PO VP6 ORF was also lost. Colony PCR results indicated the presence of the PO VP6 ORF in the *K. lactis* genome as seen in Figure 4.12b. Clone 2 indicated with an arrow was chosen for VP6 purification (Figure 4.12b).

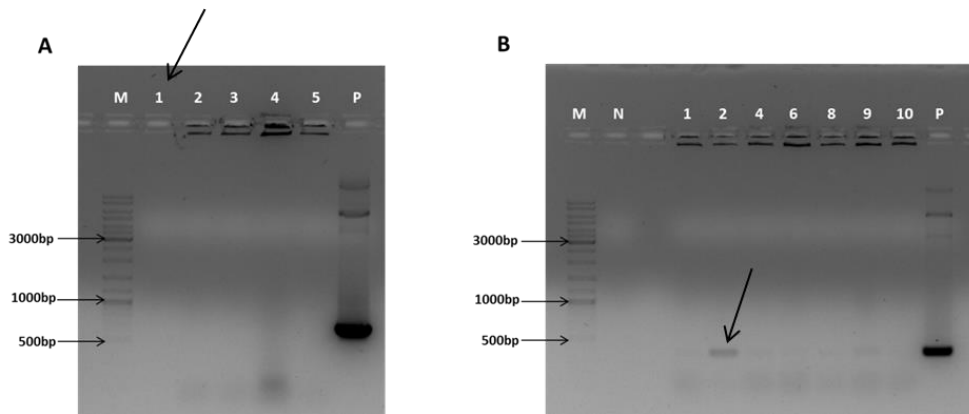


Figure 4.12: Analysis of the integration of VP6 ORF in *K. lactis* using colony PCR on 1% agarose gel. A, screening of expression cassette containing KO VP6 ORF in *K. lactis*. Lane M, GeneRuler DNA Ladder Mix (ThermoFisher Scientific), Lanes 1,-5, colonies screened for integration of KO VP6 ORF in *K. lactis* that previously showed expression. Lanes 1, colony used for purification of VP6 (arrow) Lane P, template control. B, screening of expression cassette containing PO VP6 ORF integration in *K. lactis*. Lane M, GeneRuler DNA Ladder Mix (Thermo Fisher Scientific). Lane N, negative PCR control. Lanes 1, 2, 4, 6, 8, 9, 10 colonies screened for integration of PO VP6 ORF in *K. lactis* that previously showed expression. Lane 1, newly KO VP6 ORF used for VP6 purification. Lane P, template control.

However, purification of VP6 produced in *K. lactis* was not sufficient as there were multiple bands in fractions 1-7 (Figure 4.13 a), while fractions 10-11 and 16-18 contained single bands but the bands were larger than the expected size of 45 kDa (Figure 4.13b). There were no bands seen from fractions 19-27 (Figure 4.13c), but multiple bands were seen in the last fractions, 29-36, as seen in Figure 4.13d.

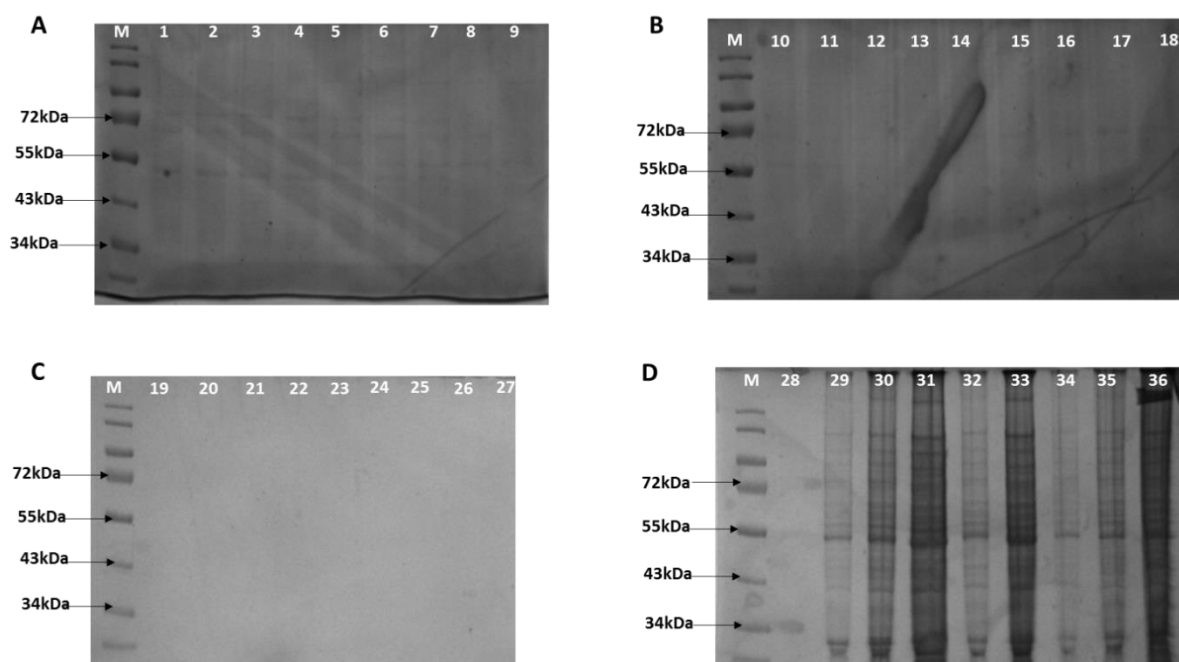


Figure 4.13: SDS-PAGE analysis of sucrose gradient fractions obtained following ultracentrifugation of the VP6 produced *K. lactis* cell lysate. Lane M, Page ladder, Lanes 1-9 sucrose gradient fractions 1-9. B, Lane M is Page Ladder, Lanes 10-18 sucrose gradient fractions 10-18. C, Lane M is Page Ladder, Lanes 19-27 sucrose gradient fractions 19-27. D, Lane M is Page Ladder, Lanes 28-34 sucrose gradient fractions 28-34.

VP6 protein could be purified from only three out of the six yeasts tested, namely *A. adenivorans* (Figure 4.3c), *P. angusta* (Figure 4.9c) and *Y. lipolytica* (Figure 4.6b). The concentrated samples were evaluated for the formation of nanotubes and nanospheres.

4.3.3 Evaluation of VP6 nanotubes and nanospheres particles

As described in Section 4.3.2, VP6 was successfully purified from only three yeasts. The samples were further concentrated through a series of filtration steps. Before assembly of nanotubes and nanospheres the VP6 protein structure should be dissociated into monomeric structures. The pH and ionic strength as well as concentration plays a vital role in the formation of the VP6 oligomeric structures of VP6 (Lappalainen *et al.*, 2016; Lepault *et al.*, 2001; Tosser *et al.*, 1992b). VP6 nanotubes were observed for the VP6 protein purified from *A. adenivorans* (Figure 4.14). However, none of the VP6 proteins purified from *P. angusta* and *Y. lipolytica* produced nanotubes. The nanotube illustrated in Figure 4.14 had a diameter of 73 nm which correlates with VP6 nanotubes that have been produced in insect cells (Lappalainen *et al.*, 2013, 2016; Lepault *et al.*, 2001). The detailed monomers structures inside the nanotubes can be seen in Figure 4.14.

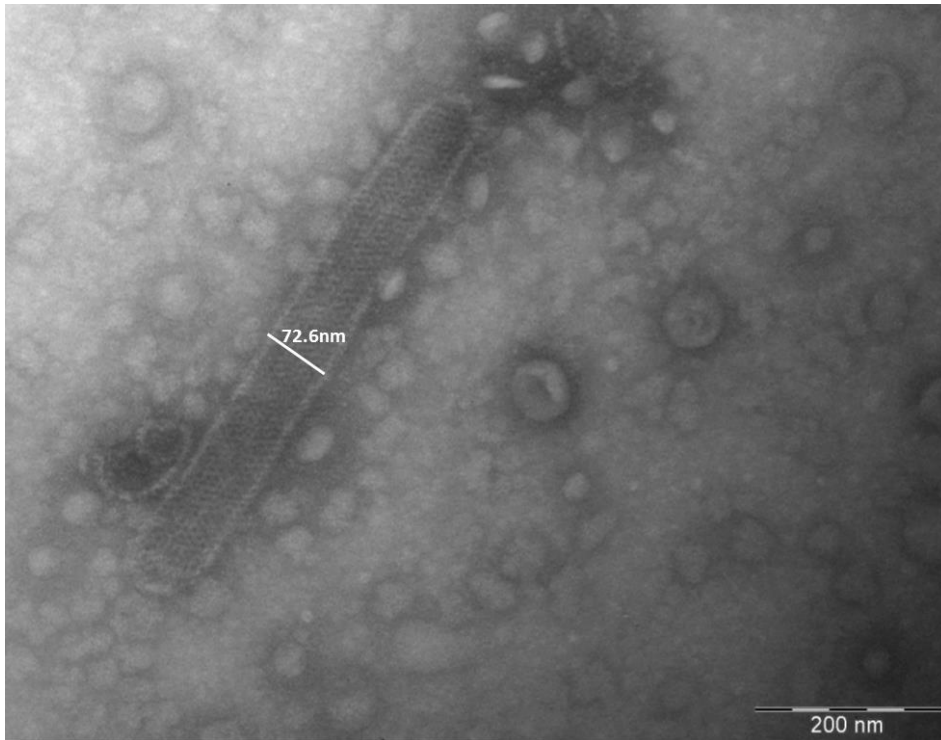


Figure 4.14: Transmission electron micrograph of rotavirus VP6 nanotubes structure produced in *A. adenivorans*. The image magnification is 20 000x.

Nanospheres were formed by VP6 purified from *A. adenivorans* and *Y. lipolytica* yeasts as seen in Figure 4.15 indicated with an arrow and no nanospheres were seen for VP6 purified for *P. angusta* (results not shown).

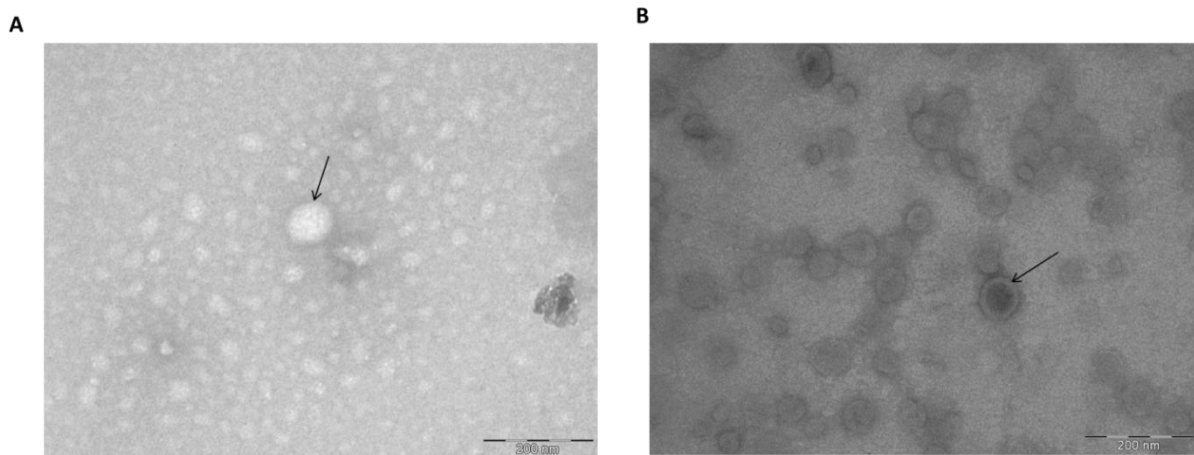


Figure 4.15: Evaluation of rotavirus VP6 nanospheres with TEM. A, rotavirus nanospheres produced in *A. adenivorans* (arrows). B, rotavirus nanospheres produced in *Y. lipolytica* (arrows).

4.4 Discussion

The growth curves indicated that the majority of yeasts producing VP6 reached the mid-exponential and exponential phases at comparable time points. There was no significant difference in total protein concentration of VP6 when *A. adenivorans*, *K. lactis* and *Y. lipolytica* cells were harvested at mid- or late-exponential phase.

It was possible to successfully purify VP6 produced by only three yeasts namely *A. adenivorans*, and *Y. lipolytica* without any impurities. Sufficient protein yield of VP6 was produced in *A. adenivorans* to result in tubular formation as compared to *Y. lipolytica*. Verification of the VP6 purified in these yeasts was carried out by western blot analysis. Density gradient ultracentrifugation is mostly used to purify viral proteins. The viral protein(s) are loaded on the sucrose density gradient and moves in the gradient until it reaches the density that corresponds to their equilibrium buoyant gradient. For the sucrose gradient results it was seen that the purification of VP6 in *A. adenivorans* had different density (Figure 4.4c and 4.10c) compared to VP6 purified in *Y. lipolytica* (Figure 4.7b). This may be due to differences in the density of the protein in the fractions.

The reason why there were no VP6 nanotubes in *Y. lipolytica* and *P. angusta* could be that the VP6 concentration recovered after sucrose gradient ultracentrifugation was too low for formation of oligomeric structures as the concentration of VP6 produced in *A. adenivorans* was higher compared VP6 produced in *P. angusta* and *Y. lipolytica*. It has been reported that *K. lactis* is an unstable host vector (Morlino *et al.*, 1999; Ooyen *et al.*, 2006) which could explain the loss of the KO VP6 ORF in the *K. lactis* genome.

A. adenivorans was the only yeast where successful assembly of both VP6 nanotubes and nanospheres were observed using TEM. The nanotubes produced in *A. adenivorans* had a similar diameter seen in previous work (Lappalainen *et al.*, 2013, 2016; Malm *et al.*, 2017). There were only VP6 nanospheres produced by *Y. lipolytica*. One reason why there were no VP6 nanotubes could be due to the ionic environment provided by the buffer, since nanotube formation is highly dependent on the ionic strength (Lepault *et al.*, 2001). Another factor could be due to the low concentration of the VP6 produced in *Y. lipolytica* which might have resulted in inefficient association of the VP6 monomers and therefore not forming nanotubes. The VP6 nanotubes produced by *A. adenivarons* may indicate that the protein is folding in its native form and this indicates that the protein might induce an immune response (Pastor *et al.*, 2014). The low resolution in our nanotubes images compared to Lepault and co-workers was due to the the fact that they used Cryo-TEM (Lepault *et al.*, 2001). TEM works on the bases of electrons interacting with organic matter which cause

damages to the sample due to creation of free radicals and breakage of chemical bonds (Egerton *et al.*, 2004; Glaeser, 1971). To overcome this, negative staining is used. The sample is stained with a chemical that is less radiation-sensitive like uranyl acetate (Brenner & Horne, 1959). However, negative staining does not penetrate into the sample (Carlo & Harris, 2012) while Cryo-TEM does not require staining of a sample. Samples are frozen with liquid nitrogen and this increases the resolution of the sample by 6-fold (Dubochet *et al.*, 1988).

This is the first time that VP6 nanotubes and nanospheres were produced in yeast cells as previous work on VP6 nanotubes and nanospheres were produced in either *E. coli* and mostly in insect cells using baculovirus expression. However, this study was not a quantitative but rather to test if rotavirus VP6 expressed in yeast cells can be able to assemble in oligomeric structures.

4.5 References

- Brenner, S. & Horne, R. W. (1959).** A negative staining method for high resolution electron microscopy of viruses. *Biochim Biophys Acta* **34**, 103–110.
- Bugli, F., Caprettini, V., Martini, C., Sterbini, F. P., Torelli, R., Longa, S. Della, Papi, M., Palmieri, V., Giardina, B. & other authors. (2014).** Synthesis and characterization of different immunogenic viral nanoconstructs from rotavirus VP6 inner capsid protein. *Int J Nanomedicine* **9**, 2727–2739.
- Carlo, S. De & Harris, J. R. (2012).** Negative staining and Cryo-negative Staining of Macromolecules and Viruses for TEM. *Micron* **42**, 117–131.
- Dubochet, J., Adrian, M., Chang, J. J., Homo, J. C., Lepault, J., McDowell, A. W. & Schultz, P. (1988).** Cryo-electron microscopy of vitrified specimens. *Q Rev Biophys* **21**, 129–228.
- Egerton, R. F., Li, P. & Malac, M. (2004).** Radiation damage in the TEM and SEM. *Micron* **35**, 399–409.
- Glaeser, R. M. (1971).** Limitations to significant information in biological electron microscopy as a result of radiation damage. *J Ultrastruct Res* **36**, 466–482.
- Lappalainen, S., Tamminen, K., Vesikari, T. & Blazevic, V. (2013).** Comparative immunogenicity in mice of rotavirus VP6 tubular structures and virus-like particles. *Hum Vaccin Immunother* **9**, 1991–2001.
- Lappalainen, S., Vesikari, T. & Blazevic, V. (2016).** Simple and efficient ultrafiltration method for purification of rotavirus VP6 oligomeric proteins. *Arch Virol* **161**, 3219–3223.
- Lepault, J., Petitpas, I., Erk, I., Navaza, J., Bigot, D., Dona, M., Vachette, P., Cohen, J. & Rey, F. A. (2001).** Structural polymorphism of the major capsid protein of rotavirus. *EMBO J* **20**, 1498–1507.
- Li, T., Lin, H., Zhang, Y., Li, M., Wang, D., Che, Y., Zhu, Y., Li, S., Zhang, J. & other authors. (2014).** Improved characteristics and protective efficacy in an animal model of E. coli derived recombinant double-layered rotavirus virus-like particles. *Vaccine* **32**, 1921–1931.
- Malm, M., Heinim, S., Vesikari, T. & Blazevic, V. (2017).** Rotavirus capsid VP6 tubular and spherical nanostructures act as local adjuvants when co-delivered with norovirus VLPs. *Clin Exp Immunology* **189**, 331–341.
- Morlino, G. B., Tizzani, L., Fleer, R., Frontali, L. & Bianchi, M. M. (1999).** Inducible Amplification of Gene Copy Number and Heterologous Protein Production in the Yeast *Kluyveromyces lactis*. *Appl Environ Microbiol* **65**, 4808–4813.
- Ooyen, A. J. J. Van, Dekker, P., Huang, M., Olsthoorn, M. M. A., Jacobs, D. I., Colussi, P. A. & Taron, C. H. (2006).** Heterologous protein production in the yeast *Kluyveromyces lactis*. *FEMS Yeast Res* **6**, 381–392.
- Pastor, A. R., Rodríguez-limas, W. A., Contreras, M. A., Esquivel, E., Esquivel-guadarrama, F., Ramírez, O. T. & Palomares, L. A. (2014).** The assembly conformation of rotavirus VP6 determines its protective efficacy against rotavirus challenge in mice. *Vaccine* **32**, 2874–2877.
- Ready, K. & Sabara, M. (1987).** In vitro assembly of bovine rotavirus nucleocapsid protein. *Virology* **157**, 189–198.
- Tosser, G., Labbe, M., Bremont, M., Cohen, J., Virologie, U. De, Moleculaires, I. & De, I. N. (1992).**

Expression of the Major Capsid Protein VP6 of Group C Rotavirus and Synthesis of Chimeric Single-Shelled Particles by Using Recombinant Baculoviruses. *J Virolgy* **66**, 5825–5831.

Chapter 5: Conclusions

In this work, the expression cassettes containing VP6 open reading frames (ORFs) codon optimised to favour expression in *A. adenivorans*, *K. lactis* and *P. angusta/P. pastoris* constructed by Mr M.S. Makatsa in a previous study were modified by site-directed mutagenesis. The expression cassettes containing the three VP6 ORFs contained an ATG in the promoter region upstream of the ORF. The VP6 ORF codon optimised for *A. adenivorans* and *K. lactis* expression cassettes were out of frame with the start codon in the promoter region. This discovery explained why there was previously no expression of the rotavirus VP6 protein in various yeasts (Makatsa, 2015). The expression cassettes containing optimised *A. adenivorans* and *K. lactis* VP6 ORF were modified by deletion-PCR to remove the ATG. Site-directed mutagenesis has been widely used to study the function of proteins and to enhance the activity of enzymes in the industry (Damián-Almazo & Saab-Rincón, 2013; Qin *et al.*, 2017).

Another factor to consider to enhance expression of VP6 protein is the Kozak sequence. The expression cassette containing VP6 ORF optimised for expression in *A. adenivorans*, contained a similar sequence to Kozak sequence of eukaryotes with the required purine (A/G) nucleotide at -3 position relative to the ATG which plays a crucial role in initiation of translation in eukaryotes (Kochetov, 2014; Kozak, 1984, 1986, 2002; Pesole *et al.*, 2000). However, the expression cassette containing the VP6 ORF optimised for expression in *K. lactis* did not contain the cytosine nucleotide at the -1 position, resulting in a sequence that differed from the Kozak sequence. The Kozak sequence was restored by subcloning the original VP6 ORF optimised for expression in *K. lactis* from GenScript into a modified vector, delATG_pKM177. The vector was modified by a colleague Mr. O.S. Folorunso who successfully removed the additional ATG.

The modified expression cassettes containing VP6 optimised for expression in *A. adenivorans* and *K. lactis* were tested for expression in various yeast strains. In addition, the VP6 ORF codon optimised for expression in *P. pastoris/P. angusta*, also modified for optimal expression by a colleague, Mr OS Folorunso, was tested for expression. In order to express the rotavirus VP6, the modified expression vectors were transformed into 14 various yeasts namely: *Arxula adenivorans* UFS1219, *Arxula adenivorans* UFS1220, *Debaryomyces hansenii* UFS0610, *Kluyveromyces lactis* UFS1167, *Pichia angusta* UFS0915, *Pichia angusta* UFS1507, *Pichia pastoris* UFS1552T, *Yarrowia lipolytica* UFS0097, *Yarrowia lipolytica* UFS 2221, *Yarrowia lipolytica* UFS2415, *Arxula adenivorans* LS3, *Saccharomyces cerevisiae* CENPK, *Pichia pastoris* GS115 and *Yarrowia lipolytica* PO 1F. All three expression cassettes containing VP6 ORFs exhibited highly effective integration

into the two *P. angusta* strains (*P. angusta* UFS0915 & *P. angusta* UFS1507). The VP6 ORFs codon optimised for *A. adenivorans* and *K. lactis* had a 93% integration into the two *A. adenivorans* strains from the UNESCO-MIRCEN Yeast Culture Collection (*A. adenivorans* UFS1219 & UFS1220). However, a low integration efficiency of the VP6 ORFs into the genome of the prototype strain, *A. adenivorans* strain (*A. adenivorans* LS3), was observed. These results were in contrast with the high integration of a foreign gene into this yeast strain reported in literature (Malak *et al.*, 2016; Wartmann *et al.*, 2002). No colonies were formed after transformation into *D. hansenii*. There were, however, colonies formed after transformation into *D. hansenii* in previous work done by Mr. M.S. Makatsa, but in none of the colonies VP6 ORFs integrated. We also saw this phenomenon in the *Y. lipolytica* strains where poor or no integration was observed, although >50 colonies formed on the hygromycin plates. This could be due to the integration of the hygromycin gene, *hph*, but not the VP6 ORFs into the genome, as seen in Mr. M.S. Makatsa's work (Makatsa, 2015). The integration of VP6 ORF codon optimised for *K. lactis* into the various yeasts tested was relatively low compared to the VP6 ORF codon optimised for *A. adenivorans* and *P. angusta/P. pastoris*.

Yeast colonies that showed integration into the various yeast genomes were screened for VP6 expression. Verification of expression was carried out by western blot analysis using the commercial polyclonal Nebraska calf diarrhoea virus (NCDV) antibody raised against a bovine rotavirus strain for detection of the VP6 protein. Successful detection of VP6 using the polyclonal NCDV antibody has been shown by Makatsa (2015) and (Jere *et al.*, 2014). All the *P. angusta* colonies that tested positive for integration, also expressed VP6, making integration and expression of the expression cassettes highly efficient in *P. angusta*. Limited integration and expression was, however, seen in *P. pastoris*. Bredell and co-workers also found *P. angusta* as a good and high yield producer of VP6 and outperformed *P. pastoris* in bioreactors (Bredell *et al.*, 2016). There was expression of rotavirus VP6 protein in other yeast strains that have not been reported in literature before, i.e. *A. adenivorans*, *K. lactis*, and *Y. lipolytica*. We identified six yeasts that showed expression of VP6 protein. Growth curves were constructed in order to evaluate the best time to harvest cells either at mid-exponential or late-exponential phase. Expression of VP6 in *P. angusta*, *P. pastoris* and *S. cerevisiae* showed a higher total protein concentration in the late-exponential phase as seen in Table 4.1.

Rotavirus VP6 protein has a unique feature to form oligomeric structures (nanospheres and nanotubes) (Lappalainen *et al.*, 2013, 2016a; Lepault *et al.*, 2001; Malm *et al.*, 2017). The VP6 nanotubes have been associated with the induction of protective immunity in mice (Lappalainen *et al.*, 2013; Pastor *et al.*, 2014). The ability of VP6 protein to assemble into

nanospheres and nanotubes mainly depend on the pH and ionic strength (Lepault *et al.*, 2001). The assembly of nanospheres ranges from pH 3-5 while assembly of nanotubes ranges from pH 5.5-7.5 (Lappalainen *et al.*, 2016a; Lepault *et al.*, 2001). Lappalainen and co-workers developed a simple and efficient ultrafiltration method to purify VP6 and assemble the oligomeric structures in insect cells (Lappalainen *et al.*, 2016a). However, to date no work has been reported on the reconstruction of VP6 nanotubes and nanosphere particles in yeasts. The Lappalainen and co-workers method was adapted to evaluate VP6 oligomeric structures in yeast cells. Firstly, to remove impurities related to the yeast proteins, the VP6 protein was purified by sucrose density gradient centrifugation. VP6 produced in *A. adenivorans* was purified in fractions 18-22. A single band of the expected size was produced in *P. angusta* in similar fractions as VP6 produced in *A. adenivorans*, but could not be confirmed as VP6. VP6 produced in *Y. lipolytica* was however purified in fractions 10-13. This indicates that the VP6 produced in *A. adenivorans* had a different density than that produced in *Y. lipolytica*. Initial experiments indicated no bands in any of the sucrose gradient fractions for VP6 produced in *K. lactis*. This led to the discovery that the KO VP6 ORF, that showed positive integration into the *K. lactis* genome (Chapter 3), was lost. It has been reported that *K. lactis* is an unstable expression host (Morlino *et al.*, 1999; Ooyen *et al.*, 2006). However, it is interesting to note that the PO VP6 ORF integration was more stable. None of the KO integrations previously seen were maintained whereas the PO VP6 ORF could be detected. Purification of VP6 protein produced in *K. lactis*, *S. cerevisiae* and *P. pastoris* was not successful as there were multiple bands in the sucrose fractions and no clear band with the correct expected size of VP6. The purified VP6 produced in *A. adenivorans* and *Y. lipolytica* were confirmed by western blot and further concentrated with Amicon Ultra-15 30kDa centrifugal filter device. There were only nanospheres assembly for VP6 produced in *Y. lipolytica*, while VP6 produced in *A. adenivorans* resulted in both nanotubes and nanosphere assembly. The nanotube assembly by VP6 produced by *A. adenivorans* is similar in diameter (72.6nm) as seen in literature (Lappalainen *et al.*, 2013, 2016a; Lepault *et al.*, 2001; Malm *et al.*, 2017).

From our results we conclude that *A. adenivorans* as an expression host for rotavirus VP6, is considered an excellent candidate for future development of a rotavirus subunit vaccine as a long term objective for cheaper rotavirus vaccines for use in Africa.

5.1 References

- Bredell, H., Smith, J. J., Prins, W. A., Görgens, J. F. & Zyl, W. H. Van. (2016).** Expression of rotavirus VP6 protein : A comparison amongst *Escherichia coli* , *Pichia pastoris* and *Hansenula polymorpha*. *FEMS Yeast Res* **16**, 1–12.
- Damián-Almazo, J. Y. & Saab-Rincón, G. (2013).** Site-Directed Mutagenesis as Applied to Biocatalysts. In *Genet Manip DNA Protein - Examples from Curr Res*, pp. 303–330. Edited by D. Figurski.
- Jere, K. C., Neill, H. G. O., Potgieter, A. C. & Van Dijk, A. A. (2014).** Chimaeric Virus-Like Particles Derived from Consensus Genome Sequences of Human Rotavirus Strains Co-Circulating in Africa. *PLoS One* **9**, 1–12.
- Kochetov, A. V. (2014).** Genome analysis AUG codons at the beginning of protein coding sequences are frequent in eukaryotic mRNAs with a suboptimal start codon context. *Bioinformatics* **21**, 837–840.
- Kozak, M. (1984).** Compilation and analysis of sequences upstream from the translational start site in eukaryotic. *Nucleic Acids Research* **12**, 857–872.
- Kozak, M. (1986).** Point Mutations Define a Sequence Flanking the AUG Initiator Codon That Modulates Translation by Eukaryotic Ribosomes. *Cell* **44**, 283–292.
- Kozak, M. (2002).** Pushing the limits of the scanning mechanism for initiation of translation. *Gene* **299**, 1–34.
- Lappalainen, S., Tamminen, K., Vesikari, T. & Blazevic, V. (2013).** Comparative immunogenicity in mice of rotavirus VP6 tubular structures and virus-like particles. *Hum Vaccin Immunother* **9**, 1991–2001.
- Lappalainen, S., Vesikari, T. & Blazevic, V. (2016).** Simple and efficient ultrafiltration method for purification of rotavirus VP6 oligomeric proteins. *Arch Virol* **161**, 3219–3223. Springer Vienna.
- Lepault, J., Petitpas, I., Erk, I., Navaza, J., Bigot, D., Dona, M., Vachette, P., Cohen, J. & Rey, F. A. (2001).** Structural polymorphism of the major capsid protein of rotavirus. *EMBO J* **20**, 1498–1507.
- Makatsa, M. S. (2015).** *Engineering yeast strains for the expression of South African G9P [6] rotavirus VP2 and VP6 structural proteins* By. University of the Free State.
- Malak, A., Baronian, K. & Kunze, G. (2016).** *Blastobotrys (Arxula) adenivorans* : a promising alternative yeast for biotechnology and basic research. *Yeast* **33**, 535–547.
- Malm, M., Heinim, S., Vesikari, T. & Blazevic, V. (2017).** Rotavirus capsid VP6 tubular and spherical nanostructures act as local adjuvants when co-delivered with norovirus VLPs. *Clin Exp Immunology* **189**, 331–341.
- Morlino, G. B., Tizzani, L., Fleer, R., Frontali, L. & Bianchi, M. M. (1999).** Inducible Amplification of Gene Copy Number and Heterologous Protein Production in the Yeast *Kluyveromyces lactis*. *Appl Environ Microbiol* **65**, 4808–4813.
- Ooyen, A. J. J. Van, Dekker, P., Huang, M., Olsthoorn, M. M. A., Jacobs, D. I., Colussi, P. A. & Taron, C. H. (2006).** Heterologous protein production in the yeast *Kluyveromyces lactis*. *FEMS Yeast Res* **6**, 381–392.

- Pastor, A. R., Rodríguez-limas, W. A., Contreras, M. A., Esquivel, E., Esquivel-guadarrama, F., Ramírez, O. T. & Palomares, L. A. (2014).** The assembly conformation of rotavirus VP6 determines its protective efficacy against rotavirus challenge in mice. *Vaccine* **32**, 2874–2877.
- Pesole, G., Gissi, C., Grillo, G., Licciulli, F., Liuni, S. & Saccone, C. (2000).** Analysis of oligonucleotide AUG start codon context in eukariotic mRNAs. *Gene* **261**, 85–91.
- Qin, N., Shen, Y., Yang, X., Su, L., Tang, R., Li, W. & Wang, M. (2017).** Site-directed mutagenesis under the direction of in silico protein docking modeling reveals the active site residues of 3-ketosteroid- Δ 1 -dehydrogenase from *Mycobacterium neoaurum*. *World J Microbiol Biotechnol* **33**, 1–9. Springer Netherlands.
- Wartmann, T., Böer, E., Pico, A. H., Sieber, H., Bartelsen, O., Gellissen, G. & Kunze, G. (2002).** High-level production and secretion of recombinant proteins by the dimorphic yeast *Arxula adenivorans*. *FEMS Yeast Res* **2**, 363–369.

Appendix A: Alignment of Sanger sequence result of delATG_pKM177_ AO VP6 with *in silico* clones using EMBOSS Needle Pairwise Sequence Alignment.

pKM177_VP6AO	301	TTGGGACTTTAGCCAAGGGTATAAAAAGACCACCGTCCCCGAATTACCTTT	350
pKM177_delVP6	1	-----	0
		yTEF promoter XhoI	
pKM177_VP6AO	351	CCTCTTCTTTCTCTCTCTCCTTGTCAACTCACACCCGAAATGCTCGAGC	400
pKM177_delVP6	1	-----CTTTTCTCTCTCTCCTTGTCAACTCACACCCGAA--CTCGAGC	41
		↑	
pKM177_VP6AO	401	ATGGATGTTTTGTATTTCGCTTTCTAAGACTCTGAAGGATGCCCGAGATAA	450
pKM177_delVP6	42	ATGGATGTTTTGTATTTCGCTTTCTAAGACTCTGAAGGATGCCCGAGATAA	91
pKM177_VP6AO	451	GATTGTTGAGGGAACTTTGTATTCTAATGTTTCTGATCTGATTCAGCAGT	500
pKM177_delVP6	92	GATTGTTGAGGGAACTTTGTATTCTAATGTTTCTGATCTGATTCAGCAGT	141
pKM177_VP6AO	501	TCAACCAGATGATTATCACTATGAACGGTAATGAGTTTCAGACCGGAGGT	550
pKM177_delVP6	142	TCAACCAGATGATTATCACTATGAACGGTAATGAGTTTCAGACCGGAGGT	191
pKM177_VP6AO	551	ATTGGAACCTCCCTATCCGAAACTGGAATTTGACTTTGGACTGCTTGG	600
pKM177_delVP6	192	ATTGGAACCTCCCTATCCGAAACTGGAATTTGACTTTGGACTGCTTGG	241
pKM177_VP6AO	601	TACTACCCTCTTGAAC TTGGATGCTAATTACGTGGAGACTGCCCGAAATA	650
pKM177_delVP6	242	TACTACCCTCTTGAAC TTGGATGCTAATTACGTGGAGACTGCCCGAAATA	291
pKM177_VP6AO	651	CCATTGACTATTTTCGTTGACTTTGTGGATAACGTCTGCATGGATGAGATG	700
pKM177_delVP6	292	CCATTGACTATTTTCGTTGACTTTGTGGATAACGTCTGCATGGATGAGATG	341
pKM177_VP6AO	701	GTCCGAGAGTCTCAGCGAAACGGTATTGCTCCTCAGTCGGACTCTCTCCG	750
pKM177_delVP6	342	GTCCGAGAGTCTCAGCGAAACGGTATTGCTCCTCAGTCGGACTCTCTCCG	391
pKM177_VP6AO	751	AAAGTTGTCCGGAATTAAGTTCAAGCGAATCAACTTCGATAATTCTTCCG	800
pKM177_delVP6	392	AAAGTTGTCCGGAATTAAGTTCAAGCGAATCAACTTCGATAATTCTTCCG	441
pKM177_VP6AO	801	AGTACATTGAGA ACTGGAATCTGCAGA ACCGACGACAGCGAACTGGATTC	850
pKM177_delVP6	442	AGTACATTGAGA ACTGGAATCTGCAGA ACCGACGACAGCGAACTGGATTC	491
pKM177_VP6AO	851	ACCTTTCACAAGCCTAACATCTTCCCCTATTCCGCTCGTTACTCTTAA	900
pKM177_delVP6	492	ACCTTTCACAAGCCTAACATCTTCCCCTATTCCGCTCGTTACTCTTAA	541
pKM177_VP6AO	901	CCGATCTCAGCCTGCTCATGACAATCTGATGGGAACCATGTGGCTTAACG	950
pKM177_delVP6	542	CCGATCTCAGCCTGCTCATGACAATCTGATGGGAACCATGTGGCTTAACG	591
pKM177_VP6AO	951	CTGGTTCGAGATTCAGGTTGCCGATTTGATTACTCGTGTGCTATCAAC	1000
pKM177_delVP6	592	CTGGTTCGAGATTCAGGTTGCCGATTTGATTACTCGTGTGCTATCAAC	641
pKM177_VP6AO	1001	GCTCCCGCAATACTCAGCAGTTCGAGCACATTGTGCAGCTCCGACGAGT	1050

pKM177_delVP6	642	GCTCCCGCCAATACTCAGCAGTTCGAGCACATTGTGCAGCTCCGACGAGT	691
pKM177_VP6AO	1051	CTTGACTACCGCCACTATCACCTGCTTCCTGACGCTGAGCGATTCTCTT	1100
pKM177_delVP6	692	CTTGACTACCGCCACTATCACCTGCTTCCTGACGCTGAGCGATTCTCTT	741
pKM177_VP6AO	1101	TTCCCCGAGTTATTAATTCGCTGATGGTGCCACTACCTGGTACTTCAAC	1150
pKM177_delVP6	742	TTCCCCGAGTTATTAATTCGCTGATGGTGCCACTACCTGGTACTTCAAC	791
pKM177_VP6AO	1151	CCTGTGATCCTCCGACCAACAATGTGGAGGTCGAGTTTCTCTTGAACGG	1200
pKM177_delVP6	792	CCTGTGATCCTCCGACCAACAATGTGGAGGTCGAGTTTCTCTTGAACGG	841
pKM177_VP6AO	1201	TCAGATTATCAATACTTATCAGGCCCGATTCGGAACCATGTGGCTCGAA	1250
pKM177_delVP6	842	TCAGATTATCAATACTTATCAGGCCCGATTCGGAACCATGTGGCTCGAA	891
pKM177_VP6AO	1251	ACTTCGACACTATCCGACTGTCTTTTCAGCTTATGCGACCTCCCAATATG	1300
pKM177_delVP6	892	ACTTCGACACTATCCGACTGTCTTTTCAGCTTATGCGACCTCCCAATATG	941
pKM177_VP6AO	1301	ACCCCTTCGTCGCTGCCCTTTTCCCTAACGCCAGCCCTTTGAGCACCA	1350
pKM177_delVP6	942	ACCCCTTCGTCGCTGCCCTTTTCCCTAACGCCAGCCCTTTGAGCACCA	991
pKM177_VP6AO	1351	TGCTACTGTTGGACTGACCCTTAAGATTGAGTCCGCCGTTTGCAGTCGG	1400
pKM177_delVP6	992	TGCTACTGTTGGACTGACCCTTAAGATTGAGTCCGCCGTTTGCAGTCGG	1041
pKM177_VP6AO	1401	TGCTCGCTGATGCCTCGGAGACTATGTTGGCCAACGTTACCTCTGTGCGA	1450
pKM177_delVP6	1042	TGCTCGCTGATGCCTCGGAGACTATGTTGGCCAACGTTACCTCTGTGCGA	1091
pKM177_VP6AO	1451	CAGGAGTACGCTATTCTGTTCGACCCGTTTTTCTCCCGGTATGAACTG	1500
pKM177_delVP6	1092	CAGGAGTACGCTATTCTGTTCGACCCGTTTTTCTCCCGGTATGAACTG	1141
pKM177_VP6AO	1501	GACTGACCTGATCACCAATTATTCTCCTTCCCAGAGGATAACCTTCAGC	1550
pKM177_delVP6	1142	GACTGACCTGATCACCAATTATTCTCCTTCCCAGAGGATAACCTTCAGC	1191
pKM177_VP6AO	1551	GAGTGTCACTGTTCGCTTCGATTCGATCTATGCTGGTCAAGTAGAGCGCT	1600
pKM177_delVP6	1192	GAGTGTCACTGTTCGCTTCGATTCGATCTATGCTGGTCAAGTAGAGCGCT	1241
pKM177_VP6AO	1601	ATTAATCCTAGGTGATCTGATCTGCTTACTTTACTTAACGACCAAAGAAA	1650
pKM177_delVP6	1242	ATTAATCCTAGGTGATCTGATCTGCTTACTTTACTTAACGACCAAAGAAA	1291
pKM177_VP6AO	1651	AACGACAAAAAAAAAATATTACTACTATTAAAATAAATTAGTATTTTTCT	1700
pKM177_delVP6	1292	AACGACAAAAAAAAAATATTACTACTATTAAAATAAATTAGTATTTTTCT	1341
pKM177_VP6AO	1701	CTTCTTACGATATGATATGATGCTATGAAATCATCATCTTCTTAACTTC	1750
pKM177_delVP6	1342	CTTCTTACGATATGATATGATGCTATGAAATCATCATCTTCTTAACTTC	1391

Figure A1: EMBOSS Needle Pairwise Sequence Alignment of VP6_AO *in silico* clone of the VP6_AO construct with modified sequence VP6_AO ORF. The aligned expression constructs consists of *Y. lipolytica* TEF promoter (yTEFp), orange, and *K. marxianus* terminator (kmINUt), blue. The VP6 AO ORF is cloned at the XhoI, purple, and Eco 47III, green restriction sites. The ATG was successful removed indicated with an arrow. NO mutation of VP6_AO ORF, black, from the start codon, red, to the stop codon, underlined.

Appendix B: Alignment of Sanger sequence result of delATG_pKM177_ KO VP6 with *in silico* clones using EMBOSS Needle Pairwise Sequence Alignment.

pKM177_VP6KO	301	TTGGGACTTTAGCCAAGGGTATAAAAGACCACCGTCCCCGAATTACCTTT	350
delATG_pKM177	123	TTGGGACTTTAGCCAAGGGTATAAAAGACCACCGTCCCCGAATTACCTTT	172
		yTEF promoter	
		XhoI	
pKM177_VP6KO	351	CCTCTTCTTTTCTCTCTCTCCTTGTCAACTCACACCCGAAATGCTCGAG-	399
delATG_pKM177	173	CCTCTTCTTTTCTCTCTCTCCTTGTCAACTCACACCCGAA---CTCGAGC	219
		↖	
pKM177_VP6KO	400	ATGATGTATTGTATTCATTGAGTAAAACCTTGAAGGATGCTAGAGATAA	449
delATG_pKM177	220	ATGATGTATTGTATTCATTGAGTAAAACCTTGAAGGATGCTAGAGATAA	269
pKM177_VP6KO	450	AATCGTGGAAGGAACCTTGTATAGTAACGTGTCTGATTTGATACAACAAT	499
delATG_pKM177	270	AATCGTGGAAGGAACCTTGTATAGTAACGTGTCTGATTTGATACAACAAT	319
pKM177_VP6KO	500	TCAACCAAATGATAATCACCATGAATGGAAACGAATTTCAAACAGGTGGA	549
delATG_pKM177	320	TCAACCAAATGATAATCACCATGAATGGAAACGAATTTCAAACAGGTGGA	369
pKM177_VP6KO	550	ATCGGTAATTTGCCAATCAGAACTGGAACCTTCGATTTTCGGTTTGTGGG	599
delATG_pKM177	370	ATCGGTAATTTGCCAATCAGAACTGGAACCTTCGATTTTCGGTTTGTGGG	419
pKM177_VP6KO	600	AACTACATTGTTGAATTTGGATGCTAACTACGTGGAAACAGCAAGAAACA	649
delATG_pKM177	420	AACTACATTGTTGAATTTGGATGCTAACTACGTGGAAACAGCAAGAAACA	469
pKM177_VP6KO	650	CCATAGATTACTTCGTCGATTTTCGTAGATAACGTTTGTATGGATGAAATG	699
delATG_pKM177	470	CCATAGATTACTTCGTCGATTTTCGTAGATAACGTTTGTATGGATGAAATG	519
pKM177_VP6KO	700	GTTAGAGAATCACAAAGAAATGGTATCGCTCCACAAAGTGATTCCTTGAG	749
delATG_pKM177	520	GTTAGAGAATCACAAAGAAATGGTATCGCTCCACAAAGTGATTCCTTGAG	569
pKM177_VP6KO	750	AAAATTATCTGGTATTTAAATTCAGAGAATCAATTTTCGATAACTCTTCAG	799
delATG_pKM177	570	AAAATTATCTGGTATTTAAATTCAGAGAATCAATTTTCGATAACTCTTCAG	619
pKM177_VP6KO	800	AATACATCGAAAACCTGGAACCTTGCAAAACAGAAGACAAAGAACCGGTTTC	849
delATG_pKM177	620	AATACATCGAAAACCTGGAACCTTGCAAAACAGAAGACAAAGAACCGGTTTC	669
pKM177_VP6KO	850	ACTTTTCATAAGCCAAATATCTTCCCTTACTCTGCATCTTTCACCTTAA	899
delATG_pKM177	670	ACTTTTCATAAGCCAAATATCTTCCCTTACTCTGCATCTTTCACCTTAA	719
pKM177_VP6KO	900	TAGATCTCAACCAGCTCATGATAACTTGATGGGTACAATGTGGTTAAATG	949
delATG_pKM177	720	TAGATCTCAACCAGCTCATGATAACTTGATGGGTACAATGTGGTTAAATG	769
pKM177_VP6KO	950	CTGGATCTGAAATCCAAGTCGCAGGTTTTGATTATTCATGTGCTATAAAT	999
delATG_pKM177	770	CTGGATCTGAAATCCAAGTCGCAGGTTTTGATTATTCATGTGCTATAAAT	819

pKM177_VP6KO	1000	GCTCCTGCAAACACTCAACAATTCGAACATATCGTACAATTGAGAAGAGT	1049
delATG_pKM177	820	GCTCCTGCAAACACTCAACAATTCGAACATATCGTACAATTGAGAAGAGT	869
pKM177_VP6KO	1050	TTTGACCACTGCAACTATCACATTGTTACCAGATGCTGAAAGATTCTCTT	1099
delATG_pKM177	870	TTTGACCACTGCAACTATCACATTGTTACCAGATGCTGAAAGATTCTCTT	919
pKM177_VP6KO	1100	TTCCCTAGAGTGATAAACTCAGCTGATGGTGCAACAACCTGGTATTTCAAT	1149
delATG_pKM177	920	TTCCCTAGAGTGATAAACTCAGCTGATGGTGCAACAACCTGGTATTTCAAT	969
pKM177_VP6KO	1150	CCAGTCATTTTGAGACCTAACCAACGTTGAAGTGGAATTCCTGTTGAACGG	1199
delATG_pKM177	970	CCAGTCATTTTGAGACCTAACCAACGTTGAAGTGGAATTCCTGTTGAACGG	1019
pKM177_VP6KO	1200	ACAAATAATTAACACTTACCAAGCAAGATTCGGTACAATCGTTGCTAGAA	1249
delATG_pKM177	1020	ACAAATAATTAACACTTACCAAGCAAGATTCGGTACAATCGTTGCTAGAA	1069
pKM177_VP6KO	1250	ACTTCGATACTATCAGATTGAGTTTCCAATTGATGAGACCACCTAACATG	1299
delATG_pKM177	1070	ACTTCGATACTATCAGATTGAGTTTCCAATTGATGAGACCACCTAACATG	1119
pKM177_VP6KO	1300	ACACCATCAGTAGCTGCATTGTTCCCAAATGCACAACCTTTTGAACATCA	1349
delATG_pKM177	1120	ACACCATCAGTAGCTGCATTGTTCCCAAATGCACAACCTTTTGAACATCA	1169
pKM177_VP6KO	1350	TGCTACTGTTGGTTTGACATTGAAGATCGAAAAGTGCAGTATGTGAATCCG	1399
delATG_pKM177	1170	TGCTACTGTTGGTTTGACATTGAAGATCGAAAAGTGCAGTATGTGAATCCG	1219
pKM177_VP6KO	1400	TTTTGGCTGATGCAAGTGAAACAATGTTAGCAAACGTGACCTCCGTCAGA	1449
delATG_pKM177	1220	TTTTGGCTGATGCAAGTGAAACAATGTTAGCAAACGTGACCTCCGTCAGA	1269
pKM177_VP6KO	1450	CAAGAATATGCTATTCCAGTAGGTCCTGTTTTTCCACCTGGAATGAATTG	1499
delATG_pKM177	1270	CAAGAATATGCTATTCCAGTAGGTCCTGTTTTTCCACCTGGAATGAATTG	1319
pKM177_VP6KO	1500	GACCGATTGATCACTAACTACAGTCCATCCAGAGAAGATAAAATTTGCAA	1549
delATG_pKM177	1320	GACCGATTGATCACTAACTACAGTCCATCCAGAGAAGAT-AAATTTGCAA	1368
		Eco47III	
pKM177_VP6KO	1550	AGAGTGTTCACTGTCGCTTCTATCAGATCAATGTTGGTTAAATAAAGCGC	1599
delATG_pKM177	1369	AGAGTGTTCACTGTCGCTTCTATCAGATCAATGTTGGTTAAATAAAGCGC	1418
		kmINU terminator	
pKM177_VP6KO	1600	TATTAATCCTAGGTGATCTGATCTGCTTACTTTACTTAAACGACCAAAGAA	1649
delATG_pKM177	1419	TATTAATCCTAGGTGATCTGATCTGCTTACTTTACTTAAACGACCAAAGAA	1468
pKM177_VP6KO	1650	AAACGACAAAAAAAAAATATTACTACTATTAAAATAAATTAGTATTTTTC	1699
delATG_pKM177	1469	AAACGACAAAAAAAAAATATTACTACTATTAAAATAAATTAGTATTTTTC	1518
pKM177_VP6KO	1700	TCTTCTTACGATATGATATGATGCTATGAAATCATCATCTTCTTAACTTT	1749
delATG_pKM177	1519	TCTTCTTACGATATGATATGATGCTATGAAATCATCATCTTCTTAACTTT	1568

Figure B1: EMBOSS Needle Pairwise Sequence Alignment of VP6_KO *in silico* clone of the VP6_KO construct with modified sequence VP6_KO ORF. The aligned expression constructs consists of *Y. lipolytica* TEF promoter (yTEFp), orange, and *K. marxianus* terminator (kmINUt), blue. The VP6 AO ORF is cloned at the XhoI, purple, and Eco 47III, green restriction sites. The ATG was successful removed and

cytosine nucleotide was introduced back to the expression cassette indicated with an arrow. NO mutation of VP6_KO ORF, black, from the start codon, red, to the stop codon, underlined.

Appendix C: Protein concentration

Before verification of the expression of VP6 ORFs by means western blot the protein concentration was calculated by using Pierce™ BCA protein assay kit (Pierce™, Biotechnology, Inc). Prior to determine unknown protein concentration, a standard curve was carried out using BSA by preparing a series of dilutions of known protein concentrations illustrated in Table C1. The wavelength used to determine the absorbance was 562nm or 540nm.

Table C1: Albumin (BSA) Standards dilutions

Vial	Volume of Diluent (µL)	Volume and Source of BSA (µL)	Final BSA Concentration (µg/mL)
A	0	300 of Stock	2000
B	125	375 of Stock	1500
C	325	325 of Stock	1000
D	325	325 of vial C dilution	500
E	325	325 of vial E dilution	250
F	325	325 of vial F dilution	125
G	400	0	0=Blank

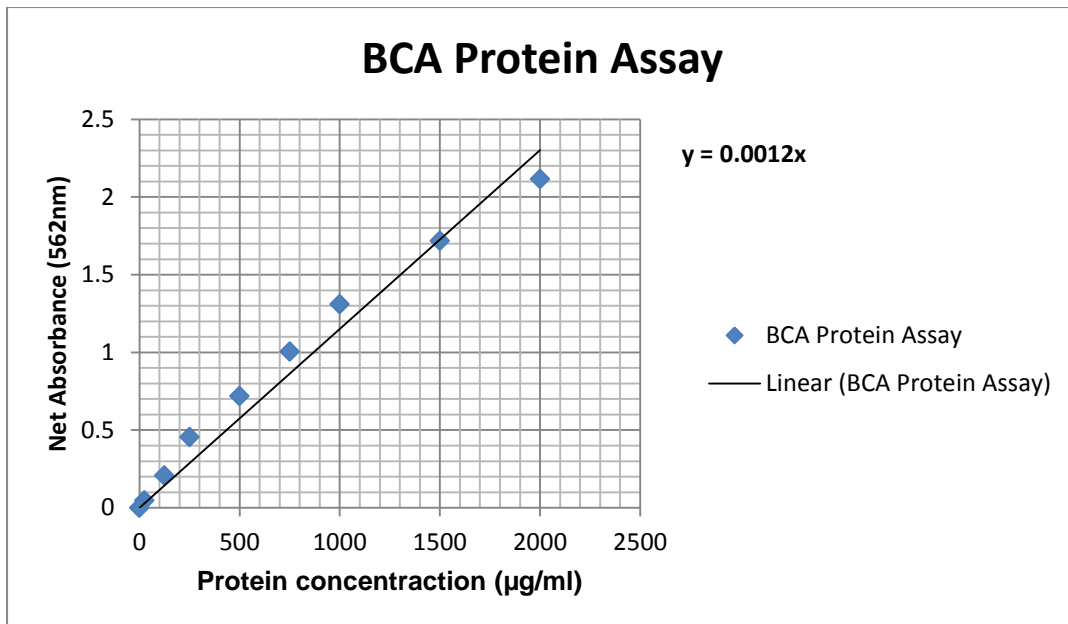


Figure C1: Standard curve of albumin standard absorbance at wavelength of 562nm of the known concentrations (ug/ml).

Appendix D: Integration of the expression cassette containing VP6 ORF codon optimised for *A. adenivorans*

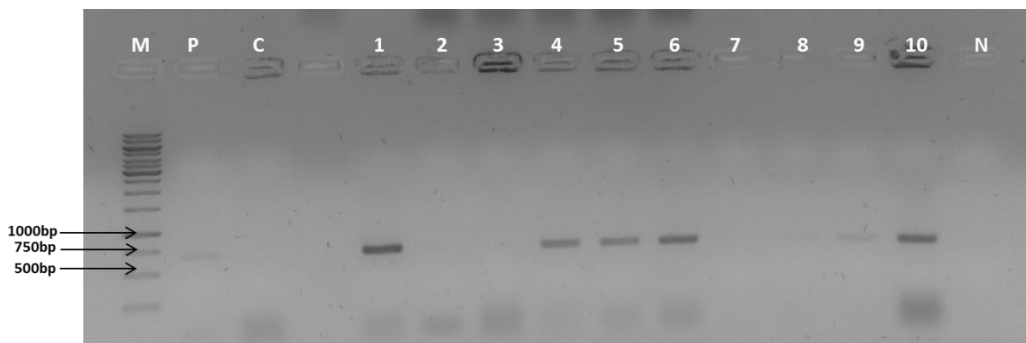


Figure D1: Analysis of the AO VP6 ORF containing expression cassette integration into the genome of *A. adenivorans* LS3 on a 1% agarose gel. Lane M: GeneRuler DNA Ladder mix. Lane N: negative PCR control, Lane C: untransformed *A. adenivorans* LS3 cells. Lane 1-10: Yeast clones screened for integration of AO VP6 ORF into *A. adenivorans* LS3. Lane P: positive control.

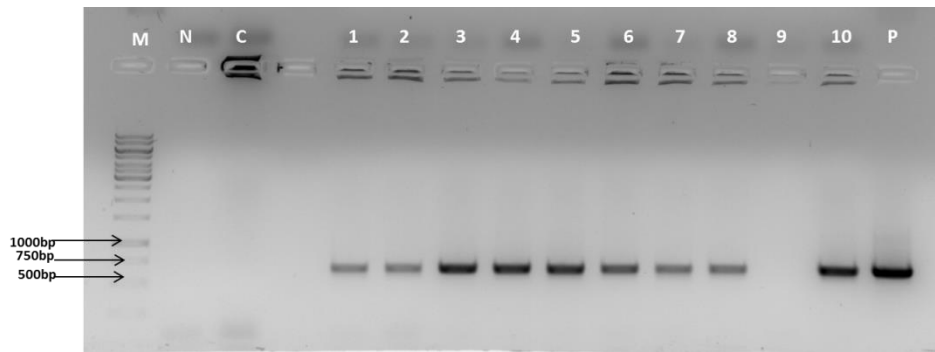


Figure D2: Analysis of the AO VP6 ORF containing expression cassette integration into the genome of *K. lactis* UFS1167 on a 1% agarose gel. Lane M: GeneRuler DNA Ladder mix. Lane N: negative PCR control, Lane C: untransformed *K. lactis* UFS1167 cells. Lane 1-10: Yeast clones screened for integration of AO VP6 ORF into *K. lactis* UFS1167. Lane P: positive control.

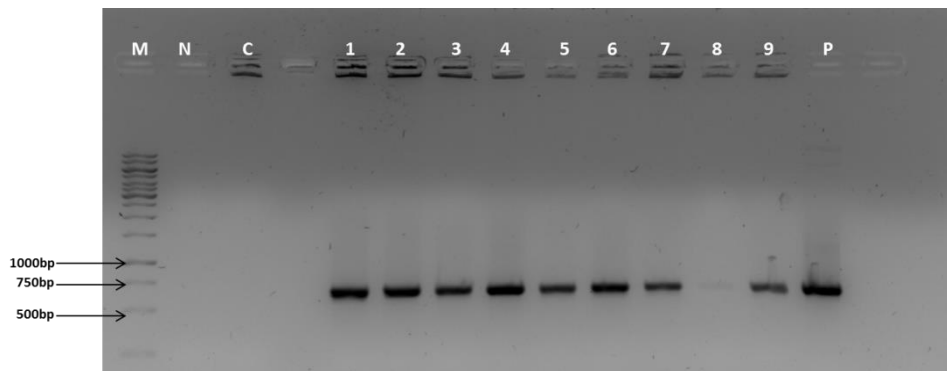


Figure D3: Analysis of the AO VP6 ORF containing expression cassette integration into the genome of *P. pastoris* GS115 on a 1% agarose gel. Lane M: GeneRuler DNA Ladder mix. Lane N: negative PCR control, Lane C: untransformed *P. pastoris* GS115 cells. Lane 1-9: Yeast clones screened for integration of AO VP6 ORF into *P. pastoris* GS115. Lane P: positive control.

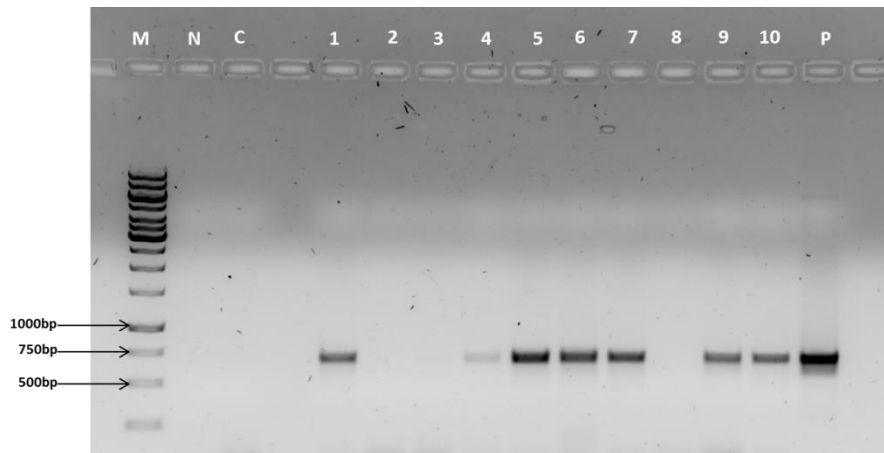


Figure D4: Analysis of the AO VP6 ORF containing expression cassette integration into the genome of *P. pastoris* UFS1552T on a 1% agarose gel. Lane M: GeneRuler DNA Ladder mix. Lane N: negative PCR control, Lane C: untransformed *P. pastoris* UFS1552T cells. Lane 1-10: Yeast clones screened for integration of AO VP6 ORF into *P. pastoris* UFS1552T. Lane P: positive control.

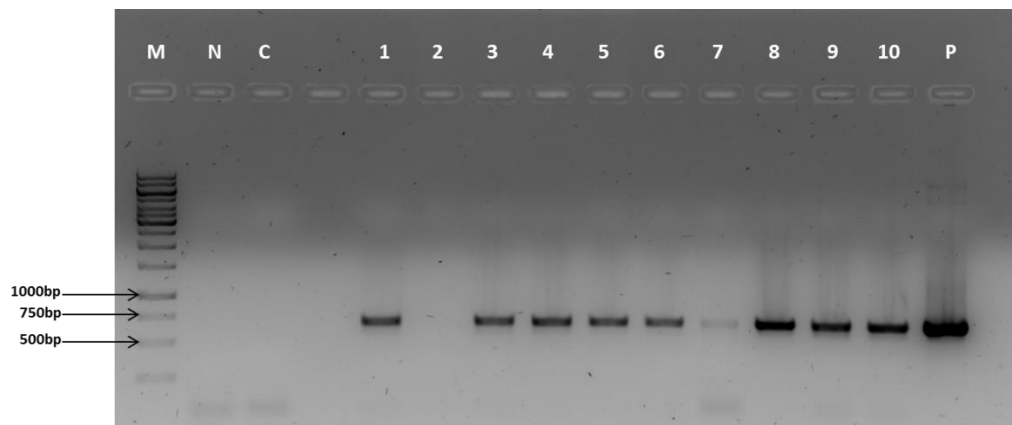


Figure D5: Analysis of the AO VP6 ORF containing expression cassette integration into the genome of *S. cerevisiae* CENPK on a 1% agarose gel. Lane M: GeneRuler DNA Ladder mix. Lane N: negative PCR control, Lane C: untransformed *S. cerevisiae* CENPK cells. Lane 1-10: Yeast clones screened for integration of AO VP6 ORF into *S. cerevisiae* CENPK. Lane P: positive control.

Appendix E: Integration of the expression cassette containing VP6 ORF codon optimised for *K. lactis* in various yeast stains

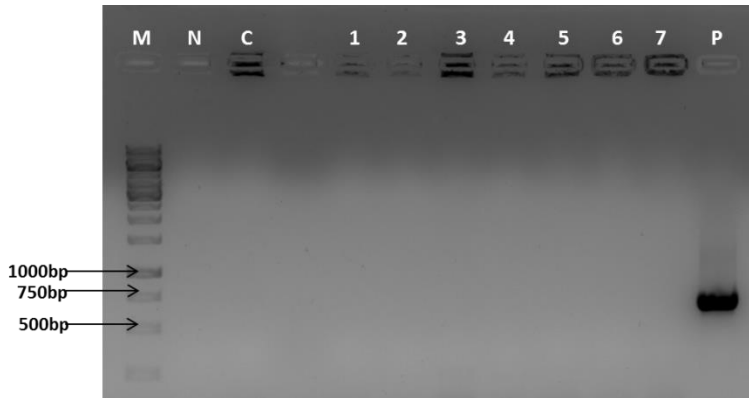


Figure E1: Analysis of the KO VP6 ORF containing expression cassette integration into the genome of *A. adenivorans* LS3 on a 1% agarose gel. Lane M: GeneRuler DNA Ladder mix. Lane N: negative PCR control, Lane C: untransformed *A. adenivorans* LS3 cells. Lane 1-7: Yeast clones screened for integration of the expression cassette containing KO VP6 ORF into *A. adenivorans* LS3. Lane P: positive control.

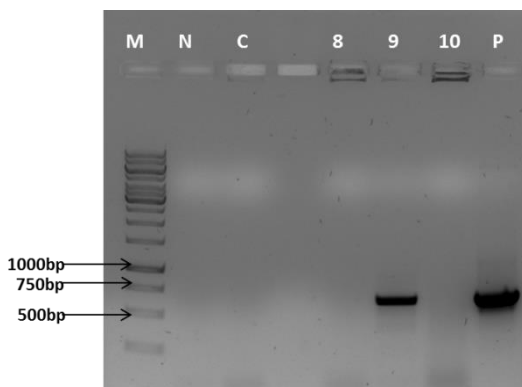


Figure E2: Analysis of the KO VP6 ORF containing expression cassette integration into the genome of *A. adenivorans* LS3 on a 1% agarose gel. Lane M: GeneRuler DNA Ladder mix. Lane N: negative PCR control, Lane C: untransformed *A. adenivorans* LS3 cells. Lane 8-10: Yeast clones screened for integration of the expression cassette containing KO VP6 ORF into *A. adenivorans* LS3. Lane P: positive control.

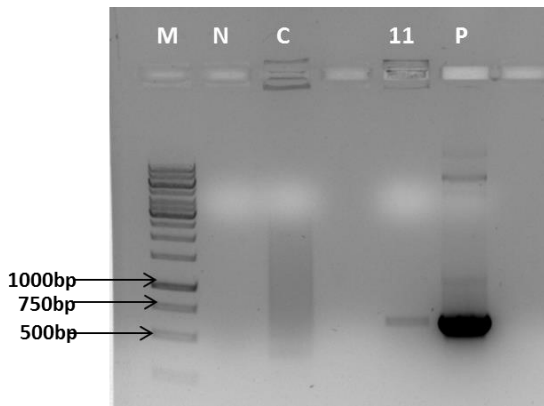


Figure E3: Analysis of the KO VP6 ORF containing expression cassette integration into the genome of *P. angusta* UFS0915 on a 1% agarose gel. Lane M: GeneRuler DNA Ladder mix. Lane N: negative PCR control, Lane C: untransformed *P. angusta* UFS0915 cells. Lane 11: Yeast clone screened for integration of the expression cassette containing KO VP6 ORF into *P. angusta* UFS0915. Lane P: positive control.

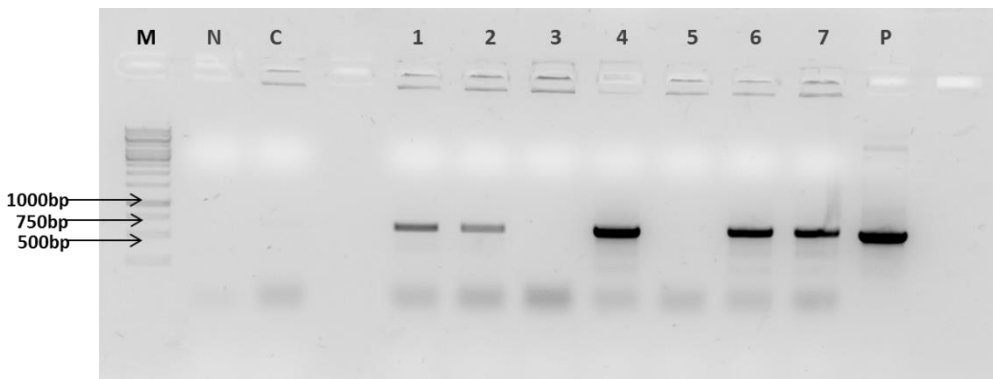


Figure E4: Analysis of the KO VP6 ORF containing expression cassette integration into the genome of *P. angusta* UFS1507 on a 1% agarose gel. Lane M: GeneRuler DNA Ladder mix. Lane N: negative PCR control, Lane C: untransformed *P. angusta* UFS1507 cells. Lane 1-7: Yeast clones screened for integration of the expression cassette containing KO VP6 ORF into *P. angusta* UFS1507. Lane P: positive control.

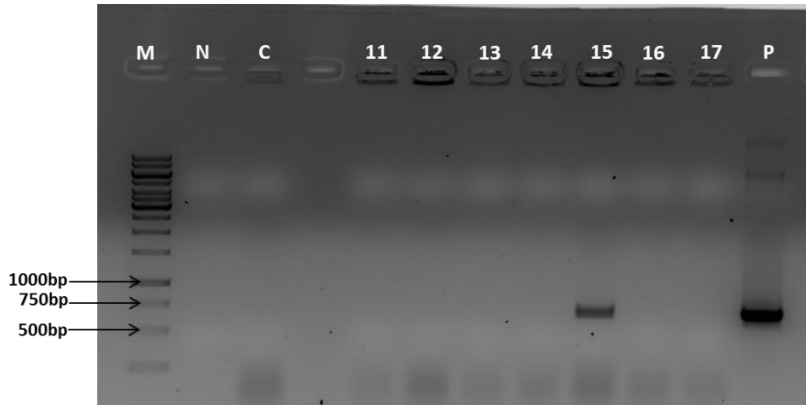


Figure E5: Analysis of the KO VP6 ORF containing expression cassette integration into the genome of *P. pastoris* GS115 on a 1% agarose gel. Lane M: GeneRuler DNA Ladder mix. Lane N: negative PCR control, Lane C: untransformed *P. pastoris*GS115 cells. Lane 11-17: Yeast clones screened for integration of the expression cassette containing KO VP6 ORF into *P. pastoris* GS115. Lane P: positive control.

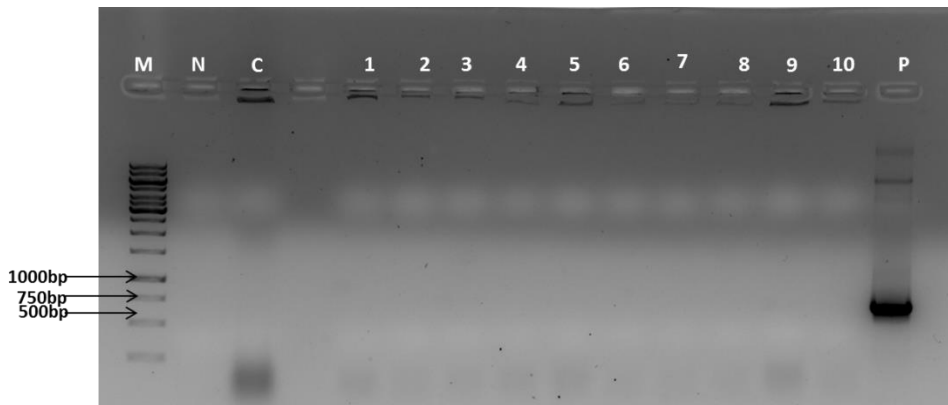


Figure E6: Analysis of the KO VP6 ORF containing expression cassette integration into the genome of *P. pastoris* UFS1552T on a 1% agarose gel. Lane M: GeneRuler DNA Ladder mix. Lane N: negative PCR control, Lane C: untransformed *P. pastoris* UFS1552T cells. Lane 1-10: Yeast clones screened for integration of the expression cassette containing KO VP6 ORF into *P. pastoris* UFS1552T. Lane P: positive control.

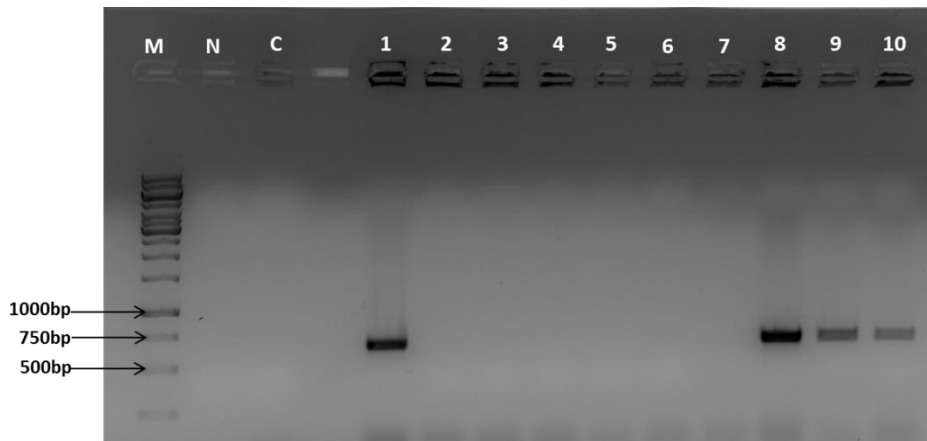


Figure E7: Analysis of the KO VP6 ORF containing expression cassette integration into the genome of *S. cerevisiae* CENPK on a 1% agarose gel. Lane M: GeneRuler DNA Ladder mix. Lane N: negative PCR control, Lane C: untransformed *S. cerevisiae* CENPK cells. Lane 1-10: Yeast clones screened for integration of the expression cassette containing KO VP6 ORF into *S. cerevisiae* CENPK.



Figure E8: Analysis of the KO VP6 ORF containing expression cassette integration into the genome of *Y. lipolytica* PO 1F on a 1% agarose gel. Lane M: GeneRuler DNA Ladder mix. Lane N: negative PCR control, Lane C: untransformed *Y. lipolytica* PO 1F cells. Lane 1-10: Yeast clones screened for integration of the expression cassette containing KO VP6 ORF into *Y. lipolytica* PO 1F. Lane P: positive control.

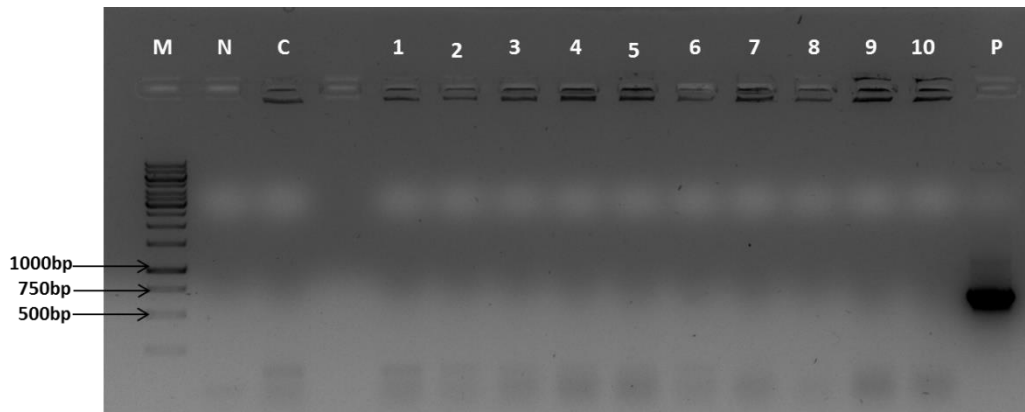


Figure E9: Analysis of the KO VP6 ORF containing expression cassette integration into the genome of *Y. lipolytica* UFS2221 on a 1% agarose gel. Lane M: GeneRuler DNA Ladder mix. Lane N: negative PCR control, Lane C: untransformed *Y. lipolytica* UFS2221 cells. Lane 1-10: Yeast clones screened for integration of the expression cassette containing KO VP6 ORF into *Y. lipolytica* UFS2221. Lane P: positive control.

Appendix F: Integration of the expression cassette containing VP6 ORF codon optimised for *P.pastoris/P.angusta* in various yeast.

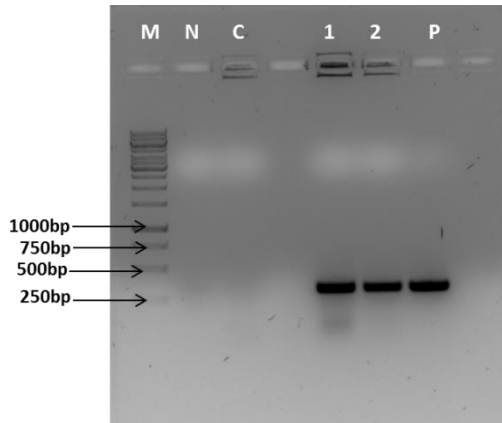


Figure F1: Analysis of the PO VP6 ORF containing expression cassette integration into the genome of *A. adenivorans* UFS1219 on a 1% agarose gel. Lane M: GeneRuler DNA Ladder mix. Lane N: negative PCR control, Lane C: untransformed *A. adenivorans* UFS1219 cells. Lane 1-2: Yeast clones screened for integration of the expression cassette containing PO VP6 ORF into *A. adenivorans* UFS1219. Lane P: positive control.

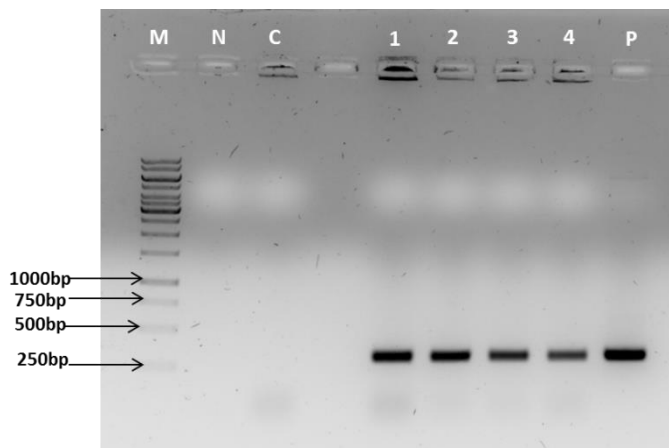


Figure F2: Analysis of the PO VP6 ORF containing expression cassette integration into the genome of *A. adenivorans* LS3 on a 1% agarose gel. Lane M: GeneRuler DNA Ladder mix. Lane N: negative PCR control, Lane C: untransformed *A. adenivorans* LS3 cells. Lane 1-4: Yeast clones screened for integration of the expression cassette containing PO VP6 ORF into *A. adenivorans* LS3. Lane P: positive control.

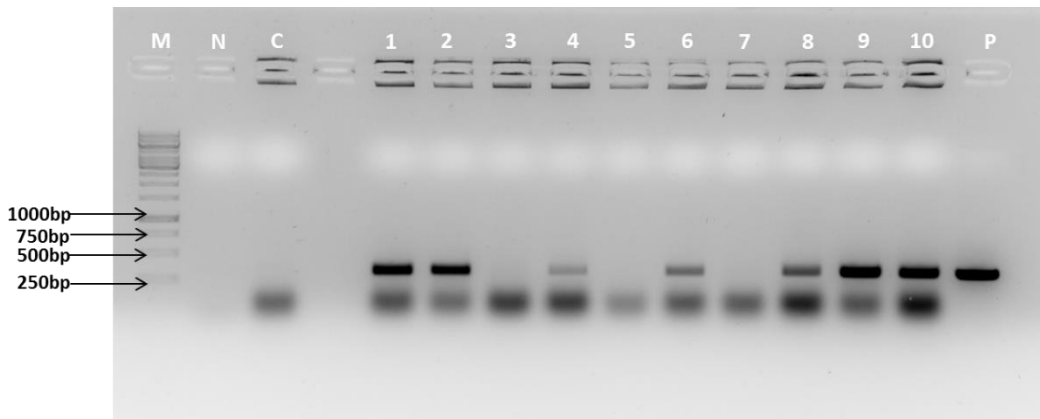


Figure F3: Analysis of the PO VP6 ORF containing expression cassette integration into the genome of *K. lactis* UFS1167 on a 1% agarose gel. Lane M: GeneRuler DNA Ladder mix. Lane N: negative PCR control, Lane C: untransformed *K. lactis* UFS1167 cells. Lane 1-10: Yeast clones screened for integration of the expression cassette containing PO VP6 ORF into *K. lactis* UFS1167. Lane P: positive control.

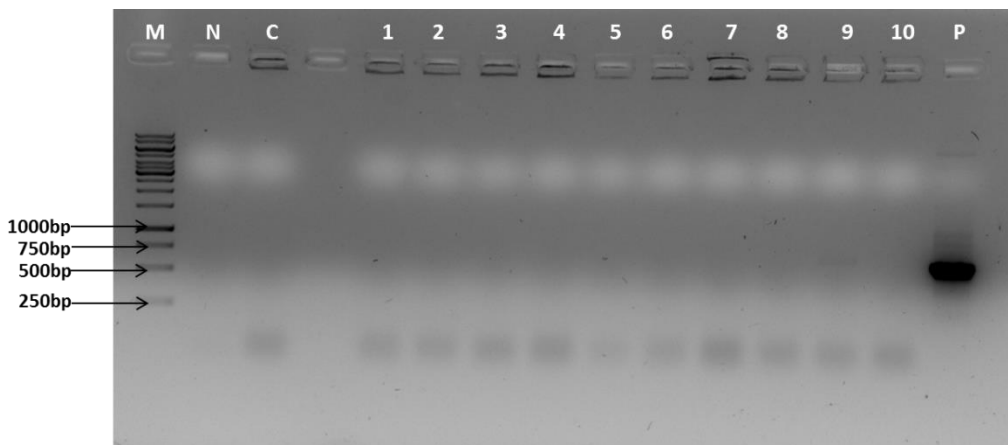


Figure F4: Analysis of the PO VP6 ORF containing expression cassette integration into the genome of *Y. lipolytica* UFS2221 on a 1% agarose gel. Lane M: GeneRuler DNA Ladder mix. Lane N: negative PCR control, Lane C: untransformed *Y. lipolytica* UF2221 cells. Lane 1-10: Yeast clones screened for integration of the expression cassette containing PO VP6 ORF into *Y. lipolytica* UFS2221. Lane P: positive control.

Appendix G: Yeast expression of rotavirus VP6 encoded by the ORF codon optimised for expression in *A. adenivorans*

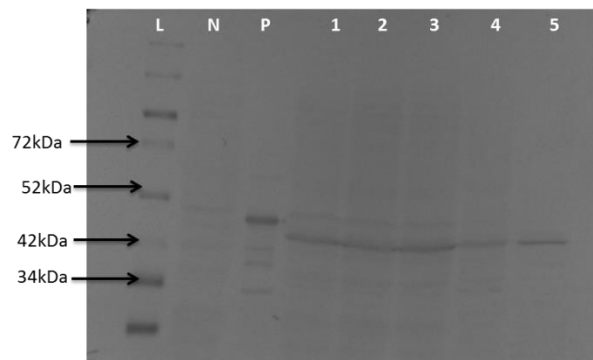


Figure G1: Western blot analysis of rotavirus VP6 expression by *A. adenivorans* UFS1219 colonies containing the AO VP6 ORF containing expression cassette. Lane L: Spectra™ Multicolor Broad Range Protein Ladder (Thermo Fisher Scientific). Lane N: untransformed *A. adenivorans* UFS1219 cells, negative control. Lane P: Bacterial expressed VP6, protein size 48 kDa. Lanes 1, 2, 3, 4, 5: *A. adenivorans* UFS1219 yeast clones screened for expression of VP6 with expected size of 45 kDa. A total protein concentration of 2.4mg/ml was used for all colonies screened.

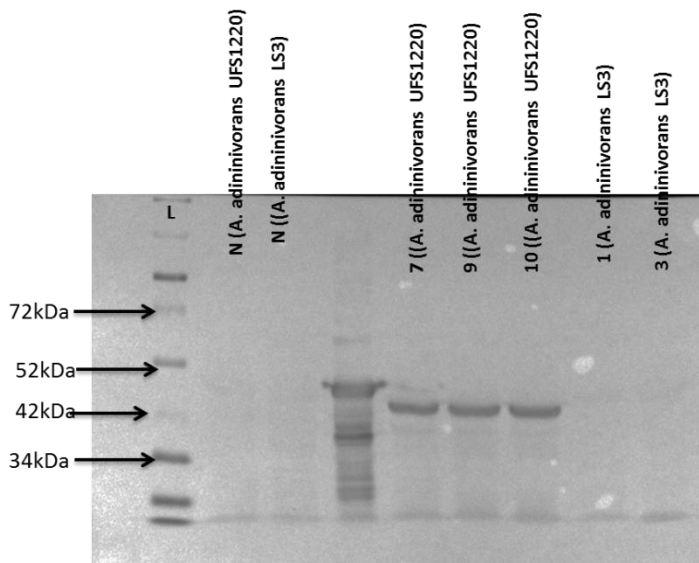


Figure G2: Western blot analysis of rotavirus VP6 expression by *A. adenivorans* UFS1219 colonies containing the AO VP6 ORF containing expression cassette. Lane L: Spectra™ Multicolor Broad Range Protein Ladder (Thermo Fisher Scientific). Lane N (*A. adenivorans* UFS1219 and Lane N (*A. adenivorans* LS3): untransformed *A. adenivorans* UFS1219 and LS3 cells, negative control. Lane P: Bacterial expressed VP6, protein size 48 kDa. Lanes 7, 9, 10 (Lane N (*A. adenivorans* UFS1219) and Lanes 1,3 (*A. adenivorans* LS3): *A. adenivorans* UFS1219 and *A. adenivorans* LS3 yeast clones screened for expression of VP6 with expected size of 45 kDa. A total protein concentration of 1.5mg/ml was used for all colonies screened.

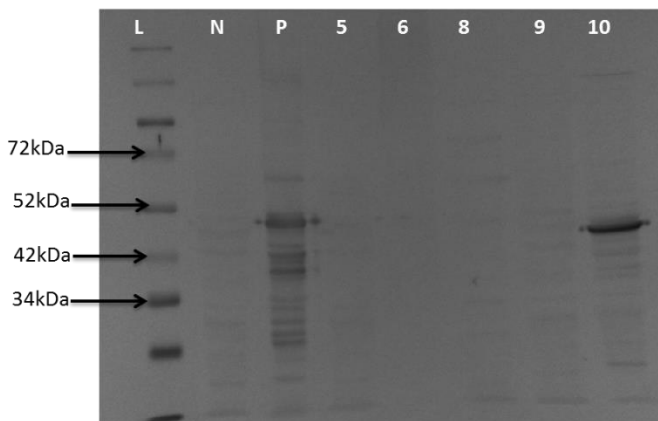


Figure G3: Western blot analysis of rotavirus VP6 expression by *A. adenivorans* LS3 colonies containing the AO VP6 ORF containing expression cassette. Lane L: Spectra™ Multicolor Broad Range Protein Ladder (Thermo Fisher Scientific). Lane N: untransformed *A. adenivorans* LS3 cells, negative control. Lane P: Bacterial expressed VP6, protein size 48 kDa. Lanes 5, 6, 8, 9, 10: *A. adenivorans* LS3 yeast clones screened for expression of VP6 with expected size of 45 kDa. A total protein concentration of 2.3mg/ml was used for all colonies screened.

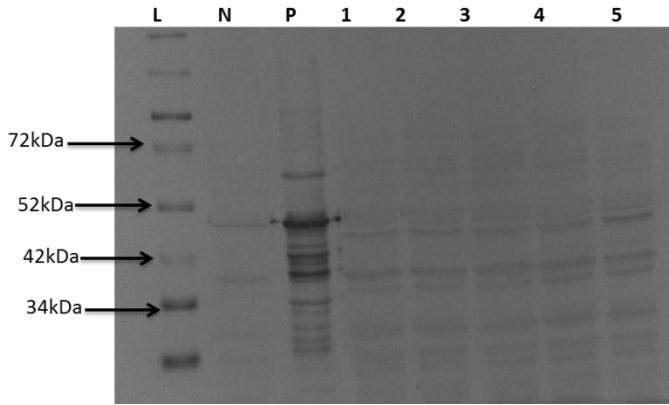


Figure G4: Western blot analysis of rotavirus VP6 expression by *K. lactis* UFS1167 colonies containing the AO VP6 ORF containing expression cassette. Lane L: Spectra™ Multicolor Broad Range Protein Ladder (Thermo Fisher Scientific). Lane N: untransformed *K. lactis* UFS1167 cells, negative control. Lane P: Bacterial expressed VP6, protein size of 48 kDa. Lanes 1-5: *K. lactis* UFS1167 yeast clones screened for expression of VP6 with expected size of 45 kDa. A total protein concentration of 2.1mg/ml was used for all colonies screened.

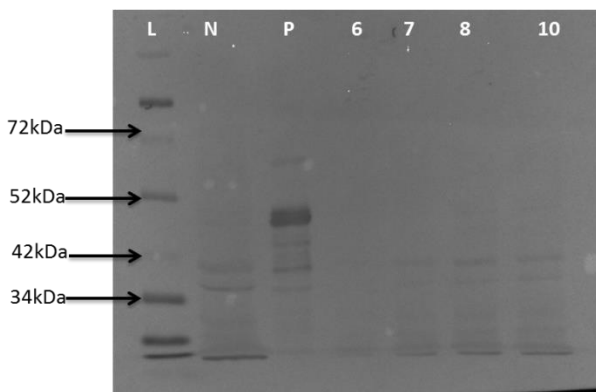


Figure G5: Western blot analysis of rotavirus VP6 expression by *K. lactis* UFS1167 colonies containing the AO VP6 ORF containing expression cassette. Lane L: Spectra™ Multicolor Broad Range Protein Ladder (Thermo Fisher Scientific). Lane N: untransformed *K. lactis* UFS1167 cells, negative control. Lane P: Bacterial expressed VP6, protein size of 48 kDa. Lanes 6, 7, 8, 10: *K. lactis* UFS1167 yeast clones screened for expression of VP6 with expected size of 45 kDa. A total protein concentration of 3.2mg/ml was used for all colonies screened.

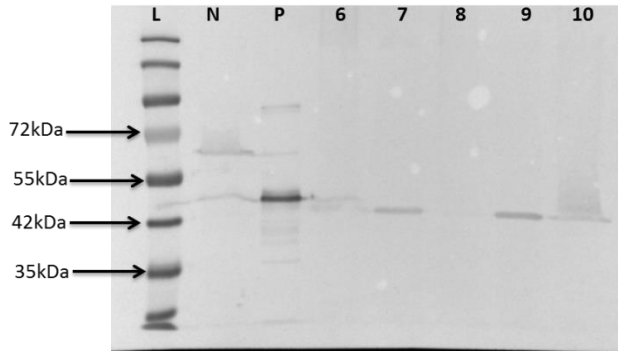


Figure G6: Western blot analysis of rotavirus VP6 expression by *P. angusta* UFS0915 colonies containing the AO VP6 ORF containing expression cassette. Lane L: PageRuler™ Prestained Protein Ladder (Thermo Fisher Scientific). Lane N: untransformed *P. angusta* UFS00915 cells, negative control. Lane P: Bacterial expressed VP6, protein size of 48 kDa. Lanes 6-10: *P. angusta* UFS0915 yeast clones screened for expression of VP6 with expected size of 45 kDa. A total protein concentration of 2.3mg/ml was used for all colonies screened.

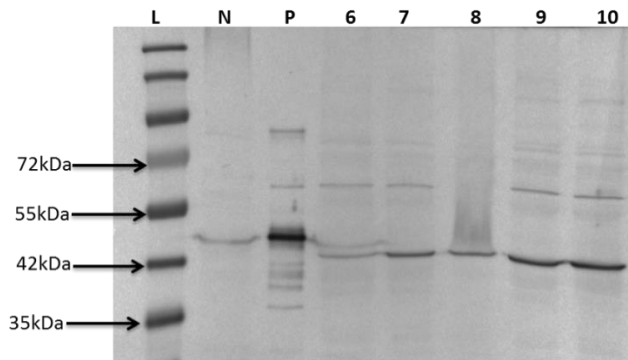


Figure G7: Western blot analysis of rotavirus VP6 expression by *P. angusta* UFS1507 colonies containing the AO VP6 ORF containing expression cassette. Lane L: PageRuler™ Prestained Protein Ladder (Thermo Fisher Scientific). Lane N: untransformed *P. angusta* UFS1507 cells, negative control. Lane P: Bacterial expressed VP6, protein size of 48 kDa. Lanes 6-10: *P. angusta* UFS0915 yeast clones screened for expression of VP6 with expected size of 45 kDa. A total protein concentration of 2.3mg/ml was used for all colonies screened.

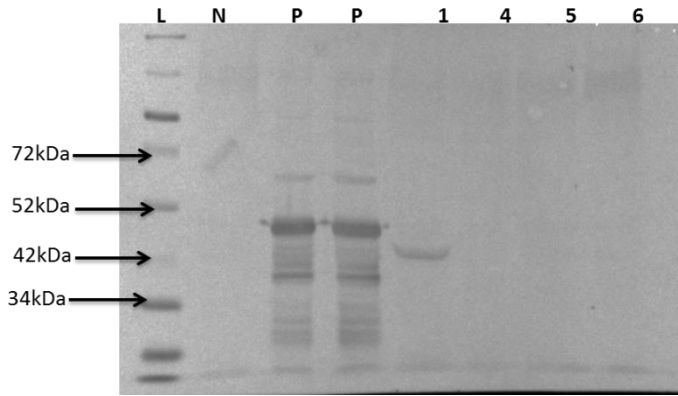


Figure G8: Western blot analysis of rotavirus VP6 expression by *P. pastoris* UFS1552T colonies containing the AO VP6 ORF containing expression cassette. Lane L: Spectra™ Multicolor Broad Range Protein Ladder (Thermo Fisher Scientific). Lane N: untransformed *P. pastoris* UFS1552T cells, negative control. Lane P: Bacterial expressed VP6, protein size of 48 kDa. Lanes 1, 4, 5, 6: *P. pastoris* UFS1552T yeast clones screened for expression of VP6 with expected size of 45 kDa. A total protein concentration of 2.0mg/ml was used for all colonies screened.

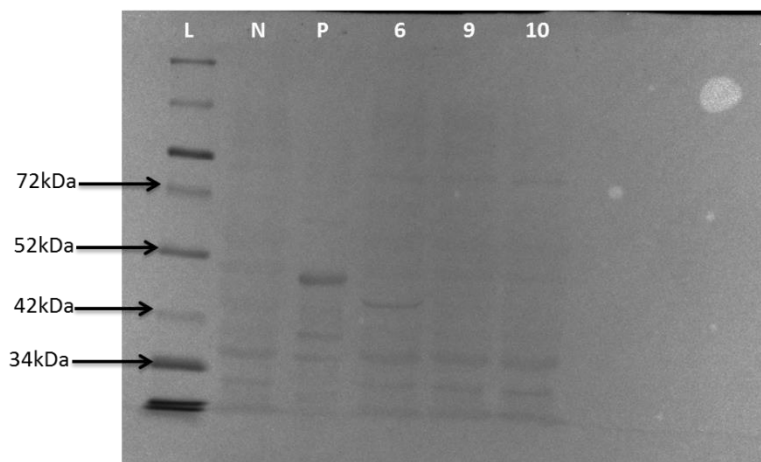


Figure G9: Western blot analysis of rotavirus VP6 expression by *P. pastoris* UFS1552T colonies containing the AO VP6 ORF containing expression cassette. Lane L: Spectra™ Multicolor Broad Range Protein Ladder (Thermo Fisher Scientific). Lane N: untransformed *P. pastoris* UFS1552T cells, negative control. Lane P: Bacterial expressed VP6, protein size of 48 kDa. Lanes 3, 9, 10: *P. pastoris* UFS1552T yeast clones screened for expression of VP6 with expected size of 45 kDa. A total protein concentration of 1.6mg/ml was used for all colonies screened.

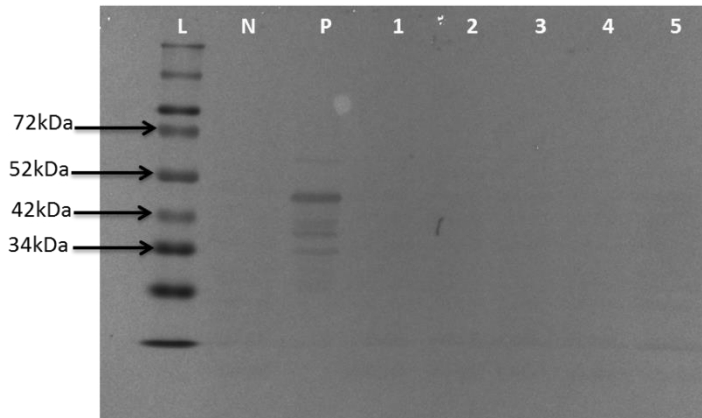


Figure G10: Western blot analysis of rotavirus VP6 expression by *P. pastoris* GS115 colonies containing the AO VP6 ORF containing expression cassette. Lane L: Spectra™ Multicolor Broad Range Protein Ladder (Thermo Fisher Scientific). Lane N: untransformed *P. pastoris* GS115 cells, negative control. Lane P: Bacterial expressed VP6, protein size of 48 kDa. Lanes 1, 2, 3, 4, 5: *P. pastoris* GS115 yeast clones screened for expression of VP6 with expected size of 45 kDa. A total protein concentration of 1.8mg/ml was used for all colonies screened.

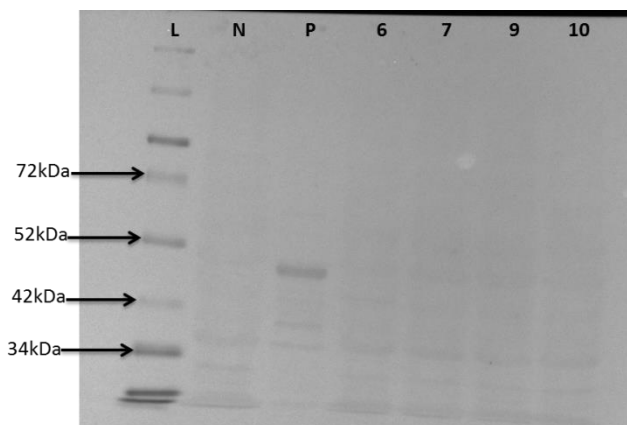


Figure G11: Western blot analysis of rotavirus VP6 expression by *P. pastoris* GS115 colonies containing the AO VP6 ORF containing expression cassette. Lane L: Spectra™ Multicolor Broad Range Protein Ladder (Thermo Fisher Scientific). Lane N: untransformed *P. pastoris* GS115 cells, negative control. Lane P: Bacterial expressed VP6, protein size of 48 kDa. Lanes 6, 7, 9, 10: *P. pastoris* GS115 yeast clones screened for expression of VP6 with expected size of 45 kDa. A total protein concentration of 1.6mg/ml was used for all colonies screened.

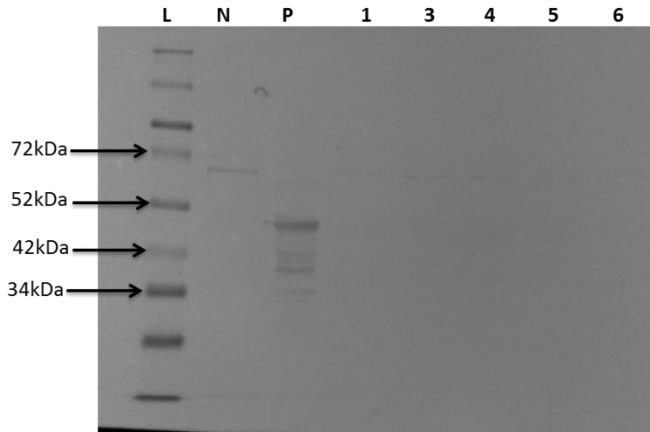


Figure G12: Western blot analysis of rotavirus VP6 expression by *S. cerevisiae* CENPK colonies containing the AO VP6 ORF containing expression cassette. Lane L: Spectra™ Multicolor Broad Range Protein Ladder (Thermo Fisher Scientific). Lane N: untransformed *S. cerevisiae* CENPK cells, negative control. Lane P: Bacterial expressed VP6, protein size of 48 kDa. Lanes 1, 3, 4, 5, 6: *S. cerevisiae* CENPK yeast clones screened for expression of VP6 with expected size of 45 kDa. A total protein concentration of 1.4mg/ml was used for all colonies screened.

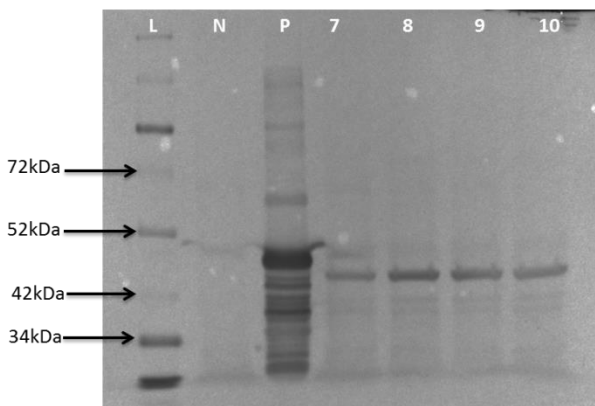


Figure G13: Western blot analysis of rotavirus VP6 expression by *S. cerevisiae* CENPK colonies containing the AO VP6 ORF containing expression cassette. Lane L: Spectra™ Multicolor Broad Range Protein Ladder (Thermo Fisher Scientific). Lane N: untransformed *S. cerevisiae* CENPK cells, negative control. Lane P: Bacterial expressed VP6, protein size of 48 kDa. Lanes 7, 8, 9, 10: *S. cerevisiae* CENPK yeast clones screened for expression of VP6 with expected size of 45 kDa. A total protein concentration of 2.1mg/ml was used for all colonies screened.

Appendix H: Yeast expression of rotavirus VP6 encoded by the ORF codon optimised for expression in *K. lactis*

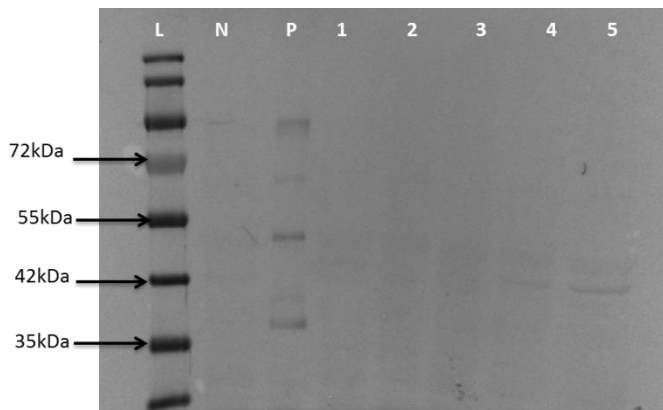


Figure H1: Western blot analysis of rotavirus VP6 expression by *A. adenivorans* UFS1219 colonies containing the KO VP6 ORF containing expression cassette. Lane L: PageRuler™ Prestained Protein Ladder (Thermo Fisher Scientific). Lane N: untransformed *A. adenivorans* UFS1219 cells, negative control. Lane P: Bacterial expressed VP6, protein size of 48 kDa. Lanes 1, 2, 3, 4, 5: *A. adenivorans* UFS1219 yeast clones screened for expression of VP6 with expected size of 45 kDa. A total protein concentration of 2.3mg/ml was used for all colonies screened.

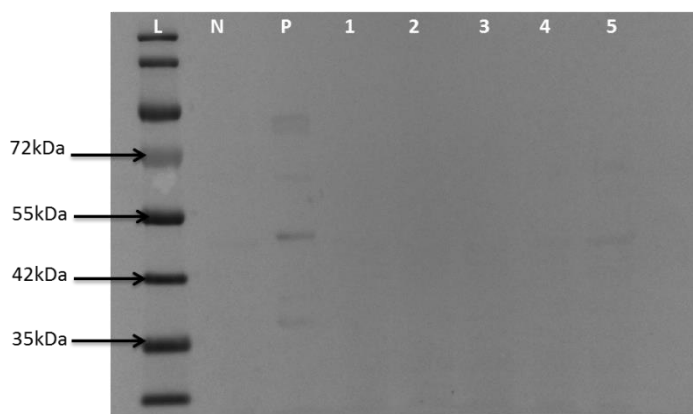


Figure H2: Western blot analysis of rotavirus VP6 expression by *A. adenivorans* UFS1220 colonies containing the KO VP6 ORF containing expression cassette. Lane L: PageRuler™ Prestained Protein Ladder (Thermo Fisher Scientific). Lane N: untransformed *A. adenivorans* UFS1220 cells, negative control. Lane P: Bacterial expressed VP6, protein size of 48 kDa. Lanes 1, 2, 3, 4, 5: *A. adenivorans* UFS1220 yeast clones screened for expression of VP6 with expected size of 45 kDa. A total protein concentration of 2.6mg/ml was used for all colonies screened.

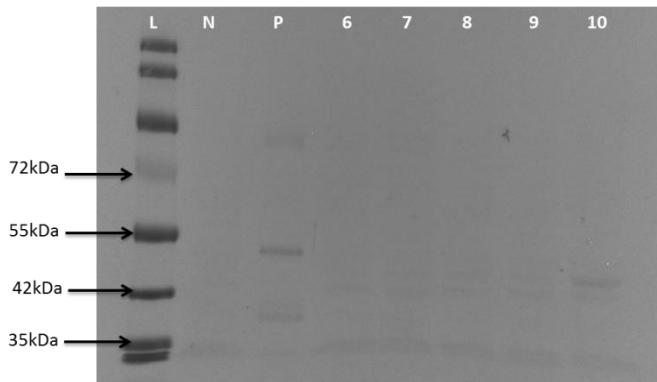


Figure H3: Western blot analysis of rotavirus VP6 expression by *A. adenivorans* UFS1220 colonies containing the KO VP6 ORF containing expression cassette. Lane L: PageRuler™ Prestained Protein Ladder (Thermo Fisher Scientific). Lane N: untransformed *A. adenivorans* UFS1220 cells, negative control. Lane P: Bacterial expressed VP6, protein size of 48 kDa. Lanes 6, 7, 8, 9, 10: *A. adenivorans* UFS1220 yeast clones screened for expression of VP6 with expected size of 45 kDa. A total protein concentration of 3.1mg/ml was used for all colonies screened.

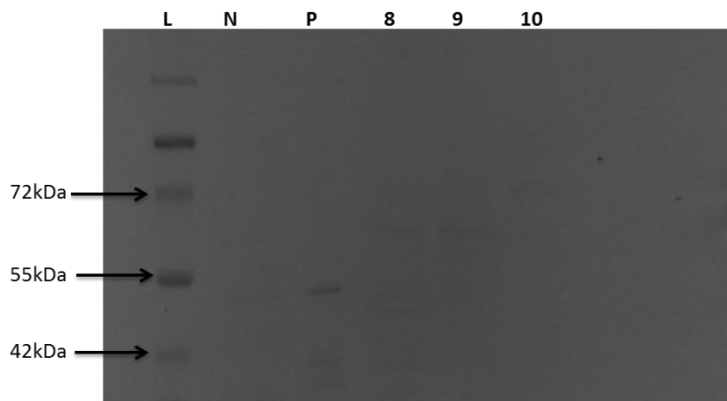


Figure H4: Western blot analysis of rotavirus VP6 expression by *K. lactis* UFS1167 colonies containing the KO VP6 ORF containing expression cassette. Lane L: PageRuler™ Prestained Protein Ladder (Thermo Fisher Scientific). Lane N: untransformed *K. lactis* UFS1167 cells, negative control. Lane P: Bacterial expressed VP6, protein size of 48 kDa. Lanes 8, 9, 10: *K. lactis* UFS1167 yeast clones screened for expression of VP6 with expected size of 45 kDa. A total protein concentration of 2.4mg/ml was used for all colonies screened.

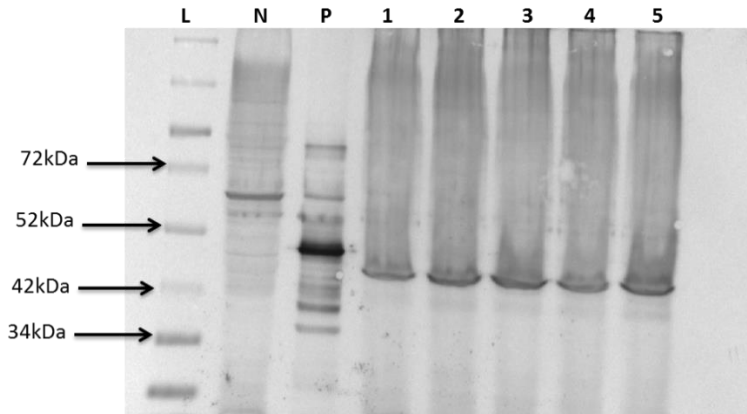


Figure H5: Western blot analysis of rotavirus VP6 expression by *P. angusta* UFS0915 colonies containing the KO VP6 ORF containing expression cassette. Lane L: Spectra™ Multicolor Broad Range Protein Ladder (Thermo Fisher Scientific). Lane N: untransformed *P. angusta* UFS0915 cells, negative control. Lane P: VP6 bacterial positive control protein size of 48 kDa. Lanes 1, 2, 3, 4, 5: *P. angusta* UFS0915 yeast clones screened for expression of VP6 with expected size of 45 kDa. A total protein concentration of 2.2mg/ml was used for all colonies screened.

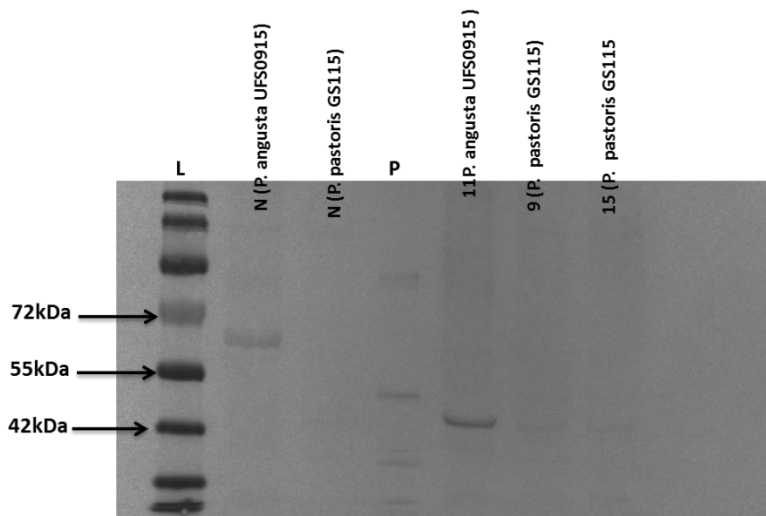


Figure H6: Western blot analysis of rotavirus VP6 expression by *P. angusta* UFS0915 and *P. pastoris* GS115 colonies containing the KO VP6 ORF containing expression cassette. Lane L: PageRuler™ Prestained Protein Ladder (Thermo Fisher Scientific). Lane N (*P. angusta* UFS0915 and Lane N (*P. pastoris* GS115): untransformed *P. angusta* UFS0915 and *P. pastoris* GS115 cells, negative control. Lane P: Bacterial expressed VP6, protein size of 48 kDa. Lanes 11 (*P. angusta* UFS0915): *P. angusta* UFS0915 yeast clone screened for expression of VP6 with expected size of 45 kDa. Lanes 9, 15 (*P. pastoris* GS115): *P. pastoris* GS115 yeast clones screened for expression of VP6 with expected size of 45 kDa. A total protein concentration of 1.4mg/ml was used for all colonies screened.

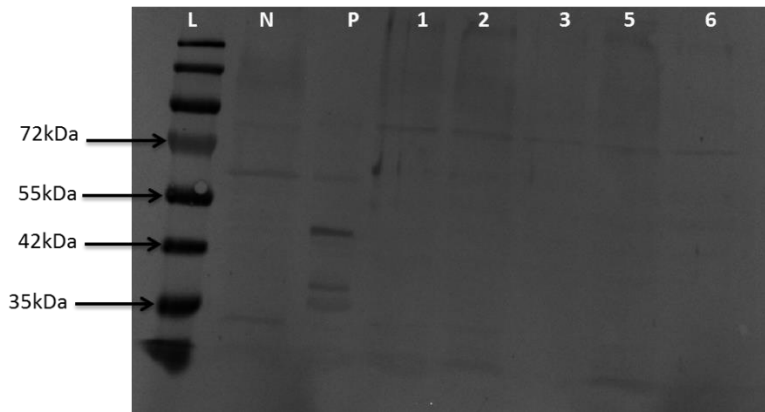


Figure H7: Western blot analysis of rotavirus VP6 expression by *P. pastoris* UFS1552T colonies containing the KO VP6 ORF containing expression cassette. Lane L: PageRuler™ Prestained Protein Ladder (Thermo Fisher Scientific). Lane N: untransformed *P. pastoris* UFS1552T cells, negative control. Lane P: Bacterial expressed VP6, protein size of 48 kDa. Lanes 1, 2, 3, 5, 6: *P. pastoris* UFS1552T yeast clones screened for expression of VP6 with expected size of 45 kDa. A total protein concentration of 2.9mg/ml was used for all colonies screened.

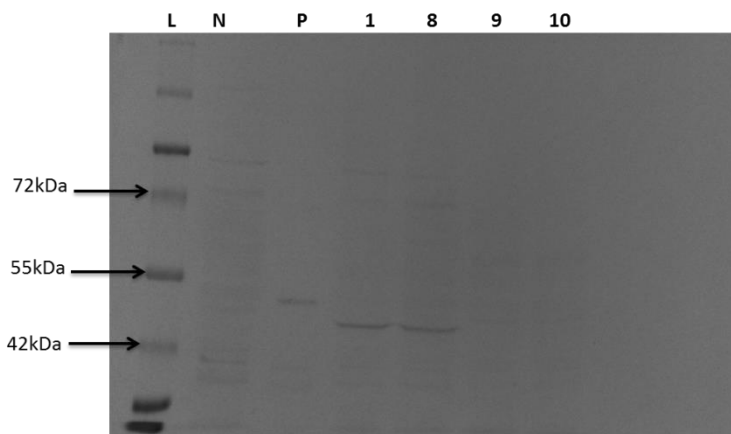


Figure H8: Western blot analysis of rotavirus VP6 expression by *S. cerevisiae* CENPK colonies containing the KO VP6 ORF containing expression cassette. Lane L: PageRuler™ Prestained Protein Ladder (Thermo Fisher Scientific). Lane N: untransformed *S. cerevisiae* CENPK cells, negative control. Lane P: Bacterial expressed VP6, protein size of 48 kDa. Lanes 1, 8, 9, 10: *S. cerevisiae* CENPK yeast clones screened for expression of VP6 with expected size of 45 kDa. A total protein concentration of 3.1mg/ml was used for all colonies screened.

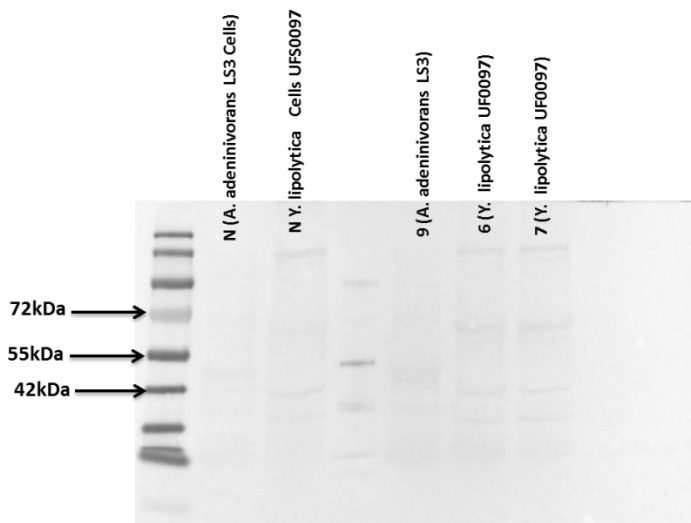


Figure H9: Western blot analysis of rotavirus VP6 expression by *A. adenivorans* LS3 and *Y. lipolytica* UFS0097 colonies containing the KO VP6 ORF containing expression cassette. Lane L: PageRuler™ Prestained Protein Ladder (Thermo Fisher Scientific). Lane N (*A. adenivorans* LS3 and Lane N (*Y. lipolytica* UFS0097): untransformed *A. adenivorans* LS3 and *Y. lipolytica* UFS0097 cells, negative control. Lane P: Bacterial expressed VP6, protein size of 48 kDa. Lanes 9 (*A. adenivorans* LS3): *A. adenivorans* LS3 yeast clone screened for expression of VP6 with expected size of 45 kDa. Lanes 6, 7 (*Y. lipolytica* UFS0097): *Y. lipolytica* UFS0097 yeast clones screened for expression of VP6 with expected size of 45 kDa. A total protein concentration of 2.1mg/ml was used for all colonies screened.

Appendix I: Yeast expression of rotavirus VP6 encoded by the ORF codon optimised for expression in *P. pastoris*/*P. angusta*

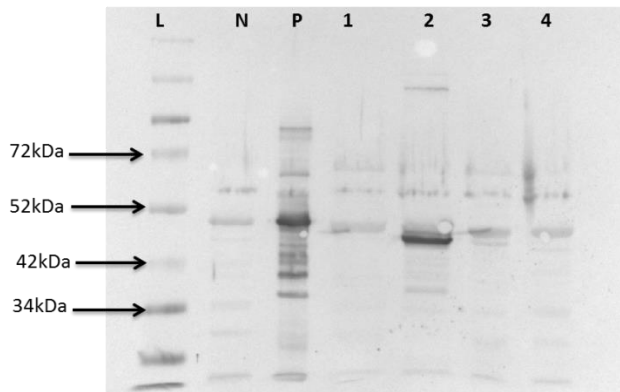


Figure I1: Western blot analysis of rotavirus VP6 expression by *A. adenivorans* LS3 colonies containing the PO VP6 ORF containing expression cassette. Lane L: (Thermo Fisher Scientific). Lane N: untransformed *A. adenivorans* LS3 cells, negative control. Lane P: Bacterial expressed VP6, protein size of 48 kDa. Lanes 1, 2, 3, 4: *A. adenivorans* LS3 yeast clones screened for expression of VP6 with expected size of 45 kDa. A total protein concentration of 1.9mg/ml was used for all colonies screened.

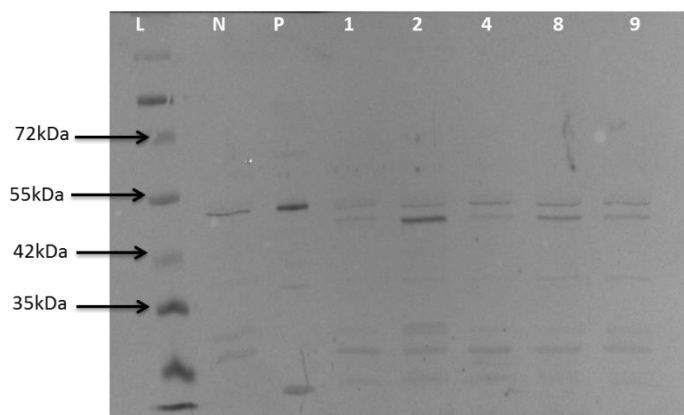


Figure I2: Western blot analysis of rotavirus VP6 expression by *K. lactis* UFS1167 colonies containing the PO VP6 ORF containing expression cassette. Lane L: PageRuler™ Prestained Protein Ladder (Thermo Fisher Scientific). Lane N: untransformed *K. lactis* UFS1167 cells, negative control. Lane P: Bacterial expressed VP6, protein size of 48 kDa. Lanes 1, 2, 4, 8, 9: *K. lactis* UFS1167 yeast clones screened for expression of VP6 with expected size of 45 kDa. A total protein concentration of 2.1mg/ml was used for all colonies screened.

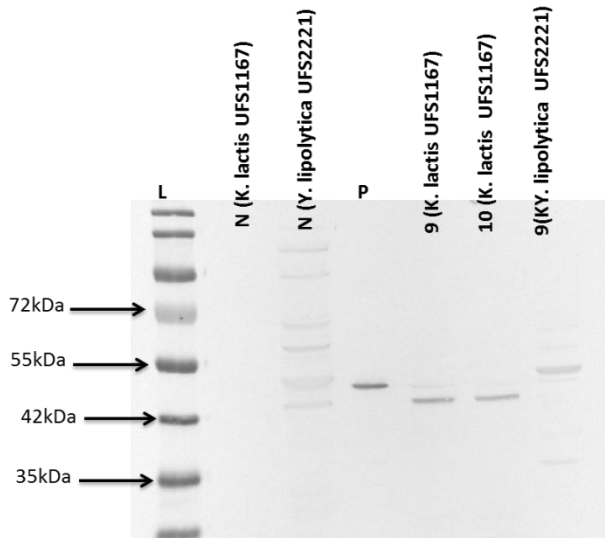


Figure I3: Western blot analysis of rotavirus VP6 expression by *K. lactis* UFS1167 and *Y. lipolytica* UFS2221 colonies containing the PO VP6 ORF-containing expression cassette. Lane L: PageRuler™ Prestained Protein Ladder (Thermo Fisher Scientific). Lane N (*K. lactis* UFS1167 and Lane N (*Y. lipolytica* UFS2221): untransformed *K. lactis* UFS1167 and *Y. lipolytica* UFS2221 cells, negative control. Lane P: Bacterial expressed VP6, protein size of 48 kDa. Lanes 9, 10 (*K. lactis* UFS1167): *K. lactis* UFS1167 yeast clones screened for expression of VP6 with expected size of 45 kDa. Lanes 9 (*Y. lipolytica* UFS2221): *Y. lipolytica* UFS2221 yeast clone screened for expression of VP6 with expected size of 45 kDa. A total protein concentration of 2.1mg/ml was used for all colonies screened.

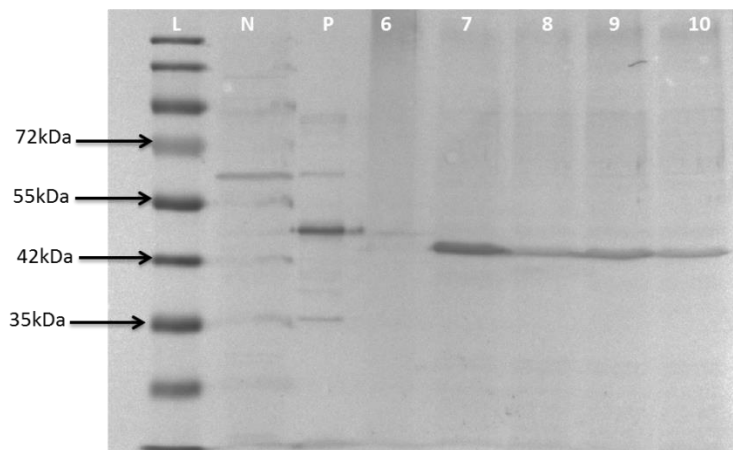


Figure I4: Western blot analysis of rotavirus VP6 expression by *P. angusta* UFS0915 colonies containing the PO VP6 ORF-containing expression cassette. Lane L: PageRuler™ Prestained Protein Ladder (Thermo Fisher Scientific). Lane N: untransformed *P. angusta* UFS0915 cells, negative control. Lane P: Bacterial expressed VP6, protein size of 48 kDa. Lanes 6, 7, 9, 9, 10: *P. angusta* UFS0915 yeast clones screened for expression of VP6 with expected size of 45 kDa. A total protein concentration of 2.1mg/ml was used for all colonies screened.

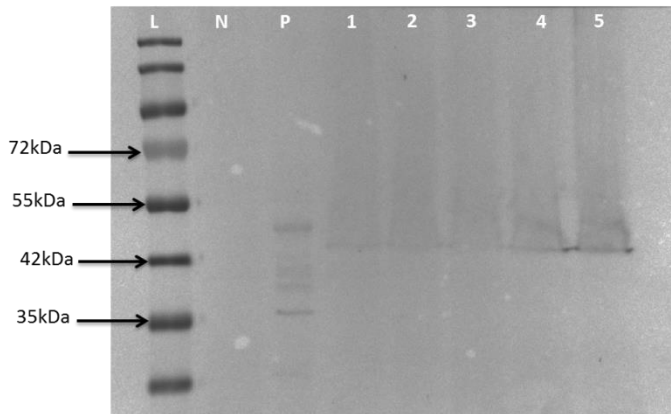


Figure I5: Western blot analysis of rotavirus VP6 expression by *P. angusta* UFS1507 colonies containing the PO VP6 ORF containing expression cassette. Lane L: PageRuler™ Prestained Protein Ladder (Thermo Fisher Scientific). Lane N: untransformed *P. angusta* UFS1507 cells, negative control. Lane P: Bacterial expressed VP6, protein size of 48 kDa. Lanes 1, 2, 3, 4, 5: *P. angusta* UFS1507 yeast clones screened for expression of VP6 with expected size of 45 kDa. A total protein concentration of 1.8mg/ml was used for all colonies screened.

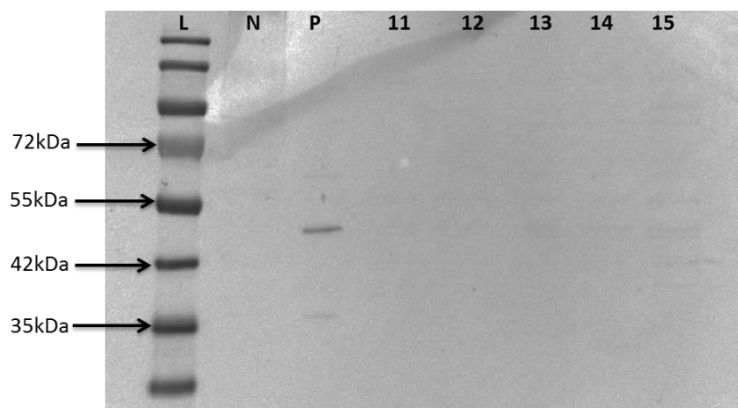


Figure I6: Western blot analysis of rotavirus VP6 expression by *P. pastoris* GS115 colonies containing the PO VP6 ORF containing expression cassette. Lane L: PageRuler™ Prestained Protein Ladder (Thermo Fisher Scientific). Lane N: untransformed *P. pastoris* GS115 cells, negative control. Lane P: Bacterial expressed VP6, protein size of 48 kDa. Lanes 11, 12, 13, 14, 15: *P. pastoris* GS115 yeast clones screened for expression of VP6 with expected size of 45 kDa. A total protein concentration of 1.6mg/ml was used for all colonies screened.

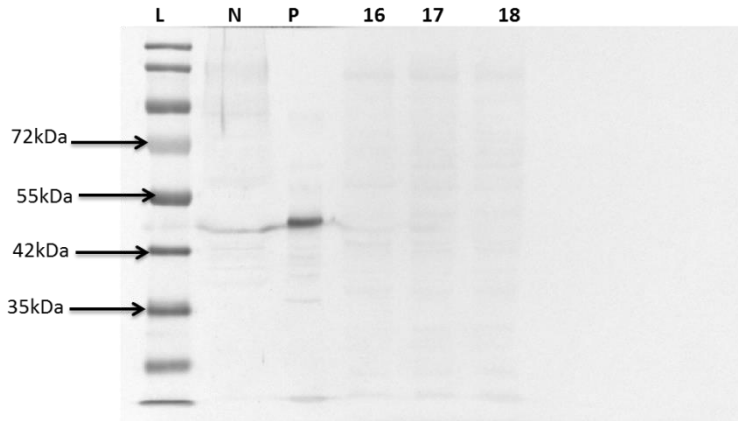


Figure I7: Western blot analysis of rotavirus VP6 expression by *P. pastoris* GS115 colonies containing the PO VP6 ORF containing expression cassette. Lane L: PageRuler™ Prestained Protein Ladder (Thermo Fisher Scientific). Lane N: untransformed *P. pastoris* GS115 cells, negative control. Lane P: VP6 bacterial positive control protein size of 48 kDa. Lanes 16, 17, 18: *P. pastoris* GS115 yeast clones screened for expression of VP6 with expected size of 45 kDa. A total protein concentration of 1.6mg/ml was used for all colonies screened.

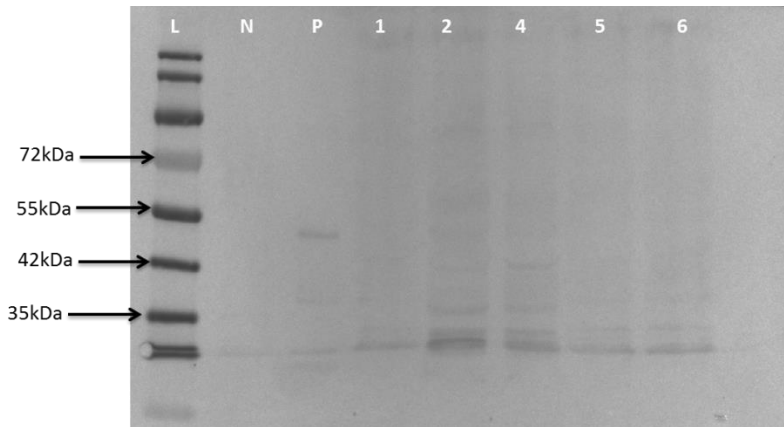


Figure I8: Western blot analysis of rotavirus VP6 expression by *P. pastoris* UFS1552T colonies containing the PO VP6 ORF-containing expression cassette. Lane L: PageRuler™ Prestained Protein Ladder (Thermo Fisher Scientific). Lane N: untransformed *P. pastoris* UFS1552T cells, negative control. Lane P: Bacterial expressed VP6, protein size of 48 kDa. Lanes 1, 2, 4, 5, 6: *P. pastoris* UFS1552T yeast clones screened for expression of VP6 with expected size of 45 kDa. A total protein concentration of 2.2mg/ml was used for all colonies screened.

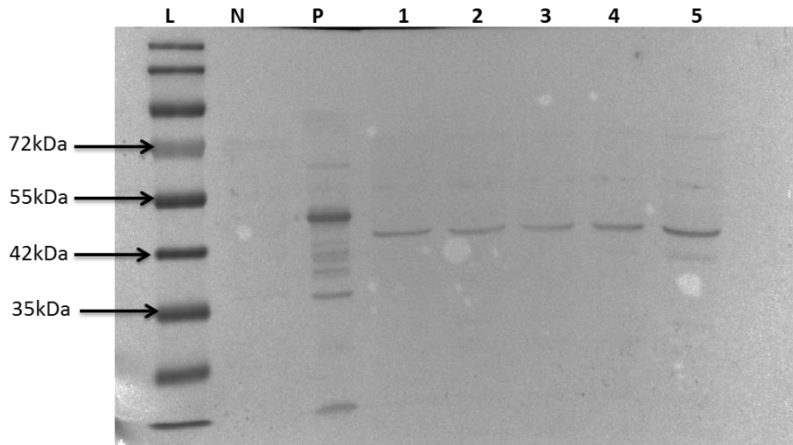


Figure I9: Western blot analysis of rotavirus VP6 expression by *S. cerevisiae* CENPK colonies containing the PO VP6 ORF containing expression cassette. Lane L: PageRuler™ Prestained Protein Ladder (Thermo Fisher Scientific). Lane N: untransformed *S. cerevisiae* CENPK cells, negative control. Lane P: Bacterial expressed VP6, protein size of 48 kDa. Lanes 1, 2, 3, 4, 5: *S. cerevisiae* CENPK yeast clones screened for expression of VP6 with expected size of 45 kDa. A total protein concentration of 20.9mg/ml was used for all colonies screened.

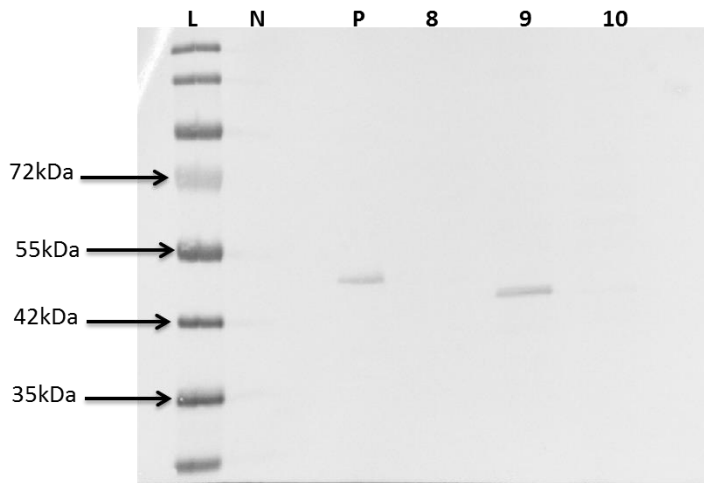


Figure I10: Western blot analysis of rotavirus VP6 expression by *Y. lipolytica* PO 1F colonies containing the PO VP6 ORF containing expression cassette. Lane L: PageRuler™ Prestained Protein Ladder (Thermo Fisher Scientific). Lane N: untransformed *Y. lipolytica* PO 1F cells, negative control. Lane P: VP6 Bacterial expressed VP6, protein size of 48 kDa. Lanes 8, 9, 10: *Y. lipolytica* PO 1F yeast clones screened for expression of VP6 with expected size of 45 kDa. A total protein concentration of 22.3mg/ml was used for all colonies screened.

Appendix J: Western blot analysis of optimal times of harvest of VP6 protein in various yeasts

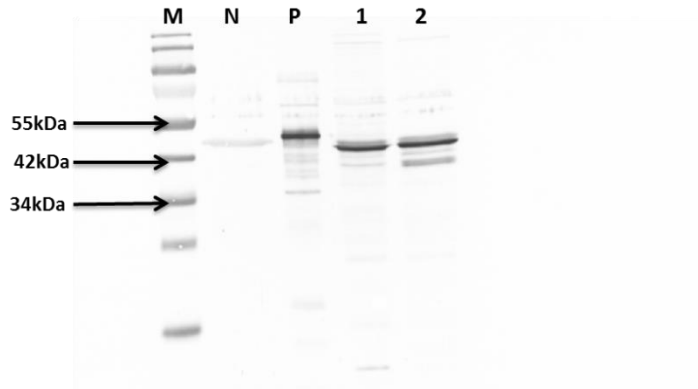


Figure J1: Western blot analysis of rotavirus VP6 expression by *A. adenivorans* UFS1219 colonies harvested either at mid- or late-exponential phase. Lane M: PageRuler™ Prestained Protein Ladder (Thermo Fisher Scientific). Lane N: untransformed cells, *A. adenivorans* UFS1219 negative control. Lane P: Bacterial expressed VP6, protein size 48 kDa. Lanes 1 *A. adenivorans* UFS1219 yeast clone screened for expression of VP6 harvested at mid-exponential phase with expected size of 45 kDa. Lanes 2 *A. adenivorans* UFS1219 yeast clone screened for expression of VP6 harvested at late-exponential phase with expected size of 45 kDa.

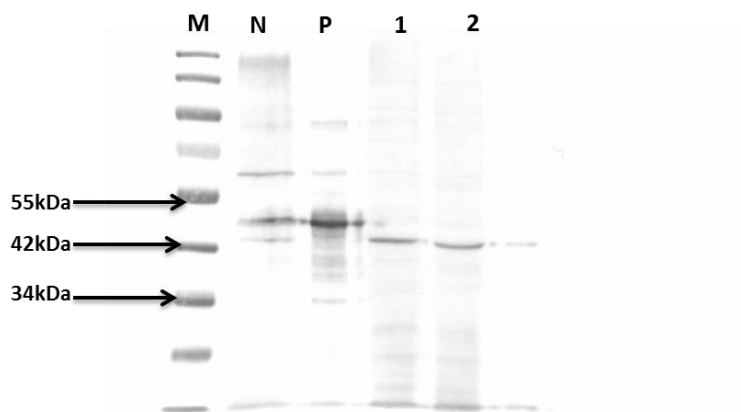


Figure J2: Western blot analysis of rotavirus VP6 expression by *P. angutsa* UFS1507 colonies harvested either at mid- or late-exponential phase. Lane M: PageRuler™ Prestained Protein Ladder (Thermo Fisher Scientific). Lane N: untransformed cells, *P. angutsa* UFS1507 negative control. Lane P: Bacterial expressed VP6, protein size 48 kDa. Lanes 1 *P. angutsa* UFS1507 yeast clone screened for expression of VP6 harvested at mid-exponential phase with expected size of 45 kDa. Lanes 2 *P. angutsa* UFS1507 yeast clone screened for expression of VP6 harvested at late-exponential phase with expected size of 45 kDa.

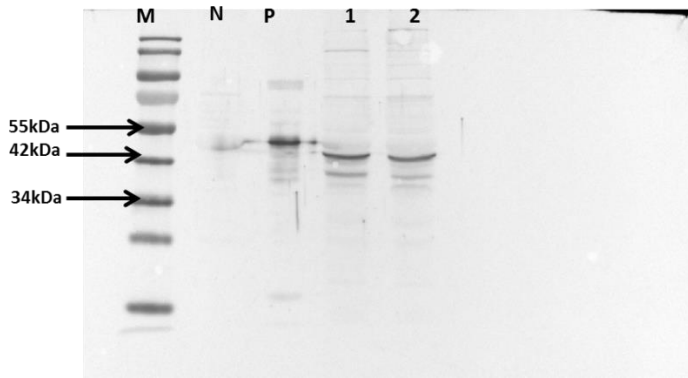


Figure J3: Western blot analysis of rotavirus VP6 expression by *S. cerevisiae* CENPK colonies harvested either at mid- or late-exponential phase. Lane M: PageRuler™ Prestained Protein Ladder (Thermo Fisher Scientific). Lane N: untransformed cells, *S. cerevisiae* CENPK negative control. Lane P: Bacterial expressed VP6, protein size 48 kDa. Lanes 1 *S. cerevisiae* CENPK yeast clone screened for expression of VP6 harvested at mid-exponential phase with expected size of 45 kDa. Lanes 2 *S. cerevisiae* CENPK yeast clone screened for expression of VP6 harvested at late-exponential phase with expected size of 45 kDa.

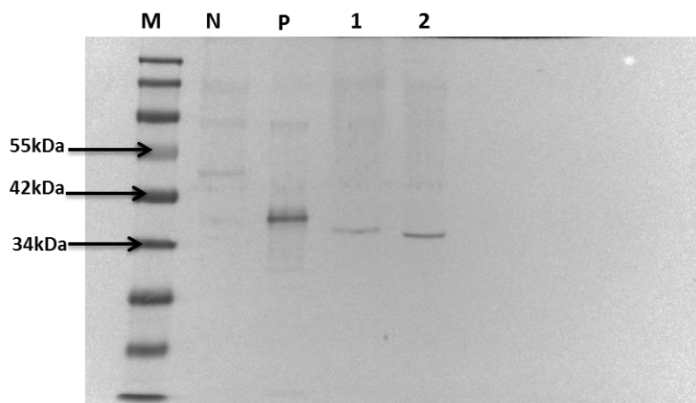


Figure J4: Western blot analysis of rotavirus VP6 expression by *S. cerevisiae* CENPK colonies harvested either at mid- or late-exponential phase. Lane M: PageRuler™ Prestained Protein Ladder (Thermo Fisher Scientific). Lane N: untransformed cells, *S. cerevisiae* CENPK negative control. Lane P: Bacterial expressed VP6, protein size 48 kDa. Lanes 1 *S. cerevisiae* CENPK yeast clone screened for expression of VP6 harvested at mid-exponential phase with expected size of 45 kDa. Lanes 2 *S. cerevisiae* CENPK yeast clone screened for expression of VP6 harvested at late-exponential phase with expected size of 45 kDa.

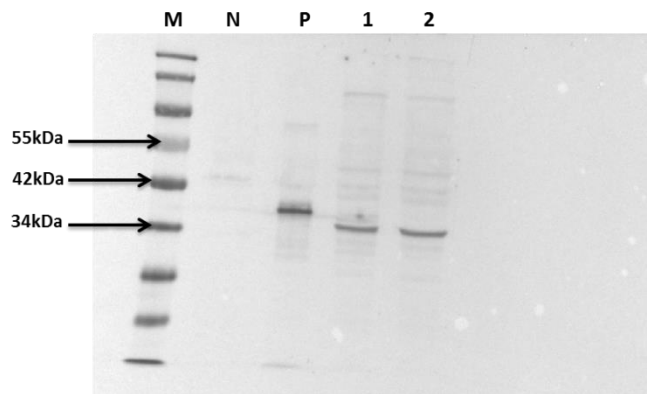


Figure J5: Western blot analysis of rotavirus VP6 expression by *Y. lipolytica* PO 1F colonies harvested either at mid- or late-exponential phase. Lane M: PageRuler™ Prestained Protein Ladder (Thermo Fisher Scientific). Lane N: untransformed cells, *Y. lipolytica* PO 1F negative control. Lane P: Bacterial expressed VP6, protein size 48 kDa. Lanes 1 *Y. lipolytica* PO 1F yeast clone screened for expression of VP6 harvested at mid-exponential phase with expected size of 45 kDa. Lanes 2 *Y. lipolytica* PO 1F yeast clone screened for expression of VP6 harvested at late-exponential phase with expected size of 45 kDa.

Appendix K: Purification of VP6 protein in *K. lactis*

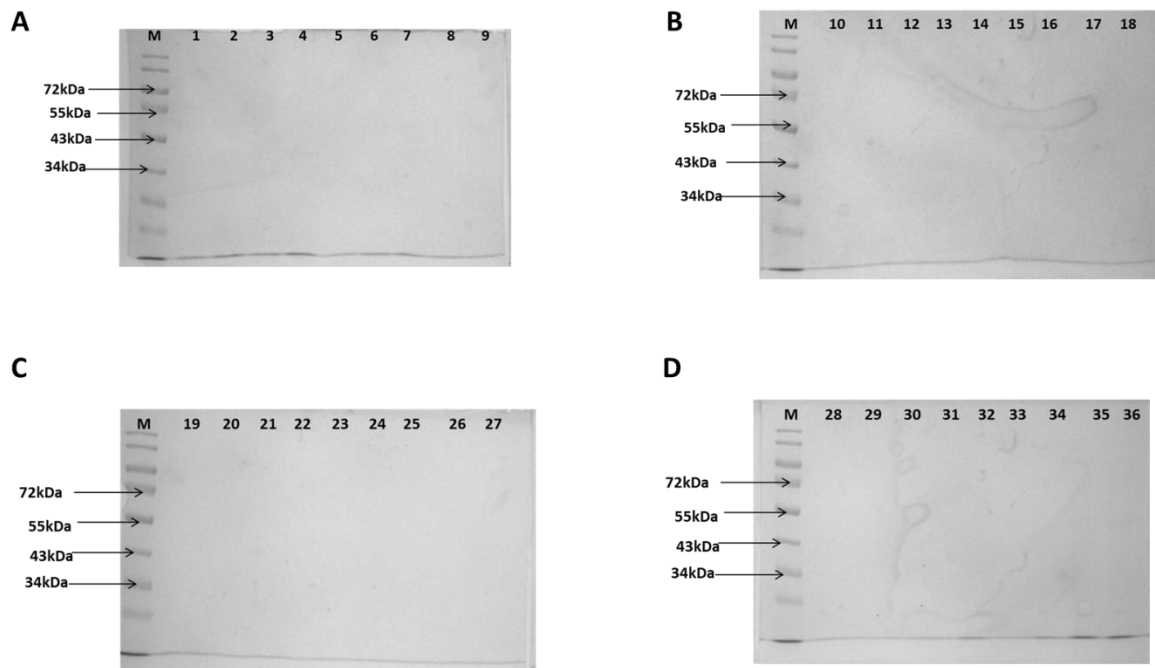


Figure K1: SDS-PAGE analysis of sucrose gradient fractions obtained following ultracentrifugation of the VP6 produced *K. lactis* cell lysate. A, Lane M is Page Ladder, Lanes 1-9 sucrose gradient fractions 1-9. B, Lane M is Page Ladder, Lanes 10-18 sucrose gradient fractions 10-18. C, Lane M is Page Ladder, Lanes 19-27 sucrose gradient fractions 19-27. D, Lane M is Page Ladder, Lanes 28-34 sucrose gradient fractions 28-34.